

Some Cosmological Implications of Extended Scalar Tensor Theories



By

Farzana Kousar

CIIT/SP13-PMATH-006/LHR

PhD Thesis

In

Mathematics

COMSATS University Islamabad

Lahore Campus - Pakistan

Fall, 2018



COMSATS University Islamabad

Some Cosmological Implications of Extended Scalar Tensor Theories

A Thesis Presented to

COMSATS University Islamabad, Lahore Campus

In partial fulfillment

of the requirement for the degree of

PhD (Mathematics)

By

Farzana Kousar

CIIT/SP13-PMATH-006/LHR

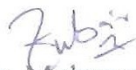
Fall, 2018

Some Cosmological Implications of Extended Scalar Tensor Theories

A Post Graduate Thesis submitted to the Department of Mathematics as partial fulfillment of the requirement for the award of Degree of PhD in Mathematics.

Name	Registration Number
Farzana Kousar	CIIT/SP13-PMATH-006/LHR

Supervisor



Dr. Muhammad Zubair
Assistant Professor Department of Mathematics
COMSATS University Islamabad (CUI) Lahore Campus

CERTIFICATE OF APPROVAL

This is to certify that the research work presented in this thesis entitled "Some Cosmological Implications of Extended Scalar Tensor Theories" was conducted by Ms. Farzana Kousar, CIIT/SP13-PMATH-006/LHR, under the supervision of Dr. Muhammad Zubair. No part of this thesis has been submitted anywhere else for any other degree. This thesis is submitted to the Department of Mathematics, COMSATS University Islamabad, Lahore Campus in the partial fulfillment of the requirements for the degree of Doctor of Philosophy in the field of Mathematics.

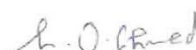
Student Name: Farzana Kousar

Signature: 

Examination Committee:




Prof. Dr. Muhammad Sharif
Chairman/Dean
Department of Mathematics
University of the Punjab
Lahore



Prof. Dr. Muhammad Ozair Ahmad
Head
Department of Mathematics
The University of Lahore (UOL)
1-Km, Raiwind Road, Lahore



Dr. Muhammad Zubair
Supervisor,
Department of Mathematics,
COMSATS University Islamabad,
Lahore Campus



Dr. Sarfraz Ahmad
HoD,
Department of Mathematics,
COMSATS University Islamabad,
Lahore Campus



Prof. Dr. Moiz ud Din Khan
Chairperson,
Department of Mathematics,
COMSATS University Islamabad

AUTHOR's DECLARATION

I Farzana Kousar, CIIT/SP13-PMATH-006/LHR, hereby state that my PhD thesis titled "Some Cosmological Implications of Extended Scalar Tensor Theories" is my own work and has not been submitted previously by me for taking any degree from this University "COMSATS University Islamabad" or anywhere else in the country/world.

At any time if my statement is found to be incorrect even after I Graduate the university has the right to withdraw my PhD degree.

Date: 18-4-2019



Farzana Kousar

CIIT/SP13-PMATH-006/LHR


PLAGIARISM UNDERTAKING

I solemnly declare that research work presented in the thesis titled “Some Cosmological Implications of Extended Scalar Tensor Theories” is solely my research work with no significant contribution from any other person. Small contribution/help wherever taken has been duly acknowledge and that complete thesis has been written by me.

I understand the zero tolerance policy of HEC and COMSATS University Islamabad towards plagiarism. Therefore, I as an author of the above titled thesis declare that no portion of my thesis has been plagiarized and any material used as reference is properly referred/cited.

I undertake that if I am found guilty of any formal plagiarism in the above titled thesis even after award of PhD degree, the University reserves the right to withdraw/revoke my PhD degree and that HEC and the University has the right to publish my name on the HEC/University website on which names of students are placed who submitted plagiarized thesis.

Date: 18-4-2019



Farzana Kousar
CIIT/SP13-PMATH-006/LHR

CERTIFICATE

It is certified that Farzana Kousar, CIIT/SP13-PMATH-006/LHR has carried out all the work related to this thesis under my supervision at the Department of Mathematics, COMSATS University Islamabad, Lahore Campus and the work fulfills the requirement for award of PhD degree.

Date: 18-4-2019

Supervisor:



Dr. Muhammad Zubair
Assistant Professor

Head of Department:



Dr. Sarfraz Ahmad
Associate Professor
Department of Mathematics

DEDICATION

To my beloved parents

and

Sisters

ACKNOWLEDGEMENTS

All praise to Almighty “ALLAH”, Who guides man in all sorts of difficulties. Above all, I must acknowledge and thanks **Almighty Allah** and **Prophet Muhammad (PBUH)** for blessing, protecting and guiding me throughout this period. Whose teachings are the building blocks of our life. I could never have accomplished this without the faith I have in the **Lord**.

I want to express my deepest gratitude to my affectionate supervisor **Dr. Muhammad Zubair** for his cooperation, keen interest suggestions and guidance during my study at COMSATS. I am grateful for his continuous support, motivation, untiring help during my PhD research work. His guidance helped me in all the time of research and writing of this thesis.

It is an honor for me to thank **Dr. Sarfraz Ahmad, Dr. Kashif Ali and Dr. Shahadat Ali Taj** for their encouraging, helping and positive attitude throughout my PhD. I would also like to say thanks to **Dr. Kashif Ali**, who guided me and recommended me **Dr. Muhammad Zubair** as a supervisor.

I can't imagine my current position without the love and support from my parents, sisters and friends. I deeply thanks my parents **Muhammad Ali Wattoo and Maqsoodan bi bi**, for their unconditional trust, timely encouragement and endless patience. I would also like to pay high regards to my sisters Kaneez Fatima, Rukhsana Kousar, Shabana Kousar, Sonia Ali and Ishrat Fatima for their endless love, prayers and encouragement which provided me inspiration at every moment of my life. **My family is my life!**

May Allah bless them all (Ameen)

Farzana Kousar
CIIT/SP13-PMATH-006/LHR

ABSTRACT

Some Cosmological Implications of Extended Scalar Tensor Theories

This thesis is devoted to explore some cosmological implications in $f(R, R_{\alpha\beta}R^{\alpha\beta}, \phi)$ gravity and generalized $f(R, \phi)$ gravity. Initially, we discuss the cosmological reconstruction of $f(R, R_{\alpha\beta}R^{\alpha\beta}, \phi)$ theory (where R , $R_{\alpha\beta}R^{\alpha\beta}$ and ϕ represent the Ricci scalar, scalar invariant and scalar field) corresponding to power law and de Sitter evolution in the framework of FRW universe model. We derive the energy conditions for this modified theory which seem to be more general and can be reduced to some known forms of these conditions in general relativity, $f(R)$ and $f(R, \phi)$ theories. We also present the general constraints in terms of recent values of snap, jerk, deceleration and Hubble parameters. The energy bounds are analyzed for reconstructed as well as known models in this theory. Finally, the free parameters are analyzed comprehensively.

First and second laws of black hole thermodynamics are examined at the apparent horizon of FRW spacetime in $f(R, R_{\alpha\beta}R^{\alpha\beta}, \phi)$ gravity. In this modified theory, Friedmann equations are formulated for any spatial curvature. These equations can be presented into the form of first law of thermodynamics for $T_h d\hat{S}_h + T_h d_i \hat{S}_h + W dV = dE$, where $d_i \hat{S}_h$ is an extra entropy term because of the non-equilibrium presentation of the equations and $T_h d\hat{S}_h + W dV = dE$ for the equilibrium presentation. The generalized second law of thermodynamics (GSLT) is expressed in an inclusive form where these results can be represented in GR, $f(R)$ and $f(R, \phi)$ gravities. Finally to check the validity of GSLT, we take some particular models and produce constraints of the parameters.

Moreover, we examine static spherically symmetric wormhole solutions in generalized $f(R, \phi)$ gravity. To do this, we consider three different kinds of fluids: anisotropic, barotropic and isotropic. We explore different $f(R, \phi)$ models and inspect the energy conditions for all of those three fluids. It is found that under some models in this theory, it is possible to obtain wormhole solutions without requiring exotic matter. From our results, one can conclude that for all three cases of fluids stable and realistic wormhole solutions can be constructed.

Further, we have considered $f(R)$ action which is non-minimally coupled to the

scalar field. In this context, we obtain the exact analytical solutions for inflationary era as well as find a graceful exit condition from inflation. We calculate the perturbed parameters, i.e., number of e-folds, slow-roll parameters, scalar and tensor power spectra, corresponding spectral indices and ultimately tensor to scalar ratio. It is showed that the power spectra lead to blue-tilt for this model. The trajectories of the perturbed parameters are plotted to compare the results with recent observations.

Finally, we will discuss cosmological models using Bianchi type I for anisotropic fluid in $f(R, \phi)$ theory of gravity which involves scalar potential. For this purpose, we consider power law assumptions of coupling function and scalar field along with the proportionality condition of expansion and shear scalars. We choose two $f(R, \phi)$ models and obtain exact solutions of field equations in both cases. For these constructed models, the behavior of different physical quantities like EoS parameter, self-interacting potential as well as deceleration and skewness parameters is explored and illustrated graphically for the feasible ranges of free parameters. It is concluded that anisotropic fluid approaches to isotropy in later cosmic times for both models which is compatible with the observational data.

LIST OF PUBLICATIONS

First five papers are included in thesis and last two are not included in the thesis.

1. M. Zubair and Farzana Kousar (2016). Cosmological reconstruction and energy bounds in $f(R, R_{\alpha\beta}R^{\alpha\beta}, \phi)$ gravity, *EPJC* **76**, 254.
2. M. Zubair a, Farzana Kousar and Sebastian Bahamonde (2016). Thermodynamics in $f(R, R_{\alpha\beta}R^{\alpha\beta}, \phi)$ theory of gravity, *Physics of the Dark Universe* **14**, 0-9.
3. M. Zubair, Farzana Kousar and Saira Waheed (2018). Evolution of anisotropic cosmic models in $f(R, \phi)$ gravity, *Int. J. Mod. Phys. D.* **27**(12), 1-19.
4. M. Zubair, Farzana Kousar and Sebastian Bahamonde (2018). Static spherically symmetric wormholes in generalized $f(R, \phi)$ gravity, *Eur. Phys. J. Plus* **133**, 523.
5. Farzana Kousar, Rabia Saleem and M. Zubair (2018). Inflation in $f(R, \phi)$ gravity with exponential model, *Adv. High Energy Phys.* **2018**, 3085761.
6. M. Zubair and Farzana Kousar (2017). Inflationary cosmology for $f(R, \phi)$ models with different potentials. *Can. J. phys.* **95** (11), 1074-1085.
7. M. Zubair, Farzana Kousar and Saira Waheed (2018). Dynamics of Scalar Potentials in $f(R, R_{\alpha\beta}R^{\alpha\beta}, \phi)$ theory of gravity, accepted in *Can. J. phys.*
8. Farzana Kousar and M. Zubair (2019). Wormholes filled with phantom fluid in $f(R, \phi)$ theory, Submitted.

TABLE OF CONTENTS

1. Introduction	1
2. Basic Concepts	10
2.1. Cosmic Expansion and Some Recent Problems of Dark Energy	11
2.2. Dark Energy	12
2.2.1. The Cosmological Constant	12
2.2.2. Quintessence	13
2.2.3. Phantom	13
2.2.4. Quintom	14
2.3. Some Cosmological Measures	14
2.3.1. Scale Factor	14
2.3.2. Hubble Parameter	14
2.3.3. Directional and Mean Hubble Parameters	14
2.3.4. Anisotropy Parameter of Expansion	15
2.3.5. Deceleration, Jerk and Snap Parameters	15
2.4. The Expansion and Shear Scalar	16
2.5. The Energy Momentum Tensor	17
2.5.1. Isotropic Fluid	18
2.5.2. Anisotropic Fluid	18
2.5.3. Barotropic fluid	19
2.5.4. Equation of State	19
2.6. The Einstein Field Equations	19
2.7. Modified Theories of Gravity	20
2.8. Scalar-Tensor Gravity	20
2.9. $f(R, \phi)$ gravity	22
2.10. $f(R, R_{\mu\nu} R^{\mu\nu}, \phi)$ gravity	22
2.11. Universe Models	23
2.11.1. Friedmann-Lemaitre-Robertson-Walker metric (FLRW) Space time	23

2.11.2. Bianchi Models	24
2.11.3. Energy Conditions	25
2.11.4. Null Energy Condition (NEC):	25
2.11.5. Weak Energy Condition (WEC):	26
2.11.6. Strong Energy Condition (SEC):	26
2.11.7. Dominant Energy Condition (DEC):	26
2.12. Black Hole Thermodynamics	26
2.12.1. Generalized Second Law of Thermodynamics (GSLT)	27
2.13. Wormhole geometries	27
2.14. Inflation	29
3. Cosmological reconstruction, energy bounds and Thermodynamics in	
$f(R, R_{\alpha\beta}R^{\alpha\beta}, \phi)$ gravity	31
3.1. Cosmological reconstruction and energy bounds in $f(R, R_{\alpha\beta}R^{\alpha\beta}, \phi)$	
gravity	32
3.1.1. Field Equations of $f(R, R_{\alpha\beta}R^{\alpha\beta}, \phi)$ gravity	32
3.1.2. Reconstruction of $f(R, Y, \phi)$ gravity	33
3.1.3. Energy Conditions	35
3.1.4. Energy Conditions of de-Sitter models and their Viability Ranges	
.	37
3.1.5. Energy Conditions of Power Law models and their validity	
ranges	42
3.1.6. Energy Conditions for Some known Models	43
3.2. Thermodynamics in $f(R, R_{\alpha\beta}R^{\alpha\beta}, \phi)$ gravity	48
3.2.1. Generalized Thermodynamics laws with non-equilibrium	
description	50
3.2.2. Validity of GSLT	53
3.2.3. Model constructed from de-Sitter Universe	53
3.2.4. Model constructed from power Law method	55
3.2.5. $f(R, \phi)$ Models	57
3.2.6. Equilibrium description of Thermodynamics laws	60

3.2.7. First Law of Thermodynamics	61
3.2.8. Generalized Second Law of Thermodynamics	62
4. Static spherically symmetric wormholes in generalized $f(R, \phi)$ gravity	64
4.1. Wormhole Geometries in extended $f(R, \phi)$ Gravity	65
4.2. Anisotropic generic fluid description	68
4.2.1. Brans-Dicke theory	69
4.2.2. Induced gravity	74
4.3. Isotropic Fluid $p_r = p_t = p$	77
4.4. Barotropic fluid with EoS $p_r = w(r)\rho$	79
4.4.1. $w(r) = w = \text{Constant}$	80
4.4.2. $w(r) = \tilde{B}r^l$	83
4.5. Barotropic fluid with EoS $p_t = w(r)\rho$	87
4.5.1. $w(r) = w = \text{Constant}$	87
4.5.2. $w(r) = \tilde{B}r^l$	90
5. Inflation in $f(R, \phi)$ gravity with exponential model	94
5.1. Model and Background Solution	95
5.1.1. Background Inflationary Solution	95
5.2. Special Case: $h_0 = h_{\tilde{n}} = 0$	96
5.3. First Order Scalar and Tensor Perturbations for the model	97
5.3.1. Perturbations	97
5.3.2. Scalar Power Spectrum	98
5.3.3. Tensor Power Spectrum	100
5.4. Stability of Inflationary Solution	101
6. Anisotropic Universe Models in $f(R, \phi)$ gravity	105
6.1. Field Equations for Bianchi I Model and Some General Parameters .	106
6.2. Solution of field Equations	108
6.2.1. The Model: $f(R, \phi) = R(1 + \xi \kappa^2 \phi^2)$	108
6.2.2. The Model: $f(R, \phi) = \frac{R - 2\Lambda(1 - e^{b_1 \phi \kappa^3 R})}{\kappa^2}$	113

7. Conclusions	119
8. References	129

LIST OF FIGURES

- Figure 3.1** Energy conditions for the dS $f(R, Y, \phi)$ model using $\alpha_1 > 0$ & $\alpha_2 > 0$.
The left plot shows the feasible regions of WEC where we fix $\zeta = -10$ (any value of ζ can be chosen since WEC is valid for all values of ζ) and the variations of α_3 & β_1 are shown. In right plot viability regions of NEC are shown for $\alpha_3 = 0$ 39
- Figure 3.2** Plot of NEC for Model-II versus the parameters ζ , β_1 and t with $n_1 = 1.1$ 45
- Figure 3.3** Validity region of the GSLT for dS $f(R, Y, \phi)$ model with $\alpha_1 = 1$ and $\alpha_2 = 3$ 54
- Figure 3.4** Validity of the GSLT for Power law- $f(R, \phi)$ versus the parameters n_1 , β_1 and t with $\alpha_1 = 1$ and $\alpha_2 = 5$ 56
- Figure 3.5** Regions where the GSLT is satisfied for the Model-II versus the parameters ζ , β_1 and t with $n_1 = 1.1$ 58
- Figure 3.6** Validity regions of the GSLT for the Model-IV for the parameters α and β_1 with $n_1 = 1.1$ 60
- Figure 4.1** Validity of $\rho \geq 0$ given by (4.2.4) for the generic anisotropic fluid in BD theory when $\sigma_2 = 1$. The yellow regions represent the regions where $\tilde{\gamma} = 1$ whereas the blue regions represent when $\tilde{\gamma} = -1$. Therefore, the green regions represent the regions where those two regions coincide. We have chosen the values $r_0 = \phi_0 = d = \omega_0 = 1$ and $\sigma_2 = 1$ 70
- Figure 4.2** Validity of NEC-1 ($\rho + p_r \geq 0$) given by (4.2.5), NEC-2 ($\rho + p_t \geq 0$) given by (4.2.6) and the full condition for the validity of NEC ($\rho + p_t \geq 0$ & $\rho + p_r \geq 0$) for the generic anisotropic fluid in BD theory. The yellow regions represent the regions where $\tilde{\gamma} = 1$ whereas the blue regions represent when $\tilde{\gamma} = -1$. For these plots, we have chosen the values $r_0 = \phi_0 = d = \omega_0 = 1$ and $\sigma_2 = 1$ 71
- Figure 4.3** Validity of NEC-1 ($\rho + p_r \geq 0$) given by (4.2.5), NEC-2 ($\rho + p_t \geq 0$) given by (4.2.6) and the full condition for the validity of NEC ($\rho + p_t \geq 0$ & $\rho + p_r \geq 0$) for the generic anisotropic fluid in BD theory. The yellow regions represent the regions where $\tilde{\gamma} = 1$ whereas the blue regions represent when

$\tilde{\gamma} = -1$. For these plots, we have chosen the values $r_0 = \phi_0 = d = \omega_0 = 1$ and $\sigma_2 = 1$ 72

Figure 4.4 Validity of WEC given by the validity of (4.2.4)-(4.2.6) for the generic anisotropic fluid in BD theory. The figure on the right represents the validity of WEC near the throat whereas the figure on the left shows the validity for locations that are not close to the throat. The yellow regions represent the regions where $\tilde{\gamma} = 1$ whereas the blue regions represent when $\tilde{\gamma} = -1$. For these plots, we have chosen the values $r_0 = \phi_0 = d = \omega_0 = 1$ and $\sigma_2 = 1$. . 73

Figure 4.5 Energy density, sum of the radial pressure and the energy density and the sum of the lateral pressure and the energy density for the generic anisotropic fluid in BD theory where $\sigma_1 = \sigma_2 = 1$ and $\tilde{\gamma} = -1$. We have further chosen the values $r_0 = \phi_0 = d = \omega_0 = 1$. For this model, the full WEC is always satisfies. 73

Figure 4.6 Validity of NEC and WEC given by the validity of (4.2.4)-(4.2.6) for the generic anisotropic fluid in BD theory. The figure on the left represents the validity of NEC for $\tilde{\gamma} = 1$ whereas the figure on the centre represents the validity for $\tilde{\gamma} = -1$. Lastly, the figure on the right shows the validity of WEC for $\tilde{\gamma} = -1$. For these plots, we have chosen the values $r_0 = \phi_0 = d = \omega_0 = 1$. We can notice that various model exist where the full WEC is valid for $\tilde{\gamma} = -1$ whereas for $\tilde{\gamma} = 1$, it is not possible to find that NEC is valid for every location. 74

Figure 4.7 Validity of NEC and WEC given by the validity of (4.2.7)-(4.2.9) for the generic anisotropic fluid in induced gravity. The figure on the left represents the validity of NEC for $\tilde{\gamma} = 1$ whereas the figure on the centre represents the validity for $\tilde{\gamma} = -1$. Lastly, the figure on the right shows the validity of WEC for $\tilde{\gamma} = -1$ and $\zeta = 2$. For these plots, we have chosen the values $r_0 = \phi_0 = d = \omega_0 = 1$. We can notice that various model exist where the full WEC is valid for $\tilde{\gamma} = -1$ whereas for $\tilde{\gamma} = 1$, it is not possible to find that NEC is valid for every location. 76

Figure 4.8 Energy density, sum of the radial pressure and the energy density and the sum of the lateral pressure and the energy density for the generic anisotropic fluid in induced gravity where $\sigma_1 = 0.5$, $\sigma_2 = \zeta = 2$ and $\tilde{\gamma} = -1$. We have further chosen the values $r_0 = \phi_0 = d = \omega_0 = 1$. For this model, the full WEC always satisfies. 76

- Figure 4.9** The behavior of $\beta(r)$ versus r taking $\eta = 1$, $\zeta = -1$, $\sigma_1 = -2.4$, $r_0 = 1$ in case of BD theory. 78
- Figure 4.10** The behavior of ρ and $\rho + p_r$ versus r taking $\eta = 1$, $\zeta = -1$, $\sigma_1 = -2.4$, $r_0 = 1$ for BD theory. 78
- Figure 4.11** The behavior of $\beta(r)$ versus r taking $\eta = 2$, $\zeta = 2$, $\sigma_1 = -2.4$, $r_0 = 1$ in case of Induced gravity. 79
- Figure 4.12** Plot shows the evolution of ρ and $\rho + p$ in case of Induced gravity for the parameters $\eta = 2$, $\zeta = 2$, $\sigma_1 = -2.4$, $r_0 = 1$, $\tilde{\gamma} = -0.5$ 79
- Figure 4.13** The behavior of $\beta(r)$ and $\beta'(r)$ versus r taking $\omega_0 = -2$, $\sigma_1 = 0.008$, $\tilde{\gamma} = -1$, $\delta_1 = 3$, $w = 15$, $\phi_0 = 10$, $V_0 = 0.1$ 80
- Figure 4.14** The behavior of $\frac{\beta(r)}{r}$ and $\beta(r) - r$ versus r taking $\omega_0 = -2$, $\sigma_1 = 0.008$, $\tilde{\gamma} = -1$, $\delta_1 = 3$, $w = 15$, $\phi_0 = 10$, $V_0 = 0.1$ 81
- Figure 4.15** The behavior of ρ , $\rho + p_r$ and $\rho + p_t$ versus r for the parameters $\omega_0 = -2$, $\sigma_1 = 0.008$, $\tilde{\gamma} = -1$, $\delta_1 = 3$, $w = 15$, $\phi_0 = 10$, $V_0 = 0.1$ 81
- Figure 4.16** The behavior of $\beta(r)$ and $\beta'(r)$ versus r taking $\omega_0 = -2$, $\sigma_1 = 0.008$, $\tilde{\gamma} = -1$, $\delta_1 = 3$, $w = 10$, $\phi_0 = 10$, $V_0 = 0.1$ 82
- Figure 4.17** The behavior of $\frac{\beta(r)}{r}$ and $\beta(r) - r$ versus r taking $\omega_0 = -2$, $\sigma_1 = 0.008$, $\tilde{\gamma} = -1$, $\delta_1 = 3$, $w = 10$, $\phi_0 = 10$, $V_0 = 0.1$ 82
- Figure 4.18** The behavior of ρ , $\rho + p_r$ and $\rho + p_t$ for the parameters $\omega_0 = -2$, $\sigma_1 = 0.008$, $\tilde{\gamma} = -1$, $\delta_1 = 3$, $w = 10$, $\phi_0 = 10$, $V_0 = 0.1$ 83
- Figure 4.19** The behavior of $\beta(r)$ and $\beta'(r)$ versus r taking $\omega_0 = -2$, $\sigma_1 = 0.008$, $\tilde{\gamma} = -1$, $\delta_1 = 5$, $\tilde{B} = 2$, $l = 5$, $\phi_0 = 10$, $V_0 = 0.1$ 84
- Figure 4.20** Left plot shows the behavior of $\frac{\beta(r)}{r}$ and right plot shows the behavior of $\beta(r) - r$ versus r for the parameters $\omega_0 = -2$, $\sigma_1 = 0.008$, $\tilde{\gamma} = -1$, $\delta_1 = 5$, $\tilde{B} = 2$, $l = 5$, $\phi_0 = 10$, $V_0 = 0.1$ 84
- Figure 4.21** The behavior of ρ , $\rho + p_r$ and $\rho + p_t$ versus r for the parameters $\omega_0 = -2$, $\sigma_1 = 0.008$, $\tilde{\gamma} = -1$, $\delta_1 = 5$, $\tilde{B} = 2$, $l = 5$, $\phi_0 = 10$, $V_0 = 0.1$ 85
- Figure 4.22** The behavior of $\beta(r)$ and $\beta'(r)$ versus r taking $\omega_0 = -2$, $\sigma_1 = 0.008$, $\tilde{\gamma} = -1$, $\delta_1 = 3$, $\tilde{B} = 2$, $l = 2.5$, $\phi_0 = 10$, $V_0 = 0.1$ 85

- Figure 4.23** The behavior of $\frac{\beta(r)}{r}$ and $\beta(r) - r$ versus r taking $\omega_0 = -2$,
 $\sigma_1 = 0.008$, $\tilde{\gamma} = -1$, $\delta_1 = 3$, $\tilde{B} = 2$, $l = 2.5$ $\phi_0 = 10$, $V_0 = 0.1$ 86
- Figure 4.24** The plot shows the evolution of ρ , $\rho + p_r$ and $\rho + p_t$ for the
parameters $\omega_0 = -2$, $\sigma_1 = 0.008$, $\tilde{\gamma} = -1$, $\delta_1 = 3$, $\tilde{B} = 2$, $l = 2.5$ $\phi_0 = 10$,
 $V_0 = 0.1$ 86
- Figure 4.25** The behavior of $\beta(r)$ and $\beta'(r)$ versus r taking $\omega_0 = -2$, $\sigma_1 = 0.009$,
 $\tilde{\gamma} = 1$, $\delta_1 = 3$, $w = 25$, $\phi_0 = 10$, $V_0 = 0.1$ 88
- Figure 4.26** Left plot shows the behavior of $\frac{\beta(r)}{r}$ versus r and right plot shows the
behavior of $\beta(r) - r$ for the parameters $\omega_0 = -2$, $\sigma_1 = 0.009$, $\tilde{\gamma} = 1$, $\delta_1 = 3$,
 $w = 25$, $\phi_0 = 10$, $V_0 = 0.1$ 88
- Figure 4.27** The plot shows the evolution of ρ , $\rho + p_r$ and $\rho + p_t$ for the
parameters $\omega_0 = -2$, $\sigma_1 = 0.009$, $\tilde{\gamma} = 1$, $\delta_1 = 3$, $w = 25$, $\phi_0 = 10$, $V_0 = 0.1$. .
. 88
- Figure 4.28** The behavior of $\beta(r)$ and $\beta'(r)$ versus r taking $\omega_0 = -2$, $\sigma_1 = 0.0008$,
 $\tilde{\gamma} = 1$, $\delta_1 = 3$, $w = 25$, $\phi_0 = 10$, $V_0 = 0.1$ 89
- Figure 4.29** Left plot shows the behavior of $\frac{\beta(r)}{r}$ versus r and right plot shows the
evolution of $\beta(r) - r$ for the parameters $\omega_0 = -2$, $\sigma_1 = 0.0008$, $\tilde{\gamma} = 1$, $\delta_1 = 3$,
 $w = 25$, $\phi_0 = 10$, $V_0 = 0.1$ 89
- Figure 4.30** The plot shows the evolution of ρ , $\rho + p_r$ and $\rho + p_t$ for the
parameters $\omega_0 = -2$, $\sigma_1 = 0.0008$, $\tilde{\gamma} = 1$, $\delta_1 = 3$, $w = 25$, $\phi_0 = 10$, $V_0 = 0.1$.
. 90
- Figure 4.31** The behavior of $\beta(r)$ and $\beta'(r)$ versus r taking $\omega_0 = -2$, $\sigma_1 = 0.008$,
 $\tilde{\gamma} = 1$, $\delta_1 = 5$, $\tilde{B} = 2$, $l = 5$ $\phi_0 = 10$, $V_0 = 1$ 91
- Figure 4.32** Left plot shows the behavior of $\frac{\beta(r)}{r}$ versus r and right plot shows the
behavior of $\beta(r) - r$ for the parameters $\omega_0 = -2$, $\sigma_1 = 0.008$, $\tilde{\gamma} = 1$, $\delta_1 = 5$,
 $\tilde{B} = 2$, $l = 5$ $\phi_0 = 10$, $V_0 = 1$ 91
- Figure 4.33** The plot shows the evolution of ρ , $\rho + p_r$ and $\rho + p_t$ for the
parameters $\omega_0 = -2$, $\sigma_1 = 0.008$, $\tilde{\gamma} = 1$, $\delta_1 = 5$, $\tilde{B} = 2$, $l = 5$ $\phi_0 = 10$, $V_0 = 1$.
. 92
- Figure 4.34** The behavior of $\beta(r)$ and $\beta'(r)$ versus r taking $\omega_0 = -2$, $\sigma_1 = 0.008$,
 $\tilde{\gamma} = 1$, $\delta_1 = 5$, $\tilde{B} = 2$, $l = 2.5$ $\phi_0 = 10$, $V_0 = 1$ 92

- Figure 4.35** Left plot shows the behavior of $\frac{\beta(r)}{r}$ versus r and right plot shows the evolution of $\beta(r) - r$ for the parameters $\omega_0 = -2$, $\sigma_1 = 0.008$, $\tilde{\gamma} = 1$, $\delta_1 = 5$, $\tilde{B} = 2$, $l = 2.5$ $\phi_0 = 10$, $V_0 = 1$ 93
- Figure 4.36** plot shows the evolution of ρ , $\rho + p_r$ and $\rho + p_t$ for the parameters $\omega_0 = -2$, $\sigma_1 = 0.008$, $\tilde{\gamma} = 1$, $\delta_1 = 5$, $\tilde{B} = 2$, $l = 2.5$ $\phi_0 = 10$, $V_0 = 1$ 93
- Figure 5.1** Evolution of ε versus N for different initial values of $\dot{\phi}$ 103
- Figure 5.2** Evolution of ϕ versus N for different initial values of $\dot{\phi}$ 104
- Figure 5.3** Left plot shows the behavior of r versus n_s for $\dot{\phi} = 0.0065\phi_D$ with $\tilde{n} = 1.6$ and right plot for $\dot{\phi} = 0.0065\phi_D$ with $\tilde{n} = 1.7$ 104
- Figure 6.1** The left plot represents the behavior of deceleration parameter q versus m while right plot indicates the behavior of energy density versus T where $n = 0.02$, $\beta_1 = 0.2$, $m = 2$, $\xi = -0.5$, $\zeta = -1.5$, $\omega_0 = 0.5$, $c_1 = -0.01$ and $c_3 = 1$ 110
- Figure 6.2** Left plot represents ρ and right plot indicates scalar potential versus T for $n = 0.02$, $\beta_1 = 1.2$, $m = 2$, $\xi = -0.5$, $\zeta = -1.5$, $\omega_0 = 0.5$, $c_1 = -0.01$ and $c_3 = 1$ 112
- Figure 6.3** Left plot refers to skewness parameter δ while right plot provides γ versus T for $n = 0.02$, $\beta_1 = 1.2$, $m = 2$, $\xi = -0.5$, $\zeta = -1.5$, $\omega_0 = 0.5$, $c_1 = -0.01$ and $c_3 = 1$ 112
- Figure 6.4** Right plot represents anisotropic expansion measure of anisotropic fluid $\frac{\delta-\gamma}{w}$ versus T and left plot corresponds to the deviation free EoS parameter w versus T for the same choice of parameters. 113
- Figure 6.5** Left plot represents ρ for three values of β while right plot indicates scalar potential versus T for $n = 0.002$, $\beta_1 = 1.2$, $m = 4$, $b_1 = 1$, $\zeta = 2.5$, $\omega_0 = 0.5$, $k_1 = 1$ and $k_3 = 1$ 117
- Figure 6.6** Plot represents skewness parameters δ and γ versus T for $n = 0.002$, $\beta_1 = 1.2$, $m = 4$, $b_1 = 1$, $\zeta = 2.5$, $\omega_0 = 0.5$, $k_1 = 1$ and $k_3 = 1$ 117
- Figure 6.7** Left plot provides the behavior of EoS parameter w versus T for $n = 0.002$, $\beta_1 = 1.2$, $m = 4$, $b_1 = 1$, $\zeta = 2.5$, $\omega_0 = 0.5$, $k_1 = 1$ and $k_3 = 1$ while right plot indicates the anisotropic expansion measure of fluid versus T for the same choice of free parameters. 118

LIST OF TABLES

Table 2.1	Classification of Bianchi Models	24
Table 3.1	Validity regions of WEC and NEC for dS $f(R, Y, \phi)$ model.	38
Table 3.2	Validity regions of $\dot{S}_{tot} = 0$ for different models.	57
Table 4.1	Some shape functions for different values of the parameter σ_2	68

LIST OF ABBREVIATIONS

We will use the following list of notations and abbreviations.

DM :	Dark Matter
DE :	Dark Energy
GR :	General Relativity
BH :	Black Hole
BD :	Brans Dicke
dS :	de-Sitter
EoS :	Equation of State
NEC :	Null Energy Condition
WEC :	Weak Energy Condition
SEC :	Strong Energy Condition
DEC :	Dominant Energy Condition
EMT :	Energy Momentum Tensor
FRW :	Friedmann-Roberston-Walker
FLRW :	Friedmann-Lemaître-Robertson-Walker
FLT :	First Law of Thermodynamics
SLT :	Second Law of Thermodynamics
GSLT :	Generalized Second Law of Thermodynamics
BI :	Bianchi Type I
BIII :	Bianchi Type III
BVI_0 :	Bianchi type VI_0
SNeIa :	Supernovae Type Ia
CMBR :	Cosmic Microwave Background Radiation
LSS :	Large Scale Structure
BAO :	Baryon Acoustic Oscillations
WMAP :	Wilkinson Microwave Anisotropy Probe
HBB :	Hot big-bang theory

LRS :	Locally Rotationally Symmetric
EFE :	Einstein Field Equation
R.H.S:	Right hand side
Λ CDM :	Λ -Cold Dark Matter
$a(t)$:	Scale Factor
H :	Hubble Parameter
q :	Deceleration Parameter
j :	Jerk Parameter
s :	Snap Parameter
Δ :	Anisotropy Parameter of Expansion
Λ :	Cosmological Constant
R :	Ricci Scalar
τ :	Torsion Scalar
ϕ :	Scalar Field
Θ :	Expansion Scalar
σ :	Shear Scalar
ρ :	Energy Density
p :	Pressure
u^μ :	4-velocity vector
σ^{ij} :	Stress density
\mathcal{L}_m :	Matter part of the Lagrangian
$T_{\mu\nu}$:	Energy Momentum Tensor
Δ^μ :	Covariant derivative
\square :	d'Alembertian operator
$g_{\mu\nu}$:	Metric Tensor
g :	Determinant of metric tensor
κ^2 :	Gravitational coupling constant.
$R_{\alpha\beta}R^{\alpha\beta}$:	Curvature Invariant
G_{eff} :	The effective gravitational coupling
N :	No. of e-folding

$n_T :$	Tensor spectral index
$n_s :$	Spectral Index
$r :$	Scalar to tensor ratio

Chapter 1

Introduction

The observational data of SNe Ia [1], CMBR [2], LSS [3] and WMAP [4] observed that the universe is facing accelerating expansion. The reason behind the cosmic expansion is DE. DE appears as distinctive energy component because of its peculiar properties. It is distinguished from ordinary matter species in the vicinity of anti gravitational behavior showing negative pressure. Despite tremendous researches and observations, origin of DE is still significant as well as challenging area for cosmologists. Present Planck's data [5] yield matter distribution of the universe in the ratio: 4.9% baryonic or shining matter, 26.8% dark matter and 68.3% exotic matter, i.e., DE. The classification of this unknown component is still under consideration as different possibilities have been proposed [6]-[8] in the background of GR. In GR, cosmological constant Λ was proposed by Einstein in 1917 [9], considering the universe as static. After the discovery of cosmic expansion with the help of Hubble, Einstein admitted the inclusion of Λ as his "biggest blunder. After the observational results Λ appeared to be the merest candidate for the DE in which the energy density is constant [10] but still it involves some issues to be settled. Now, if the Λ is not the origin of DE then cosmologists need some alternate models or ways for the description of cosmic expansion.

To describe the reality of DE, various approaches have been reported in literature through different strategies. These efforts are usually distributed in two groups: modifications on the right side of dynamical equations and the second one is to modify the left side of Einstein equations. Cosmological constant [8, 11], Chaplygin gas matter with its different modified versions [12], scalar field models like quintessence and k-essence [13] are some prominent cases among the candidates belonging to the first category, whereas the large-distance modifications of gravity, i.e., modified theories of gravity belong to second class [14]. Although the members of the first group are fascinating but due to the existence of ambiguities these could not be proved much promising. On the other hand, modified frameworks of gravity are regarded as more appropriate candidates due to their successful cosmological applications. Some well motivated examples of modified theories include $f(R)$ gravity [15], $f(\tau)$ gravity [16], Gauss-Bonnet gravity [17], $f(R, T)$ gravity, (where T is the trace of EMT) [18] and the scalar-tensor theories (based on both scalar and tensor fields) [19, 20] etc.

In 1961, Brans and Dicke introduced a scalar-tensor gravity as an effort to incorporate the Mach's proposal [21] in the Einstein-Hilbert gravitational framework which is known in the literature as BD theory. Scalar tensor theory is one of the attractive generalizations of GR in which gravity is manifested by both scalar and tensor fields. This theory is an example of non-minimally interacting theories yielding a dynamical framework due to the presence of variable gravitational constant given by the scalar field reciprocal. For a successful prediction of solar system tests, the BD parameter should assume a very large value or should behave asymptotically approaching to infinity [22]. The other physical laws like weak equivalence principle and Dirac's large number hypothesis also remain valid in this gravity. In literature [23], there are two conformally related frames to formulate this theory namely, Jordan and Einstein conformal frames. There is a long term clash between the physical and mathematical equivalence of these frames and also about their validity [24]. There are many arguments in the literature [25] but still this issue is debateable. There are numerous interesting versions of scalar tensor theory due to its increasing applications in cosmology. Some well-famed versions include generalized BD theory, BD gravity with curvature correction and chameleonic BD gravity. The curvature corrected version of BD gravity is motivated by the argument that the introduction of the inverse of R in the Einstein-Hilbert Lagrangian leads to a coherent phenomenon of cosmic acceleration [26, 27]. Chameleonic BD gravity is defined on the basis of non-minimal coupling between the scalar field and the matter.

One of important aspects of cosmology in modified theories is cosmological reconstruction. The reconstruction procedure in modified theories has been utilized in many ways to describe the well known cosmic eras. In this perspective, one way is to pick the known cosmic evolution and utilize the dynamical equations to determine specific form of Lagrangian that can procreate the defined evolution background. Using FRW spacetime, the power law cosmology is examined in these modified theories. Generic $f(R)$ gravity models were developed by Nojiri et al. [28] and further applied to modified Gauss-Bonnet theories and $f(R, G)$ gravity [29]. In [30], Carloni et al. has developed a new method for the reconstruction of $f(R)$ gravity models by using cosmic parameters rather than scale factor. Employing different cosmological scenarios, many authors [31]-[33] have reconstructed

the some viable models in $f(R, T)$ gravity.

Energy conditions are very important as these can yield the physical viable solutions by ensuring the positivity of the matter density. From these conditions, we have four inequalities known as strong, weak, null and dominant conditions [34]. The SEC provides a basis for the conjecture regarding the existence of singularities proposed by Hawking and Penrose [35] whereas NEC and DEC are taken as the basic ingredients to validate the SLT for BH and positive mass theorem, respectively [34, 36]. Although these constraints are earlier derived in GR, but later their application are also extended to other modified gravitational frameworks. On cosmological grounds, these conditions are used to restrict the parameters of the extra added degree of freedom like $f(R)$ or $f(\phi)$ functions so that they could be compatible with their corresponding values already found in cosmology. Visser [37] expressed some cosmological parameters including deceleration, jerk and snap parameters, distance formulae as well as lookback cosmic time in terms of red shift using energy bounds. Banijamali et al. [38] used energy constraints to investigate the possible bounds on some $f(G)$ models in modified Gauss-Bonnet theory. They argued that in spite of all physical motivations, the application of energy conditions to modified theories still remains as an open problem for the researchers that can further be linked with the consistency of the theory with the observations. For a detailed discussion on the cosmological applications of these conditions to modified theories, we may refer the readers to study the literature [31], [39]-[41].

The energy conditions have been discussed in many theories like $f(R)$ gravity [42], BD theory [40], $f(G)$ theory [43] and $f(T)$ theory [43, 44]. Sharif and Saira have discussed the energy bounds in generalized scalar tensor theory of second order [45]. Further Sharif and Zubair studied these constraints in $f(R, T)$ gravity [31] and $f(R, T, R_{\mu\nu}T^{\mu\nu})$ gravity [46] in which Ricci tensor and EMT are non-minimally coupled. Moreover, Saira and Zubair examined these constraints in $F(T, T_G)$ gravity where T is the torsion invariant along with T_G which is equivalent to the Gauss-Bonnet term and teleparallel [47].

The BH thermodynamics was first time introduced in 1970s. At that time, physicists found that there must be some relation between Einstein's equations and thermodynamics due to the connection between entropy (thermodynamical quantity) and horizon area

(geometric quantity) of BH. The full attention was on thermodynamic studies to analyze these in the context of black hole due to the connection between surface gravity (geometric quantity) and its temperature (thermodynamical quantity) [48]. By the revelation of BH thermodynamics, Bardeen et al. showed that gravitation and thermodynamics are strongly connected [49]. Using the FLT $\delta Q = TdS$ and proportionality between entropy and horizon area of the BH, Jacobson formulated the Einstein's equations [50]. Verlinde [51] discovered that for radiation dominated (FRW) universe, field equation can be written in the form of Cardy-Verlinde formula. For conformal field theory, this relation represents an entropy formula in higher dimensional spacetime. It can also be seen that radiation can be expressed by conformal field theory. Using entropy formula, radiation thermodynamics in the universe has been derived and also can be written on the pattern of Friedmann equation that represents the dynamics of the space-time. Moreover, the relationship between Einstein's equations and thermodynamics was discovered by Verlinde, the related discussion can be seen in [52].

In Einstein theory and modified gravities, the relation between the field equations and FLT has been extensively discussed. In Einstein gravity, for spherically symmetric BH, Padmanabhan [53] has defined such connection and established that the field equations can be written in the form of FLT stated as $dE + PdV = TdS$. In case of Lanczos-Lovelock gravity, same work was done for general static and spherically symmetric spacetimes [54]. Considering the geometric entropy equals to quarter of the apparent horizon area and employing FLT to the apparent horizon of FRW spacetime, Cai and Kim calculated the Friedmann equations that shows the dynamics of the universe having any spatial curvature [55]. In 2006, Akbar has discussed the relation between FLT and Friedmann equations in case of $f(R)$ gravity and scalar tensor gravity [56]. In phantom dominated era, Sadjadi described the constraints on GSLT and apply restrictions on Hubble parameter H , future horizon R_h and temperature T [57]. Akbar [58] has expressed that in FRW universe, the Friedmann equations filled with viscous fluid can be described in the form of FLT at apparent horizon. In $f(R)$ theories, the existence of Kerr-Newman and RN BHs were examined and further discuss the properties of thermodynamics in extended electromagnetic theories and $f(R)$ theory [59]. In Palatini formalism, Bamba has discussed the FLT and SLT in $f(R)$ grav-

ity at apparent horizon [60, 61]. He also discussed the equilibrium and non-equilibrium descriptions of $f(R)$ gravity and concluded that equilibrium is more transparent than the non-equilibrium. Furthermore, Sharif et al. [62]-[64] have considered the modified theories with non-minimal coupling and discussed the laws of thermodynamics in FRW universe at apparent horizon. In $f(R, T)$ and $f(R, T, Q)$ gravities they have explored that equilibrium thermodynamics does not satisfy and discussed the non-equilibrium thermodynamics. In [65], Huang et al. have discussed the laws of thermodynamics for the scalar tensor theory involving non-minimally coupling.

Wormholes are hypothetical topological objects that provide a shortcut connecting two distant regions in a space-time or bridging two distinct universes. The study of such geometrical objects started in 1916 by Flamm [66] and then followed by the work of Einstein and Rosen in 1935 [67]. In the later work, they found a space-time solution whose geometry consists of two mouths and a throat known as an Einstein-Rosen bridge. Misner and Wheeler introduced the word wormhole for such objects in 1957 [68]. They also showed that wormholes cannot be traversable for standard matter due to its instability. The current interest in wormholes started after the important works done by Morris et al. [69]. They formally presented a metric, the so called Morris-Thorne metric, and give some conditions in order to have a traversable wormhole. They showed that wormholes can be traversable provided that they are backed by exotic form of matter, which involves EMT that violates the NEC. There already exist an important number of works exploring the possible existence of wormhole geometries in various physical scenarios. In the literature, some attempts have been made to reduce the impact of exotic matter and minimize the violation of energy conditions [70]-[72]. An interesting approach is the one made by alternative theories of gravity. The main idea of this approach lies in assuming that the matter which supports the wormhole does not violate the energy conditions but all the new terms coming from the theory lead towards this violation [73]-[75]. The procedure is the following. In all of those modified theories, it is possible to rewrite the field equations using effective fluids defined as the sum of the standard fluid and a new fluid which represents all the new terms coming from the modified theory. In this scenario, one can see that the standard matter fluid satisfies the energy conditions (NEC and WEC) but the effective fluids do not.

Hence, one can say that those new terms coming from modified gravity are responsible for the violation of the standard energy.

Existence of wormhole solutions has been discussed in various theories such as $f(R)$ gravity [73], $f(T)$ gravity [74], $f(R, T)$ gravity [75], BD theory [76]-[79], metric Palatini hybrid $f(R)$ [80], scalar tensor teleparallel gravity [81], in Gauss Bonnet gravity [82] and in many others. In [76], Agnese and Camera found static spherically symmetric solutions in BD theory which can describe wormhole solutions depending on the choice of post Newtonian parameter $\gamma > 1$. BD theory could admit traversable wormhole solutions for both positive and negative values of BD parameter ($\omega < -2$ & $\omega < \infty$). In this study, scalar field plays the role of the exotic matter [77, 78]. Ebrahimi and Riazi [79] used a traceless EMT to find two classes of Lorentizan wormhole solutions in BD theory. The first one was obtained in an open universe whereas the second wormhole solution was obtained for both open and closed universes. However, the WEC is violated for these solutions. The existence of Euclidean wormhole solutions has also been explored in BD theory and induced gravity [83].

In GR, to construct the wormholes without exotic matter is not an easy task. For this purpose, the thin shell wormholes were introduced by Visser [71] in which exotic matter is minimized at the throat. Many thin shell wormholes has been discovered, discussed in the literature [84]-[89] but all have two drawbacks: limited or non-physical stability and the exotic matter as a source. For thin-shell wormholes, stability analysis has been done by many authors using perturbations that preserve the original symmetries. In [84], Poisson and Visser have discussed the linearized analysis of a thin-shell wormhole taking two Schwarzschild geometries jointly. Barceló and Visser [90] applied this method to construct wormholes taking brans into account with negative tensions. The linearized stability analysis was discussed: using ReissnerNordström thin-shell geometries [87], wormholes with a cosmological constant [85] and dynamical thin-shell wormholes [91].

In literature, Bianchi universe models have been studied by numerous authors. In this respect, Rodrigues [92] constructed a BI Λ CDM cosmic model. He concluded that the DE component produces anisotropic vacuum pressure which maintains its non-dynamical character. Koivisto and Mota [93] have studied the BI model in the presence of DE.

They investigated that if anisotropic EoS is taken into account, then the cosmic expansion rate becomes direction dependent, in later cosmic times. They also suggested that using anisotropic EoS, the cosmological models can resolve some of observed deviations of CMB. In another study [94], this model is examined for the combination of perfect fluid and DE. In [95, 96], Akarsu and Kilinc proposed that it is not necessary for anisotropic fluid to support anisotropy, such fluid may support isotropic behavior of the cosmos. It is also shown [95, 96] that anisotropic BI model with perfect fluid and DE matter contents corresponds to isotropic behavior in the earlier cosmic times. Sharif and Zubair [97] have investigated BVI_0 model for anisotropic DE. They examined the anisotropic behavior of DE and the effects of electromagnetic field on cosmic dynamics. It is found that electromagnetic field supports the anisotropic behavior of DE that further becomes isotropic in later stages of the universe. In another study [98], same authors studied BVI_0 model for magnetized anisotropic DE. It is found that universe model and anisotropic fluid do not approach to isotropy in any cosmic epoch. Sharif and Zubair [99, 100] have studied BI model for perfect fluid in $f(R, T)$ gravity. In [99], they found that perfect fluid solutions are quite similar to the massless scalar field models while in [100], they found solutions of dynamical equations using power and exponential expansion laws. They also examined different kinematical and physical quantities and concluded that these are satisfied in accordance with observational data.

In BD scalar tensor theory, Sharif and Waheed [101] studied BI model in the presence of perfect, anisotropic and magnetized anisotropic fluids. They concluded that in all cases, anisotropic fluid approaches to isotropy in later cosmic times according to the observational studies. In another paper [102], they explored the solution of BI field equations in the presence of charged viscous cosmological strings fluid. They found that this model shows the accelerated cosmic expansion for some specific values of the free parameters. Also, Zubair and Hassan [103] examined the nature of NEC, energy density and deceleration parameter for BI, BIII and Kantowski-Sachs universe models in $f(R, T)$ gravity. They concluded that in all cases, the cosmic models corresponds to phantom cosmic evolution. Sahoo and Reddy [104] studied BI cosmic model containing bulk viscous fluid by taking linear $f(R, T)$ model along with time varying deceleration parameter. They concluded that

their constructed model is physically viable. Ramesh and Umadevi [105] investigated FRW universe model using perfect fluid in $f(R, T)$ gravity. Recently, Shamir [106] explored the solutions of $f(R, T)$ field equations for BI universe model by using the proportionality condition of shear and expansion scalars. He found three different solutions and explored the behavior of corresponding physical quantities.

In 1981, Guth [107] introduced the term cosmological inflation, an influential research aspect in modern cosmology. Idea of inflation is applied on very initial era of cosmic evolution in the view of HBB theory. Regardless of all of the improvements, there are some unsatisfactory issues with HBB theory which cultivated inflation [108]. Liddle and Samuel [109] discussed the impact of substandard evolution between the current stage and end of inflation, showing that the expected number of e-folding (N) can be modified. Walliser [110] solved generic scalar tensor theories and found the differential equations which successfully inflate the universe. Garcia-Bellido and Quiros [111] discussed the problem of inflation, based on a generic scalar-tensor theory. They determined a particular class of models with a BD like behavior during inflation. The result are converted continuously to GR during the epochs of radiation and matter dominated. They solved dynamical equations numerically and find a subclass of models. Lahiri and Bhattacharya [112] formulated a general mechanism to analyze the linear perturbations during inflation based on the gauge-ready approach. They solved the first order slow-roll equations for scalar and tensor perturbations and obtained the super-horizon solutions for different perturbations after inflation.

Myrzakulov et al. [113] described the inflation with the reference of $f(R, \phi)$ -theories and generated a class of models which support early-time acceleration. Sharif and Saleem [114] studied the warm inflation using LRS BI universe model. They presented the plots of the perturbed parameters to check the comparability of the considered model with recent observations. Mathew et al. [115] constructed exact analytical solution in Jordan frame with non-minimally coupling of $f(R)$ action to a massive scalar field. They proved that the solutions were same as in scalar tensor theory. They also explained the dynamics of tensor power spectrum for this model.

Chapter 2

Basic Concepts

The nature of our universe, its formation and ultimate fate are some mysterious problems for researchers. Cosmology is a subject which describes the universe intellectually upto some extent, still some mysteries are unresolved. This global picture of the universe is supported by the recent advances in modern cosmology on both observational as well as theoretical grounds. In this chapter we will explain the DE and its candidates, especially we emphasize on scalar-tensor theories. We will also explain some cosmological notations and basic concepts.

2.1 Cosmic Expansion and Some Recent Problems of Dark Energy

Herschelian picture of Milky way was the first effort to understand the galactic structure [116], which describes that our galaxy is like a disk upon which all the stars are distributed with the Sun at its center. This picture remains acceptable for astronomers till 19th century. In 1912, Harlow Shapely argued that the Sun is not located at the galactic center rather it lies far away from it. In 1915, Einstein also attempted to formulate a mathematical model of cosmos that would be compatible with the expansion. Edwin Hubble was the first person who reported the cosmic expansion in 1929, which is a cornerstone for cosmology. The expanding behavior of cosmos was affirmed by the examination of spectral lines coming from the galaxies that turned out to be red shifted.

The first effort was made in (1912-1925) by an American astronomer Slipher who analyzed more than twenty extragalactic objects for the spectra shifts. Furthermore, Hubble strengthened this expanding picture of cosmos in 1929 by extending those observations to the other galaxies. He concluded that with time transition, the distance between extragalactic objects is increasing continuously. On the basis of well-known Friedman relationship, Hubble presented an amazing law dubbed as Hubble law according to which there is a proportional relationship between the recessional velocity v and the distance between the Earth and the galaxy D , i.e., $v = HD$, where the proportionality constant is taken as Hubble parameter H . This law arose a lot of enthusiasm among the cosmologists in subsequent decades.

An interesting question that always arises is about the formation of our cosmos: how our

universe came into existence? A possible satisfactory answer to this question is given by the phenomenon of big-bang explosion. It is argued that the accelerated cosmic expansion is the reason to make the form of our cosmos less dense day by day. Thus the existence of bigbang point (an extremely dense and hot form that is small enough like a point) can be ensured by assuming this expanding phenomenon of cosmos as a reversible process.

2.2 Dark Energy

In cosmology, DE is mysterious type of energy which is supposed to fill all of the space, tending to accelerate the cosmic expansion. The DE is a mysterious force which is responsible for driving the galaxies away from each other against the force of gravity. The evidence of DE has not been detected directly. It appeared as the anti-gravity force whose properties are still unknown. The identification of DE appears as a major source in this cosmos which started a new era of theoretical physics and urged astrophysicists to launch new probes for detection of its properties. Significant number of attempts have been made to explain this issue, however the nature of DE is still an open question. Recently, Planck satellite data [5] shows that only 4.9% of the universe consists of visible matter; the DM makes up 26.8% whereas “DE” exists in 68.3% of the universe. Most part of the universe is made up of DE.

2.2.1 The Cosmological Constant

Einstein obtained a static and finite cosmological solution using the cosmological constant Λ in his dynamical equations [9]. According to him, the universe is positively curved and attractive gravity is balanced by repulsive gravity of Λ . After the discovery of expansion of the universe, the cosmological constant was neglected. The energy linked with the vacuum, i.e., cosmological constant having EoS $\omega = -1$ is the simplest form of DE. Vacuum energy is opposite to that matter, matter slows down the expansion and finally stops while vacuum energy shows expansion speedily.

Linde presented a model in 1983, for the expansion of the universe known as chaotic inflationary model. He also proposed that there is no phase transition and cooling. Accord-

ing to quantum theory, the spacetime is filled with quantum fluctuations. In spectrometric theory, the infinitely large positive and negative energies of the ground states are canceled out between particles of different spin. In some regions, quantum fluctuations would have large values that's why all energies would not be canceled. The vacuum energy of those regions would behave like cosmological constant and hence would expand in an inflationary manner due to the repulsive gravitational effect of vacuum energy [116, 117].

2.2.2 Quintessence

To avoid the extreme fine tuning, Wetterich [118], Caldwell [119], Ratra and Peebles [120] introduced the quintessence which is needed to adjust cosmological constant at recent epochs. Quintessence is represented by a scalar field whose evolution depends on its potential. In accelerating universe, the dynamical scalar field explain the role of DE. Taking constant energy density ρ , pressure p and EoS $\omega = -1$, the cosmological constant is assigned to vacuum energy, whereas quintessence is an inhomogeneous field with varying time have EoS $-1 < \omega < -1/3$ [118]-[122]. In future evolution of the universe, dark energy dominates the cosmic acceleration in case of quintessence. As the value of ω increases, dominance of quintessence field will also increase.

2.2.3 Phantom

It is the hypothetical form of DE having EoS $\omega < -1$. If we consider the expansion of the universe we can get the clear idea about the difference between DE with $\omega < -1$ and $\omega > -1$. The dominated energy condition [123] is violated for phantom energy [124] that might result in the existence of wormholes. For phantom energy, the energy density grows speedily and goes to infinity in finite time. The gravitational repulsion is increased by phantom energy which will destroy the galaxies and then any bound system including elementary particles [124, 125]. In a finite time the expansion factor of the universe dominated by phantom energy will diverge to future singularity (Big Rip) [125, 126], which is also stated as cosmic doomsday when all the objects, from galaxies to nucleons, will be ripped apart. According to Baushev [127], phantom energy is not enough to produce Big Rip because ω does not seem to be constant throughout the evolution of the universe.

2.2.4 Quintom

As the name indicates, this DE model is a unification of both the quintessence and phantom models of scalar field yielding the crossing of cosmological constant barrier from one of the both sides. The effects of cosmic age and SNe Ia limits were considered by Feng et al. [128] taking the variations of EoS parameter ω . They found that the variations of amplitude on the EoS parameter can be lowered by age limits. The transition of ω from quintessence ($\omega > -1$) epoch to phantom ($\omega < -1$) era is favored by SNe Ia data [1]. The quintom model predicts some interesting features related to the evolution and fate of the universe. In quintom scenario, the universe would avoid the singularities such as Big Bang, Big Rip [129, 130].

2.3 Some Cosmological Measures

Here we will present some important cosmological parameters [131] that are used to measure the cosmic expansion rate.

2.3.1 Scale Factor

Scale factor is a dimensionless time-dependent positive function which is used to parameterize the expansion of the universe and determine its size (the distance between galaxies). It is also called expansion factor or cosmological radius. It is used as a spatial component of the metric which describes the universe models.

2.3.2 Hubble Parameter

It is used to measure the cosmic expansion rate and is stated as the quotient of the expansion factor with its first-order time rate, i.e., $H = \frac{\dot{a}}{a}$. The current value of Hubble parameter can be estimated using the red shift of different galaxies.

2.3.3 Directional and Mean Hubble Parameters

In the case of isotropic expansion, the Hubble parameter H is stated as above but for anisotropic expansion mean Hubble parameter is used. The average of directional Hubble

parameters H_i is known as mean Hubble parameter. With the passage of time if directional Hubble parameters i.e., along x , y and z axes varies then it is defined as

$$H = \frac{1}{3}(\ln V) = (\ln a) = \frac{1}{3}(H_1 + H_2 + H_3), \quad (2.3.1)$$

where $H_i (i = 1, 2, 3)$ is the expansion rate in each particular direction.

2.3.4 Anisotropy Parameter of Expansion

The anisotropy parameter of expansion can be described as

$$\Delta = \frac{1}{3} \sum_{i=1}^3 \left(\frac{H_i - H}{H} \right)^2. \quad (2.3.2)$$

In the case of isotropic cosmic expansion, the anisotropy parameter becomes zero, i.e., $\Delta = 0$.

2.3.5 Deceleration, Jerk and Snap Parameters

These are some geometrical parameters which are known for the explanation of DE models and cosmic expansion. The point is that if we can measure the change in the Hubble parameter then we have important information to explore the nature and fate of cosmos. The deceleration parameter “ q ” describes the change of rate at which the cosmic expansion is slowing as a result of self gravitation. It is defined as the quotient of the time rates of scale factor, i.e., $a(t)$ and can be defined as

$$q = -\frac{a\ddot{a}}{\dot{a}^2},$$

where $a(t)$ denotes scale factor and dot indicates the time derivative. According to the recent observations, expansion rate of the cosmos is currently accelerating, it is due to the effects of DE. This yields negative values for the deceleration parameter.

The sign of q shows whether the cosmic expansion is decelerating or accelerating. The positive sign of q shows the decelerating expansion of the cosmos and negative sign of q indicates the accelerated cosmic expansion. According to the recent observations, q possesses the negative value which ensures the accelerating cosmic expansion. The deceleration parameter stated in terms of Hubble parameter H is as follows

$$q = -\frac{1}{H^2} \frac{\ddot{a}}{a}. \quad (2.3.3)$$

Sahni et al. [132] presented the concept of dimensionless diagnostic pair which are the generalization of usual cosmological parameters H and q depending upon the third-order time rate of expansion factor referred as statefinders. These parameters are given by

$$j = \frac{1}{H^3} \frac{\ddot{a}}{a}, \quad s = \frac{1}{H^4} \frac{\dddot{a}}{a}. \quad (2.3.4)$$

Here, the parameter s can also be represented as a linear combination of parameters r and q i.e., $s = \frac{r-1}{3(q-1/2)}$. The parameter j can also be expressed in terms of second-order time rate of Hubble parameter as $r = \frac{\ddot{H}}{H^3} - 3q - 2$. The most impressive feature of these variables is that these are universal in nature and determine the features of DE without any specified model. These are also known as jerk and snap parameters. The motivation behind these parameters was the fact that it is critical to decide which one DE model is the most effective for the description of cosmos dynamics in the presence of variety of DE proposals.

These parameters help to investigate the correspondence between constructed DE models and standard models of cosmos by plotting trajectories in the $j-s$ plane. Some specific (j, s) pairs correspond to standard models of DE like $(1, 0)$ represents the constant cosmological constant, $(1, 1)$ corresponds to standard cold dark matter while $(-\infty, \infty)$ shows static Einstein universe. If the $j-s$ trajectories of a DE model are moving away from these standard points, then it may be concluded that the models have distinct features from the standard models of cosmos. Basically, these factors emerge from the Taylors series expansion of $a(t)$ about the present time t_0 given by

$$a(t) = a_0 \left[1 + H_0(t-t_0) - \frac{1}{2}q_0H_0^2(t-t_0)^2 + \frac{1}{6}j_0H_0^3(t-t_0)^3 + \dots \right],$$

where H_0 , q_0 and j_0 denote the present day values of corresponding parameters respectively.

2.4 The Expansion and Shear Scalar

A congruence in an open region of space-time is a class of curves such that through each point of the domain one curve of this family passes [133]. The generation of congruences by null, spacelike and timelike curves are known as null, spacelike and timelike congruences. Considering the congruence of timelike geodesics and associated timelike vector

field u^a (timelike vector connects two events that are causally connected, that is the second event is in the light cone of the first event). The timelike curves are also known as world-lines or field lines [134].

The measure of fractional rate of change of volume per unit time is called expansion scalar and is defined as [133]

$$\Theta = u^a_{;a} = u^a_{,a} + \Gamma^a_{ab} u^b. \quad (2.4.1)$$

The congruence is divergent (geodesic flying apart) if $\Theta > 0$, that shows the expanding universe and $\Theta < 0$ gives convergent congruence (geodesics coming closer) and shows the decelerating behavior of the universe. The measure of distortion in timelike curves is called shear tensor and the volume remains constant. It presents the feasibility of distortion to ellipsoidal shape from initial sphere. This is defined as

$$\sigma_{cd} = \Theta_{cd} - \frac{1}{3}\Theta h_{cd} = u_{(c;d)} + \dot{u}_{(c}u_{d)} - \frac{1}{3}\Theta h_{cd}. \quad (2.4.2)$$

The indices of shear tensor are symmetric. The shear scalar σ is defined as

$$\sigma^2 = \frac{1}{2}\sigma_{cd}\sigma^{cd}. \quad (2.4.3)$$

2.5 The Energy Momentum Tensor

The EMT is a symmetric tensor having rank two and is denoted by $T^{\alpha\beta}$, which represents the flux and density of energy and momentum in space-time. This tensor plays the role of gravitational field in field equations of GR, as the mass density plays similar role in Newtonian gravity. In case of vacuum, its value is zero. For an arbitrary manifold it takes the form as

$$T^{\alpha\beta} = \rho u^\alpha u^\beta + \sigma^{ij} \delta_i^\alpha \delta_j^\beta, \quad (2.5.1)$$

where u^α is the 4-velocity vector, ρ is the matter density and σ^{ij} is the stress density defined by

$$\sigma^{ij} = \frac{dF^i}{dS_j}, \quad (i, j = 1, 2, 3) \quad (2.5.2)$$

where dF^i denotes the force acting on dS_j , the area element. The components of $T^{\alpha\beta}$ have the following meaning:

- T^{00} component represents the energy density of matter and is represented by ρ .
- T^{i0} components represent the energy flux.
- T^{0i} components denote the momentum flux.
- T^{ij} components represents the stress tensor that is pressure.

Now, we discuss the energy-momentum tensor for perfect fluid.

2.5.1 Isotropic Fluid

A fluid having no heat conduction and viscosity is called perfect fluid and defined in terms of ρ and p . For perfect fluid, the stress energy tensor with signature $(+, -, -, -)$ can be described as

$$T_{\alpha\beta} = (\rho + p)u_\alpha u_\beta - pg_{\alpha\beta}. \quad (2.5.3)$$

If we use the signature $(-, +, +, +)$ then it is stated as

$$T_{\alpha\beta} = (\rho + p)u_\alpha u_\beta + pg_{\alpha\beta}. \quad (2.5.4)$$

In case of dust, we have $p = 0$ and EMT reduced to

$$T_{\alpha\beta} = \rho u_\alpha u_\beta. \quad (2.5.5)$$

In co-moving frame i.e., $(u^\alpha = (1, 0, 0, 0))$, the trace of $T_{\alpha\beta}$ for signature $(+, -, -, -)$ is

$$T = \rho - 3p. \quad (2.5.6)$$

2.5.2 Anisotropic Fluid

For perfect fluid or isotropic fluid, pressure remains constant in every direction but in case of anisotropic fluid, pressure varies in spatial directions. It can be stated that anisotropic fluid is the simplest generalization of the perfect fluid in which we vary pressure on each axis separately. For an anisotropic fluid, the EMT with signature $(+, -, -, -)$ is defined as follows

$$T_{\alpha\beta} = (\rho + p_t)V_\alpha V_\beta - p_r g_{\alpha\beta} + (p_r - p_t)X_\alpha X_\beta, \quad (2.5.7)$$

where ρ , p_r and p_t indicate the energy density, directional pressures of the fluid, respectively, measured in the orthogonal direction of the unit space-like vector in the radial vector $X_\alpha = \frac{1}{\sqrt{-g_{11}}} \delta_1^\alpha$. Additionally, $V_\alpha = \frac{1}{\sqrt{g_{00}}} \delta_0^\alpha$ is the 4-velocity which satisfies the conditions $X^\alpha X_\alpha = -1$, $V^\alpha V_\alpha = 1$ and also $X^\alpha V_\alpha = 0$.

2.5.3 Barotropic fluid

In fluid dynamics, barotropic fluid is defined as the fluid whose density is a function of pressure only. It is stated as

$$\rho = \rho(p). \quad (2.5.8)$$

In our work, we apply an EoS parameter involving energy density and radial pressure, i.e., $\omega = p/\rho$. EoS is a dimensionless parameter, not necessarily constant. The quintessence yields dynamical EoS describing the relationship between the state variables like fluid energy density and pressure.

2.5.4 Equation of State

The EoS in cosmology is described by dimensionless number ω as, $\omega = p/\rho$ where ρ , p are notions of matter density and pressure. If we evaluate the EoS by considering the universe isotropic, homogeneous, and taking the FLRW space-time at the background, then EoS for ω_{DE} is exactly equal to -1 in Λ CDM model whereas in quintessence model it is dynamical quantity, and $-1 < \omega_{DE} < -1/3$. Moreover ω_{DE} varies with time and $\omega_{DE} < -1$ in phantom model.

2.6 The Einstein Field Equations

Einstein formulated the equations which relate the geometry and matter of the spacetime known as the EFEs and given by

$$G_{\alpha\beta} = R_{\alpha\beta} - \frac{1}{2} R g_{\alpha\beta} = \kappa T_{\alpha\beta}, \quad (2.6.1)$$

where R , $g_{\alpha\beta}$, $G_{\alpha\beta}$, $R_{\alpha\beta}$, $T_{\alpha\beta}$ and κ denote the Ricci scalar, the metric tensor, Einstein tensor, Ricci tensor, the EMT and coupling constant respectively. The EFEs show the

relation of energy and matter, how they are related to the curvature of spacetime. These can also be written as

$$R_{\alpha\beta} = 8\pi(T_{\alpha\beta} - \frac{1}{2}Tg_{\alpha\beta}). \quad (2.6.2)$$

The metric tensor $g_{\alpha\beta}$ in GR and the scalar potential ϕ in Newtonian theory of gravitation play the same role. In weak field approximation (Newtonian limit), the EFEs are reduced to the Poisson's equations. These are the second order coupled non-linear system of differential equations for the metric components [135].

To determine the metric tensor $g_{\alpha\beta}$, these equations can be solved if EMT ' $T_{\alpha\beta}$ ' is given. Until the $g_{\alpha\beta}$ is unknown we cannot explain the EMT $T_{\alpha\beta}$ physically. If the components of metric are known, we can find the Einstein tensor and also EMT. In most of the cases, the $T_{\alpha\beta}$ is found to be non-physical and even it violates the energy bounds. Thus we should solve these EFEs simultaneously for matter distribution and spacetime metric. In case of vacuum these equations are solved by taking $T_{\alpha\beta} = 0$. These equations satisfy the principle of conservation of energy and momentum, i.e. $T_{;\beta}^{\alpha\beta} = 0$ for matter distribution which gives information about the behavior of the matter [135].

2.7 Modified Theories of Gravity

To interpret the behavior of DE, modified theories of gravity are introduced by adding an extra degree of freedom that may be vector, scalar or tensor field. There is a class of DE models in which role of gravity is played by different parameters. Some famous theories are $f(R)$ gravity, $f(R, T)$ gravity, $f(\tau)$ gravity, Gauss-Bonnet theory and its generalizations, $f(R, G)$ gravity with Ricci scalar R , trace of EMT T , torsion scalar τ and Gauss-Bonnet invariant term G and scalar-tensor gravity accommodating both scalar and tensor fields.

In this chapter, we shall discuss only the modified approach of scalar-tensor gravity in detail.

2.8 Scalar-Tensor Gravity

For the modification of GR, one of oldest approach is scalar-tensor gravity in which the simplest field of nature, i.e., scalar field is included [20]. This gravitational proposal is

very old even before the elegant publication of Einstein. In 1912, Nordström presented the first idea and introduced the conformally flat scalar-tensor gravity [136]. Dirac presented a new idea in 1937, regarding dynamical Newton gravitational coupling [137]. He drew his conclusion after analyzing the quotients of various cosmological as well as fundamental constants used in physics and argued that one of these constants in such ratios should vary over the time scales in cosmology. In 1959, Jordan presented a gravitational proposal with varying Newton's coupling of gravity on the basis of Dirac's idea. Another important idea was given by Ernst Mach (1893) which states that inertia is a property of matter as well as of the background provided by rest of the universe.

Later on, Brans and Dicke (1961) attempted to formulate a new scalar-tensor gravity by accommodating both the Dirac's hypothesis and the well-known Mach's principle. This was named as BD gravity and is considered as the most strong competent of GR. In scalar-tensor gravity, the reciprocal of the scalar-field plays the role of Newton's gravitational coupling. The action proposed by Brans-Dicke is given by [20]

$$S = \int dx^4 \sqrt{-g} \left[\phi R - \frac{\omega_0}{\phi} \phi_{;\alpha} \phi^{;\alpha} + \mathcal{L}_m \right], \quad \alpha = 0, 1, 2, 3, \quad (2.8.1)$$

where ω_0 is the BD coupling parameter, \mathcal{L}_m is the matter part of the Lagrangian and ϕ is the scalar field. Varying this action with respect to both metric tensor and scalar field one can find the following set of field equations

$$G_{\alpha\beta} = \frac{\omega_0}{\phi^2} \left[\phi_{;\alpha} \phi_{;\beta} - \frac{1}{2} g_{\alpha\beta} \phi_{;\alpha} \phi^{;\alpha} \right] + \frac{1}{\phi} [\phi_{;\alpha;\beta} - g_{\alpha\beta} \square \phi] + \frac{T_{\alpha\beta}}{\phi}, \quad (2.8.2)$$

$$\square \phi = \frac{T}{3 + 2\omega_0}. \quad (2.8.3)$$

The notations $T_{\alpha\beta}$, T , Δ^α and \square are used for the EMT, its trace, covariant derivative and box or d'Alembertian operator ($\square = \Delta^\alpha \Delta_\alpha$), respectively.

Eq.(2.8.3) is the Klein-Gordon equation for this framework. Choosing scalar field as a constant and asymptotically large BD coupling parameter ($\omega_0 \rightarrow \infty$), GR can be recovered. However, it does not seem true for exact solutions. For non-vanishing trace of EMT this limit recovers GR. Scalar-tensor gravity have correspondence with other modified theories for different values of ω_0 ; we can get $f(R)$ gravity, Palatini metric and string theory with low energy by replacing $\omega_0 = 0$, $\omega_0 = -3/2$ and $\omega_0 = -1$, respectively.

The generalization of the action (2.8.1) can be discussed by taking the scalar field and geometry coupling by a general function $f(\phi)$ and the BD constant by a dynamical coupling $\omega(\phi)$ and also including scalar field potential. It can be written as

$$S = \int d^4x \sqrt{-g} \left[f(\phi) R - \frac{\omega(\phi)}{\phi} \phi_{;\alpha} \phi^{;\alpha} - U(\phi) + \mathcal{L}_m \right]. \quad (2.8.4)$$

This theory is known as generalized scalar-tensor gravity.

2.9 $f(R, \phi)$ gravity

The $f(R, \phi)$ theory with scalar potential is given by

$$S_m = \int d^4x \sqrt{-g} \left[\frac{1}{\kappa^2} (f(R, \phi) + \omega(\phi) \phi_{;\alpha} \phi^{;\alpha}) + V(\phi) \right], \quad (2.9.1)$$

where f is a function of R and ϕ , $V(\phi)$ denotes the scalar field potential and $\omega(\phi)$ denotes the coupling function.

Varying the action (2.9.1) with respect to metric we have field equations of the form

$$f_R R_{\alpha\beta} - \frac{1}{2} (f + \omega(\phi) \phi_{;\alpha} \phi^{;\alpha}) g_{\alpha\beta} - f_{R;\alpha\beta} + g_{\alpha\beta} \square f_R + \omega(\phi) \phi_{;\alpha} \phi_{;\beta} = \kappa^2 T_{\alpha\beta}, \quad (2.9.2)$$

$$2\omega(\phi) \square \phi + \omega_\phi(\phi) \phi_{;\alpha} \phi^{;\alpha} - f_\phi + V_\phi(\phi) = 0, \quad (2.9.3)$$

where $\square = g^{\alpha\beta} \nabla_\alpha \nabla_\beta$ and $\kappa^2 \equiv 8\pi G$.

2.10 $f(R, R_{\mu\nu} R^{\mu\nu}, \phi)$ gravity

In generalized scalar tensor theories, the $f(R, R_{\mu\nu} R^{\mu\nu}, \phi)$ gravity have very interesting prospects. The action of $f(R, R_{\mu\nu} R^{\mu\nu}, \phi)$ theory is [138],

$$S_m = \int d^4x \sqrt{-g} \left[\frac{1}{\kappa^2} (f(R, R_{\mu\nu} R^{\mu\nu}, \phi) + \omega(\phi) \phi_{;\alpha} \phi^{;\alpha}) + \mathcal{L}_m \right], \quad (2.10.1)$$

where the unspecified function f is depending on R , ϕ and $R_{\alpha\beta} R^{\alpha\beta} \equiv Y$.

One can find the field equations corresponding to (2.10.1) of the form

$$\begin{aligned} f_R R_{\mu\nu} - \frac{1}{2} (f + \omega(\phi) \phi_{;\alpha} \phi^{;\alpha}) g_{\mu\nu} - f_{R;\mu\nu} + g_{\mu\nu} \square f_R + 2f_Y R_\mu^\alpha R_{\alpha\nu} - 2[f_Y R_{(\mu}^\alpha]_{;\nu)\alpha} \\ + \square[f_Y R_{\mu\nu}] + [f_Y R_{\alpha\beta}]^{;\alpha\beta} g_{\mu\nu} + \omega(\phi) \phi_{;\mu} \phi_{;\nu} = \kappa^2 T_{\mu\nu}, \end{aligned} \quad (2.10.2)$$

$$2\omega(\phi) \square \phi + \omega_\phi(\phi) \phi_{;\alpha} \phi^{;\alpha} - f_\phi = 0, \quad (2.10.3)$$

where $\square = g^{\mu\nu} \nabla_\mu \nabla_\nu$ and $\kappa^2 \equiv 8\pi G$.

2.11 Universe Models

2.11.1 Friedmann-Lemaitre-Robertson-Walker metric (FLRW) Space time

The FLRW model is compatible with the Copernican principle of cosmology having specifications spatially homogeneous and isotropic but not necessarily flat. In cosmology it is considered as the most realistic standard model. This model was first time formulated in 1922 by Alexander Friedman. Later on, in 1935 its modification was presented by Howard Percy Robertson and Arthur Geoffrey Walker. The metric of this model in terms of curvature index $k = \{-1, 0, 1\}$ (open, flat and closed, respectively) and expansion factor $a(t)$ can be written as [131]

$$ds^2 = c^2 dt^2 - a(t)^2 \left[\frac{dr^2}{1 - kr^2} + r^2 d\theta^2 + r^2 \sin^2 \theta d\phi^2 \right]. \quad (2.11.1)$$

- de-Sitter (dS) Universe Models

The dS cosmic solutions seems very useful in explaining the current picture of cosmos. In dS model, the Hubble parameter, scale factor and Ricci tensor are defined as,

$$H = H_0, \quad a(t) = a_0 e^{H_0 t}, \quad R = 12H_0^2. \quad (2.11.2)$$

One of the major characteristic of such model is constant EoS ω , so that

$$\rho = \rho_0 e^{-3(1+\omega)H_0 t}, \quad \omega \neq -1. \quad (2.11.3)$$

- Power Law Solutions

These solutions are very effective to discuss different eras of cosmic evolution. These solutions are very helpful in explaining the all cosmic evolutions such as DE, DM and radiation dominated eras. In this case, the scale factor, Hubble parameter and Ricci scalar are defined as [31, 33]

$$a(t) = a_0 t^{n_1}, \quad H(t) = \frac{n_1}{t}, \quad R = 6n_1(1 - 2n_1)t^{-2}, \quad (2.11.4)$$

where $n_1 > 0$. If $0 < n_1 < 1$, we have decelerated universe which leads to the dust dominated era ($n_1 = \frac{2}{3}$) or radiation dominated ($n_1 = \frac{1}{2}$) while $n_1 > 1$ leads to the accelerating picture of the universe.

2.11.2 Bianchi Models

Homogeneity refers to the similar pictures to observers at different locations of the cosmos whereas isotropy implies the results independent of directions. The FLRW models are spatially homogeneous, but these models are in a very limited subclass of cosmic candidates due to their property of isotropy. Bianchi models are homogeneous and anisotropic. There have been a large number of papers to investigate the Bianchi models, finding the exact solution of the field equations and explaining the dynamical behavior of the models. The BI model points to the generalization of flat FLRW models which confirms the distinct expansion factors. BI model is given by

$$ds^2 = dt^2 - A^2(t)dx^2 - B^2(t)dy^2 - C^2(t)dz^2, \quad (2.11.5)$$

where $A(t)$, $B(t)$ and $C(t)$ are the scale factors, x is transverse direction and y, z are equivalent longitudinal directions. The average expansion scale factor is $a = (ABC)^{\frac{1}{3}}$. The volume V , for the above BI spacetime, is $V = a^3 = ABC$.

For LRS BI model we set $C = B$ so that metric of the form

$$ds^2 = dt^2 - A^2(t)dx^2 - B^2(t)(dy^2 + dz^2), \quad (2.11.6)$$

Here, the average expansion scale factor is $a = (AB^2)^{\frac{1}{3}}$ and volume V is $V = a^3 = AB^2$. Here, we represent the Bianchi type classification in the following table.

Class	A						B				
Type	I	II	VI_0	VII_0	VIII	IX	V	IV	VI_h	III	$VIII_h$
$n^{(1)}$	0	+ve	0	0	-ve	+ve	0	0	0	0	0
$n^{(2)}$	0	0	+ve	+ve	+ve	+ve	0	0	+ve	+ve	+ve
$n^{(3)}$	0	0	-ve	-ve	+ve	+ve	0	+ve	-ve	-ve	+ve
a	0	0	0	0	0	0	+ve	+ve	+ve	$\sqrt{-n^{(2)}n^{(3)}}$	+ve

Table 2.1: Classification of Bianchi Models

These parameters $n^{(i)}$ and a can be set to either ± 1 or zero.

2.12 Energy Conditions

The energy conditions play an important role in GR and also have useful applications in modified theories of gravity. Here, we firstly present the energy conditions in GR and then describe the extended version of these bounds in modified gravitational framework. In GR, energy conditions have four explicit forms named as: the NEC, WEC, SEC and DEC [34] which are obtained using Raychaudhuri equation along with appealing properties of gravity. Assuming u^α and k^α , the tangent vectors to the timelike and null curves of a spacetime manifold, the Raychaudhuri equation yields the temporal evolution of expansion θ for the corresponding timelike curves in terms of the Ricci tensor $\mathcal{R}_{\alpha\beta}$, shear tensor $\sigma^{\alpha\beta}$ and rotation $\omega^{\alpha\beta}$ and is given by

$$\frac{d\theta}{d\tau} = -\frac{\theta^2}{3} - \sigma_{\alpha\beta}\sigma^{\alpha\beta} + \omega_{\alpha\beta}\omega^{\alpha\beta} - \mathcal{R}_{\alpha\beta}u^\alpha u^\beta, \quad (2.12.1)$$

$$\frac{d\theta}{d\tau} = -\frac{\theta^2}{3} - \sigma_{\alpha\beta}\sigma^{\alpha\beta} + \omega_{\alpha\beta}\omega^{\alpha\beta} - \mathcal{R}_{\alpha\beta}k^\alpha k^\beta. \quad (2.12.2)$$

Since the attractive property of gravity implies $\frac{d\theta}{d\tau} < 0$ indicating the geodesics become closer to each other and hence corresponds to converging congruence of geodesics. It further imposes,

$$\mathcal{R}_{\alpha\beta}u^\alpha u^\beta \geq 0, \text{ and } \mathcal{R}_{\alpha\beta}k^\alpha k^\beta \geq 0. \quad (2.12.3)$$

for time-like and null vectors, respectively. We obtain the energy conditions by replacing Ricci tensor $\mathcal{R}_{\alpha\beta}$ with the EMT $T_{\alpha\beta}$ of perfect fluid. We get the following forms of the point-wise energy conditions.

2.12.1 Null Energy Condition (NEC):

For any null vector k^α the relation for NEC is given by $T_{\alpha\beta}k^\alpha k^\beta \geq 0$. In terms of $T_{\alpha\beta}$ (2.5.7) it implies, $\rho + p_i \geq 0 \quad \forall i$. In modified gravitational framework, assuming that the total matter contents act like a perfect fluid, these constraints can be determined by replacing p with p_{eff} and ρ with ρ_{eff}

$$\rho_{(eff)} + p_{i(eff)} \geq 0 \quad \forall i. \quad (2.12.4)$$

2.12.2 Weak Energy Condition (WEC):

For any timelike vector u^α , WEC is represented as $T_{\alpha\beta}u^\alpha u^\beta \geq 0$. Physically, $T_{\alpha\beta}u^\alpha u^\beta$ represents matter density which is evaluated by any observer in timelike position having four-velocity u^α . In case of generalized theories we can write

$$\rho_{(eff)} \geq 0 \quad \text{and} \quad \rho_{(eff)} + p_{i(eff)} \geq 0 \quad \forall i. \quad (2.12.5)$$

2.12.3 Strong Energy Condition (SEC):

In case of u^α the timelike vector, we have the inequality, $\left(T_{\alpha\beta} - \frac{T}{2}g_{\alpha\beta}\right)u^\alpha u^\beta \geq 0$. For perfect fluid it takes the form as $\rho + p_i \geq 0, \rho + \sum p_i \geq 0 \quad \forall i$, which can be generalized as

$$\rho_{(eff)} + p_{i(eff)} \geq 0 \quad \text{and} \quad \rho_{(eff)} + \sum p_{i(eff)} \geq 0 \quad \forall i. \quad (2.12.6)$$

The SEC holds the NEC but it is not necessary that it holds WEC too.

2.12.4 Dominant Energy Condition (DEC):

DEC is given by $T_{\alpha\beta}u^\alpha u^\beta \geq 0$, where $T_{\alpha\beta}u^\alpha$ is not spacelike. For $T_{\alpha\beta}$ (2.5.7), we have the conditions, $\rho \geq 0, \rho \pm p_i \geq 0 \quad \forall i$, for effective components it takes the form

$$\rho_{(eff)} \geq 0 \quad \text{and} \quad \rho_{(eff)} \pm p_{i(eff)} \geq 0 \quad \forall i. \quad (2.12.7)$$

DEC reduces to WEC and hence the NEC.

2.13 Black Hole Thermodynamics

The relation between black hole (BH) mechanism and laws of thermodynamics is known as BH thermodynamics. To setup the BH thermodynamics one can generalize the law of BH dynamics depending on their counterparts in classical theory. BHs satisfy specific mathematical laws which correspond to classical laws. Classically, BHs appear as perfect absorbers but do not radiate, however, these objects do not emit particles beyond the horizon. In fact, this theory helped us to formulate a coherent relation between thermodynamics and gravity.

2.13.1 Generalized Second Law of Thermodynamics (GSLT)

Here, we discuss some theoretical parameters which helped to formulate GSLT. Classically theory argues that total entropy of the entire cosmos can never decrease, however the presence of BHs can create some issues. In the presence of BH we have to concentrate on its surroundings (matter and radiations outside it). Matter falls into a singularity as BH accretes, then it is not easy for external observer to get the complete information beyond the horizon. As a result, entropy of external contents of BHs decreases which cannot be recovered through any means. In [139], Bekenstein introduced a relation of BH entropy in terms of the horizon area. A new generalized entropy was proposed as a combination of BH entropy (S_{BH}) and entropy associated to radiation and matter outside. Thus the SLT was replaced by GSLT, i.e. the total entropy can never decrease $dS = d(S_{BH} + S_m) \geq 0$ [140].

Hawking presented a theorem about BHs which states that the surface area of a BH can never be decreased i.e., $dA \geq 0$. It can be seen that due to the presence of BH, quantum effects and area theorem, the GSLT is violated. Initially, Bekenstein presented GSLT without considering the possibility of this decrease in area. Bekenstein also stated that increase in horizon area compensates the loss of matter outside the BH. The condition of validity for area theorem is violated by quantum effects, that can be stated as “BH evaporation is accompanied by a rise in entropy in the surroundings space through the emitted thermal radiations”. Thus the GSLT can be stated as the total cosmic entropy including BH entropy cannot be decreased, i.e. $dS = d(S_{ext} + S) > 0$ and S_{ext} denotes the cosmic entropy excluding BH.

2.14 Wormhole geometries

The existence of spacetimes having non-trivial topological structure makes GR more fascinating. Misner and Wheeler [68] named such solutions of the field equations as wormhole solutions. The following equation gives the line element for static and spherically symmetric wormhole spacetime, established by Morris and Thorne [69]

$$ds^2 = e^{a(r)} dt^2 - e^{b(r)} dr^2 - r^2(d\theta^2 + \sin^2\theta d\phi^2), \quad (2.14.1)$$

where,

$$e^{-b(r)} = 1 - \frac{\beta(r)}{r}.$$

Redshift function $a(r)$ determines the gravitational redshift of very light particle (photon) and $\beta(r)$ represent the shape of the wormhole. So, they must have some characteristics for wormhole geometry [72]. These properties as function of radial coordinate r are discussed bellow.

- The behavior of r is non-monotonic as it decreases from ∞ to minimum value r_0 which represents the location of wormhole throat, i.e., $\beta(r_0) = r_0$ then it increases back from r_0 to ∞ .
- The proper radial distance, $\mathcal{L}(r)$ should be finite throughout the space. Nevertheless, we can have the following real and regular integral outside the throat,

$$\mathcal{L}(r) = \pm \int_{r_0}^r \left(1 - \frac{\beta(r)}{r}\right)^{-1/2} dr, \quad r \geq r_0.$$

The signs \pm are associated with the configuration of two portions joined together by the wormhole.

- In order to have geometries and proper shape of wormhole at the throat which flares outward, the following condition is imposed,

$$\frac{\beta(r) - r\beta'(r)}{\beta^2(r)} > 0.$$

The above inequality is accountable for the violation of NEC in GR. If the throat radius is denoted by r_0 , then this condition implies $\beta(r_0) = r_0$ while $\beta'(r_0) \leq 1$.

- For the proper length, the function should be finite and well defined everywhere. So, it is required that:

$$1 - \frac{\beta(r)}{r} \geq 0.$$

- For two way travel through wormhole and keeping the throat open, requirement is that there are no horizons present, i.e. $e^{a(r)} \rightarrow 0$. The magnitude of $a(r)$ should be limited (finite) everywhere. For this purpose, we may take constant redshift function i.e., $a'(r) = 0$.

We notice that the schwarzschild wormhole depends on the mass of wormhole, but the Morris-Thorne wormhole is a particular case that does not depend on its mass. For arbitrary choices of shape function and as well as of redshift function there exist various solutions that satisfy the above conditions.

2.15 Inflation

In cosmology, inflation represents the early time expansion of the universe. Inflationary theory was developed in 1981 by Alan Guth and Sato [107, 141], who explain the thermalization of the universe and resolved the issues associated with the initial conditions on Friedmann cosmos. Inflation states that our universe goes under the superluminal expansion in early times. Inflation describes why our universe is homogeneous, flat and so large. The field moves gradually at the end of inflation through a minimum of the potential and reheating happens for the creation of particle. In the scenario of “warm inflation” the reheating is not necessary, only radiation arises at the end of inflation.

Many models have been proposed which can produce the deceleration, expansion and early time cosmic acceleration. One interesting approach to derive inflation is the use of modified theories of gravity. A model is compatible for inflation if for Friedmann universe spectral index and tensor to scalar ratio can be derived at the origin of the cosmological fluctuations.

For inflation, the necessary condition in terms of comoving Hubble length $\frac{H^{-1}}{a}$ is stated as

$$\text{Inflation} \Leftrightarrow \frac{d}{dt} \left(\frac{H^{-1}}{a} \right) < 0.$$

In the context of GR, the condition for inflation is given by

$$\text{Inflation} \Leftrightarrow \rho + 3p < 0.$$

The energy density ρ is taken as positive, so in this case p should be negative to fulfill this condition.

In inflationary models, the scalar potential has scalar field having slow evolution [142, 143]. Sometimes, exact solution exists but in detail it can be studied numerically or by

using approximation scheme, the approximation mostly used is “slow-roll approximation” [139, 144, 145]. ρ and p associated with the scalar field are defined as [21]

$$\rho = \frac{\dot{\phi}^2}{2} + V(\phi), \quad p = \frac{\dot{\phi}^2}{2} - V(\phi).$$

Depending on different choices of $V(\phi)$ there are various inflationary models. Using above expressions in continuity and Friedmann equations we find equations of motions of the form

$$\ddot{\phi} - 3H\dot{\phi} + \frac{dV}{d\phi} = 0, \quad H^2 - \frac{1}{3} \left(V(\phi) + \frac{\dot{\phi}^2}{2} \right) = 0.$$

For inflation, the ρ and p meet the condition $\dot{\phi}^2 \ll V(\phi)$. Using this approximation we have equations of the form

$$H^2 \simeq \frac{V(\phi)}{3}, \quad 3H\dot{\phi} \simeq -\frac{dV}{d\phi},$$

where dot indicates the derivative with respect to time and \simeq shows that for slow-roll approximation the quantities are equal.

Validity of slow-roll approximation is a sufficient condition for inflation but not necessary. To show this, one can express the condition for inflation as

$$\frac{\ddot{a}}{a} = \dot{H} + H^2 > 0,$$

which will be valid if $\dot{H} > 0$ or $-\frac{\dot{H}}{H^2} < 1$. The standard slow-roll parameters are

$$\epsilon_1 = -\frac{\dot{H}}{H^2} \ll 1, \quad \epsilon_2 = \frac{\ddot{\phi}}{H\dot{\phi}} \ll 1, \quad \epsilon_3 = \frac{\dot{F}}{2HF} \ll 1, \quad \epsilon_4 = \frac{\dot{E}}{2HE} \ll 1.$$

The inflation is guaranteed if $\epsilon \ll 1$. These parameters tell about the inflation, it might occur for a certain potential e.g., $V(\phi) = \frac{m^2\phi^2}{2}$. For this potential, one can find the validity of above conditions subject to $\phi^2 > 2$.

Chapter 3

Cosmological reconstruction, energy bounds and Thermodynamics in

$f(R, R_{\alpha\beta}R^{\alpha\beta}, \phi)$ **gravity**

3.1 Cosmological reconstruction and energy bounds in $f(R, R_{\alpha\beta}R^{\alpha\beta}, \phi)$ gravity

3.1.1 Field Equations of $f(R, R_{\alpha\beta}R^{\alpha\beta}, \phi)$ gravity

We are considering the FRW space time with $a(t)$ as

$$ds^2 = dt^2 - a^2(t)dx^2 - a^2(t)dy^2 - a^2(t)dz^2. \quad (3.1.1)$$

The gravitational field equations (2.10.2) corresponding to perfect fluid (2.5.3) as matter content, are given by

$$\begin{aligned} \kappa^2 \rho &= -3(H^2 + \dot{H})f_R + 3H\partial_t f_R + \frac{1}{2}(\omega(\phi)\dot{\phi}^2 - f) - 6H(2H + \dot{H})\partial_t f_Y + (24\dot{H}^2 \\ &+ 114\dot{H}H^2 + 42H^4)f_Y, \end{aligned} \quad (3.1.2)$$

$$\begin{aligned} \kappa^2 p &= -\partial_{tt} f_R - 2H\partial_t f_R + \frac{1}{2}(f + \omega(\phi)\dot{\phi}^2) + (\dot{H} + 3H^2)f_R + 4H(3H^2 + \dot{H})\partial_t f_Y + (6H^2 \\ &+ 4\dot{H})\partial_{tt} f_Y + (4\ddot{H} + 20\dot{H}H + 10\ddot{H}H^2 + 16\dot{H}^2 - 18H^4)f_Y. \end{aligned} \quad (3.1.3)$$

The field equation (2.10.2) can be rearranged in the following form

$$G_{\mu\nu} = R_{\mu\nu} - \frac{1}{2}Rg_{\mu\nu} = T_{\mu\nu}^{eff}, \quad (3.1.4)$$

that is similar to the standard field equations in GR and $T_{\mu\nu}^{eff}$ in $f(R, Y, \phi)$ gravity is defined as

$$\begin{aligned} T_{\mu\nu}^{eff} &= \frac{1}{f_R} \left[\kappa^2 T_{\mu\nu} + \frac{1}{2}(f + \omega(\phi)\phi_{;\alpha}\phi^{;\alpha} - Rf_R)g_{\mu\nu} + f_{R;\mu\nu} - g_{\mu\nu}\square f_R - 2f_Y R_{\mu}^{\alpha} R_{\alpha\mu} \right. \\ &+ \left. 2[f_Y R_{(\mu}^{\alpha}{}_{;\nu)\alpha} - \square[f_Y R_{\mu\nu}] - [f_Y R_{\alpha\beta}]^{;\alpha\beta} g_{\mu\nu} - \omega(\phi)\phi_{;\mu}\phi_{;\nu} \right]. \end{aligned}$$

The effective energy density and pressure can be defined in the form

$$\begin{aligned} \rho_{eff} &= \frac{1}{f_R} \left[\kappa^2 \rho - \frac{1}{2}(\omega(\phi)\dot{\phi}^2 - f) + 3\left(\frac{\dot{a}^2}{a^2} + \frac{\ddot{a}}{a}\right)f_R - 3\frac{\dot{a}}{a}\partial_t f_R + 6\left(\frac{\dot{a}^3}{a^3} + 2\frac{\dot{a}\ddot{a}}{a^2}\right)\partial_t f_Y \right. \\ &+ \left. \left(24\frac{\ddot{a}^2}{a^2} - 66\frac{\dot{a}^2\ddot{a}}{a^3} + 48\frac{\ddot{a}^4}{a^4}\right)f_Y \right], \end{aligned} \quad (3.1.5)$$

and

$$\begin{aligned} p_{eff} &= \frac{1}{f_R} \left[\kappa^2 p - \frac{1}{2}(f + \omega(\phi)\dot{\phi}^2) - 3\left(\frac{\ddot{a}}{a} + \frac{\dot{a}^2}{a^2}\right)f_R + 2\frac{\dot{a}}{a}\partial_t f_R + \partial_{tt} f_R - 2\left(\frac{\ddot{a}}{a} + 2\frac{\dot{a}^2}{a^2}\right) \right. \\ &\times \left. \partial_{tt} f_Y - 4\left(\frac{\dot{a}\ddot{a}}{a^2} + 2\frac{\dot{a}^3}{a^3}\right)\partial_t f_Y - \left(4\frac{\ddot{a}^3}{a} + 4\frac{\dot{a}\ddot{a}^2}{a^2} - 34\frac{\dot{a}^2\ddot{a}}{a^3} - 4\frac{\ddot{a}^2}{a^2} - 4\frac{\dot{a}^4}{a^4}\right)f_Y \right]. \end{aligned} \quad (3.1.6)$$

3.1.2 Reconstruction of $f(R, Y, \phi)$ gravity

Now, we are presenting the reconstruction of $f(R, Y, \phi)$ gravity by applying dS and power law cosmologies which are established cosmological solutions.

- de-Sitter $f(R, Y, \phi)$ Model

Here we are using [146]

$$\omega(\phi) = \omega_0 \phi^\zeta, \quad \phi(t) \sim a(t)^{\beta_1}. \quad (3.1.7)$$

Using these quantities along with Eqs.(2.11.2) and (2.11.3) in Eq.(3.1.2), we obtain

$$\begin{aligned} & 3H_0^2 \beta_1 \phi f_{R\phi} - 18H_0^4 \beta_1 \phi f_{Y\phi} - 3H_0^2 f_R + 42H_0^4 f_Y - \frac{1}{2} f(R, Y, \phi) + \frac{1}{2} \beta_1^2 \omega_0 H_0^2 \phi^{\zeta+2} \\ & - \kappa^2 \rho_0 a_0^{3(1+w)} \phi^{-\frac{3}{\beta_1}} = 0, \end{aligned} \quad (3.1.8)$$

which is a partial differential equation of second order that is converted into canonical form and solving we have solution of the form

$$f(R, Y, \phi) = \alpha_1 \alpha_2 \alpha_3 e^{\alpha_1 R} e^{\alpha_2 Y} \phi^{\gamma_1} + \gamma_2 \phi^{\gamma_3} + \gamma_4 \phi^{\gamma_5}, \quad (3.1.9)$$

where α_i/s are constants of integration and

$$\begin{aligned} \gamma_1 &= \frac{18\beta_1 \alpha_1 H_0^2 - 108\beta_1 \alpha_2 H_0^4 - 5 + 6\alpha_1 H_0^2 - 84\alpha_2 H_0^4}{6(H_0^2 \alpha_1 \beta_1 - 6\beta_1 \alpha_2 H_0^4)} \\ \gamma_2 &= \omega_0 \beta_1^2 H_0^2, \quad \gamma_3 = \zeta + 2, \quad \gamma_4 = -2\kappa^2 \rho_0 a_0^{3(1+w)}, \quad \gamma_5 = -\frac{3}{\beta_1}. \end{aligned} \quad (3.1.10)$$

- de-Sitter model independent of Y

Here we are taking function $f(R, \phi)$ and inserting Eq.(3.1.7) along with Eqs.(2.11.2) and (2.11.3) in Eq. (3.1.2) we obtain

$$3H_0^2 \beta_1 \phi f_{R\phi} - 3H_0^2 f_R - \frac{1}{2} f(R, \phi) + \frac{1}{2} \omega_0 \beta_1^2 H_0^2 \phi^{\zeta+2} - \kappa^2 \rho_0 a_0^{3(1+w)} \phi^{-\frac{3}{\beta_1}} = 0. \quad (3.1.11)$$

Solving the above equation, we have solution of the form

$$f(R, \phi) = \alpha_1 \alpha_2 e^{\alpha_1 R} \phi^{\gamma_1} + \gamma_2 \phi^{\gamma_3} + \gamma_4 \phi^{\gamma_5}, \quad (3.1.12)$$

where α_i/s are constants of integration and

$$\begin{aligned} \gamma_1 &= -\frac{1}{\beta_1} \left(1 + \frac{1}{6H_0^2 \alpha_1} \right), \quad \gamma_2 = \omega_0 \beta_1^2 H_0^2, \\ \gamma_3 &= \zeta + 2, \quad \gamma_4 = -2\kappa^2 \rho_0 a_0^{3(1+w)}, \quad \gamma_5 = -\frac{3}{\beta_1}. \end{aligned} \quad (3.1.13)$$

- **de-Sitter model independent of R**

Now we are taking function $f(Y, \phi)$ and inserting Eq.(3.1.7) along with Eqs.(2.11.2) and (2.11.3) in Eq.(3.1.2) we get

$$18H_0^4\beta_1\phi f_{Y\phi} - 42H_0^4f_Y + \frac{1}{2}f(Y, \phi) - \frac{1}{2}\omega_0\beta_1^2H_0^2\phi^{\zeta+2} - \kappa^2\rho_0a_0^{3(1+w)}\phi^{-\frac{3}{\beta_1}} = 0, \quad (3.1.14)$$

whose solution yields

$$f(Y, \phi) = \alpha_1\alpha_2e^{\alpha_1Y}\phi^{\gamma_1} + \gamma_2\phi^{\gamma_3} + \gamma_4\phi^{\gamma_5}, \quad (3.1.15)$$

where α_i 's are constants of integration and

$$\begin{aligned} \gamma_1 &= -\frac{7}{3\beta_1} + \frac{1}{36H_0^4\alpha_1\beta_1}, \quad \gamma_2 = \omega_0\beta_1^2H_0^2, \\ \gamma_3 &= \zeta + 2, \quad \gamma_4 = -2\kappa^2\rho_0a_0^{3(1+w)}, \quad \gamma_5 = -\frac{3}{\beta_1}. \end{aligned} \quad (3.1.16)$$

- **Power Law Solution independent of R**

Here, we are taking $f(Y, \phi)$ function, using Eqs.(2.11.3), (3.1.7) and (2.11.4) in Eq.(3.1.2) we obtain

$$\begin{aligned} &\frac{2(3n_1-2)}{4n_1^2-3n_1+1}Y^2f_{YY} - \frac{n_1(3n_1-2)}{2(4n_1^2-3n_1+1)}\phi Y f_{Y\phi} + \frac{7n_1^2-19n_1+4}{2(4n_1^2-3n_1+1)}Y f_Y - \frac{1}{2}f \\ &- \kappa^2\rho_0\phi^{-\frac{3}{\beta_1}}a_0^{3(1+w)} + \frac{1}{2}\omega_0\beta_1^2n_1^2a_0^{\frac{2}{n_1}}\phi^{\zeta+2-\frac{2}{n_1\beta_1}} = 0, \end{aligned} \quad (3.1.17)$$

solving it we have the following $f(Y, \phi)$ model

$$f(Y, \phi) = \alpha_1\alpha_2\phi^{\gamma_1}Y^{\gamma_2} + \gamma_3\phi^{\gamma_4} + \gamma_5\phi^{\gamma_6}, \quad (3.1.18)$$

where α_i 's are constants of integration and

$$\begin{aligned} \gamma_1 &= \frac{2(3n_1-2)\alpha_1}{4n_1^2-3n_1+1} + \frac{7n_1^2-31n_1+12}{n_1(3n_1-2)} - \frac{2(4n_1^2-3n_1+1)^2}{n_1^2(3n_1-2)^2\alpha_1}, \\ \gamma_2 &= \frac{n_1(3n_1-2)\alpha_1}{2(4n_1^2-3n_1+1)}, \quad \gamma_3 = -\omega_0\beta_1^2n_1^2a_0^{\frac{2}{n_1}}, \quad \gamma_4 = \zeta + 2 - \frac{2}{n_1\beta_1}, \\ \gamma_5 &= -2\kappa^2\rho_0a_0^{3(1+w)}, \quad \gamma_6 = -\frac{3}{\beta_1}. \end{aligned} \quad (3.1.19)$$

• **Power Law Solution independent of Y**

Now we are taking function $f(R, \phi)$, using Eq.(2.11.3) along with Eqs.(3.1.7) and (2.11.4) in Eq.(3.1.2) yields

$$\begin{aligned} & \frac{1}{3n_1-1} R^2 f_{RR} + \frac{n_1-1}{2(3n_1-1)} R f_R - \frac{n_1 \beta_1}{2(3n_1-1)} \phi R f_{R\phi} - \kappa^2 \rho_0 a_0^{3(1+w)} \phi^{-\frac{3}{\beta_1}} - \frac{1}{2} f \\ & + \frac{1}{2} \omega_0 \beta_1^2 n_1^2 a_0^{\frac{2}{n_1}} \phi^{\zeta+2-\frac{2}{n_1 \beta_1}} = 0. \end{aligned} \quad (3.1.20)$$

Solving this we have,

$$f(R, \phi) = \alpha_1 \alpha_2 \phi^{\gamma_1} R^{\gamma_2} + \gamma_3 \phi^{\gamma_4} + \gamma_5 \phi^{\gamma_6}, \quad (3.1.21)$$

where α_i 's are constants of integration and

$$\begin{aligned} \gamma_1 &= \frac{\alpha_1}{3n_1-1} + \frac{n_1-3}{n_1 \beta_1} - \frac{2(3n_1-1)^2}{n_1^2 \beta_1^2 \alpha_1}, \quad \gamma_2 = \frac{n_1(n_1-3) \beta_1 \alpha_1}{(3n_1-1)^2}, \\ \gamma_3 &= \omega_0 \beta_1^2 n_1^2 a_0^{\frac{2}{n_1}}, \quad \gamma_4 = \zeta + 2 - \frac{2}{n_1 \beta_1}, \quad \gamma_5 = -2 \kappa^2 \rho_0 a_0^{3(1+w)}, \quad \gamma_6 = -\frac{3}{\beta_1}. \end{aligned} \quad (3.1.22)$$

3.1.3 Energy Conditions

The energy conditions (2.12.4)-(2.12.7) for scalar tensor fourth order gravity are:

$$\begin{aligned} \text{NEC: } \rho_{eff} + p_{eff} &= \frac{1}{f_R} \left[\kappa^2 (\rho + p) - \omega(\phi) \dot{\phi}^2 + \partial_t f_R - H \partial_t f_R - 2(2\dot{H} + 3H^2) \partial_t f_Y \right. \\ & \left. + (8\dot{H}H + 6H^3) \partial_t f_Y - (4\ddot{H} + 20H\ddot{H} + 28\dot{H}H^2 + 40\dot{H}^2) f_Y \right], \end{aligned} \quad (3.1.23)$$

$$\begin{aligned} \text{WEC: } \rho_{eff} &= \frac{1}{f_R} \left[\kappa^2 \rho + \frac{1}{2} (f - \omega(\phi) \dot{\phi}^2 - R f_R) - 3H \partial_t f_R + 6H (2\dot{H} + 3H^2) \partial_t f_Y \right. \\ & \left. - f_Y (18\dot{H}H^2 + 24\dot{H}^2 + 18H^4) \right], \end{aligned} \quad (3.1.24)$$

$$\begin{aligned} \text{SEC: } \rho_{eff} + 3p_{eff} &= \frac{1}{f_R} \left[\kappa^2 (\rho + 3p) - 2\omega(\phi) \dot{\phi}^2 - f + R f_R + 3H \partial_t f_R + 3\partial_t f_R \right. \\ & \left. - 6(2\dot{H} + 3H^2) \partial_t f_Y - 18H^3 \partial_t f_Y - (12\ddot{H} + 60\dot{H}H + 48\dot{H}H^2 + 72\dot{H}^2 - 36H^4) f_Y \right], \end{aligned} \quad (3.1.25)$$

$$\begin{aligned} \text{DEC: } \rho_{eff} - p_{eff} &= \frac{1}{f_R} \left[\kappa^2 (\rho - p) + f - R f_R - \partial_t f_R - 5H \partial_t f_R + 2(2\dot{H} + 3H^2) \right. \\ & \left. \times \partial_t f_Y + (16\dot{H}H + 30H^3) \partial_t f_Y + (4\ddot{H} + 20H\ddot{H} - 8\dot{H}H^2 - 8\dot{H}^2 - 36H^4) f_Y \right]. \end{aligned} \quad (3.1.26)$$

Inequalities (3.1.23)-(3.1.26) represent the NEC, WEC, SEC and DEC of $f(R, Y, \phi)$ gravity with FRW spacetime.

In terms of deceleration, jerk and snap parameters [147, 148], the Ricci scalar and its derivatives can be written as

$$R = 6H^2(q-1), \quad \dot{R} = 6H^3(q-j+2), \quad \ddot{R} = 6H^4(s+q^2+8q+6), \quad (3.1.27)$$

where q, j, s are defined in (2.3.3), (2.3.4) and using these parameters, Hubble parameter and its time derivatives can be expressed as [46, 47]

$$H = \frac{\dot{a}}{a}, \quad \dot{H} = -H^2(q+1), \quad \ddot{H} = (3q+j+2)H^3, \quad \dddot{H} = H^4(s-6-4j-12q-3q^2). \quad (3.1.28)$$

Using the above definitions, the energy conditions (3.1.23)-(3.1.26) can be rewritten as

$$\begin{aligned} \text{NEC: } & -\omega(\phi)\dot{\phi}^2\kappa^2(\rho+p) - 6H^4\{s-j+(q+8)(q+1)\}f_{RR} + \{\ddot{Y} - H\dot{Y} + 12H^6 \\ & \times \{s(1-2q) + j(4q+1) + (1+q)(4-2q^2-17q)\}\}f_{RY} - f_{R\phi}(H\dot{\phi} - \ddot{\phi}) - 2H^2 \\ & \times (H\dot{Y} + \ddot{Y}) - 2qf_{YY}(\ddot{Y} - 2H\dot{Y}) - 2H^2f_{Y\phi}\{(H\dot{\phi} + \ddot{\phi}) + 2q(2H\dot{\phi} - \ddot{\phi})\} + 36H^6 \\ & \times (j-2-q)^2f_{RRR} - 12H^3(j-2-q)\{6H^5(j-2-q)(1-2q) + \dot{Y}\}f_{RRY} - 12\dot{\phi}H^3 \\ & \times (j-2-q)f_{RR\phi} + \dot{Y}f_{RYY}\{\dot{Y} + 24H^5(j-q-2)(1-2q)\} + \dot{\phi}^2f_{R\phi\phi} + 2\dot{\phi}\{\dot{Y} \\ & + 12H^5(j-q-2)(1-2q)\}f_{RY\phi} + \dot{Y}(\dot{Y}f_{YYY} + \dot{\phi}f_{YY\phi}) + \dot{\phi}(\dot{\phi}f_{Y\phi\phi} + \dot{Y}f_{YY\phi}) - 4H^4 \\ & \times (s+j+7q^2+16q+7)f_Y \geq 0, \end{aligned} \quad (3.1.29)$$

$$\begin{aligned} \text{WEC: } & \kappa^2\rho + \frac{1}{2}(f - \omega(\phi)\dot{\phi}^2) - \frac{1}{2}Rf_R + 18H^4(j-q-2)\{f_{RR} - 2H^2(1-2q)f_{RY}\} \\ & - 3H(\dot{Y}f_{RY} + \dot{\phi}f_{R\phi}) + 6H^3(1-2q)(\dot{Y}f_{YY} + \dot{\phi}f_{Y\phi}) - 6H^4(4q^2+5q+4)f_Y \geq 0, \end{aligned} \quad (3.1.30)$$

$$\begin{aligned} \text{SEC: } & \kappa^2(\rho+3p) - f - 2\omega(\phi)\dot{\phi}^2 + Rf_R - 6H^4(2s+2j-6q^2+14q) + 17f_Y - 18H^4 \\ & \times (s+q^2+j+4+7q)f_{RR} + 3\{\ddot{Y} + H\dot{Y} + 12H^6(s+8q+q^2+6)(1-2q) + 36H^6 \\ & \times (j-2-q)\}f_{RY} + 3(\ddot{\phi} + H\dot{\phi})f_{R\phi} - 6H^2f_{YY}\{3\dot{Y}H + \ddot{Y}(1-2q)\} - 6H^2\{\ddot{\phi}(1-2q) \\ & + 3\dot{\phi}H\}f_{Y\phi} + 108H^6f_{RRR}(j-q-2)^2 - 36H^3(j-2-q)\{6H^5(j-q-2)(1-2q) \\ & + \dot{Y}\}f_{RRY} - 36H^3(j-q-2)\{\dot{Y} + 6H^5(1-2q)(j-q-2)\}f_{RRY} - 36H^3\dot{\phi} \end{aligned}$$

$$\begin{aligned}
& \times (j-2-q)f_{RR\phi} + 3\{24H^5(1-2q)(j-q-2)\dot{Y} + \dot{Y}^2\}f_{RYY} + 3\dot{\phi}^2 f_{R\phi\phi} + 6\{\dot{\phi}\dot{Y} \\
& + 12H^5\dot{\phi}(1-2q)(j-q-2)\}f_{RY\phi} - 6H^2\dot{\phi}(1-2q)(\dot{\phi}f_{Y\phi\phi} + \dot{Y}f_{YY}) - 6H^2\dot{Y}(1-2q) \\
& (\dot{\phi}f_{YY\phi} + \dot{Y}f_{YYY}) \geq 0,
\end{aligned} \tag{3.1.31}$$

$$\begin{aligned}
\textbf{DEC: } & \kappa^2(\rho - p) + f - Rf_R - (\ddot{R} + 5H\dot{R})f_{RR} - \{\ddot{Y} + 5H\dot{Y} - 2H^2\ddot{R}(1-2q) - 2\dot{R}H^3 \\
& \times (7-8q)\}f_{RY} - (5H\dot{\phi} + \ddot{\phi})f_{R\phi} - \dot{R}^2 f_{RRR} - 2\dot{R}(\dot{Y} - \dot{R}H^2(1-2q))f_{RRY} - 2\dot{\phi}\dot{R} \\
& \times f_{RR\phi} + (4H^2(1-2q)\dot{R} - \dot{Y})\dot{Y}f_{RYY} - \dot{\phi}^2 f_{R\phi\phi} + 2\dot{\phi}\{2H^2\dot{R}(1-2q) - \dot{Y}\}f_{RY\phi} \\
& - 2H^2\dot{Y}(2q-1)(\dot{\phi}f_{YY\phi} + \dot{Y}f_{YYY}) - 2H^2\dot{\phi}(2q-1)(\dot{\phi}f_{Y\phi\phi} + \dot{Y}f_{YY\phi}) + H^2\{2\ddot{Y} \\
& \times (1-2q) + 2\dot{Y}H(7-8q)\}f_{YY} - 2H^2\{(2q-1)\ddot{\phi} + H\dot{\phi}(8q-7)\} + 4H^4(j+s \\
& - 5q^2 - 5 - q)f_Y \geq 0.
\end{aligned} \tag{3.1.32}$$

3.1.4 Energy Conditions of de-Sitter models and their Viability Ranges

- de-Sitter $f(R, Y, \phi)$ model

Introducing model (3.1.9) in the energy conditions (3.1.23)-(3.1.26), it follows

$$\begin{aligned}
\textbf{NEC: } & \kappa^2 p + \kappa^2 \rho_0 e^{-3H_0(1+w)t} - \omega_0 \beta_1^2 H_0^2 a_0^{\beta_1(\zeta+2)} e^{\beta_1(\zeta+2)H_0 t} + \beta_1(\beta_1 \gamma_1 - 1)\alpha_1 \alpha_2 \alpha_3 \\
& \times \gamma_1 H_0^2 (\alpha_1 - 6\alpha_2 H_0^2) a_0^{\beta_1 \gamma_1} e^{\beta_1 \gamma_1 H_0 t + 12\alpha_1 H_0^2 + 36\alpha_2 H_0^4} + \beta_1^2 \alpha_1 \alpha_2 \alpha_3 \gamma_1 H_0^2 a_0^{\beta_1 \gamma_1} (\gamma_1 - 1) \\
& \times (\alpha_1 - 6\alpha_2 H_0^2) e^{\beta_1 \gamma_1 H_0 t + 12\alpha_1 H_0^2 + 36\alpha_2 H_0^4} \geq 0,
\end{aligned} \tag{3.1.33}$$

$$\begin{aligned}
\textbf{WEC: } & \kappa^2 \rho_0 e^{-3H_0(1+w)t} + \frac{1}{2} \alpha_1 \alpha_2 \alpha_3 a_0^{\beta_1 \gamma_1} e^{\beta_1 \gamma_1 H_0 t + 12\alpha_1 H_0^2 + 36\alpha_2 H_0^4} (1 - 12\alpha_1 H_0^2 - 36\alpha_2 \\
& \times H_0^4) + \gamma_2 a_0^{\beta_1 \gamma_3} e^{\beta_1 \gamma_3 H_0 t} + \gamma_4 a_0^{\beta_1 \gamma_5} e^{\beta_1 \gamma_5 H_0 t} - \frac{1}{2} \omega_0 \beta_1^2 H_0^2 a_0^{\beta_1(\zeta+2)} e^{\beta_1(\zeta+2)H_0 t} - 3\beta_1 \alpha_1 \alpha_2 \\
& \alpha_3 \gamma_1 H_0^2 (\alpha_1 - 6\alpha_2 H_0^2) a_0^{\beta_1 \gamma_1} e^{\beta_1 \gamma_1 H_0 t + 12\alpha_1 H_0^2 + 36\alpha_2 H_0^4} \geq 0,
\end{aligned} \tag{3.1.34}$$

$$\begin{aligned}
\textbf{SEC: } & \kappa^2 \rho_0 e^{-3H_0(1+w)t} + 3\kappa^2 p + \alpha_1 \alpha_2 \alpha_3 a_0^{\beta_1 \gamma_1} e^{\beta_1 \gamma_1 H_0 t + 12\alpha_1 H_0^2 + 36\alpha_2 H_0^4} (36\alpha_2 H_0^4 - 1 \\
& + 12\alpha_1 H_0^2) - \gamma_2 a_0^{\beta_1 \gamma_3} e^{\beta_1 \gamma_3 H_0 t} - \gamma_4 a_0^{\beta_1 \gamma_5} e^{\beta_1 \gamma_5 H_0 t} - 2\omega_0 \beta_1^2 H_0^2 a_0^{\beta_1(\zeta+2)} e^{\beta_1(\zeta+2)H_0 t} + 3\beta_1 \\
& \times (1 + \beta_1) \alpha_1 \alpha_2 \alpha_3 \gamma_1 H_0^2 (\alpha_1 - 6\alpha_2 H_0^2) e^{\beta_1 \gamma_1 H_0 t + 12\alpha_1 H_0^2 + 36\alpha_2 H_0^4} a_0^{\beta_1 \gamma_1} + 3\beta_1^2 \alpha_1 \alpha_2 \alpha_3 \gamma_1 \\
& \times (\gamma_1 - 1) H_0^2 (\alpha_1 - 6\alpha_2 H_0^2) a_0^{\beta_1 \gamma_1} e^{\beta_1 \gamma_1 H_0 t + 12\alpha_1 H_0^2 + 36\alpha_2 H_0^4} \geq 0,
\end{aligned}$$

$$\begin{aligned}
\text{DEC: } & \kappa^2 \rho_0 e^{-3H_0(1+w)t} - \kappa^2 p + \alpha_1 \alpha_2 \alpha_3 a_0^{\beta_1 \gamma_1} e^{\beta_1 \gamma_1 H_0 t + 12\alpha_1 H_0^2 + 36\alpha_2 H_0^4} (1 - 12\alpha_1 H_0^2 \\
& - 36\alpha_2 H_0^4) + \gamma_2 a_0^{\beta_1 \gamma_3} e^{\beta_1 \gamma_3 H_0 t} + \gamma_4 a_0^{\beta_1 \gamma_5} e^{\beta_1 \gamma_5 H_0 t} + \beta_1 (\beta_1 + 5) \alpha_1 \alpha_2 \alpha_3 \gamma_1 H_0^2 (6\alpha_2 H_0^2 - \alpha_1) \\
& \times a_0^{\beta_1 \gamma_1} e^{\beta_1 \gamma_1 H_0 t + 12\alpha_1 H_0^2 + 36\alpha_2 H_0^4} + \beta_1^2 \alpha_1 \alpha_2 \alpha_3 \gamma_1 (\gamma_1 - 1) H_0^2 (6\alpha_2 H_0^2 - \alpha_1) a_0^{\beta_1 \gamma_1} \\
& \times e^{\beta_1 \gamma_1 H_0 t + 12\alpha_1 H_0^2 + 36\alpha_2 H_0^4} \geq 0.
\end{aligned} \tag{3.1.35}$$

Variations of $\alpha'_i s$	Validity of WEC	Validity of NEC
$\alpha_1 > 0, \alpha_2 > 0$	$\alpha_3 = 0, \forall \beta_1 \text{ \& } \zeta$	$\alpha_3 < 0$ with $\forall \zeta \text{ \& } \beta_1$
	$\alpha_3 > 0, \beta_1 \geq 0, \forall \zeta$	$\alpha_3 = 0$ with $(\zeta \geq 0, \beta_1 \leq -1)$ or $(\zeta \leq -2.8, \beta_1 \geq 2)$
	$\alpha_3 < 0, \beta_1 \leq -1, \forall \zeta$	
$\alpha_1 < 0, \alpha_2 > 0$	$\forall \alpha_3, \zeta \text{ \& } \beta_1 \geq 0$	$\alpha_3 = 0$ with $(\zeta \geq 0, \beta_1 \leq -2)$ or $(\zeta \leq -2.8, \beta_1 \geq 2)$
		$\alpha_3 > 0$ with $\beta_1 > 0$ or $\beta_1 < 0 \vee \zeta$
$\alpha_1 > 0, \alpha_2 < 0$	$\forall \alpha_3, \beta_1, \zeta \text{ \& } t \geq 3.6$	$\forall \alpha_3$ with $(\zeta \geq 0, \beta_1 \leq -1.5)$ or $(\zeta \leq -3, \beta_1 \geq 2.8)$
$\alpha_1 < 0, \alpha_2 < 0$	$\forall \alpha_3, \beta_1, \zeta \text{ \& } t \geq 3.6$	$\forall \alpha_3$ with $(\zeta \geq 0, \beta_1 \leq -1.4)$ or $(\zeta \leq -3.6, \beta_1 \geq 1)$
$\alpha_2 > 0, \alpha_3 > 0$	$\alpha_1 < 0$ with $\beta_1 \leq -1, \forall \zeta$	$\alpha_1 < 0$ with $\beta_1 > 0$ or $\beta_1 < 0 \text{ \& } \forall \zeta$
	$\alpha_1 = 0$ with $t \geq 3.6, \forall \zeta \text{ \& } \beta_1$	$\alpha_1 = 0$ with $(\zeta \leq -3, \beta_1 \geq 2.8)$ or $(\zeta \geq 0, \beta_1 \leq -1)$
	$\alpha_1 > 0$ with $\beta_1 > 0, t \geq 3.6, \forall \zeta$	
$\alpha_2 > 0, \alpha_3 < 0$	$\alpha_1 < 0, \beta_1 > 0, \forall \zeta$	$\alpha_1 = 0$ with $(\zeta \leq -3, \beta_1 \geq 1)$ or $(\zeta \geq -1, \beta_1 \leq -1)$
	$\alpha_1 > 0, \beta_1 \leq -1, \forall \zeta$	$\alpha_1 > 0$ with $\beta_1 < 0$ or $\beta_1 > 0 \text{ \& } \forall \zeta$
	$\alpha_1 = 0, t \geq 3.6, \forall \beta_1 \text{ \& } \zeta$	
$\alpha_2 < 0, \alpha_3 > 0$	$\forall \alpha_1, \beta_1 \text{ \& } \zeta$ with $t \geq 3.6$	$\forall \alpha_1$ with $(\beta_1 \leq -1, \zeta \geq 1)$ or $(\beta_1 \geq 2.8, \zeta \leq -3)$
$\alpha_2 < 0, \alpha_3 < 0$	$\forall \alpha_1, \beta_1 \text{ \& } \zeta$ with $t \geq 3.6$	$\forall \alpha_1$ with $(\beta_1 \leq -1, \zeta \geq 0.8)$ or $(\beta_1 \geq 2.5, \zeta \leq -3.5)$
$\alpha_1 > 0, \alpha_3 > 0$	$\alpha_2 > 0$ with $\beta_1 > 0, \forall \zeta$	$\alpha_2 \leq 0$ with $(\beta_1 \leq -1.5, \zeta \geq 0)$ or $(\beta_1 \geq 2.8, \zeta \leq -3)$
	$\alpha_2 \leq 0$ with $\forall \beta_1, \zeta \text{ \& } t \geq 3.6$	
$\alpha_1 > 0, \alpha_3 < 0$	$\alpha_2 \leq 0$ with $\forall \beta_1, \zeta \text{ \& } t \geq 3.6$	$\forall \alpha_2$ with $(\beta_1 \leq -2, \zeta \geq 0)$ or $(\beta_1 \geq 1, \zeta \leq -3)$
	$\alpha_2 > 0$ with $\beta_1 \leq -0.5 \text{ \& } \forall \zeta$	
$\alpha_1 < 0, \alpha_3 > 0$	$\alpha_2 \leq 0$ with $\forall \beta_1, \zeta \text{ \& } t \geq 3.6$	$\alpha_2 > 0$ with $\forall \beta_1 \text{ \& } \zeta$
	$\alpha_2 > 0$ with $\beta_1 \leq -0.5 \text{ \& } \forall \zeta$	$\alpha_2 \leq 0$ with $(\beta_1 \geq 2.8, \zeta \leq -3)$ or $(\beta_1 \leq -1.4, \zeta \geq 0)$
$\alpha_1 < 0, \alpha_3 < 0$	$\alpha_2 > 0, \beta_1 \geq 0 \text{ \& } \zeta$	$\alpha_2 \leq 0$ with $(\beta_1 \geq 2, \zeta \leq -3.5)$ or $(\beta_1 \leq -1.4, \zeta \geq 0)$
	$\alpha_2 \leq 0$ with $\forall \beta_1, \zeta \text{ \& } t \geq 3.6$	

Table 3.1: Validity regions of WEC and NEC for dS $f(R, Y, \phi)$ model.

The inequalities (3.1.33)-(3.1.35) depend on six parameters $\alpha_1, \alpha_2, \alpha_3, \beta_1, \zeta$ and t . First we will fix two parameters and discuss the validity region taking the feasible ranges of other parameters. We will fix the constants of integration and discuss the NEC and WEC. Here we will use the present day values of fractional energy density, Hubble parameter and cosmographic parameters as $\Omega_{m0} = 0.315, H_0 = 67.3$ [146], $s = -0.22, j = 2.16$,

$q = -0.81$ [31]. The validity ranges of all cases for dS $f(R, Y, \phi)$ model are given in Table 3.1.

First we will vary α_1 and α_2 to show the viability of NEC and WEC for different values of β_1 , α_3 and ζ . Taking both α_1 and α_2 as positive, the WEC is valid for all values of ζ but some particular ranges for β_1 are: $(\alpha_3 > 0, \beta_1 \geq 0)$, $(\alpha_3 = 0, \forall \beta_1)$ and $(\alpha_3 < 0, \beta_1 \leq -1)$. The validity of NEC depends on $\alpha_3 \leq 0$ and the validity regions of α_3 and ζ are $(\alpha_3 < 0, \forall \zeta, \beta_1)$, $(\alpha_3 = 0, \zeta \geq 0, \beta_1 \leq -1)$ and $(\alpha_3 = 0, \zeta \leq -2.8, \beta_1 \geq 2)$. In Fig. 3.1, we have shown the evolution of NEC and WEC to show the validity regions in this case.

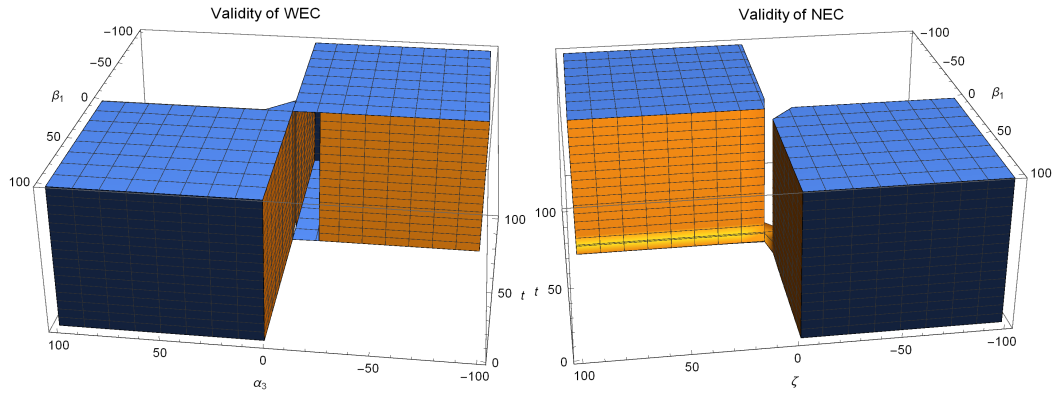


Figure 3.1: Energy conditions for the dS $f(R, Y, \phi)$ model using $\alpha_1 > 0$ & $\alpha_2 > 0$. The left plot shows the feasible regions of WEC where we fix $\zeta = -10$ (any value of ζ can be chosen since WEC is valid for all values of ζ) and the variations of α_3 & β_1 are shown. In right plot viability regions of NEC are shown for $\alpha_3 = 0$.

If $\alpha_1 < 0$ and $\alpha_2 > 0$, for $\beta_1 \geq 0$ WEC is satisfied for all ranges of α_3 & ζ . The validity of NEC is stated in cases: (i) $\alpha_3 > 0$ with all values of ζ and β_1 except $\beta_1 = 0$ (ii) $\alpha_3 = 0$ with $(\zeta \geq 0, \beta_1 \leq -2)$ or $(\zeta \leq -2.8, \beta_1 \geq 2)$. Taking $\alpha_1 > 0$ and $\alpha_2 < 0$, the validity of WEC requires $t > 3.6$ for all values of α_3 , β_1 , ζ and the NEC is valid for all values of α_3 with $(\beta_1 \leq -1.5, \zeta \geq 0)$ or $(\beta_1 \geq 2.8, \zeta \leq -3)$. If $\alpha_1 < 0$ and $\alpha_2 < 0$, the validity of WEC requires $t \geq 3.6$ and for all values of α_3 , β_1 and ζ . The validity of NEC requires $(\beta_1 \leq -1.4, \zeta \geq 0)$ or $(\beta_1 \geq 1, \zeta \leq -3.6)$ and all values of α_3 .

Next we will vary α_2 and α_3 , first we will take $\alpha_2 > 0$ and $\alpha_3 > 0$. For $\alpha_1 < 0$, NEC is satisfied for all values of ζ & β_1 except $\beta_1 = 0$, for $\alpha_1 > 0$ it violates and for $\alpha_1 = 0$, it is valid for $(\zeta \geq 0, \beta_1 \leq -1)$ and $(\zeta \leq -3, \beta_1 \geq 2.8)$. The WEC is valid for all values

of ζ with three cases: (i) $\alpha_1 > 0$ with ($\beta_1 > 0$ & $t \geq 3.6$), (ii) $\alpha_1 < 0$ with $\beta_1 \leq -1$, (iii) $\alpha_1 = 0$ with $\beta_1 \leq -1$. Now we are taking $\alpha_2 > 0$ and $\alpha_3 < 0$, first we will discuss the NEC. For $\alpha_1 < 0$ NEC violates, for $\alpha_1 > 0$ it is valid for all values of ζ & β_1 except $\beta_1 = 0$ and for $\alpha_1 = 0$, its validity depends on ($\beta_1 \geq 1$, $\zeta \leq -3$) and ($\beta_1 \leq -1$, $\zeta \geq -1$). Now we will discuss the validity of WEC. If $\alpha_1 < 0$, WEC is valid for $\beta_1 > 0$ & all values of ζ , for $\alpha_1 > 0$, it is valid for $\beta_1 \leq -1$ & all values of ζ and if $\alpha_1 = 0$, for all values of β_1 & ζ the WEC is valid with $t \geq 3.6$. Taking $\alpha_2 < 0$ & $\alpha_3 > 0$, NEC is valid for all α_1 with ($\beta_1 \leq -1$, $\zeta \geq 1$) or ($\beta_1 \geq 2.8$, $\zeta \leq -3$) while WEC is satisfied for all values of α_1 , β_1 & ζ with $t \geq 3.6$. Next we are taking $\alpha_2 < 0$ and $\alpha_3 < 0$, NEC is valid for ($\beta_1 \leq -1$, $\zeta \geq 0.8$) or ($\beta_1 \geq 2.5$, $\zeta \leq -3.5$) for all α_1 and WEC is satisfied for all values of α_1 , β_1 , and ζ with $t \geq 3.6$.

Now we will vary α_1 and α_3 , first we will take $\alpha_1 > 0$ & $\alpha_3 > 0$. Taking $\alpha_2 > 0$, NEC violates and WEC is valid for all values of ζ & $\beta_1 > 0$. Taking $\alpha_2 \leq 0$, for all values of β_1 WEC is valid for $t \geq 3.6$ & for all values of ζ while NEC is satisfied for ($\beta_1 \leq -1.5$, $\zeta \geq 0$) or ($\beta_1 \geq 2.8$, $\zeta \leq -3$). Choosing $\alpha_1 > 0$ and $\alpha_3 < 0$. The NEC is valid for all values of α_2 with ($\beta_1 \leq -2$, $\zeta \geq 0$) and ($\beta_1 \geq 1$, $\zeta \leq -3$) and for all values of ζ , WEC is valid for $\alpha_2 > 0$ with $\beta_1 \leq -0.5$ and for $\alpha_2 \leq 0$ with $t \geq 3.6$ & for all values of β_1 . Next we are choosing $\alpha_1 < 0$ and $\alpha_3 > 0$. For $\alpha_2 > 0$, NEC is valid for all values of ζ & $\beta_1 \leq -0.5$ while for $\alpha_2 \leq 0$ its validity regions are ($\beta_1 \geq 2.8$, $\zeta \leq -3$) and ($\beta_1 \leq -1.4$, $\zeta \geq 0$). The WEC is valid in both cases for all values of β_1 & ζ while for $\alpha_2 \leq 0$ it requires $t \geq 3.6$. Now we will take $\alpha_1 < 0$ and $\alpha_3 < 0$. For $\alpha_2 > 0$, NEC violates and for $\alpha_2 \leq 0$ the validity regions are ($\beta_1 \geq 2$, $\zeta \leq -3.5$) and ($\beta_1 \leq -1.4$, $\zeta \geq 0$) while WEC is valid for all values of ζ : (i) $\alpha_2 > 0$ with $\beta_1 \geq 0$, (ii) $\alpha_2 \leq 0$ with $t \geq 3.6$ and $\forall \beta_1$.

- de-Sitter $f(R, \phi)$ model

Introducing model (3.1.12) in inequalities (3.1.23)-(3.1.26) it follows,

$$\text{NEC: } \kappa^2 \rho_0 e^{-3H_0(1+w)t} + \kappa^2 p - \omega_0 \beta_1^2 H_0^2 a_0^{\beta_1(\zeta+2)} e^{\beta_1(\zeta+2)H_0 t} + \beta_1(\beta_1 - 1) \alpha_1^2 \alpha_2 \gamma_1 H_0^2 \times a_0^{\beta_1 \gamma_1} e^{\beta_1 \gamma_1 H_0 t + 12\alpha_1 H_0^2} + \beta_1^2 \alpha_1^2 \alpha_2 \gamma_1 (\gamma_1 - 1) H_0^2 a_0^{\beta_1 \gamma_1} e^{\beta_1 \gamma_1 H_0 t + 12\alpha_1 H_0^2} \geq 0, \quad (3.1.36)$$

$$\text{WEC: } \kappa^2 \rho_0 e^{-3H_0(1+w)t} + \frac{1}{2} \alpha_1 \alpha_2 a_0^{\beta_1 \gamma_1} e^{\beta_1 \gamma_1 H_0 t + 18\alpha_1 H_0^2} + \frac{1}{2} \gamma_4 a_0^{\beta_1 \gamma_5} e^{\beta_1 \gamma_5 H_0 t} - 6\alpha_1^2 \alpha_2 H_0^2 \times a_0^{\beta_1 \gamma_1} e^{\beta_1 \gamma_1 H_0 t + 12\alpha_1 H_0^2} - 3\beta_1 \alpha_1^2 \alpha_2 \gamma_1 H_0^2 a_0^{\beta_1 \gamma_1} e^{\beta_1 \gamma_1 H_0 t + 12\alpha_1 H_0^2} \geq 0, \quad (3.1.37)$$

$$\begin{aligned}
\text{SEC: } & \kappa^2 \rho_0 e^{-3H_0(1+w)t} + 3\kappa^2 p - \alpha_1 \alpha_2 a_0^{\beta_1 \gamma_1} e^{\beta_1 \gamma_1 H_0 t + 12\alpha_1 H_0^2} - \gamma_2 a_0^{\beta_1 \gamma_3} e^{\beta_1 \gamma_3 H_0 t} - \gamma_4 a_0^{\beta_1 \gamma_5} \\
& \times e^{\beta_1 \gamma_5 H_0 t} - 2\omega_0 \beta_1^2 H_0^2 a_0^{\beta_1(\zeta+2)} e^{\beta_1(\zeta+2)H_0 t} + 12\alpha_1^2 \alpha_2 H_0^2 a_0^{\beta_1 \gamma_1} e^{\beta_1 \gamma_1 H_0 t + 12\alpha_1 H_0^2} + 3\beta_1 \alpha_1^2 \alpha_2 \\
& \times (1 + \beta_1) \gamma_1 H_0^2 a_0^{\beta_1 \gamma_1} e^{\beta_1 \gamma_1 H_0 t + 12\alpha_1 H_0^2} + 3\beta_1^2 \alpha_1^2 \alpha_2 \gamma_1 (\gamma_1 - 1) H_0^2 a_0^{\beta_1 \gamma_1} e^{\beta_1 \gamma_1 H_0 t + 12\alpha_1 H_0^2} \geq 0,
\end{aligned} \tag{3.1.38}$$

$$\begin{aligned}
\text{DEC: } & \kappa^2 \rho_0 e^{-3H_0(1+w)t} - \kappa^2 p + \alpha_1 \alpha_2 a_0^{\beta_1 \gamma_1} e^{\beta_1 \gamma_1 H_0 t + 12\alpha_1 H_0^2} + \gamma_2 a_0^{\beta_1 \gamma_3} e^{\beta_1 \gamma_3 H_0 t} + \gamma_4 a_0^{\beta_1 \gamma_5} \\
& \times e^{\beta_1 \gamma_5 H_0 t} - 12\alpha_1^2 \alpha_2 H_0^2 a_0^{\beta_1 \gamma_1} e^{\beta_1 \gamma_1 H_0 t + 12\alpha_1 H_0^2} - \beta_1 (\beta_1 + 5) \alpha_1^2 \alpha_2 \gamma_1 H_0^2 a_0^{\beta_1 \gamma_1} e^{\beta_1 \gamma_1 H_0 t + 12\alpha_1 H_0^2} \\
& - \beta_1^2 \alpha_1^2 \alpha_2 \gamma_1 (\gamma_1 - 1) H_0^2 a_0^{\beta_1 \gamma_1} e^{\beta_1 \gamma_1 H_0 t + 12\alpha_1 H_0^2} \geq 0.
\end{aligned} \tag{3.1.39}$$

Now we will discuss the energy bounds for $f(R, \phi)$ dS model, above constraints show that these bounds involve five parameters, α_1 , α_2 , β_1 , ζ and t . It can be noted that WEC involve only α_1 , α_2 and t . We have observed that the validity of WEC stated for two choices of α_1 : (i) $\alpha_1 > 0$ with $\alpha_2 \geq 0$ (ii) $\alpha_1 < 0$ with for all α_2 . Now we will discuss NEC in three cases: first we take $\alpha_1 > 0$ and $\alpha_2 > 0$, the validity regions for NEC are ($\beta_1 < 0$, $\zeta > -2$) and ($\beta_1 > 0$, $\zeta \leq -2$). Choosing $\alpha_1 < 0$ and $\alpha_2 > 0$, NEC is satisfied for ($\beta_1 \geq 3$, $\zeta \leq -5$) & ($\beta_1 \leq -1$, $\zeta \geq 0.8$). Taking $\alpha_1 < 0$, $\alpha_2 < 0$ NEC is valid for ($\beta_1 \geq 3.5$, $\zeta \leq -5$) and ($\beta_1 \leq -1$, $\zeta \geq 1$).

- de-Sitter $f(Y, \phi)$ model

Using model (3.1.15) in constraints (3.1.23)-(3.1.26), it follows

$$\begin{aligned}
\text{NEC: } & \kappa^2 \rho_0 e^{-3H_0(1+w)t} + \kappa^2 p - \omega_0 \beta_1^2 H_0^2 a_0^{\beta_1(\zeta+2)} e^{\beta_1(\zeta+2)H_0 t} - 6\beta_1 (\beta_1 - 1) \alpha_1^2 \alpha_2 H_0^4 \\
& \times \gamma_1 a_0^{\beta_1 \gamma_1} e^{\beta_1 \gamma_1 H_0 t + 36\alpha_1 H_0^4} - 6\beta_1^2 \alpha_1^2 \alpha_2 \gamma_1 (\gamma_1 - 1) H_0^4 a_0^{\beta_1 \gamma_1} e^{\beta_1 \gamma_1 H_0 t + 36\alpha_1 H_0^4} \geq 0,
\end{aligned} \tag{3.1.40}$$

$$\begin{aligned}
\text{WEC: } & \kappa^2 \rho_0 e^{-3H_0(1+w)t} + \frac{1}{2} \alpha_1 \alpha_2 a_0^{\beta_1 \gamma_1} e^{\beta_1 \gamma_1 H_0 t + 36\alpha_1 H_0^4} + \frac{1}{2} \gamma_4 a_0^{\beta_1 \gamma_5} e^{\beta_1 \gamma_5 H_0 t} + 18\alpha_1^2 \alpha_2 \gamma_1 \\
& \times H_0^4 a_0^{\beta_1 \gamma_1} e^{\beta_1 \gamma_1 H_0 t + 36\alpha_1 H_0^4} - 18\alpha_1^2 \alpha_2 H_0^4 a_0^{\beta_1 \gamma_1} e^{\beta_1 \gamma_1 H_0 t + 36\alpha_1 H_0^4} \geq 0,
\end{aligned} \tag{3.1.41}$$

$$\begin{aligned}
\text{SEC: } & \kappa^2 \rho_0 e^{-3H_0(1+w)t} + 3\kappa^2 p - \alpha_1 \alpha_2 a_0^{\beta_1 \gamma_1} e^{\beta_1 \gamma_1 H_0 t + 36\alpha_1 H_0^4} - \gamma_2 a_0^{\beta_1 \gamma_3} e^{\beta_1 \gamma_3 H_0 t} - \gamma_4 a_0^{\beta_1 \gamma_5} \\
& \times e^{\beta_1 \gamma_5 H_0 t} - 2\omega_0 \beta_1^2 H_0^2 a_0^{\beta_1(\zeta+2)} e^{\beta_1(\zeta+2)H_0 t} - 18\beta_1 (1 + \beta_1) \alpha_1^2 \alpha_2 \gamma_1 H_0^4 e^{\beta_1 \gamma_1 H_0 t + 36\alpha_1 H_0^4} \\
& \times a_0^{\beta_1 \gamma_1} - 18\beta_1^2 \alpha_1^2 \alpha_2 \gamma_1 (\gamma_1 - 1) H_0^4 a_0^{\beta_1 \gamma_1} e^{\beta_1 \gamma_1 H_0 t + 36\alpha_1 H_0^4} + 36\alpha_1^2 \alpha_2 H_0^4 e^{\beta_1 \gamma_1 H_0 t + 36\alpha_1 H_0^4} \\
& \times a_0^{\beta_1 \gamma_1} \geq 0,
\end{aligned} \tag{3.1.42}$$

$$\begin{aligned}
\text{DEC: } & \kappa^2 \rho_0 e^{-3H_0(1+w)t} - \kappa^2 p + \alpha_1 \alpha_2 a_0^{\beta_1 \gamma_1} e^{\beta_1 \gamma_1 H_0 t + 36 \alpha_1 H_0^4} + \gamma_2 a_0^{\beta_1 \gamma_3} e^{\beta_1 \gamma_3 H_0 t} + \gamma_4 a_0^{\beta_1 \gamma_5} \\
& \times e^{\beta_1 \gamma_5 H_0 t} + 6\beta_1(\beta_1 + 5)\alpha_1^2 \alpha_2 \gamma_1 H_0^4 a_0^{\beta_1 \gamma_1} e^{\beta_1 \gamma_1 H_0 t + 36 \alpha_1 H_0^4} + 6\beta_1^2 \alpha_1^2 \alpha_2 \gamma_1 (\gamma_1 - 1) H_0^4 a_0^{\beta_1 \gamma_1} \\
& \times e^{\beta_1 \gamma_1 H_0 t + 36 \alpha_1 H_0^4} - 36\alpha_1^2 \alpha_2 H_0^4 a_0^{\beta_1 \gamma_1} e^{\beta_1 \gamma_1 H_0 t + 36 \alpha_1 H_0^4} \geq 0.
\end{aligned} \tag{3.1.43}$$

Here, the dependence of WEC is only on t , α_1 & α_2 . The validity of WEC holds only for $\alpha_2 \leq 0$ and for all values of α_1 . Varying α_1 and α_2 we will discuss the ranges for which NEC holds. If we choose $\alpha_1 > 0$ & $\alpha_2 > 0$ then NEC violates although in all remaining cases, $(\alpha_1 < 0, \alpha_2 > 0)$, $(\alpha_1 > 0, \alpha_2 < 0)$ and $(\alpha_1 < 0, \alpha_2 < 0)$ NEC is valid for all values of ζ and β_1 except $\beta_1 = 0$.

3.1.5 Energy Conditions of Power Law models and their validity ranges

- Power Law $f(Y, \phi)$ model

Introducing (3.1.18) in the energy constraints (3.1.23)-(3.1.26), it can be seen that the inequalities involve six parameters t , α_1 , α_2 , β_1 , ζ and n_1 . We are discussing here only NEC and WEC by fixing n_1 and α_i 's where $i = 1, 2$ for different values of β_1 and ζ . We start with $\alpha_1 > 0$ and $\alpha_2 > 0$, the validity of WEC requires $n_1 > 1$, $t \geq 1.1$, $\beta_1 \leq -0.1$ & $\zeta \geq 0$ while NEC is valid for $n_1 > 1$, $\beta_1 \geq 0$ and all values of ζ . Now taking $\alpha_1 < 0$ and $\alpha_2 > 0$, the validity of WEC requires $1 < n_1 \leq 1.8$ with $\zeta \geq 0$, $\beta_1 \leq -3$ and $n_1 \geq 2.3$ with $\beta_1 \geq 2$ & $\zeta \leq -1$. Similarly, the validity of NEC requires $t \geq 1.01$, $n_1 > 1$, $\beta_1 \leq -0.12$ and all values of ζ . Now taking $\alpha_1 > 0$ and $\alpha_2 < 0$, NEC requires $t \geq 1.07$, $n_1 > 1$, $\beta_1 \geq 0$ and all values of ζ for the validity while WEC requires $n_1 \geq 1.7$ with $\beta_1 \geq 0.1$ & $\zeta \leq -10$. For $\alpha_1 < 0$ and $\alpha_2 < 0$, WEC has two validity regions $1 < n_1 \leq 1.9$ with $(t > 1, \beta_1 > 0$ and $\zeta \leq -6.5)$ and $n_1 \geq 2$ with $(\beta_1 \leq 0$ & $\zeta \geq 4)$ while NEC also have two validity regions (i) $1 < n_1 \leq 1.5$ with $(t \geq 1.9, \beta_1 \geq 0$ & $\zeta \leq -2.6)$, (ii) $n_1 \geq 2$ with $(t \geq 1.05, \beta_1 < 0$ & $\zeta \geq 0)$ and $(t \geq 1.08, \beta_1 \geq 0$ & $\zeta \leq -4)$.

- Power Law $f(R, \phi)$ model

Inserting (3.1.21) in the energy conditions (3.1.23)-(3.1.26) we can calculate the energy bounds for $f(R, \phi)$ model. Now we will discuss the viability of NEC and WEC taking different values of β_1 , ζ , t and some specific values of n_1 , α_i 's where $i = 1, 2$. Taking

$\alpha_1 > 0$ and $\alpha_2 > 0$, WEC is viable for $n_1 = 3$ with $\beta_1 \neq 0$ and for all values of ζ while the validity of NEC requires $n_1 = 3$ with $t \geq 1.03$, $\beta_1 \leq -2$ and $\zeta \geq 0$. For $\alpha_1 < 0$ and $\alpha_2 > 0$, the validity of NEC requires $n_1 > 1$ with $t \geq 1.05$, $\beta_1 > 1$ and $\zeta \leq -5$ while in case of WEC, we have two validity regions for $n_1 = 3$: ($\zeta \geq 0$, $\beta_1 \geq 2.6$, $t \geq 0.65$) and ($\zeta \leq -2$, $\beta_1 \geq 22.5$). Now taking $\alpha_1 > 0$ and $\alpha_2 < 0$, the validity of NEC is satisfied for $n_1 = 3$, all values of ζ and β_1 except $\beta_1 = 0$ while in case of WEC we have $n_1 = 3$ with ($\beta_1 \geq 2.7$, $\zeta \geq 0$ & $t \geq 0.65$) and ($\beta_1 \leq -2$, $\zeta \leq -5.5$ & $t \geq 0.65$). Taking $\alpha_1 < 0$ and $\alpha_2 < 0$, NEC and WEC both are valid for $n_1 = 3$, $\beta_1 \neq 0$ and for all values of ζ .

3.1.6 Energy Conditions for Some known Models

Now we will show that using energy bounds how limits can be applied on $f(R, Y, \phi)$ gravity. For this purpose, we are taking some familiar models given below.

- $f(R, \phi)$ Models

Here, we are taking $f(R, Y, \phi)$ gravity models independent of Y represented as $f(R, \phi)$ gravity. We will find the energy conditions for these models

$$\left. \begin{aligned} f(R, \phi) &= \frac{R - 2\Lambda(1 - e^{b_1\phi\kappa^3 R})}{\kappa^2}, \\ f(R, \phi) &= R \left(\frac{\omega_0 \beta_1^2 n_1^2 a_0^{2/n_1} (\zeta n_1 \beta_1 + 2n_1 \beta_1 + 6n_1 - 2)}{\zeta n_1 \beta_1 + 2n_1 \beta_1 - 2} \right) \phi^{\zeta + 2 - \frac{2}{n_1 \beta_1}}, \\ f(R, \phi) &= R(1 + \xi \kappa^2 \phi^2), \\ f(R, \phi) &= \phi(R + \alpha R^2). \end{aligned} \right\} \quad (3.1.44)$$

Now we will explore the energy conditions for these models in the background of power law solutions with $n_1 > 1$ which favors the accelerated expansion of the universe.

Model-I

Myrzakulov et al. [113] have studied the inflation in $f(R, \phi)$ theory by analysing the tensor-to-scalar ratio and spectral index and found the results compatible with the recent observational data. Here, we are using the following $f(R, \phi)$ model [113]

$$f(R, \phi) = \frac{R - 2\Lambda(1 - e^{b_1\phi\kappa^3 R})}{\kappa^2}, \quad \omega(\phi) = 1. \quad (3.1.45)$$

The term κ^3 is introduced for dimensional reasons and b_1 is a dimensionless number of order unity.

Using model (3.1.45) into the energy bounds (3.1.23)-(3.1.26) along with Eqs.(2.11.3), (3.1.7) and (2.11.4), we find the following constraints

$$\begin{aligned} \text{NEC: } & \kappa^2(\rho_0 t^{-3n_1(1+w)} + p) - \beta_1^2 H^2 a_0^{2\beta_1} t^{2n_1\beta_1} + 2\Lambda b_1 \kappa \beta_1 H^2 a_0^{\beta_1} t^{n_1\beta_1} e^{-6b_1\phi\kappa^3(1-q)H^2} \\ & \times (\beta_1 - 2 - q) - 12\Lambda b_1^2 \kappa^4 H^4 t^{2n_1\beta_1} a_0^{2\beta_1} [(q^2 + s + 6 + 8q) + \beta_1(\beta_1 - 1 - q)(1 - q) \\ & + 2\beta_1(j - 2 - q) + 2\beta_1^2(1 - q) - (j - 2 - q) - \beta_1(1 - q)] e^{-6b_1\phi\kappa^3H^2(1-q)} + 72\Lambda b_1^3 \\ & \times \kappa^7 H^6 a_0^{3\beta_1} t^{3n_1\beta_1} [\beta_1^2(1 - q)^2 + 2\beta_1(j - 2 - q)(1 - q)] e^{-6b_1\phi\kappa^3(1-q)H^2} \geq 0, \quad (3.1.46) \end{aligned}$$

$$\begin{aligned} \text{WEC: } & \kappa^2 \rho_0 t^{-3n_1(1+w)} + \frac{1}{\kappa^2} [3(1 - q)H^2 - \Lambda(1 - e^{-6b_1\phi\kappa^3(1-q)H^2})] - \frac{1}{2}\beta_1^2 H^2 a_0^{2\beta_1} \\ & \times t^{2n_1\beta_1} - \Lambda b_1 \kappa H^2 a_0^{\beta_1} t^{n_1\beta_1} (\beta_1 - 6 + 6q) e^{-6b_1\phi\kappa^3(1-q)H^2} + 36\Lambda b_1^2 \kappa^4 H^4 a_0^{2\beta_1} t^{2n_1\beta_1} \\ & \times \{\beta_1(1 - q) + (j - q - 2)\} e^{-6b_1\phi\kappa^3(1-q)H^2} \geq 0, \quad (3.1.47) \end{aligned}$$

$$\begin{aligned} \text{SEC: } & \kappa^2(\rho_0 t^{-3n_1(1+w)} + 3p) + \frac{2\Lambda}{\kappa^2} (1 - e^{-6b_1\phi\kappa^3(1-q)H^2}) - 2\beta_1^2 H^2 a_0^{2\beta_1} t^{2n_1\beta_1} + 6\Lambda b_1 \\ & \times \kappa H^2 a_0^{2\beta_1} t^{2n_1\beta_1} [\beta_1(\beta_1 - 1 - q) + \beta_1 - 2(1 - q)] e^{-6b_1\phi\kappa^3(1-q)H^2} - 36\Lambda b_1^2 \kappa^4 H^4 a_0^{2\beta_1} \\ & \times t^{2n_1\beta_1} [(q^2 + s + 6 + 8q) + \beta_1(\beta_1 - q - 1)(1 - q) + 4\beta_1(j - 2 - q) + 2\beta_1^2(1 - q) \\ & + (j - 2 - q) + \beta_1(1 - q)] e^{-6b_1\phi\kappa^3H^2(1-q)} + 216\Lambda b_1^3 \kappa^7 H^6 a_0^{3\beta_1} t^{3n_1\beta_1} [\beta_1^2(1 - q)^2 \\ & + 2\beta_1(j - 2 - q)(1 - q) + (j - 2 - q)^2] e^{-6b_1\phi\kappa^3H^2(1-q)} \geq 0, \quad (3.1.48) \end{aligned}$$

$$\begin{aligned} \text{DEC: } & \kappa^2(\rho_0 t^{-3n_1(1+w)} - p) - \frac{2\Lambda}{\kappa^2} (1 - e^{-6b_1\phi\kappa^3(1-q)H^2}) - 2\Lambda b_1 \kappa H^2 a_0^{\beta_1} t^{n_1\beta_1} [\beta_1(\beta_1 \\ & - q - 1) + 5\beta_1 - 6(1 - q)] e^{-6b_1\phi\kappa^3H^2(1-q)} + 12\Lambda b_1^2 \kappa^4 H^4 t^{2n_1\beta_1} a_0^{2\beta_1} [(s + q^2 + 6 + 8q) \\ & + \beta_1(1 - q)(\beta_1 - 1 - q) + 4\beta_1(j - 2 - q) + 2\beta_1^2(1 - q) + 5(j - 2 - q) + 5\beta_1(1 - q)] \\ & \times e^{-6b_1\phi\kappa^3H^2(1-q)} - 72\Lambda b_1^3 \kappa^7 H^6 a_0^{3\beta_1} t^{3n_1\beta_1} [\beta_1^2(1 - q)^2 + 2\beta_1(j - q - 2)(1 - q) \\ & + (j - 2 - q)^2] e^{-6b_1\phi\kappa^3(1-q)H^2} \geq 0. \quad (3.1.49) \end{aligned}$$

Now we have only four parameters t , b_1 , β_1 and n_1 , we will find the ranges of these parameters according to NEC and WEC. First we will take $b_1 \geq 0$, the validity of WEC requires $b_1 = 0$, $n_1 > 1$, $t \geq 1.1$ and $\beta_1 \leq 0$ whereas NEC requires $n_1 > 1$ with $\beta_1 \leq -1.5$. Now taking $b_1 < 0$, NEC and WEC both are valid for $n_1 > 1$ and all values of β_1 . In Fig. 3.2, the plot of NEC is shown for this model taking $n_1 > 1$ verses the parameters ζ , β_1 and t .

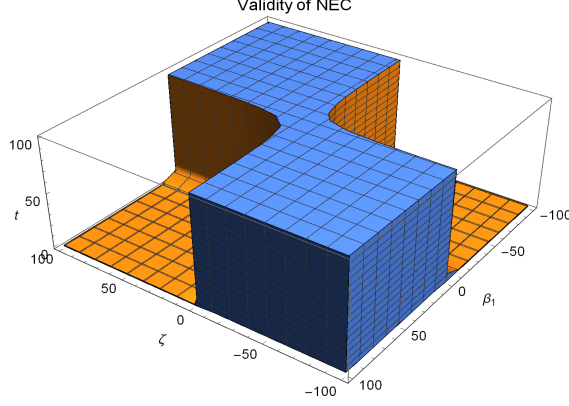


Figure 3.2: Plot of NEC for Model-I versus the parameters ζ , β_1 and t with $n_1 = 1.1$.

Model-II

In $f(R, \phi)$ gravity, we have calculated this model using the form $Rf(\phi)$. Using Klein-Gordon equation (2.10.3) with power law assumptions (3.1.7) we have derived $f(\phi)$ form. Using $f(\phi)$ we have the following model

$$f(R, \phi) = R \left(\frac{\omega_0 \beta_1^2 n_1^2 a_0^{2/n_1} (\zeta n_1 \beta_1 + 2n_1 \beta_1 + 6n_1 - 2)}{\zeta n_1 \beta_1 + 2n_1 \beta_1 - 2} \right) \phi^{\zeta+2-\frac{2}{n_1 \beta_1}}, \quad (3.1.50)$$

where ω_0 and a_0 are constants. Inserting this model in energy bounds (3.1.23)-(3.1.26) along with Eqs.(2.11.3), (3.1.7) and (2.11.4) we have energy conditions,

$$\text{NEC: } \kappa^2 \rho_0 t^{-3n_1(1+w)} + \kappa^2 p - \omega_0 \beta_1^2 H^2 a_0^{(\zeta+2)\beta_1} t^{(\zeta+2)n_1 \beta_1} + \omega_0 \beta_1^2 H^2 a_0^{(\zeta+2)\beta_1} \{n_1 \beta_1 \times (\zeta + 2) + 2(3n_1 - 1)\} \{(\zeta + 2)n_1 \beta_1 - 2(n_1 + 1) - n_1 q\} t^{(\zeta n_1 \beta_1 + 2n_1 \beta_1 - 2)} \geq 0, \quad (3.1.51)$$

$$\text{WEC: } \kappa^2 \rho_0 t^{-3n_1(1+w)} - \frac{1}{2} \omega_0 \beta_1^2 H^2 a_0^{(\zeta+2)\beta_1} t^{(\zeta+2)n_1 \beta_1} - 3\omega_0 n_1 \beta_1^2 H^2 a_0^{(\zeta+2)\beta_1} \{n_1 \beta_1 \times (\zeta + 2) + 2(3n_1 - 1)\} t^{\zeta n_1 \beta_1 + 2n_1 \beta_1 - 2} \geq 0, \quad (3.1.52)$$

$$\text{SEC: } \kappa^2 (\rho_0 t^{-3n_1(1+w)} + 3p) - 2\omega_0 \beta_1^2 H^2 a_0^{(\zeta+2)\beta_1} t^{(\zeta+2)n_1 \beta_1} + 3\omega_0 \beta_1^2 H^2 a_0^{(\zeta+2)\beta_1} \{(\zeta + 2)n_1 \beta_1 + 2(3n_1 - 1)\} t^{(\zeta n_1 \beta_1 + 2n_1 \beta_1 - 2)} \{(\zeta \beta_1 - q)n_1 + 2(n_1 \beta_1 - 1)\} \geq 0, \quad (3.1.53)$$

$$\text{DEC: } \kappa^2 (\rho_0 t^{-3n_1(1+w)} - p) + \omega_0 \beta_1^2 H^2 a_0^{(\zeta+2)\beta_1} \{(\zeta + 2)n_1 \beta_1 + 2(3n_1 - 1)\} \{n_1 (q - \zeta \beta_1) + 2(1 - 2n_1 - n_1 \beta_1)\} t^{\zeta n_1 \beta_1 + 2n_1 \beta_1 - 2} \geq 0. \quad (3.1.54)$$

We have examined the WEC and NEC versus the parameters t , β_1 , n_1 and ζ . We have found that for $t \geq 1.3$, WEC is valid for all values of ζ and β_1 whereas the validity of NEC is divided in two parts: $\zeta \geq 0$ with ($t \geq 1.5$ & $\beta_1 \leq 0$) and $\zeta < -2$ with ($t \geq 1.2$ & $\beta_1 \geq 0$).

Model-III

Now we choose the model [149] and discuss the energy conditions

$$f(R, \phi) = R(1 + \xi \kappa^2 \phi^2), \quad (3.1.55)$$

where ξ denotes the coupling constant. This model is already used to study the cosmological perturbations for non-minimally coupled scalar field DE in both Palatini and metric formalisms. The interaction has been analyzed depending on the coupling constant. Inserting this model in energy bounds (3.1.23)-(3.1.26) along with Eqs.(2.11.3), (3.1.7) and (2.11.4) we get,

$$\begin{aligned} \text{NEC: } & \kappa^2(\rho_0 t^{-3n_1(1+w)} + p) - \omega_0 \beta_1^2 H^2 a_0^{(\zeta+2)\beta_1} t^{(\zeta+2)n_1\beta_1} + 2\beta_1 \xi \kappa^2 H^2 a_0^{2\beta_1} t^{2n_1\beta_1} (\beta_1 \\ & - q - 1) + 2\beta_1^2 \xi \kappa^2 H^2 a_0^{2\beta_1} t^{2n_1\beta_1} - 2\beta_1 \xi \kappa^2 H^2 a_0^{2\beta_1} t^{2n_1\beta_1} \geq 0, \end{aligned} \quad (3.1.56)$$

$$\begin{aligned} \text{WEC: } & \kappa^2 \rho_0 t^{-3n_1(1+w)} - \frac{1}{2} \omega_0 \beta_1^2 H^2 a_0^{(\zeta+2)\beta_1} t^{(\zeta+2)n_1\beta_1} - 6\beta_1 H^2 \xi \kappa^2 a_0^{2\beta_1} t^{2n_1\beta_1} \geq 0, \\ \text{SEC: } & \kappa^2(\rho_0 t^{-3n_1(1+w)} + 3p) - 2\omega_0 \beta_1^2 H^2 a_0^{(\zeta+2)\beta_1} t^{(\zeta+2)n_1\beta_1} + 6\xi \kappa^2 \beta_1 H^2 a_0^{2\beta_1} t^{2n_1\beta_1} \\ & + 6\xi \kappa^2 \beta_1 H^2 (\beta_1 - 1 - q) a_0^{2\beta_1} t^{2n_1\beta_1} + 6\xi \kappa^2 \beta_1^2 H^2 a_0^{2\beta_1} t^{2n_1\beta_1} \geq 0, \end{aligned} \quad (3.1.57)$$

$$\begin{aligned} \text{DEC: } & \kappa^2(\rho_0 t^{-3n_1(1+w)} - p) - 10\beta_1 H^2 \xi \kappa^2 a_0^{2\beta_1} t^{2n_1\beta_1} - 2\beta_1 H^2 \xi \kappa^2 (\beta_1 - 1 - q) a_0^{2\beta_1} \\ & \times t^{2n_1\beta_1} - 2\beta_1^2 H^2 \xi \kappa^2 a_0^{2\beta_1} t^{2n_1\beta_1} \geq 0. \end{aligned} \quad (3.1.58)$$

We will discuss the validity of WEC, NEC and find the feasible ranges of the parameters t , β_1 , ξ , n_1 and ζ . Here, we develop three cases depending on the value of ζ . First we will take $\zeta > 0$ and $n_1 > 1$, for all values of ξ , WEC is valid for $t \geq 2.8$ with $\beta_1 \leq -3.4$ and NEC is valid for $t \geq 3$ with $\beta_1 \leq -3.7$. Now we will take $\zeta < 0$ with $n_1 > 1$, NEC is viable for $t \geq 3.1$ with $\beta_1 \leq -3.7$ and $\forall t$ with $\xi > 0$, $\beta_1 > 0$. For $\beta_1 \leq -3.4$, validity of WEC requires $t \geq 2.8$ & $\forall \xi$ and for $\beta_1 \geq 0$ WEC requires all values of t with $\xi \leq 0$. Now taking $\zeta = 0$ and $n_1 > 1$, the validity of WEC requires $\xi \leq -8.35$ with $\beta_1 \geq 0$ and $\forall \xi$ with $t \geq 2.8$ & $\beta_1 \leq -3.4$ while NEC is valid for $\beta_1 \geq 0$ with $\xi \geq 0.28$ and $\beta_1 \leq -3.7$ with $t \geq 3$ & $\forall \xi$.

Model-IV

Bahamonde, S. et al has used the expression $f(R)$ [150]

$$f(R, \phi) = \phi(R + \alpha R^2), \quad (3.1.59)$$

where α is a constant with suitable dimensions. This gravitational action is very familiar in the text as it is able to reproduce inflation. Inserting this model in the energy conditions (3.1.23)-(3.1.26) along with Eqs.(2.11.3), (3.1.7) and (2.11.4) we have energy conditions,

$$\begin{aligned} \text{NEC: } & \kappa^2(\rho_0 t^{-3n_1(1+w)} + p) - \omega_0 \beta_1^2 H^2 a_0^{(\zeta+2)\beta_1} t^{(\zeta+2)n_1\beta_1} - 24\alpha\beta_1 H^4 a_0^{\beta_1} t^{n_1\beta_1} (j - q \\ & - 2) - 12\alpha H^4 (s + q^2 + 8q + 6) a_0^{\beta_1} t^{n_1\beta_1} + \beta_1 (\beta_1 - 1 - q) H^2 a_0^{\beta_1} t^{n_1\beta_1} - 12\alpha\beta_1 H^4 (\beta_1 \\ & - q - 1)(1 - q) a_0^{\beta_1} t^{n_1\beta_1} + 12\alpha H^4 (j - q - 2) a_0^{\beta_1} t^{n_1\beta_1} - \beta_1 H^2 a_0^{\beta_1} t^{n_1\beta_1} + 12\alpha\beta_1 H^4 a_0^{\beta_1} \\ & \times (1 - q) t^{n_1\beta_1} \geq 0, \end{aligned} \quad (3.1.60)$$

$$\begin{aligned} \text{WEC: } & \kappa^2 \rho_0 t^{-3n_1(1+w)} - \frac{1}{2} \omega_0 \beta_1 H a_0^{(\zeta+2)\beta_1} t^{(\zeta+2)n_1\beta_1} - 18\alpha H^4 (1 - q)^2 a_0^{\beta_1} t^{n_1\beta_1} + 36\alpha \\ & \times H^4 (j - q - 2) a_0^{\beta_1} t^{n_1\beta_1} - 3\beta_1 H^2 a_0^{\beta_1} t^{n_1\beta_1} + 36\alpha\beta_1 H^4 (1 - q) a_0^{\beta_1} t^{n_1\beta_1} \geq 0, \end{aligned} \quad (3.1.61)$$

$$\begin{aligned} \text{SEC: } & \kappa^2(\rho_0 t^{-3n_1(1+w)} + 3p) - 2\omega_0 \beta_1^2 H^2 a_0^{(\zeta+2)\beta_1} t^{(\zeta+2)n_1\beta_1} + 36\alpha H^4 (1 - q)^2 a_0^{\beta_1} t^{n_1\beta_1} \\ & - 36\alpha H^4 (j - q - 2) a_0^{\beta_1} t^{n_1\beta_1} + 3\beta_1 H^2 a_0^{\beta_1} t^{n_1\beta_1} - 36\alpha H^4 (s + q^2 + 8q + 6) a_0^{\beta_1} t^{n_1\beta_1} - 36\alpha \\ & \times \beta_1 H^4 a_0^{\beta_1} t^{n_1\beta_1} + 3\beta_1 H^2 (\beta_1 - 1 - q) a_0^{\beta_1} t^{n_1\beta_1} - 72\alpha\beta_1 H^4 (j - q - 2) a_0^{\beta_1} t^{n_1\beta_1} - 36\alpha\beta_1 \\ & \times H^4 (\beta_1 - 1 - q)(1 - q) a_0^{\beta_1} t^{n_1\beta_1} \geq 0, \end{aligned} \quad (3.1.62)$$

$$\begin{aligned} \text{DEC: } & \kappa^2(\rho_0 t^{-3n_1(1+w)} - p) + 36\alpha H^4 (1 - q)^2 a_0^{\beta_1} t^{n_1\beta_1} + 60\alpha H^4 (j - q - 2) a_0^{\beta_1} t^{n_1\beta_1} \\ & - 5\beta_1 H^2 a_0^{\beta_1} t^{n_1\beta_1} + 60\alpha\beta_1 H^4 (1 - q) a_0^{\beta_1} t^{n_1\beta_1} + 24\alpha\beta_1 H^4 (j - q - 2) a_0^{\beta_1} t^{n_1\beta_1} + 12\alpha H^4 \\ & \times a_0^{\beta_1} (s + q^2 + 8q + 6) t^{n_1\beta_1} - \beta_1 H^2 (\beta_1 - 1 - q) a_0^{\beta_1} t^{n_1\beta_1} + 12\alpha\beta_1 H^4 (\beta_1 - 1 - q) \\ & \times (1 - q) a_0^{\beta_1} t^{n_1\beta_1} \geq 0. \end{aligned} \quad (3.1.63)$$

Here, we are considering WEC, NEC and will examine the viability for different values of t , β_1 , α , n_1 and ζ . Now we will vary the coupling parameter α and find the ranges of other parameters for which the NEC and WEC are valid. For $\alpha > 0$, WEC is valid for $n_1 > 1$ with $(\beta_1 \geq 0, \zeta \leq -1 \text{ \& } t \geq 1)$ and $(\beta_1 \leq -9, t \geq 6 \text{ \& all values of } \zeta)$. Taking $\alpha < 0$ then validity of WEC requires $n_1 > 1$, all values of ζ and $\beta_1 \leq 0$ while for validity of NEC we have two regions with $n_1 > 1$; $(\beta_1 \leq -0.7, \zeta \geq 0 \text{ \& } t \geq 1)$ and $(\beta_1 \geq 0.85, \zeta \leq -1 \text{ \& } t \geq 1)$.

Now we are taking $\alpha = 0$ with $n_1 > 1$, the validity of WEC requires $\beta_1 \leq 0$ and all values of ζ whereas for NEC we have two regions: $\beta_1 \geq 0$ with $(\zeta \leq -1.05, t > 1.01)$ and $\beta_1 \leq 0$ with $(\zeta \geq 0, t \geq 1)$.

3.2 Thermodynamics in $f(R, R_{\alpha\beta_1} R^{\alpha\beta_1}, \phi)$ gravity

For a perfect fluid, the EMT is defined in (2.5.3), we are writing in this way

$$T_{\mu\nu}^{(m)} = (\rho_m + p_m)u_\mu u_\nu + p_m g_{\mu\nu}. \quad (3.2.1)$$

Here, we are assuming that matter of the universe has zero pressure $p_m = 0$ (dust). From Eq. (2.10.2) we can write an effective EFE as

$$R_{\mu\nu} - \frac{1}{2}Rg_{\mu\nu} = 8\pi G_{eff} T_{\mu\nu}^{(m)} + T_{\mu\nu}^{(d)}, \quad (3.2.2)$$

where G_{eff} denotes the effective gravitational matter and $T_{\mu\nu}^{(d)}$ represents an effective EMT related with all the new terms of the theory defined as

$$G_{eff} = \frac{G}{f_R}, \quad (3.2.3)$$

$$\begin{aligned} T_{\mu\nu}^{(d)} = & \frac{1}{f_R} \left[-\frac{1}{2}Rg_{\mu\nu}f_R + \frac{1}{2}(f + \omega(\phi)\phi_{;\alpha}\phi^{;\alpha})g_{\mu\nu} + f_{R;\mu\nu} - g_{\mu\nu}\square f_R - 2f_Y R_\mu^\alpha R_{\alpha\nu} \right. \\ & \left. + 2[f_Y R_{(\mu}^\alpha]_{;\nu)\alpha} - \square[f_Y R_{\mu\nu}] - [f_Y R_{\alpha\beta}]^{;\alpha\beta}g_{\mu\nu} - \omega(\phi)\phi_{;\mu}\phi_{;\nu} \right]. \end{aligned} \quad (3.2.4)$$

The metric describing the FRW universe is

$$ds^2 = h_{\alpha\beta} dx^\alpha dx^\beta + \tilde{r}^2 d\Omega^2, \quad (3.2.5)$$

with the 2-dimensional metric $h_{\alpha\beta} = \text{diag}\left(-1, \frac{a(t)^2}{1-kr^2}\right)$, $(x^0, x^1) = (t, r)$, and $k = \pm 1, 0$ is the spacial curvature. The second term is $\tilde{r} = a(t)r$ and $d\Omega^2 = d\theta^2 + \sin^2\theta d\varphi^2$ is the 2-dimensional sphere with unit radius. The gravitational field equations for the metric (3.2.5) are given by

$$\begin{aligned} 3\left(H^2 + \frac{k}{a^2}\right) = & 8\pi G_{eff}\rho_m + \frac{1}{f_R} \left[\frac{1}{2}(Rf_R - f) - \frac{1}{2}\omega(\phi)\dot{\phi}^2 - 3H\partial_t f_R - 6H(2\dot{H} \right. \\ & \left. + 3H^2 + \frac{k}{a^2})\partial_t f_Y - f_Y \left(\ddot{H} + 4H\dot{H} + 6\dot{H}H^2 - 2H^4 - \frac{4kH^2}{a^2} \right) \right], \end{aligned} \quad (3.2.6)$$

$$\begin{aligned}
-\left(2\dot{H} + 3H^2 + \frac{k}{a^2}\right) &= \frac{1}{f_R} \left[\frac{1}{2} (f - Rf_R) - \frac{1}{2} \omega(\phi) \dot{\phi}^2 + \partial_{tt} f_R + 2H \partial_t f_R + (4\dot{H} + 6H^2 \right. \\
&\quad + \left. \frac{2k}{a^2}) \partial_{tt} f_Y + 4H \left(\dot{H} + 3H^2 + \frac{2k}{a^2} \right) \partial_t f_Y + f_Y \left(4\ddot{H} + 20H\ddot{H} \right. \right. \\
&\quad + \left. \left. 10\dot{H}H^2 + 16\dot{H}^2 - 18H^4 - \frac{18k\dot{H}}{a^2} - \frac{20kH^2}{a^2} - \frac{18k^2}{a^4} \right) \right]. \quad (3.2.7)
\end{aligned}$$

Here, dot represents the total derivative and ∂_t represents the partial derivative with respect to time t . The term $H = \dot{a}/a$ represents the Hubble parameter, these equations can be rewritten as

$$3 \left(H^2 + \frac{k}{a^2} \right) = 8\pi G_{eff} (\rho_m + \rho_d), \quad (3.2.8)$$

$$-2 \left(\dot{H} - \frac{k}{a^2} \right) = 8\pi G_{eff} (\rho_m + \rho_d + p_d), \quad (3.2.9)$$

where ρ_d and p_d are the energy density and pressure of dark components with $G = f_R G_{eff}$, are given by

$$\begin{aligned}
\rho_d &= \frac{1}{8\pi G} \left[\frac{1}{2} (Rf_R - f) - \frac{1}{2} \omega(\phi) \dot{\phi}^2 - 3H \partial_t f_R - 6H \left(2\dot{H} + 3H^2 + \frac{k}{a^2} \right) \partial_t f_Y - f_Y (\ddot{H} \right. \\
&\quad + \left. 4H\ddot{H} + 6\dot{H}H^2 - 2H^4 - \frac{4kH^2}{a^2} \right)], \quad (3.2.10)
\end{aligned}$$

$$\begin{aligned}
p_d &= \frac{1}{8\pi G} \left[\frac{1}{2} (f - Rf_R) - \frac{1}{2} \omega(\phi) \dot{\phi}^2 + \partial_{tt} f_R + 2H \partial_t f_R + \left(4\dot{H} + 6H^2 + \frac{2k}{a^2} \right) \partial_{tt} f_Y \right. \\
&\quad + \left. 4H \left(\dot{H} + 3H^2 + \frac{2k}{a^2} \right) \partial_t f_Y + f_Y \left(4\ddot{H} + 20H\ddot{H} + 10\dot{H}H^2 + 16\dot{H}^2 - 18H^4 - \frac{8k^2}{a^4} \right. \right. \\
&\quad + \left. \left. - \frac{18k\dot{H}}{a^2} - \frac{20kH^2}{a^2} \right) \right]. \quad (3.2.11)
\end{aligned}$$

The EoS parameter ω_d for a dark fluid can be obtained from ($\omega_d = \frac{p_d}{\rho_d}$)

$$\begin{aligned}
\omega_d &= -1 + \frac{1}{\rho_d} \left[-\omega(\phi) \dot{\phi}^2 + \partial_{tt} \Psi - H \partial_t \Psi + \left(4\dot{H} + 6H^2 + \frac{2k}{a^2} \right) \partial_{tt} f_Y - 2H (4\dot{H} \right. \\
&\quad + \left. 3H^2 + \frac{k}{a^2}) \partial_t f_Y + f_Y \left(3\ddot{H} + 16H\ddot{H} + 4\dot{H}H^2 + 16\dot{H}^2 - 16H^4 - \frac{18k\dot{H}}{a^2} - \frac{8k^2}{a^4} \right. \right. \\
&\quad + \left. \left. - \frac{16kH^2}{a^2} \right) \right]. \quad (3.2.12)
\end{aligned}$$

The semi-conservation equation for an ordinary matter is

$$\dot{\rho} + 3H\rho = q, \quad (3.2.13)$$

and the conservation equation for dark component is

$$\dot{\rho}_d + 3H(\rho_d + p_d) = q_d, \quad (3.2.14)$$

$$\dot{\rho}_{\text{total}} + 3H(\rho_{\text{total}} + p_{\text{total}}) = q_{\text{total}}, \quad (3.2.15)$$

where $\rho_{\text{total}} = \rho_m + \rho_d$, $p_{\text{total}} = p_m + p_d$, $q_{\text{total}} = q + q_d$ represents the total energy exchange term and q_d denotes the energy exchange term for dark component. Substituting Eq's. (3.2.8) and (3.2.9) in the above equation, we have

$$q_{\text{total}} = \frac{3}{8\pi G} \left(H^2 + \frac{k}{a^2} \right) \partial_t f_R. \quad (3.2.16)$$

Taking $f(R, Y, \phi) = f(R)$, we can get the energy exchange term for the gravity and in GR taking $f(R, Y, \phi) = R$ we will get $q_{\text{total}} = 0$.

3.2.1 Generalized Thermodynamics laws with non-equilibrium description

Here, for a more general $f(R, Y, \phi)$ gravity we will discuss the FLT and SLT at the apparent horizon of FRW universe.

First Law of Thermodynamics

Now, we will analyze the viability of FLT for $f(R, Y, \phi)$ gravity at apparent horizon in FRW universe. The dynamical apparent horizon is calculated by the relation $h^{\alpha\beta} \partial_\alpha \tilde{r} \partial_\beta \tilde{r} = 0$ from which we have the radius of apparent horizon as $\tilde{r}_A = (H^2 + k/a^2)^{-\frac{1}{2}}$. Taking time derivative of \tilde{r}_A and using Eq. (3.2.9), we have

$$f_R d\tilde{r}_A = 4\pi G H \tilde{r}_A^3 (\hat{\rho}_{\text{total}} + \hat{p}_{\text{total}}) dt, \quad (3.2.17)$$

where $\hat{\rho}_{\text{total}} = \hat{\rho}_m + \hat{\rho}_d$ is total energy density and $\hat{p}_{\text{total}} = \hat{p}_d$ is total pressure. Here, $d\tilde{r}_A$ denotes the infinitesimal change in the radius of the apparent horizon during an infinitesimal time interval dt . Through surface gravity K_{sg} , the temperature of apparent horizon is defined as $T_h = |K_{sg}|/(2\pi)$ and the K_{sg} [55] is given by

$$K_{sg} = -\frac{1}{\tilde{r}_A} \left(1 - \frac{\dot{\tilde{r}}_A}{2H\tilde{r}_A} \right). \quad (3.2.18)$$

The horizon entropy in GR defined by Bekenstein and Hawking is $S_h = A/4G$, where A denotes the area of apparent horizon given by $A = 4\pi\tilde{r}_A^2$ [48, 49, 151]. In the literature of modified theories of gravity, the horizon entropy with a Noether charge was introduced by Wald [152], that can be obtained by varying the Lagrangian density of the modified theory with respect to Riemann tensor. Wald entropy is defined as $\hat{S}_h = A/4G_{eff}$ [153], where G_{eff} represents the effective gravitational coupling. In $f(R, Y, \phi)$ gravity, the Wald's entropy is defined as

$$\hat{S}_h = \frac{f_R A}{4G}. \quad (3.2.19)$$

By differentiating Eq. (3.2.19) and using (3.2.17), we have

$$\frac{1}{2\pi\tilde{r}_A} d\hat{S}_h = 4\pi\tilde{r}_A^3 (\hat{\rho}_{total} + \hat{p}_{total}) H dt + \frac{\tilde{r}_A}{2G} df_R. \quad (3.2.20)$$

Multiplying the above equation by $1 - \dot{\tilde{r}}_A/(2H\tilde{r}_A)$ on both sides, we have

$$T_h d\hat{S}_h = -4\pi\tilde{r}_A^3 (\hat{\rho}_{total} + \hat{p}_{total}) H dt + 2\pi\tilde{r}_A^2 (\hat{\rho}_{total} + \hat{p}_{total}) d\tilde{r}_A + \frac{\pi\tilde{r}_A^2 T_h}{G} df_R. \quad (3.2.21)$$

Now, we will define the energy of the universe inside the apparent horizon. The defined Misner-Sharp energy is $E = \tilde{r}_A/(2G)$ [154] while for $f(R, Y, \phi)$ gravity it can be written as [155]

$$\hat{E} = \frac{\tilde{r}_A}{2G_{eff}}. \quad (3.2.22)$$

Further, using the relation $V = (4/3)\pi\tilde{r}_A^3$, above equation can also be rewritten as

$$\hat{E} = \frac{3V}{8\pi G_{eff}} \left(H^2 + \frac{k}{a^2} \right) = V \hat{\rho}_{total}, \quad (3.2.23)$$

which represents the total energy inside the sphere of radius \tilde{r}_A . In $f(R, Y, \phi)$ gravity, choosing positive G_{eff} we have $G_{eff} = G/f_R > 0$. It can be concluded that $\hat{E} > 0$. From Eqs. (3.2.8) and (3.2.23) we will have

$$d\hat{E} = 4\pi\tilde{r}_A^2 \hat{\rho}_{total} d\tilde{r}_A - 4\pi\tilde{r}_A^3 (\hat{\rho}_{total} + \hat{p}_{total}) H dt + \frac{\tilde{r}_A}{2G} df_R. \quad (3.2.24)$$

Using Eq. (3.2.24) in (3.2.21), it follows that

$$T_h d\hat{S}_h = d\hat{E} - \hat{W} dV - \frac{(1 - 2\pi\tilde{r}_A T_h) \tilde{r}_A}{2G} df_R, \quad (3.2.25)$$

where the work density $\hat{W} = (1/2)(\hat{\rho}_{total} - \hat{p}_{total})$ [156] is used. Rewriting the above equation we have

$$T_h d\hat{S}_h + T_h d_i \hat{S}_h = d\hat{E} - \hat{W} dV, \quad (3.2.26)$$

where

$$d_i \hat{S}_h = \frac{(1 - 2\pi \tilde{r}_A T_h) \tilde{r}_A}{2GT_h} df_R = \frac{(\hat{E} - \hat{S}_h T_h)}{T_h} \frac{df_R}{f_R}. \quad (3.2.27)$$

Comparing the above expression of $f(R, Y, \phi)$ gravity with GR, Gauss-Bonnet gravity and Lovelock gravity it can be seen that in FLT we have an additional term $d_i \hat{S}_h$. That extra term is known as the entropy production term which is produced due to the non-equilibrium behaviour of $f(R, Y, \phi)$ gravity. In this expression taking $f(R, Y, \phi) = f(R)$ we can get the non-equilibrium FLT for $f(R)$ gravity [60]. Moreover, taking $f(R, Y, \phi) = R$, we can get the standard FLT in GR.

Generalized Second Law of Thermodynamics

In modified gravitational theories, the GSLT has been widely discussed [60]-[65],[155, 157, 158]. For the validity of GSLT in $f(R, Y, \phi)$ gravity, the following inequality [155] must be satisfied

$$\dot{\hat{S}}_h + d_i \dot{\hat{S}}_h + \dot{\hat{S}}_v \geq 0, \quad (3.2.28)$$

where \hat{S}_h is the horizon entropy, $d_i \hat{S}_h = \partial_t (d_i \hat{S}_h)$ is entropy due to all the matter inside the horizon and \hat{S}_v is the entropy due to energy sources inside the horizon. The Gibb's equation which includes the entropy of matter and energy fluid is given by [159]

$$T_v d\hat{S}_v = d(\hat{\rho}_{total} V) + \hat{p}_{total} dV, \quad (3.2.29)$$

where T_v is the temperature inside the horizon. Assuming the relation between the temperature of the apparent horizon and the temperature inside the horizon given by

$$T_v = b T_h, \quad (3.2.30)$$

where b is a constant having range $0 < b < 1$ and it guarantees the positivity of the temperature T_v and also assure that temperature is smaller than the horizon temperature. Substituting Eqs. (3.2.26) and (3.2.29) in Eq. (3.2.28), we obtain

$$\dot{S}_{tot} = \dot{\hat{S}}_h + d_i \dot{\hat{S}}_h + \dot{\hat{S}}_v = \frac{2\pi\Sigma}{\tilde{r}_A b R} \geq 0, \quad (3.2.31)$$

where

$$\Sigma = (1-b)\dot{\hat{p}}_{total}V + (1-\frac{b}{2})(\hat{p}_{total} + \dot{\hat{p}}_{total})\dot{V},$$

which is the general condition in modified gravitational theories [155] to satisfy the GSLT.

Utilizing Eqs. (3.2.8) and (3.2.9), the condition (3.2.31) is reduced to

$$\frac{2\pi\Xi}{Gb\left(H^2 + \frac{k}{a^2}\right)\left(\dot{H} + 2H^2 + \frac{k}{a^2}\right)} \geq 0, \quad (3.2.32)$$

where

$$\begin{aligned} \Xi &= (b-1)\partial_t f_R \left(H^2 + \frac{k}{a^2}\right) + 2Hf_R(b-1) \left(\dot{H} - \frac{k}{a^2}\right) + (b-2)f_R H \left(\dot{H} - \frac{k}{a^2}\right)^2 \\ &\times \left(H^2 + \frac{k}{a^2}\right)^{-1}. \end{aligned} \quad (3.2.33)$$

In flat FRW universe, the GSLT is valid for $\partial_t f_R \geq 0$, $f_R \geq 0$, $\dot{H} \geq 0$ and $H \geq 0$. To protect the GSLT, the condition (3.2.32) is equivalent to $\Xi \geq 0$.

3.2.2 Validity of GSLT

To check the validity of GSLT, $\dot{S}_{tot} \geq 0$ for different cosmological solutions we will use some interesting models in $f(R, Y, \phi)$ gravity and some specific $f(R, \phi)$ models.

3.2.3 Model constructed from de-Sitter Universe

- **de-Sitter model $f(R, Y, \phi)$**

The $f(R, Y, \phi)$ model is defined in (3.1.9). To examine the viability of GSLT we will use this model. Introducing this model in (3.2.31), the GSLT will be valid if the following inequality holds

$$\begin{aligned} \dot{S}_{tot} &= \frac{2\pi}{Gb} \left[-12kH_0(b-1)\alpha_1^3\alpha_2\alpha_3a_0^{\beta_1\gamma_1}e^{\alpha_1R+\alpha_2Y}(a_0^2H_0^2+ke^{-2H_0t})e^{-2H_0t}e^{\beta_1\gamma_1H_0t} \right. \\ &- \frac{24}{a_0^2}kH_0(b-1)(a_0^2H_0^2+ke^{-2H_0t})(3a_0H_0^2e^{-3H_0t}+2ke^{-4H_0t})\alpha_1^2\alpha_2^2\alpha_3a_0^{\beta_1\gamma_1}e^{\alpha_1R+\alpha_2Y} \\ &\times e^{\beta_1\gamma_1H_0t} + \beta_1H_0(b-1)\alpha_1^2\alpha_2\alpha_3\gamma_1a_0^{\beta_1+2}e^{\beta_1H_0t}(a_0^2H_0^2+ke^{-2H_0t})e^{\alpha_1R+\alpha_2Y}a_0^{\beta_1(\gamma_1-1)} \\ &\times e^{\beta_1(\gamma_1-1)H_0t} - 2kH_0a_0^2(b-1)\alpha_1^2\alpha_2\alpha_3e^{-2H_0t}a_0^{\beta_1\gamma_1}e^{\alpha_1R+\alpha_2Y}e^{\beta_1\gamma_1H_0t} + 2k^2H_0a_0^2\alpha_1^2\alpha_2 \\ &\times \alpha_3\left(\frac{b}{2}-1\right)(a_0^2H_0^2+ke^{-2H_0t})^{-1}e^{-4H_0t}e^{\alpha_1R+\alpha_2Y}a_0^{\beta_1\gamma_1}e^{\beta_1\gamma_1H_0t} \left. \right] (a_0^2H_0^2+ke^{-2H_0t})^{-1} \\ &\times (2a_0^2H_0^2+ke^{-2H_0t})^{-1} \geq 0. \end{aligned} \quad (3.2.34)$$

For dS $f(R, Y, \phi)$ model, the validity of GSLT depends on five parameters t , α_1 , α_2 , α_3 and β_1 . In this perspective, fixing two parameters we can observe the feasible ranges of other parameters. In our case, we are fixing α_1 , α_2 and will check the validity of \dot{S}_{tot} . We are setting here the present day values of cosmographic parameters and Hubble parameter as $j = 2.16$, $q = -0.81$, $s = -0.22$, and $H_0 = 67.3$ [5]. The feasible ranges for all dS $f(R, Y, \phi)$ models are presented in Table 3.2.

First we start with the variations of α_1 and α_2 to show the validity of \dot{S}_{tot} for different values of t , α_3 and β_1 . Taking $\alpha_1 > 0$ and $\alpha_2 > 0$ the validity of $\dot{S}_{tot} \geq 0$ holds for every time, however α_3 and β_1 must be in the ranges ($\alpha_3 \geq 0$, $\beta_1 \leq -0.78$) and ($\alpha_3 \leq 0$, $\beta_1 \geq 0$).

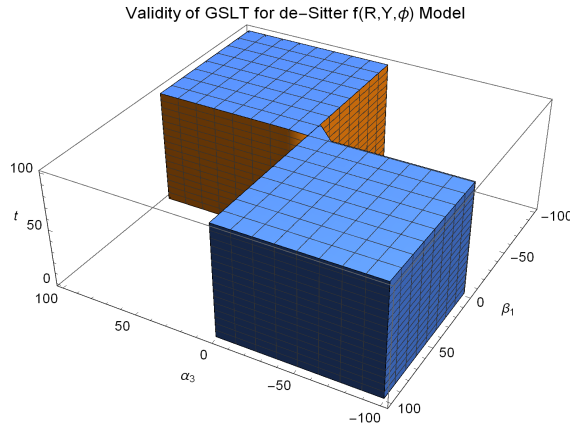


Figure 3.3: Validity region of the GSLT for dS $f(R, Y, \phi)$ model with $\alpha_1 = 1$ and $\alpha_2 = 3$.

If $\alpha_1 < 0$ and $\alpha_2 > 0$, the GSLT is valid for all times with ($\alpha_3 \geq 0$, $\beta_1 \leq -0.78$) or ($\alpha_3 \leq 0$, $\beta_1 \geq 0$). For ($\alpha_1 > 0$, $\alpha_2 < 0$), $\dot{S}_{tot} \geq 0$ holds for all values of α_3 , β_1 and t . For ($\alpha_1 > 0$, $\alpha_2 < 0$) and ($\alpha_1 < 0$, $\alpha_2 < 0$), the GSLT is valid for all values of t , α_3 and β_1 . Fig. 3.3 is shown as an example for the evolution of GSLT verses the parameters t , α_3 and β_1 by fixing $\alpha_1 > 0$ and $\alpha_2 > 0$.

- de-Sitter model independent of Y

Now taking $f(R, \phi)$ model that is independent of Y given by (3.1.12). Introducing this model in (3.2.31), the GSLT will be valid if the following inequality holds

$$\begin{aligned}
\dot{S}_{tot} = & \frac{2\pi}{Gb} \left[-12kH_0(b-1)\alpha_1^3\alpha_2a_0^{\beta_1\gamma_1}e^{\alpha_1R}e^{-2H_0t}e^{\beta_1\gamma_1H_0t} + \beta_1H_0(b-1)\alpha_1^2\alpha_2\gamma_1a_0^2a_0^{\beta_1\gamma_1} \right. \\
& \times (a_0^2H_0^2 + ke^{-2H_0t})e^{\alpha_1R}e^{\beta_1\gamma_1H_0t} - 2kH_0(b-1)\alpha_1^2\alpha_2a_0^2a_0^{\beta_1\gamma_1}e^{\alpha_1R}e^{\beta_1\gamma_1H_0t}e^{-2H_0t} + 2k^2H_0 \\
& \times a_0^2e^{-4H_0t} \left(\frac{b}{2} - 1 \right) (H_0^2a_0^2 + ke^{-2H_0t})^{-1} \alpha_1^2\alpha_2e^{\alpha_1R}e^{\beta_1\gamma_1H_0t}a_0^{\beta_1\gamma_1} \left. \right] (a_0^2H_0^2 + ke^{-2H_0t})^{-1} \\
& \times (2a_0^2H_0^2 + ke^{-2H_0t})^{-1} \geq 0.
\end{aligned} \tag{3.2.35}$$

In dS $f(R, \phi)$ model, viability of GSLT involves four parameters t , α_1 , α_2 and β_1 . We will fix β_1 and check the variations of α_1 , α_2 for the validity of GSLT. The GSLT is valid for all values of t and β_1 whereas we have two cases for other parameters (i) $\alpha_1 \leq -0.1$ with all values of α_2 (ii) $\alpha_1 > 0$ with $\alpha_2 \geq 0$.

3.2.4 Model constructed from power Law method

- **Power Law model independent of Y**

The power law $f(R, \phi)$ model is defined in (3.1.21). Now our concentration is on this model to check the validity of GSLT. By substituting this $f(R, \phi)$ model in (3.2.31) we get

$$\begin{aligned}
\dot{S}_{tot} = & \frac{2\pi}{Gb} \left[H_0(b-1)\alpha_1\alpha_2\gamma_2 \left\{ (j-q-2)H_0^2 + \frac{k}{a_0^2t^{2n_1}} \right\} \left\{ (1-q)H_0^2 + \frac{k}{a_0^2t^{2n_1}} \right\}^{\gamma_2-2} \right. \\
& \times (\gamma_2-1)a_0^{\beta_1\gamma_1}t^{n_1\beta_1\gamma_1} + \beta_1H_0\alpha_1\alpha_2\gamma_1\gamma_2(b-1)a_0^{\beta_1\gamma_1}t^{n_1\beta_1\gamma_1} \left\{ (1-q)H_0^2 + \frac{k}{a_0^2t^{2n_1}} \right\}^{\gamma_2-1} \\
& - 2H_0(b-1)\alpha_1\alpha_2\gamma_2a_0^{\beta_1\gamma_1}t^{n_1\beta_1\gamma_1} \left\{ (1-q)H_0^2 + \frac{k}{a_0^2t^{2n_1}} \right\}^{\gamma_2-1} \left\{ 1 + \frac{qH_0^2}{H_0^2 + \frac{k}{a_0^2t^{2n_1}}} \right\} \\
& \left. + 2H_0\alpha_1\alpha_2\gamma_2a_0^{\beta_1\gamma_1}t^{n_1\beta_1\gamma_1} \left((1-q)H_0^2 + \frac{k}{a_0^2t^{2n_1}} \right)^{\gamma_2-1} \left(\frac{b}{2} - 1 \right) \left(1 + \frac{qH_0^2}{H_0^2 + \frac{k}{a_0^2t^{2n_1}}} \right)^2 \right] \\
& \times \left((1-q)H_0^2 + \frac{k}{a_0^2t^{2n_1}} \right)^{-1} \geq 0.
\end{aligned} \tag{3.2.36}$$

The above constraint has five parameters t , α_1 , α_2 , n_1 and β_1 . Now, we will fix α_1 , α_2 and check the validity of $\dot{S}_{tot} \geq 0$ for the possible ranges of t , n_1 and β_1 . All possible cases of this model are written in Table 3.2.

We are starting with $\alpha_1 > 0$ and find the viable ranges of t , α_2 and β_1 . Considering this we will discuss the three cases depending on α_2 ,

- (i) $\alpha_2 < 0$, $n_1 \geq 3$ with $(t \geq 1, \beta_1 \leq -35.8)$ or $(t \geq 0.94, \beta_1 \geq 2.81)$.
- (ii) $\alpha_2 = 0$, $n_1 > 1$ and $\forall t$ with $\beta_1 > 0$ or $\beta_1 < 0$.
- (iii) $\alpha_2 > 0$ with $(t \geq 0.8, n_1 \geq 8.6, 0 < \beta_1 \leq 20)$ or $(t \geq 0.9, n_1 \geq 12.7, -20 \leq \beta_1 < 0)$.

Now taking $\alpha_1 < 0$, again we have three cases for the validity of the GSLT

- (i) $\alpha_2 < 0$ with $(t \geq 0.8, n_1 \geq 8.6, -20 \leq \beta_1 < 0)$ or $(t \geq 0.9, n_1 \geq 12.7, 0 < \beta_1 \leq 20)$.
- (ii) $\alpha_2 = 0$, $n_1 > 1$ and $\forall t$ with $\beta_1 > 0$ or $\beta_1 < 0$.
- (iii) $\alpha_2 > 0$, $n_1 \geq 3$ and $\forall t$ with $(\beta_1 \leq -28.1)$ or $(\beta_1 \geq 35.7)$.

We have observed that by taking α_1 and α_2 both with the same sign, for initial values of n_1 and t the GSLT is not valid whereas β_1 is restricted to $\beta_1 \leq 20$ or $\beta_1 \geq -20$. The Fig. 3.4 shows the validity region of the GSLT for $\alpha_1 > 0$ and $\alpha_2 = 5$.

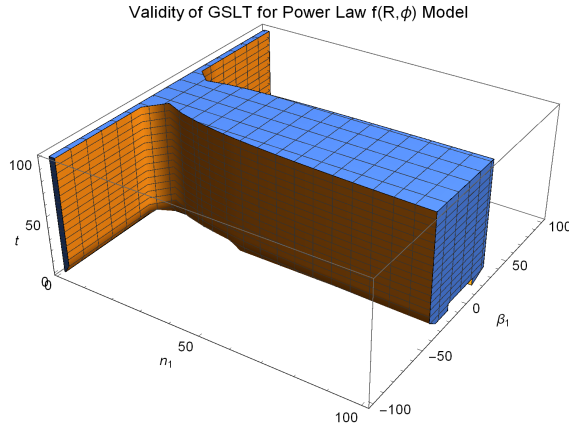


Figure 3.4: Validity of the GSLT for Power law- $f(R, \phi)$ versus the parameters n_1 , β_1 and t with $\alpha_1 = 1$ and $\alpha_2 = 5$.

Models	Variations of parameters	Validity of $\dot{S}_{tot} \geq 0$
de-Sitter Model $f(R, Y, \phi)$	$\alpha_1 > 0, \alpha_2 > 0$ and $\alpha_1 < 0, \alpha_2 > 0$	$\forall t$ with $(\alpha_3 \geq 0, \beta_1 \leq -0.78)$ or $(\alpha_3 \leq 0, \beta_1 \geq 0)$
	$\alpha_1 > 0, \alpha_2 < 0$ and $\alpha_1 < 0, \alpha_2 < 0$	$\forall \alpha_3, \beta_1$ and t
de-Sitter Model $f(R, \phi)$	$\forall \beta_1$	$\forall t$ with $(\alpha_1 \leq -0.1, \forall \alpha_2)$ or $(\alpha_1 > 0, \alpha_2 \geq 0)$
Power Law Model $f(R, \phi)$	$\alpha_1 > 0$ with $\alpha_2 < 0$	$n_1 \geq 3$ with $(\beta_1 \leq -35.8, t \geq 1)$ or $(\beta_1 \geq 2.81, t \geq 0.94)$
	$\alpha_2 = 0$	$n_1 > 1, \beta_1 > 0$ or $\beta_1 < 0, \forall t$
	$\alpha_2 > 0$	$(n_1 \geq 8.6, 0 < \beta_1 \leq 20, t \geq 0.8)$ or $(n_1 \geq 12.7, -20 \leq \beta_1 < 0, t \geq 0.9)$
	$\alpha_1 < 0$ with $\alpha_2 < 0$	$(n_1 \geq 8.6, -20 \leq \beta_1 < 0, t \geq 0.8)$ or $(n_1 \geq 12.7, 0 < \beta_1 \leq 20, t \geq 0.9)$
Model-I	$\alpha_2 = 0$	$n_1 > 1, \beta_1 > 0$ or $\beta_1 < 0, \forall t$
	$\alpha_2 > 0$	$n_1 \geq 3$ and $\forall t$ with $(\beta_1 \leq -28.1)$ or $(\beta_1 \geq 35.7)$
	$b_1 = 0$	$n_1 > 1, \forall \beta_1, t \geq 0.96$
	$b_1 > 0$	$(n_1 > 1$ with $\beta_1 \leq -0.6, \forall t)$ or $(n_1 \geq 2.5$ with $\beta_1 \geq 6, t \geq 2.5)$
Model-II	$b_1 < 0$	not valid
Model-III	$n_1 > 1$	$\forall t$ with $(\zeta \geq 2, \beta_1 \leq -1.5)$ or $(\zeta \leq -3.2, \beta_1 \geq 5)$
Model-IV	$n_1 > 1$	$(\forall \xi, \beta_1 \leq -3.5$ and $t \geq 4)$ or $(\xi \leq 0, \beta_1 \geq 0.15$ and $t \geq 1)$
Model-IV	$n_1 > 1$	$(\beta_1 \geq 0, \alpha < 0$ and $\forall t)$ or $(\beta_1 \leq -0.25, \alpha \geq 0$ and $t \geq 1)$

Table 3.2: Validity regions of $\dot{S}_{tot} \geq 0$ for different models.

3.2.5 $f(R, \phi)$ Models

Now we will use the $f(R, \phi)$ gravity models stated in (3.1.44) and discuss the validity of the GSLT.

First we are using model (3.1.45), inserting the model in (3.2.31) we have inequality of the form

$$\begin{aligned}
\dot{S}_{tot} = & \frac{2\pi}{Gb} \left[2H_0(b-1)\Lambda b_1^2 a_0^{2\beta_1} t^{2n_1\beta_1} \kappa^4 R e^{b_1 a_0^{\beta_1} t^{n_1\beta_1} \kappa^3 R} + 2\Lambda b_1 \kappa \left(1 + b_1 a_0^{\beta_1} t^{n_1\beta_1} \kappa^3 R \right) \right. \\
& \times (b-1) \beta_1 H_0 a_0^{\beta_1} t^{n_1\beta_1} e^{b_1 a_0^{\beta_1} t^{n_1\beta_1} \kappa^3 R} - \frac{2}{\kappa^2} H_0(b-1) \left\{ 1 + 2\Lambda b_1 a_0^{\beta_1} t^{n_1\beta_1} \kappa^3 e^{b_1 a_0^{\beta_1} t^{n_1\beta_1} \kappa^3 R} \right\} \\
& \times \left(1 + \frac{qH_0^2}{H_0^2 + \frac{k}{a_0^2 t^{2n_1}}} \right) + \frac{2H}{\kappa^2} \left\{ 1 + 2\Lambda b_1 a_0^{\beta_1} t^{n_1\beta_1} \kappa^3 e^{b_1 a_0^{\beta_1} t^{n_1\beta_1} \kappa^3 R} \right\} \left(1 + \frac{qH_0^2}{H_0^2 + \frac{k}{a_0^2 t^{2n_1}}} \right)^2 \\
& \left. \times \left(\frac{b}{2} - 1 \right) \right] \left(H_0^2(1-q) + \frac{k}{a_0^2 t^{2n_1}} \right)^{-1} \geq 0, \tag{3.2.37}
\end{aligned}$$

where $R = 6 [H_0^2(1-q) + k/(a_0^2 t^{2n_1})]$. It can be seen that the above inequality involves four parameters t , b_1 , n_1 and β_1 . We have observed that the GSLT is valid for two cases

depending on the choice of b_1 :

(i) $b_1 = 0$ with $t \geq 0.96$, $n_1 > 1$ & $\forall \beta_1$.

(ii) $b_1 > 0$ with $(\beta_1 \leq -0.6, n_1 > 1 \text{ \& } \forall t)$ and $(\beta_1 \geq 6, n_1 \geq 2.5 \text{ \& } t \geq 2.5)$.

Now we will use the model (3.1.50) into (3.2.31) and have the constraint

$$\begin{aligned} \dot{S}_{tot} = & \frac{2\pi}{Gb} \left[\beta_1^2 H_0 (b-1) \omega_0 n_1 (\zeta n_1 \beta_1 + 2n_1 \beta_1 + 6n_1 - 2) a_0^{\beta_1(\zeta+2)} t^{\zeta n_1 \beta_1 + 2n_1 \beta_1 - 2} - 2H_0 \right. \\ & \times (b-1) \left\{ \frac{\omega_0 \beta_1^2 n_1^2 a_0^{2/n_1} (\zeta n_1 \beta_1 + 2n_1 \beta_1 + 6n_1 - 2)}{\zeta n_1 \beta_1 + 2n_1 \beta_1 - 2} \right\} \left\{ 1 + qH_0^2 (H_0^2 + \frac{k}{a_0^2} t^{2n_1})^{-1} \right\} \\ & \times a_0^{\beta_1(\zeta+2-\frac{2}{n_1 \beta_1})} t^{\zeta n_1 \beta_1 + 2n_1 \beta_1 - 2} + 2 \left(\frac{b}{2} - 1 \right) H_0 a_0^{\beta_1(\zeta+2-\frac{2}{n_1 \beta_1})} \left(1 + \frac{qH_0^2}{H_0^2 + \frac{k}{a_0^2} t^{2n_1}} \right)^2 \\ & \times t^{\zeta n_1 \beta_1 + 2n_1 \beta_1 - 2} \left\{ \frac{\omega_0 \beta_1^2 n_1^2 a_0^{2/n_1} (\zeta n_1 \beta_1 + 2n_1 \beta_1 + 6n_1 - 2)}{\zeta n_1 \beta_1 + 2n_1 \beta_1 - 2} \right\} \left. \right] (H_0^2 (1-q) \\ & + \frac{k}{a_0^2 t^{2n_1}})^{-1} \geq 0. \end{aligned} \quad (3.2.38)$$

It can be observed that the inequality of GSLT for this model involves four parameters t , β_1 , ζ and n_1 . Now by fixing n_1 we will check the validity of GSLT for different values of ζ and β_1 . For every time t and $n_1 > 1$ we observed two cases for the validity of $\dot{S}_{tot} \geq 0$: ($\zeta \geq 2$ with $\beta_1 \leq -1.5$) and ($\zeta \leq -3.2$ with $\beta_1 \geq 5$). By fixing $n_1 > 1$, validity of the GSLT verses the parameters t , ζ and β_1 is shown in Fig. 3.5.

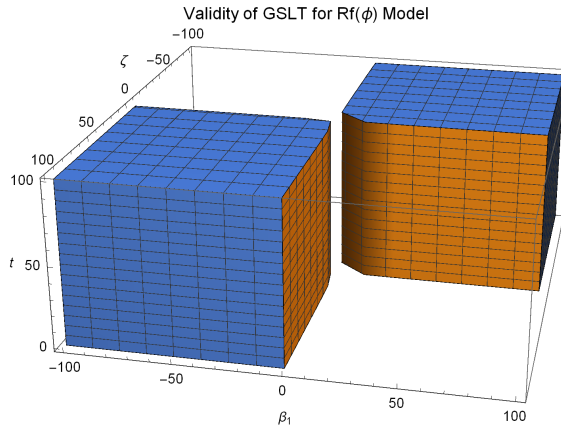


Figure 3.5: Regions where the GSLT is satisfied for the Model-II versus the parameters ζ , β_1 and t with $n_1 = 1.1$.

Further we are taking model (3.1.55), using this model in (3.2.31) we have

$$\begin{aligned} \dot{S}_{tot} = & \frac{2\pi}{Gb} \left[2\beta_1 H_0 \xi \kappa^2 (b-1) a_0^{2\beta_1} t^{2n_1\beta_1} - 2H_0(b-1) \left\{ 1 + qH_0^2 \left(H_0^2 + \frac{k}{a_0^2} t^{2n_1} \right)^{-1} \right\} \right. \\ & \left. \left(1 + \xi \kappa^2 a_0^{2\beta_1} t^{2n_1\beta_1} \right) + 2 \left(\frac{b}{2} - 1 \right) H_0 \left(1 + \xi \kappa^2 a_0^{2\beta_1} t^{2n_1\beta_1} \right) \left(1 + \frac{qH_0^2}{H_0^2 + \frac{k}{a_0^2} t^{2n_1}} \right)^2 \right] \\ & \times \left(H_0^2(1-q) + \frac{k}{a_0^2 t^{2n_1}} \right)^{-1} \geq 0. \end{aligned} \quad (3.2.39)$$

Here, the above constraint involves four parameters t , n_1 , ξ and β_1 . To check the validity of GSLT we fix n_1 and find the feasible values of β_1 and ξ . We have two validity regions for $n_1 > 1$ depending on the choice of β_1 : $\beta_1 \leq -3.5$ with $(t \geq 4 \text{ \& } \forall \xi)$ and $\beta_1 \geq 0.15$ with $(t \geq 1 \text{ \& } \xi \leq 0)$.

Moreover, introducing the model (3.1.59) in (3.2.31) we have inequality of the form

$$\begin{aligned} \dot{S}_{tot} = & \frac{2\pi}{Gb} \left[12\alpha H_0(b-1) a_0^{\beta_1} t^{n_1\beta_1} \left\{ (j-q-2)H_0^2 + \frac{k}{a_0^2 t^{2n_1}} \right\} + \beta_1 H_0(b-1) a_0^{\beta_1} t^{n_1\beta_1} \right. \\ & \times \left\{ 1 + 12\alpha \left((1-q)H_0^2 + \frac{k}{a_0^2 t^{2n_1}} \right) \right\} - 2H_0(b-1) \left\{ 1 + 12\alpha \left((1-q)H_0^2 + \frac{k}{a_0^2 t^{2n_1}} \right) \right\} \\ & \times a_0^{\beta_1} t^{n_1\beta_1} \left\{ 1 + qH_0^2 \left(H_0^2 + \frac{k}{a_0^2 t^{2n_1}} \right)^{-1} \right\} + 2H_0 a_0^{\beta_1} \left\{ 1 + 12\alpha \left((1-q)H_0^2 + \frac{k}{a_0^2 t^{2n_1}} \right) \right\} \\ & \left. \times t^{n_1\beta_1} \left(\frac{b}{2} - 1 \right) \left(1 + \frac{qH_0^2}{H_0^2 + \frac{k}{a_0^2} t^{2n_1}} \right)^2 \right] \left(H_0^2(1-q) + \frac{k}{a_0^2 t^{2n_1}} \right)^{-1} \geq 0. \end{aligned} \quad (3.2.40)$$

The above inequality involves four parameters t , n_1 , α and β_1 . To constraint the above relation we have $n_1 > 1$ and two validity ranges depending on the choice of α :

- (i) $\alpha < 0$ with $(\beta_1 \geq 0 \text{ \& } \forall t)$.
- (ii) $\alpha \geq 0$ with $(t \geq 1 \text{ \& } \beta_1 \leq -0.25)$.

The Fig. 3.6 shows the validity region of the GSLT for a specific choice of the parameter $n_1 = 1.1$

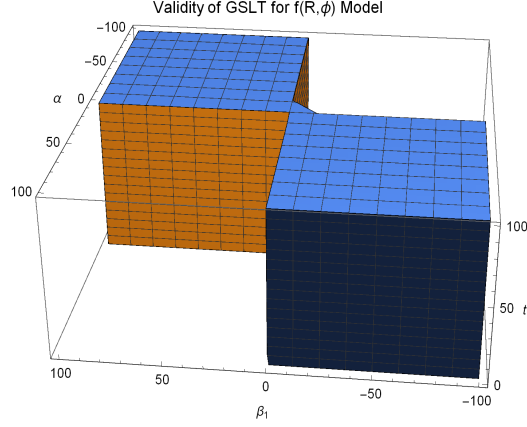


Figure 3.6: Validity regions of the GSLT for the Model-IV for the parameters α and β_1 with $n_1 = 1.1$.

3.2.6 Equilibrium description of Thermodynamics laws

In entropy production, the existence of non-equilibrium term $d_i S$ is due to ρ_d , p_d given in eqs. (3.2.10), (3.2.11) which satisfy the continuity Eq. (3.2.16) and in $f(R, Y, \phi)$ gravity its R.H.S. will not vanish because $\partial_t f_R \neq 0$. Otherwise the standard continuity equation does not satisfy. Now we will define ρ_d and p_d which satisfy the continuity equation and no extra entropy production term occur, that is known as equilibrium description. Now we will discuss the equilibrium description of thermodynamics in $f(R, Y, \phi)$ gravity. The field equation (2.10.2) is redefined as

$$G_{\mu\nu} + f_R R_{\mu\nu} - \frac{1}{2} (f + \omega(\phi) \phi_{;\alpha} \phi^{;\alpha}) g_{\mu\nu} - f_{R;\mu\nu} + g_{\mu\nu} \square f_R + 2f_Y R_{\mu}^{\alpha} R_{\alpha\nu} + \square [f_Y R_{\mu\nu}] - 2[f_Y R_{(\mu}^{\alpha}{}_{;\nu)\alpha} + [f_Y R_{\alpha\beta}]^{;\alpha\beta} g_{\mu\nu} + \omega(\phi) \phi_{;\mu} \phi_{;\nu} = G_{\mu\nu} + \kappa T_{\mu\nu}^{(m)}. \quad (3.2.41)$$

For EMT of a perfect fluid (3.2.1), we are assuming here that the matter of the universe has zero pressure $p_m = 0$ (dust). From Eq. (3.2.41), the EFE can be written as

$$R_{\mu\nu} - \frac{1}{2} R g_{\mu\nu} = 8\pi G T_{\mu\nu}^{(m)} + T_{\mu\nu}^{(d)}, \quad (3.2.42)$$

where

$$T_{\mu\nu}^{(d)} = -\frac{1}{2} R g_{\mu\nu} f_R + \frac{1}{2} (f + \omega(\phi) \phi_{;\alpha} \phi^{;\alpha}) g_{\mu\nu} + f_{R;\mu\nu} - g_{\mu\nu} \square f_R - 2f_Y R_{\mu}^{\alpha} R_{\alpha\nu} + 2[f_Y R_{(\mu}^{\alpha}{}_{;\nu)\alpha} - \square [f_Y R_{\mu\nu}] - [f_Y R_{\alpha\beta}]^{;\alpha\beta} g_{\mu\nu} - \omega(\phi) \phi_{;\mu} \phi_{;\nu} + (1 - f_R) G_{\mu\nu}, \quad (3.2.43)$$

represents an effective EMT which involves all the new terms of the theory.

3.2.7 First Law of Thermodynamics

Now, redefining Eq. (3.2.8) and Eq. (3.2.9) in the form

$$3 \left(H^2 + \frac{k}{a^2} \right) = 8\pi G(\rho_m + \rho_d), \quad (3.2.44)$$

$$-2 \left(\dot{H} - \frac{k}{a^2} \right) = 8\pi G(\rho_m + \rho_d + p_d), \quad (3.2.45)$$

where the redefined ρ_d and p_d are

$$\begin{aligned} \rho_d = & \frac{1}{8\pi G} \left[\frac{1}{2} (Rf_R - f) - \frac{1}{2} \omega(\phi) \dot{\phi}^2 - 3H \partial_t f_R - 6H \left(2\dot{H} + 3H^2 + \frac{k}{a^2} \right) \partial_t f_Y - f_Y (\ddot{H} \right. \\ & \left. + 4H\ddot{H} + 6\dot{H}H^2 - 2H^4 - \frac{4kH^2}{a^2} \right) + 3(1 - f_R) \left(H^2 + \frac{k}{a^2} \right) \right], \end{aligned} \quad (3.2.46)$$

$$\begin{aligned} p_d = & \frac{1}{8\pi G} \left[\frac{1}{2} (f - Rf_R) - \frac{1}{2} \omega(\phi) \dot{\phi}^2 + \partial_{tt} f_R + 2H \partial_t f_R + \left(4\dot{H} + 6H^2 + \frac{2k}{a^2} \right) \partial_{tt} f_Y \right. \\ & + 4H \left(\dot{H} + 3H^2 + \frac{2k}{a^2} \right) \partial_t f_Y + f_Y \left(4\ddot{H} + 20H\ddot{H} + 10\dot{H}H^2 + 16\dot{H}^2 - 18H^4 - \frac{8k^2}{a^4} \right. \\ & \left. \left. - \frac{18k\dot{H}}{a^2} - \frac{20kH^2}{a^2} \right) - (1 - f_R) \left(2\dot{H} + 3H^2 + \frac{k}{a^2} \right) \right]. \end{aligned} \quad (3.2.47)$$

In this representation, eq. (3.2.17) becomes

$$d\tilde{r}_A = 4\pi G H \tilde{r}_A^3 (\hat{\rho}_{total} + \hat{p}_{total}) dt, \quad (3.2.48)$$

by using the horizon entropy \hat{S}_h of the form

$$\hat{S}_h = \frac{A}{4G}, \quad (3.2.49)$$

differentiating Eq. (3.2.49) and using (3.2.48), we have

$$\frac{1}{2\pi\tilde{r}_A} d\hat{S}_h = 4\pi\tilde{r}_A^3 (\hat{\rho}_{total} + \hat{p}_{total}) H dt, \quad (3.2.50)$$

multiplying both sides of the above equation by $1 - \dot{\tilde{r}}_A / (2H\tilde{r}_A)$, we have

$$T_h d\hat{S}_h = -4\pi\tilde{r}_A^3 (\hat{\rho}_{total} + \hat{p}_{total}) H dt + 2\pi\tilde{r}_A^2 (\hat{\rho}_{total} + \hat{p}_{total}) d\tilde{r}_A. \quad (3.2.51)$$

By defining the Misner-Sharp energy as

$$\hat{E} = \frac{\tilde{r}_A}{2G} = V \hat{\rho}_{total}, \quad (3.2.52)$$

we get

$$d\hat{E} = 4\pi\tilde{r}_A^2\hat{\rho}_{total}d\tilde{r}_A - 4\pi\tilde{r}_A^3(\hat{\rho}_{total} + \hat{p}_{total})Hdt. \quad (3.2.53)$$

Using Eq. (3.2.53) in (3.2.51), we get

$$T_h d\hat{S}_h = d\hat{E} - \hat{W}dV, \quad (3.2.54)$$

where we have used the work density $\hat{W} = (1/2)(\hat{\rho}_{total} - \hat{p}_{total})$ [156]. The equilibrium description of thermodynamics can be derived by redefining ρ_d and p_d to satisfy the continuity equation.

3.2.8 Generalized Second Law of Thermodynamics

To analyze the SLT for equilibrium description, the Gibb's equation in terms of all matter and DE fluid can be written as

$$T_v d\hat{S}_v = d(\hat{\rho}_{total}V) + \hat{p}_{total}dV, \quad (3.2.55)$$

where T_v denotes the temperature within the horizon. The SLT can be expressed as

$$\dot{\hat{S}}_h + \dot{\hat{S}}_v \geq 0, \quad (3.2.56)$$

where \hat{S}_h denotes the horizon entropy and \hat{S}_v denotes the entropy due to energy sources inside the horizon. Now, assuming the relation between the temperature within the horizon and temperature of the apparent horizon as

$$T_v = T_h. \quad (3.2.57)$$

By substituting Eqs. (3.2.54) and (3.2.55) in Eq. (3.2.56), we obtain

$$\dot{S}_{tot} = \dot{\hat{S}}_h + \dot{\hat{S}}_v = \frac{2\pi\Sigma}{\tilde{r}_A R} \geq 0, \quad (3.2.58)$$

where

$$\Sigma = \frac{1}{2}(\hat{\rho}_{total} + \hat{p}_{total})\dot{V},$$

which is the general condition for the validity of the GSLT. Using Eqs. (3.2.44) and (3.2.45), the condition (3.2.58) reduced to

$$\frac{2\pi H \left(\frac{2k\dot{H}}{a^2} - \dot{H}^2 - \frac{k^2}{a^4} \right)}{G \left(\dot{H} + 2H^2 + \frac{k}{a^2} \right) \left(H^2 + \frac{k}{a^2} \right)^2} \geq 0, \quad (3.2.59)$$

In case of flat FRW universe, for the validity of the GSLT, the condition (3.2.59) must be satisfied.

Chapter 4

Static spherically symmetric wormholes in generalized $f(R, \phi)$ gravity

4.1 Wormhole Geometries in extended $f(R, \phi)$ Gravity

In this section we will present the field equations (2.9.2) in the Morris-Thorne geometry (2.14.1) and then study its generic properties to find out the general energy conditions. The action of extended $f(R, \phi)$ theory is defined in (2.9.1) and field eq's are (2.9.2), (2.9.3).

We can rewrite the field equation (2.9.2) in an effective form,

$$G_{\mu\nu} = R_{\mu\nu} - \frac{1}{2}Rg_{\mu\nu} = T_{\mu\nu}^{eff}, \quad (4.1.1)$$

where $T_{\mu\nu}^{eff}$ is defined as

$$T_{\mu\nu}^{eff} = \frac{1}{f_R} \left[\kappa^2 T_{\mu\nu} + \frac{1}{2} (f + \omega(\phi)\phi_{;\alpha}\phi^{;\alpha} - Rf_R) g_{\mu\nu} + f_{R;\mu\nu} - g_{\mu\nu} \square f_R - \omega(\phi)\phi_{;\mu}\phi_{;\nu} - g_{\mu\nu} V(\phi) \right]. \quad (4.1.2)$$

The shape function must satisfy the condition that at the throat r_0 is equal to $\beta(r = r_0) = r_0$ and then it must increases from r_0 to ∞ . For the existence of standard wormholes, the shape function must also satisfy the flaring-out condition which reads

$$\frac{\beta(r) - \beta'(r)r}{\beta(r)^2} > 0, \quad \text{at } r = r_0. \quad (4.1.3)$$

The above condition can be also written in a short way, namely $\beta'(r = r_0) < 1$. In addition, to do not change the signature of the metric, the shape function must also satisfy the condition $1 - \beta(r)/r > 0$.

Since we are interested on studying wormhole geometries for anisotropic, isotropic and barotropic fluids, we will first derive the equation for the most general of those fluids, i.e., the anisotropic fluid. Then, when it is necessary, the other particular cases (barotropic and isotropic) can be easily recovered. For an anisotropic fluid, the EMT is defined in (2.5.7). If we consider the EMT (2.5.7) and the Morris-Thorne metric (2.14.1), the generalized $f(R, \phi)$ field equations (2.9.2) become

$$\begin{aligned} \kappa^2 \rho &= -e^{-b} f_R'' + \frac{1}{2r} e^{-b} (rb' + 4) f_R' + \frac{1}{4r} e^{-b} (2ra'' + ra'^2 - ra'b' + 4a') f_R - \frac{1}{2} f \\ &+ \frac{1}{2} \omega(\phi) e^{-b} \phi'^2 + V(\phi), \end{aligned} \quad (4.1.4)$$

$$\begin{aligned}\kappa^2 p_r &= \frac{1}{2r}e^{-b}(ra' + 4)f'_R - \frac{1}{4r}e^{-b}\left(2ra'' + ra'^2 - ra'b' - 4b'\right)f_R - \frac{1}{2}e^{-b}\omega(\phi)\phi'^2 \\ &+ \frac{1}{2}f - V(\phi),\end{aligned}\quad (4.1.5)$$

$$\begin{aligned}\kappa^2 p_t &= e^{-b}f''_R + \frac{1}{2r}e^{-b}(ra' - rb' + 2)f'_R + \frac{1}{2r^2}e^{-b}\left(rb' - ra' + 2e^b - 2\right)f_R + \frac{1}{2}f \\ &- \frac{1}{2}e^{-b}\omega(\phi)\phi'^2 - V(\phi),\end{aligned}\quad (4.1.6)$$

where primes denote differentiation with respect to the radial coordinate r . In GR, wormhole geometries are supported by exotic matter which requires the violation of NEC and WEC. In [160], Harko et al. discussed wormholes in modified theories and showed that these geometries can be theoretically constructed without the presence of exotic matter. In such scenario, matter threading a wormhole satisfies the energy conditions and the additional geometric components coming from the modified theory are the responsible of the violation of the energy conditions. Hence, the violation of the NEC and WEC are described in terms of the effective EMT, i.e.,

$$\text{WEC} : W^\mu W^\nu T_{\mu\nu}^{eff} < 0, \quad \text{NEC} : k^\mu k^\nu T_{\mu\nu}^{eff} < 0, \quad (4.1.7)$$

for any W^μ time-like vector and any k^μ null-like vector. By doing that, we can then impose that the matter satisfies those conditions:

$$\text{WEC} : W^\mu W^\nu T_{\mu\nu} > 0, \quad \text{NEC} : k^\mu k^\nu T_{\mu\nu} > 0. \quad (4.1.8)$$

Clearly, if NEC is violated then WEC will be also violated and if WEC is valid, it does not imply that the NEC is satisfied. In the literature, this approach has been discussed in different contexts including $f(R)$ gravity [73], curvature-matter couplings [161], braneworlds [162], $f(T)$ theory [74] and hybrid metric-Palatini $f(R)$ [80].

Applying the flaring out condition (4.1.3), one directly notice that NEC needs to be violated for the effective fluid. Hence, to have traversable wormhole geometries we must impose the conditions $\rho^{eff} + p_r^{eff} < 0$ and $\rho^{eff} + p_t^{eff} < 0$. As we discussed above, those conditions do not imply that the standard matter violates NEC. Thus, we can then impose $\rho + p_r > 0$ and $\rho + p_t > 0$ to ensure that the matter satisfies the NEC, which gives us

$$\rho + p_r = -e^{-b}f''_R + \frac{1}{2r}e^{-b}\left(r(a' + b') + 8\right)f'_R + \frac{1}{r}e^{-b}(a' + b')f_R > 0, \quad (4.1.9)$$

$$\rho + p_t = \frac{1}{2r}e^{-b}(ra' + 6)f'_R + \frac{e^{-b}}{4r^2} \left[2r^2a'' + ra'(2 - rb') + r^2a'^2 + 2rb' + 4e^b - 4 \right] f_R > 0. \quad (4.1.10)$$

Let us clarify that WEC will be valid if the above conditions are true and also assuming that the energy density is always positive $\rho > 0$. Thus, for the validity of WEC, we also need to impose that the R.H.S in Eq. (4.1.4) is always positive. For the specific case where there are not tidal forces, i.e., when $a'(r) = 0$, the above conditions become

$$\rho + p_r = -e^{-b}f''_R + \frac{1}{2r}e^{-b}(rb' + 8)f'_R + \frac{b'}{r}e^{-b}f_R > 0, \quad (4.1.11)$$

$$\rho + p_t = \frac{3}{r}e^{-b}f'_R + \frac{e^{-b}}{4r^2} \left[2rb' + 4e^b - 4 \right] f_R > 0. \quad (4.1.12)$$

Hereafter, we will consider $f(R, \phi)$ models given in a power-law way given by [163]

$$f(R, \phi) = \tilde{\gamma}R\phi^\eta, \quad (4.1.13)$$

where $\tilde{\gamma}$ and η are constants. Using this model, the field equations become

$$\begin{aligned} 2\kappa^2\rho &= \frac{\tilde{\gamma}^2e^{-3b}}{16r^3}\omega(\phi)\phi'^2\phi^{2\eta}(2ra'' - ra'b' + ra'^2 + 4a')(-2r^2a'' + r^2a'b' - r^2a'^2 - 4 \\ &\quad - 4ra' + 4rb' + 4e^b) + \frac{\eta\tilde{\gamma}e^{-b}}{r}(rb' + 4)\phi'\phi^{\eta-1} - 2\eta\tilde{\gamma}e^{-b}\phi''\phi^{\eta-1} - 2\tilde{\gamma}\eta(\eta - 1) \\ &\quad \times e^{-b}\phi'^2\phi^{\eta-2} + 2\kappa^2V(\phi), \end{aligned} \quad (4.1.14)$$

$$\begin{aligned} 2\kappa^2p_r &= \frac{\eta\tilde{\gamma}e^{-b}}{r}(ra' + 4)\phi'\phi^{\eta-1} - \frac{\tilde{\gamma}e^{-b}}{2r^2}(-2r^2a'' + r^2a'b' - r^2a'^2 - 4ra' + 4rb' + 4e^b \\ &\quad - 4)\phi^\eta - e^{-b}\omega(\phi)\phi'^2 - \frac{\tilde{\gamma}e^{-b}}{2r}(2ra'' - ra'b' + ra'^2 - 4b')\phi^\eta - 2\kappa^2V(\phi), \end{aligned} \quad (4.1.15)$$

$$\begin{aligned} 2\kappa^2p_t &= \frac{\tilde{\gamma}e^{-b}}{r^2}(-ra' + rb' + 2e^b - 2)\phi^\eta + \frac{\eta\tilde{\gamma}e^{-b}}{r}(ra' - rb' + 2)\phi'\phi^{\eta-1} + 2\eta\tilde{\gamma}e^{-b}\phi'' \\ &\quad \times \phi^{\eta-1} - \frac{\tilde{\gamma}e^{-b}}{2r^2}(-2r^2a'' + r^2a'b' - r^2a'^2 - 4ra' + 4rb' + 4e^b - 4)\phi^\eta + 2\tilde{\gamma}\eta e^{-b} \\ &\quad \times (\eta - 1)\phi'^2\phi^{\eta-2} - e^{-b}\omega(\phi)\phi'^2 - 2\kappa^2V(\phi). \end{aligned} \quad (4.1.16)$$

Now, if we replace (4.1.13) into (2.9.3) we get

$$\begin{aligned} \frac{dV}{d\phi} &= -\frac{\eta\tilde{\gamma}e^{-b}}{2r^2} \left\{ -2r^2a'' + r^2a'b' - r^2a'^2 - 4ra' + 4rb' + 4e^b - 4 \right\} \phi^{\eta-1} + e^{-b}\frac{d\omega}{d\phi}\phi'^2 \\ &\quad + 2\omega(\phi)e^{-b} \left\{ \phi'' + \left(\frac{a' - b'}{2} + \frac{2}{r} \right) \phi' \right\}. \end{aligned} \quad (4.1.17)$$

Additionally, the following power-law functions for the BD function (3.1.7) and the scalar field [164]

$$\phi(r) = \phi_0 \left(\frac{d}{r} \right)^{\sigma_1}, \quad (4.1.18)$$

where ϕ_0 , d and σ_1 are constants.

4.2 Anisotropic generic fluid description

This section is devoted to study wormholes supported by an anisotropic fluid characterized by ρ , p_r and p_t without specifying any EoS. Our principal aim is to check the validity of the energy conditions (WEC and NEC) for our model. To do this, we will specify the $b(r)$ radial function as follows [74], [165]-[170]

$$b(r) = -\ln \left[1 - \left(\frac{r_0}{r} \right)^{\sigma_2+1} \right], \quad (4.2.1)$$

where σ_2 is a constant and r_0 denotes the throat of the wormhole, which gives us that the shape function is

$$\beta(r) = r_0 \left(\frac{r_0}{r} \right)^{\sigma_2}. \quad (4.2.2)$$

This kind of shape function has been used widely in the literature and satisfies all the conditions needed to have a wormhole geometry if $\sigma_2 > -1$ (see the flaring-out condition given by (4.1.3)). Table 4.1 shows the values that the shape function takes for different constants σ_2 .

Table 4.1: Some shape functions for different values of the parameter σ_2

σ_2	$\sigma_2 = 1$	$\sigma_2 = 1/2$	$\sigma_2 = 1/5$	$\sigma_2 = 0$	$\sigma_2 = -1/2$
Shape function $\beta(r)$	r_0^2/r	$r_0\sqrt{r_0/r}$	$r_0^{6/5}r^{-1/5}$	r_0	$\sqrt{r_0r}$

Additionally, for this section we will also assume that the redshift function is constant ($a'(r) = 0$), or in other words, we will assume zero tidal forces. Using power law ansatz with model (4.1.13) and radial function (4.2.1) into (4.1.17) and integrating we have scalar potential of the form

$$\begin{aligned}
V(\phi) = & \frac{\eta \tilde{\gamma} r_0^{\sigma_2+1} \sigma_1 (\sigma_2 - 3) \phi^{\eta + \frac{\sigma_2+3}{\sigma_1}}}{2 d^{\sigma_2+3} \phi_0^{\frac{\sigma_2+3}{\sigma_1}} (\eta \sigma_1 + \sigma_2 + 3)} + \frac{\omega_0 \zeta \sigma_1^3 r_0^{\sigma_2+1} \phi^{\zeta+2 + \frac{\sigma_2+2}{\sigma_1}}}{d^{\sigma_2+3} \phi_0^{\frac{\sigma_2+3}{\sigma_1}} (\zeta \sigma_1 + 2 \sigma_1 + \sigma_2 + 2)} \\
& - \frac{\omega_0 \zeta \sigma_1^3 \phi^{\zeta+2 + \frac{1}{\sigma_1}}}{d^2 \phi_0^{2/\sigma_1} (\zeta \sigma_1 + 2 \sigma_1 + 1)} + \frac{\omega_0 \sigma_1^2 (2 \sigma_1 - \zeta \sigma_1 - 2) \phi^{\zeta+2 + \frac{2}{\sigma_1}}}{d^2 \phi_0^{2/\sigma_1} (\zeta \sigma_1 + 2 \sigma_1 + 2)} \\
& + \frac{\omega_0 \sigma_1^2 r_0^{\sigma_2+1} (\zeta \sigma_1 - \sigma_2 + 3) \phi^{\zeta+2 + \frac{\sigma_2+3}{\sigma_1}}}{d^{\sigma_2+3} \phi_0^{\frac{\sigma_2+3}{\sigma_1}} (\zeta \sigma_1 + 2 \sigma_1 + \sigma_2 + 3)} + c_0.
\end{aligned} \tag{4.2.3}$$

In the following discussion, we will study the validity of WEC and NEC for the standard matter (see Eqs. (4.1.9) and (4.1.10)). Let us then study different cases for σ_2 to study the validity of the the energy conditions. To do this, we will fix $r_0 = \phi_0 = d = \omega_0 = 1$ and $\kappa^2 = 8\pi$ for simplicity. Additionally, it can be noticed from the equations that the constant $\tilde{\gamma}$ which appears from the model (see (4.1.13)) only will change the behaviour of the wormhole depending on its sign. Hence, we will study mainly two cases for this parameter, namely, when $\tilde{\gamma} = 1$ and $\tilde{\gamma} = -1$. Let us also divide our study into two main theories: BD and induced gravity.

4.2.1 Brans-Dicke theory

To recover the case of BD theory we need to choose $\eta = 1$ with $\zeta = -1$. Now, we will examine the validity of the energy bounds for the remaining parameters $\tilde{\gamma}$, σ_1 and σ_2 . As we have pointed out before, only the sign of $\tilde{\gamma}$ changes the physical motion of the wormholes so we will set either $\tilde{\gamma} = 1$ and $\tilde{\gamma} = -1$. Since we have two free parameter (σ_1 and σ_2), we will make region plots to check the validity of all the important energy conditions. For this model we have that the corresponding energy conditions are

$$\begin{aligned}
\rho = & \frac{(2\tilde{\gamma}-1)\sigma_1^2}{\tilde{\gamma}} + \frac{8\pi\sigma_1(\tilde{\gamma}(\sigma_2-3) - 2\sigma_1(\sigma_1+\sigma_2-3))}{\tilde{\gamma}(\sigma_1+\sigma_2+3)} + \frac{16\pi\sigma_1^3 r^{\sigma_2+2}}{\tilde{\gamma}\sigma_1 + \tilde{\gamma}} \\
& + \frac{16\pi r^{\sigma_1+\sigma_2+3}}{\tilde{\gamma}} + \frac{\sigma_1(\sigma_1 + 16\pi(3\sigma_1-2) + 2) - 2\tilde{\gamma}(\sigma_1^2 + 5\sigma_1 + 6)}{\tilde{\gamma}(\sigma_1+2)} r^{\sigma_2+1} \\
& - \frac{16\pi r \sigma_1^3}{\tilde{\gamma}(\sigma_1+\sigma_2+2)} + \sigma_1 \sigma_2 + 7\sigma_1 - 2\sigma_2 \geq 0,
\end{aligned} \tag{4.2.4}$$

$$\rho + p_r = -2\sigma_1(\sigma_1 + 5)r^{\sigma_2+1} + 2\sigma_1^2 + \sigma_1(\sigma_2 + 11) - 2(\sigma_2 + 1) \geq 0, \tag{4.2.5}$$

$$\rho + p_t = -6\sigma_1 r^{\sigma_2+1} + 6\sigma_1 - \sigma_2 + 1 \geq 0. \tag{4.2.6}$$

We can see that it is not so easy to check the validity of the energy conditions. Let us first study the case where $\sigma_2 = 1$ to visualize better the behavior of the energy conditions. In that case, we are able to create 2D region plots for the validity of the energy conditions. Fig. 4.1 shows the validity of $\rho \geq 0$ (see (4.2.4)) for different values of σ_1 and $\tilde{\gamma} = 1$ or $\tilde{\gamma} = -1$. Each blue(yellow) regions represent the validity of this condition for $\tilde{\gamma} = -1(\tilde{\gamma} = 1)$. The green regions are the intersection regions where this condition is valid for $\tilde{\gamma} = 1$ and $\tilde{\gamma} = -1$. As we can see from the figure, there is not so much difference in the valid region for positive or negative values of $\tilde{\gamma}$. However, one can directly see that for the region where $-2 \lesssim \sigma_1 \lesssim -1.3$, this condition will be never true. For other values, one can notice that the validity of this condition depends on the location of the observer. For an observer who is far away from the throat (located at $r_0 = 1$), the condition $\rho \geq 0$ will be always true. However, for an observer who is located near the throat, this condition will be violated for some values of σ_1 .

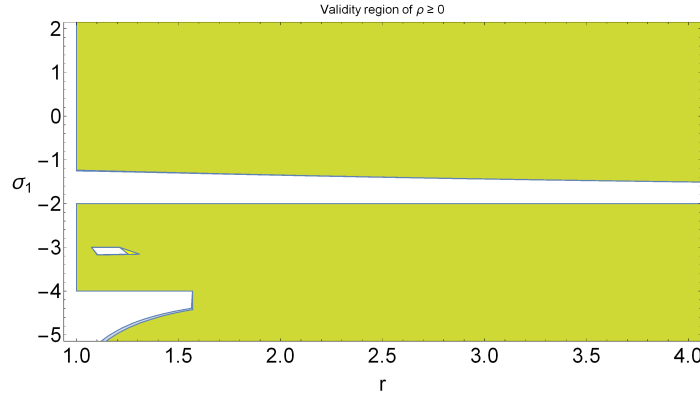


Figure 4.1: Validity of $\rho \geq 0$ given by (4.2.4) for the generic anisotropic fluid in BD theory when $\sigma_2 = 1$. The yellow regions represent the regions where $\tilde{\gamma} = 1$ whereas the blue regions represent when $\tilde{\gamma} = -1$. Therefore, the green regions represent the regions where those two regions coincide. We have chosen the values $r_0 = \phi_0 = d = \omega_0 = 1$ and $\sigma_2 = 1$.

Figs. 4.3a and 4.3b show similar region plots for the validity of NEC-1 ($\rho + p_r \geq 0$) and NEC-2 ($\rho + p_t \geq 0$) given by the validity of the inequalities (4.2.5) and (4.2.6) respectively. For almost all σ_1 , NEC-1 depends on the location of the observer and the sign of $\tilde{\gamma}$. However, there exists a region for $\tilde{\gamma} = -1$ given by $-1 \lesssim \sigma_1 \lesssim 2$ where NEC-1 is always valid independently of the location of the observer. For positive values of $\tilde{\gamma}$, it does not exist

a region where NEC-1 is valid everywhere. NEC-2 is independent of the location of the observer. For $\tilde{\gamma} = -1$, NEC-2 is satisfied always if $\sigma_1 \gtrsim 0$ and for $\tilde{\gamma} = 1$, $\sigma_1 \lesssim 0$ is required. Hence, there are not regions where NEC-1 and NEC-2 are valid for the intersections $\tilde{\gamma} = 1$ and $\tilde{\gamma} = -1$ regions.

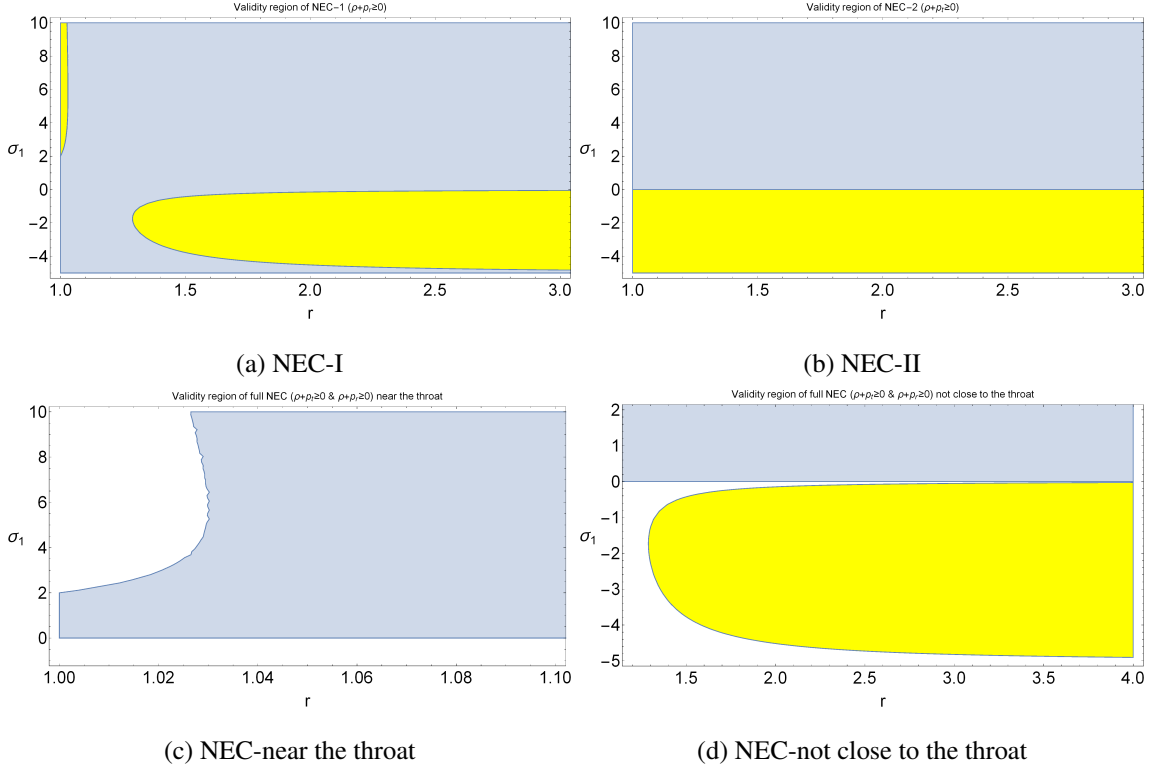


Figure 4.2: Validity of NEC-1 ($\rho + p_r \geq 0$) given by (4.2.5), NEC-2 ($\rho + p_t \geq 0$) given by (4.2.6) and the full condition for the validity of NEC ($\rho + p_t \geq 0$ & $\rho + p_r \geq 0$) for the generic anisotropic fluid in BD theory. The yellow regions represent the regions where $\tilde{\gamma} = 1$ whereas the blue regions represent when $\tilde{\gamma} = -1$. For these plots, we have chosen the values $r_0 = \phi_0 = d = \omega_0 = 1$ and $\sigma_2 = 1$.

In Figs. 4.3c and 4.3d are depicted region plots for the validity of the full NEC ($\rho + p_r \geq 0$ & $\rho + p_t \geq 0$) near the throat and also for locations that are not so close to the throat. The full NEC is satisfied if Eqs. (4.2.5) and (4.2.5) are true. As we can see from the figures, for $\tilde{\gamma} = 1$, it is not possible to find a suitable σ_1 where the full NEC is valid at every point of the space. Moreover, at points near the throat, NEC is always invalid for $\tilde{\gamma} = 1$. Although, for $\tilde{\gamma} = -1$, in the region $0 \lesssim \sigma_1 \lesssim 2$, the full NEC is valid everywhere.

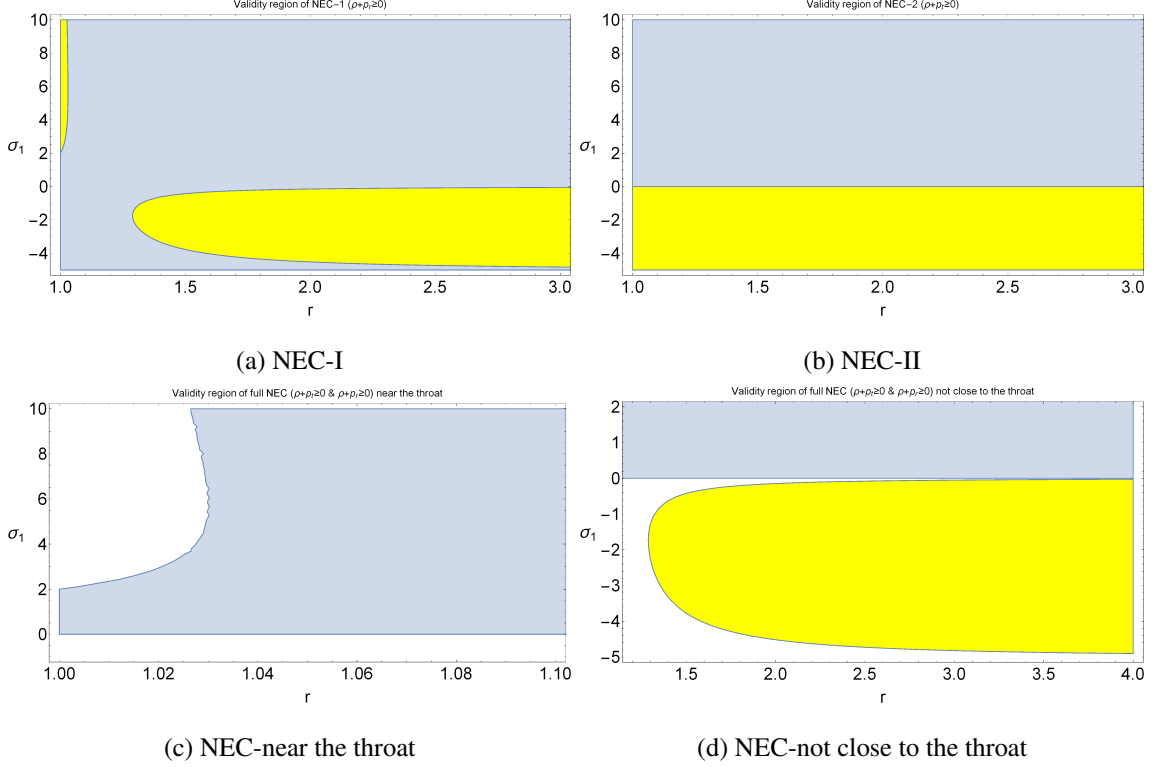


Figure 4.3: Validity of NEC-1 ($\rho + p_r \geq 0$) given by (4.2.5), NEC-2 ($\rho + p_t \geq 0$) given by (4.2.6) and the full condition for the validity of NEC ($\rho + p_t \geq 0$ & $\rho + p_r \geq 0$) for the generic anisotropic fluid in BD theory. The yellow regions represent the regions where $\tilde{\gamma} = 1$ whereas the blue regions represent when $\tilde{\gamma} = -1$. For these plots, we have chosen the values $r_0 = \phi_0 = d = \omega_0 = 1$ and $\sigma_2 = 1$.

Finally, Figs. 4.4a and 4.4b show the validity of the full WEC ($\rho \geq 0$ & $\rho + p_r \geq 0$ & $\rho + p_t \geq 0$) close and not so close to the throat respectively. From those figures, we can see that the full WEC is valid only for some very special regions for $\tilde{\gamma} = 1$ and moreover for observers closer to the throat, it would be always invalid. This is consistent with the full NEC (see Figs. 4.3c and 4.3d) since if NEC is violated, then WEC will be also violated. On the other hand, for $\tilde{\gamma} = -1$, there are different ranges where WEC is valid but only for the range where $0 \lesssim \sigma_1 \lesssim 2$, WEC is valid independently of the location of the observer. As a consistency checking, Fig. 4.5 shows the behaviour of ρ , $\rho + p_r$ and $\rho + p_t$ for a special model where $\tilde{\gamma} = -1$ and $\sigma_1 = 1$. In this model, WEC is satisfied at all locations since all the important quantities are always positive.

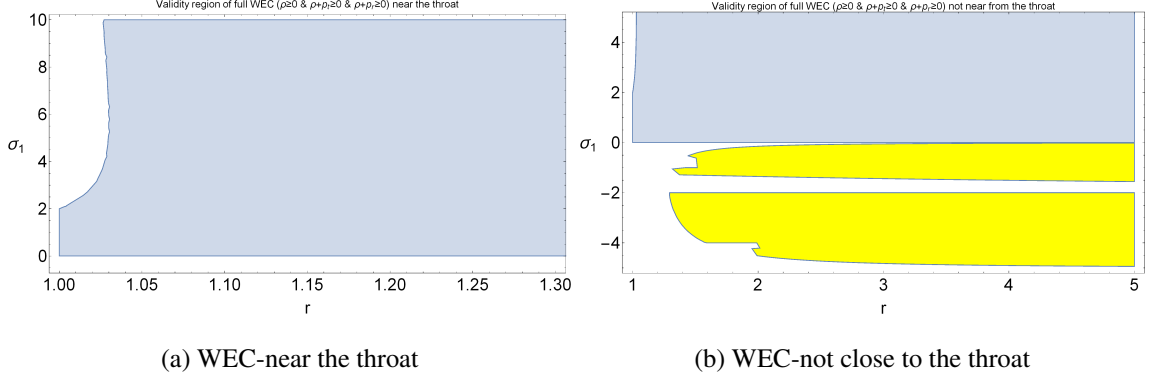


Figure 4.4: Validity of WEC given by the validity of (4.2.4)-(4.2.6) for the generic anisotropic fluid in BD theory. The figure on the right represents the validity of WEC near the throat whereas the figure on the left shows the validity for locations that are not close to the throat. The yellow regions represent the regions where $\tilde{\gamma} = 1$ whereas the blue regions represent when $\tilde{\gamma} = -1$. For these plots, we have chosen the values $r_0 = \phi_0 = d = \omega_0 = 1$ and $\sigma_2 = 1$.

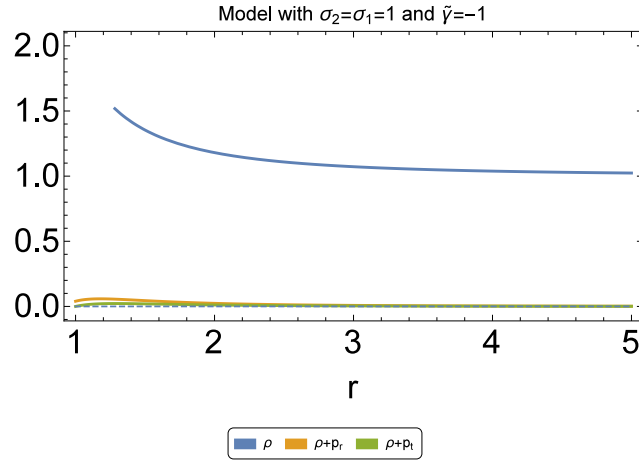


Figure 4.5: Energy density, sum of the radial pressure and the energy density and the sum of the lateral pressure and the energy density for the generic anisotropic fluid in BD theory where $\sigma_1 = \sigma_2 = 1$ and $\tilde{\gamma} = -1$. We have further chosen the values $r_0 = \phi_0 = d = \omega_0 = 1$. For this model, the full WEC is always satisfies.

Let us now try to analyse the model for an arbitrary shape function parameter σ_2 . In this case, we have three parameters, namely, $\tilde{\gamma}$, σ_1 and σ_2 . As we have said before, the sign of $\tilde{\gamma}$

is important but not its strength. Figs. 4.6 show region plots for the validity of the full NEC and WEC for positive and negatives values of $\tilde{\gamma}$. One can notice that it is not possible to model wormholes satisfying the full NEC everywhere for positive $\tilde{\gamma}$ since depending on the location of the observer, that energy condition would be valid or not. For negative values of $\tilde{\gamma}$, there are different models depending on σ_2 and σ_1 which ensures that the wormhole is supported by non-exotic matter at every point of the space. In those specific models, the full WEC is always satisfied.

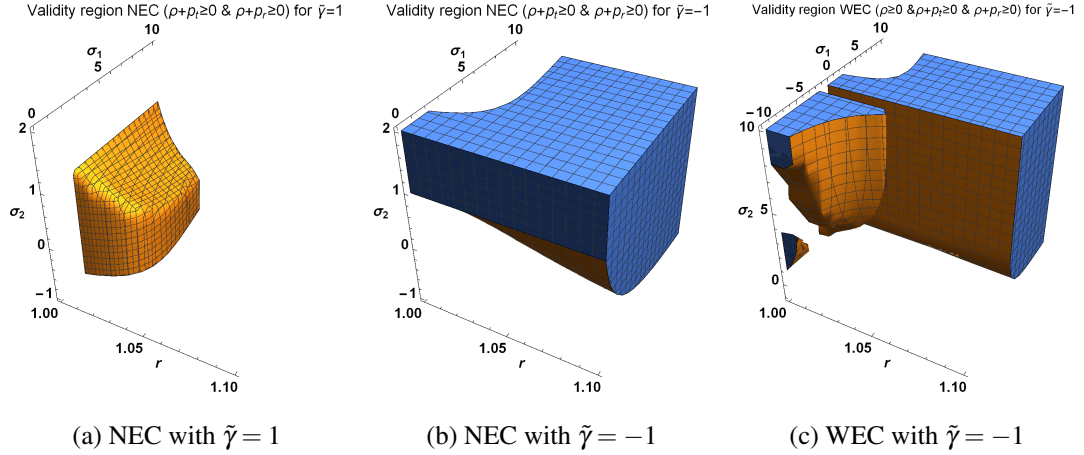


Figure 4.6: Validity of NEC and WEC given by the validity of (4.2.4)-(4.2.6) for the generic anisotropic fluid in BD theory. The figure on the left represents the validity of NEC for $\tilde{\gamma} = 1$ whereas the figure on the centre represents the validity for $\tilde{\gamma} = -1$. Lastly, the figure on the right shows the validity of WEC for $\tilde{\gamma} = -1$. For these plots, we have chosen the values $r_0 = \phi_0 = d = \omega_0 = 1$. We can notice that various model exist where the full WEC is valid for $\tilde{\gamma} = -1$ whereas for $\tilde{\gamma} = 1$, it is not possible to find that NEC is valid for every location.

4.2.2 Induced gravity

In this section, we will study the energy conditions for the induced gravity case. To recover this case, we must choose $\eta = 2$ with $\zeta > 0$. Then, we have four free parameters, namely ζ , σ_1 , σ_2 and $\tilde{\gamma}$. Doing a similar approach as we did in the previous section, we can distinguish between models that do not violate the energy conditions. Without going into too much details as in the previous section, in this section we will only show the validity of the full

NEC and full WEC. If WEC is valid, all the other energy conditions will be valid too. The validity of WEC will be true if all the following three inequalities hold,

$$\begin{aligned} \rho = & -\frac{\zeta \sigma_1^3 r^{-(\zeta+2)\sigma_1-1}}{(\zeta+2)\sigma_1+1} + \frac{1}{16} \sigma_1^2 r^{-(\zeta+2)\sigma_1-2} \left(\frac{16\zeta \sigma_1 r^{-\sigma_2}}{(\zeta+2)\sigma_1+\sigma_2+2} - \frac{16((\zeta-2)\sigma_1+2)}{(\zeta+2)\sigma_1+2} \right. \\ & \left. + \frac{1}{\pi} \right) + \frac{\sigma_1^2}{16\pi} \left\{ (16\pi(\zeta \sigma_1 - \sigma_2 + 3) - (\zeta+2)\sigma_1 - \sigma_2 - 3) r^{-(\zeta+2)\sigma_1-\sigma_2-3} \right\} \{ \sigma_2 + 3 \\ & + (\zeta+2)\sigma_1 \}^{-1} + \frac{\tilde{\gamma}}{8\pi} \left[\{ 8\sigma_1^3 + \sigma_1^2(6\sigma_2+26) + \sigma_1(\sigma_2^2+8\sigma_2+8\pi(\sigma_2-3)+21) - \sigma_2 \right. \\ & \left. \times (\sigma_2+3) \} r^{-2\sigma_1-\sigma_2-3} \right] (2\sigma_1+\sigma_2+3)^{-1} - \frac{1}{4\pi} \{ \tilde{\gamma} \sigma_1 (2\sigma_1+3) r^{-2\sigma_1-2} \} + 1 \geq 0, \end{aligned} \quad (4.2.7)$$

$$\rho + p_r = \frac{\tilde{\gamma}(4\sigma_1^2 + \sigma_1(\sigma_2+11) - \sigma_2 - 1) r^{-2\sigma_1-\sigma_2-3}}{8\pi} - \frac{\tilde{\gamma} \sigma_1 (2\sigma_1+5) r^{-2\sigma_1-2}}{4\pi} \geq 0, \quad (4.2.8)$$

$$\rho + p_t = \frac{\tilde{\gamma}(12\sigma_1 - \sigma_2 + 1) r^{-2\sigma_1-\sigma_2-3}}{16\pi} - \frac{3\tilde{\gamma} \sigma_1 r^{-2\sigma_1-2}}{4\pi} \geq 0. \quad (4.2.9)$$

Note that the validity of the last two inequalities do not depend on the parameter ζ . Hence, the validity of the full NEC will not depend on the parameter ζ . Figs. 4.7a and 4.7b show the validity of NEC for $\tilde{\gamma} = 1$ and $\tilde{\gamma} = -1$ respectively. Exactly as the BD case, NEC cannot be true for every location when $\tilde{\gamma}$ is positive. Moreover, the problem comes near the throat. Hence, the full WEC will be also not true at every location for induced gravity when $\tilde{\gamma}$ is positive. On the other hand, for negative $\tilde{\gamma}$, it is possible to ensure the validity of NEC for some parameters σ_1 and σ_2 . Fig. 4.7c shows the validity of WEC for $\zeta = 2$ and $\tilde{\gamma} = -1$. Since ρ depends on ζ , the validity of WEC will depend on ζ too. For bigger values of ζ , the validity of WEC is more constraint. However, it always exists a small range of values of σ_1 and σ_2 where WEC will be true at every location (even near the throat). From the figure one can notice that this small region is $-1 \lesssim \sigma_1 \lesssim 1$. Fig. 4.8 depicts the energy density and the sum of the pressures with the energy density for a model in this range, where $\sigma_1 = 0.5$. In the latter figure, we have further chosen $\zeta = \sigma_2 = 2$ and $\tilde{\gamma} = -1$. One can see from the figure, that WEC is always true in this model.

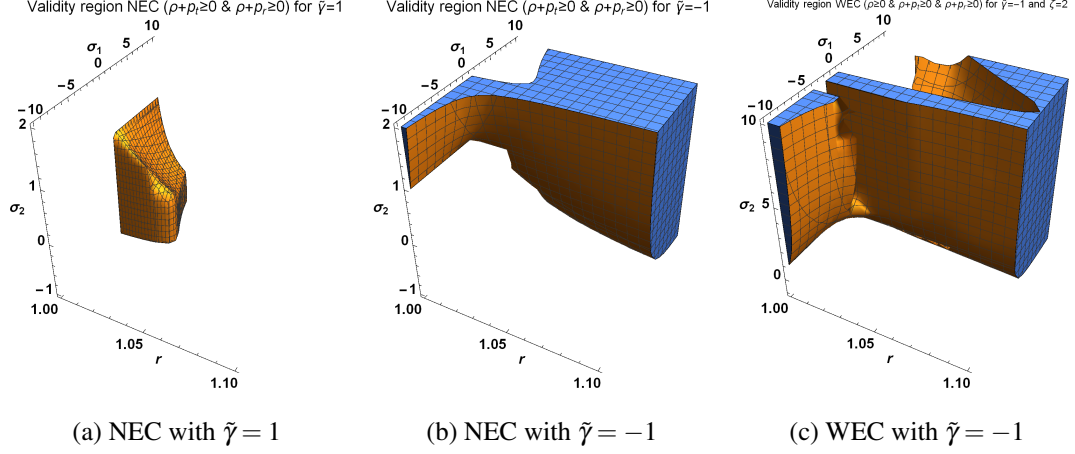


Figure 4.7: Validity of NEC and WEC given by the validity of (4.2.7)-(4.2.9) for the generic anisotropic fluid in induced gravity. The figure on the left represents the validity of NEC for $\tilde{\gamma} = 1$ whereas the figure on the centre represents the validity for $\tilde{\gamma} = -1$. Lastly, the figure on the right shows the validity of WEC for $\tilde{\gamma} = -1$ and $\zeta = 2$. For these plots, we have chosen the values $r_0 = \phi_0 = d = \omega_0 = 1$. We can notice that various model exist where the full WEC is valid for $\tilde{\gamma} = -1$ whereas for $\tilde{\gamma} = 1$, it is not possible to find that NEC is valid for every location.

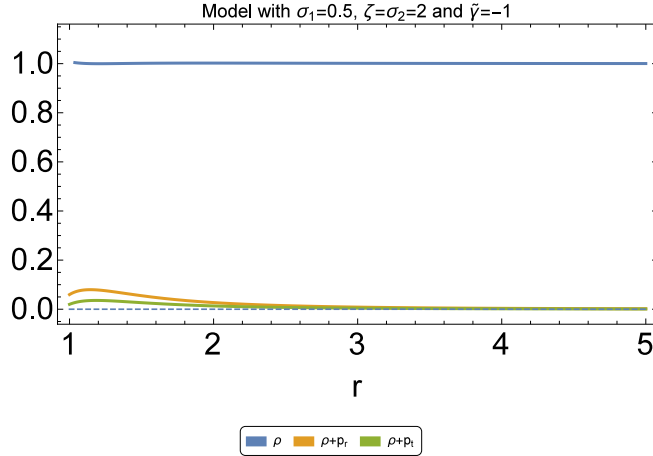


Figure 4.8: Energy density, sum of the radial pressure and the energy density and the sum of the lateral pressure and the energy density for the generic anisotropic fluid in induced gravity where $\sigma_1 = 0.5$, $\sigma_2 = \zeta = 2$ and $\tilde{\gamma} = -1$. We have further chosen the values $r_0 = \phi_0 = d = \omega_0 = 1$. For this model, the full WEC always satisfies.

4.3 Isotropic Fluid ($p_r = p_t = p$)

In this case we will take $p_r = p_t = p$ and substituting $e^{-b(r)} = 1 - \frac{\beta(r)}{r}$ we have equation in terms of shape function of the form:

$$\frac{\tilde{\gamma}}{dr\kappa^2}\phi_0^\eta\left(\frac{d}{r}\right)^{\eta\sigma_1}\left[d^2r(\eta\sigma_1-1)\beta'(r)+\{-2\eta\sigma_1^3(\sigma_1-1)+d^2(3-7\eta\sigma_1+2\eta\sigma_1^2-2\eta^2\sigma_1^2)\}\beta(r)+2\eta r\sigma_1\{\sigma_1^2(\sigma_1-1)+d^2(3+\eta\sigma_1-\sigma_1)\}\right]=0. \quad (4.3.1)$$

We can easily solve this equation analytically and we have shape function of the form

$$\beta(r) = -\xi_1 r + c_1 r^{-\eta_1}, \quad (4.3.2)$$

where c_1 is constant of integration and $A_1 = d^2(\eta\sigma_1 - 1)$,

$$A_2 = -2\eta\sigma_1^3(\sigma_1 - 1) + d^2\{3 - 7\eta\sigma_1 + 2\eta\sigma_1^2 - 2\eta^2\sigma_1^2\},$$

$$A_3 = 2\eta\sigma_1\{\sigma_1^2(\sigma_1 - 1) + d^2(3 + \eta\sigma_1 - \sigma_1)\}, \quad \xi_1 = \frac{A_3}{A_1 + A_2} \text{ and } \eta_1 = \frac{A_2}{A_1}.$$

Using power law ansatz with model (4.1.13) and radial function (4.3.2) into (2.9.3) and integrating we have scalar potential of the form

$$\begin{aligned} V(\phi) &= \frac{2\eta\tilde{\gamma}\xi_1\sigma_1 d^{-2}\phi_0^{-2/\sigma_1}}{\eta\sigma_1 + 2}\phi^{\frac{\eta\sigma_1+2}{\sigma_1}} + \frac{\omega_0\sigma_1^2(1+\xi_1)(-2+2\sigma_1+\zeta\sigma_1)d^{-2}\phi_0^{-2/\sigma_1}}{\zeta\sigma_1+2\sigma_1+2} \\ &\times \phi^{\frac{\zeta\sigma_1+2\sigma_1+2}{\sigma_1}} - \frac{\omega_0 c_1 \sigma_1^2(-1+\eta_1+2\sigma_1+\zeta\sigma_1)d^{-3-\eta_1}\phi_0^{\frac{-3-\eta_1}{\sigma_1}}}{\zeta\sigma_1+2\sigma_1+\eta_1+3}\phi^{\zeta+2+\frac{\eta_1+3}{\sigma_1}} \\ &+ \frac{2\eta c_1 \eta_1 \tilde{\gamma} \sigma_1 d^{-\eta_1-3}\phi_0^{\frac{-\eta_1-3}{\sigma_1}}}{\eta\sigma_1+\eta_1+3}\phi^{\frac{\eta\sigma_1+\eta_1+3}{\sigma_1}} + c_0. \end{aligned} \quad (4.3.3)$$

The throat is located at $r = r_0$ if it satisfy the condition $\beta(r_0) = r_0$. Using this relation we have calculated that the throat is located at $r_0 = \left(\frac{c_1}{1+\xi_1}\right)^{\frac{1}{\eta_1+1}}$. The constant of integration is calculated $c_1 = (1+\xi_1)r_0^{1+\eta_1}$ by using the relation $\beta(r_0) = r_0$. Using $\beta'(r_0) = -\xi_1 - c_1\eta_1 r_0^{-1-\eta_1}$ one can also conclude that $\beta'(r_0) < 1$ imposes the restriction $\eta_1 > -1$. The asymptotically flatness condition is $\frac{\beta(r)}{r} \rightarrow -\xi_1$ as $r \rightarrow \infty$.

Taking $\eta = 1$ and $\zeta = -1$, we get $f(R, \phi) = \tilde{\gamma}R\phi$ which describes the BD theory. We will discuss the behavior of $\beta(r)$, ρ and $\rho + p$ by taking the parameters $d = \omega_0 = c_0 = \phi_0 = 1$, $\sigma_1 = -2.4$, $r_0 = 1$ and $\tilde{\gamma} = -0.5$. The behavior of the shape function is shown in Fig. 4.9. It shows that $\beta(r)$ is increasing and also satisfy $\beta(r) < r$. The behavior of NEC

and WEC is shown in Fig.4.10. In that case, $\rho > 0$ and $\rho + p > 0$ are satisfied throughout the evolution.

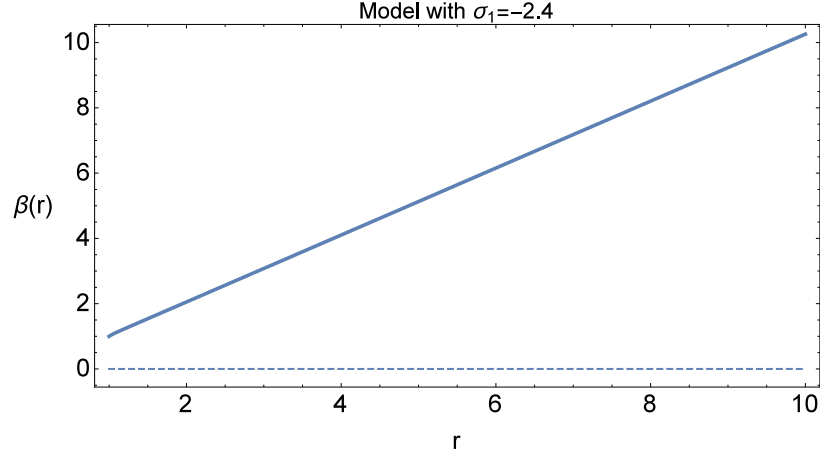


Figure 4.9: The behavior of $\beta(r)$ versus r taking $\eta = 1$, $\zeta = -1$, $\sigma_1 = -2.4$, $r_0 = 1$ in case of BD theory.

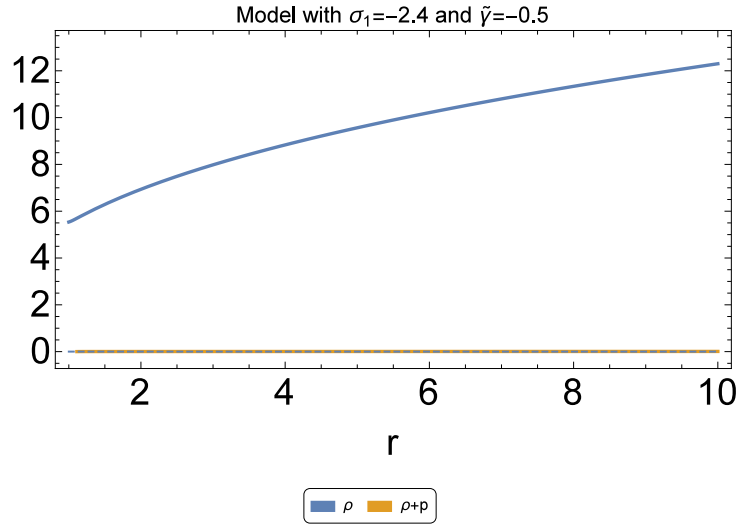


Figure 4.10: The behavior of ρ and $\rho + p_r$ versus r taking $\eta = 1$, $\zeta = -1$, $\sigma_1 = -2.4$, $r_0 = 1$ for BD theory.

For induced gravity, we have taken $\eta = 2$, $\zeta > 0$. To analyze the plots of $\beta(r)$, ρ and $\rho + p$ we have chosen the parameters $\omega_0 = -0.5$, $r_0 = d = c_0 = 1$, $\phi_0 = 0.05$, $\sigma_1 = -2.4$ and $\tilde{\gamma} = -0.5$.

In Fig.4.11, plot shows the increasing behavior of shape function and validate the term $\beta(r) < r$. The behavior of NEC and WEC is shown in Fig.4.12, which shows the validity

throughout the evolution.

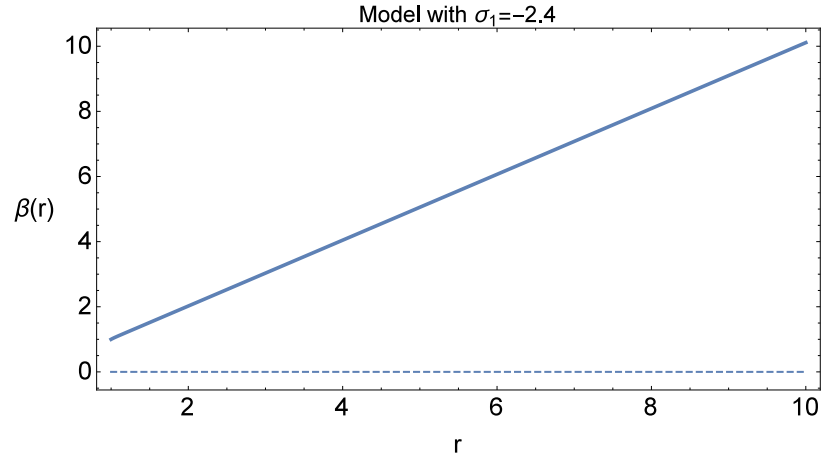


Figure 4.11: The behavior of $\beta(r)$ versus r taking $\eta = 2$, $\zeta = 2$, $\sigma_1 = -2.4$, $r_0 = 1$ in case of Induced gravity.

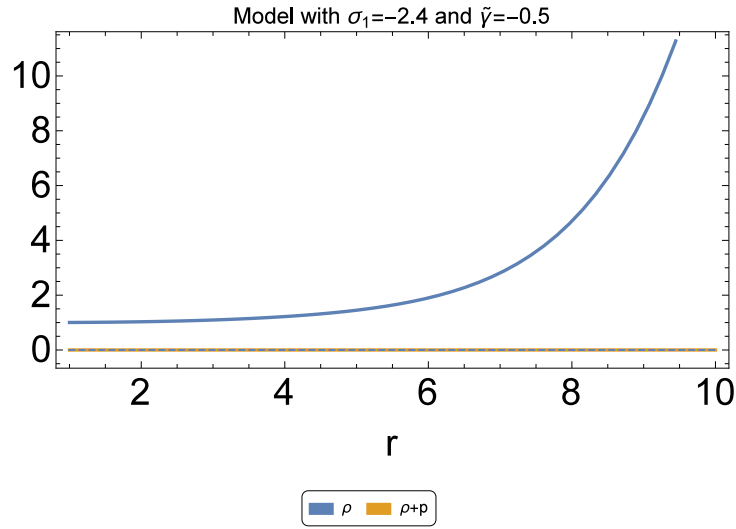


Figure 4.12: Plot shows the evolution of ρ and $\rho + p$ in case of Induced gravity for the parameters $\eta = 2$, $\zeta = 2$, $\sigma_1 = -2.4$, $r_0 = 1$, $\tilde{\gamma} = -0.5$.

4.4 Barotropic fluid with EoS $p_r = w(r)\rho$

In this section, we are applying a specific EoS $p_r = w(r)\rho$ which involves radial pressure, energy density and a positive radial function $w(r)$. In [171], Rahaman et al. has used that

type of EoS with varying parameter. We are using here scalar potential of the form

$$V(\phi) = \frac{V_0}{\phi^{\delta_1}}$$

4.4.1 $w(r) = w = \text{Constant}$

First we are taking $w(r) = w = \text{constant}$. Utilizing the above EoS with constant parameter for our field equations (4.1.14), (4.1.15), we have constraint of the following form

$$\begin{aligned} & \frac{\phi_0^{-\delta_1}}{r\kappa^2} \left(\frac{d}{r} \right)^{-\delta_1\sigma_1} \left[-2\kappa^2 r^3 V_0(w+1) + 2\eta r \tilde{\gamma} \sigma_1 (-2+3w+\eta\sigma_1 w) \phi_0^{\eta+\delta_1} \left(\frac{d}{r} \right)^{\sigma_1(\eta+\delta_1)} \right. \\ & - r\omega_0 \sigma_1^2 (w+1) \phi_0^{\zeta+2+\delta_1} \left(\frac{d}{r} \right)^{\sigma_1(\zeta+2+\delta_1)} + \omega_0 \sigma_1^2 (w+1) \beta(r) \left(\frac{d}{r} \right)^{\sigma_1(\zeta+2+\delta_1)} \\ & \times \phi_0^{\zeta+2+\delta_1} - \tilde{\gamma} \phi_0^{\eta+\delta_1} \left(\frac{d}{r} \right)^{\sigma_1(\eta+\delta_1)} \{ (2-4\eta\sigma_1+7\eta\sigma_1 w+2\eta^2\sigma_1^2 w) \beta(r) + rw \\ & \left. \times (2-\eta\sigma_1) \beta'(r) \} \right] = 0. \end{aligned} \quad (4.4.1)$$

It cannot be solved analytically, that's why we are solving it numerically and results are shown below.

- Brans-Dicke Theory:

In case of BD we are using $\eta = 1$, $\zeta = -1$ and by varying the parameters ω_0 , σ_1 , $\tilde{\gamma}$, δ_1 , w , ϕ_0 , V_0 we will discuss the behavior of $\beta(r)$, $\beta'(r)$, $\frac{\beta(r)}{r}$, $\beta(r) - r$, ρ , $\rho + p_r$ and $\rho + p_t$.

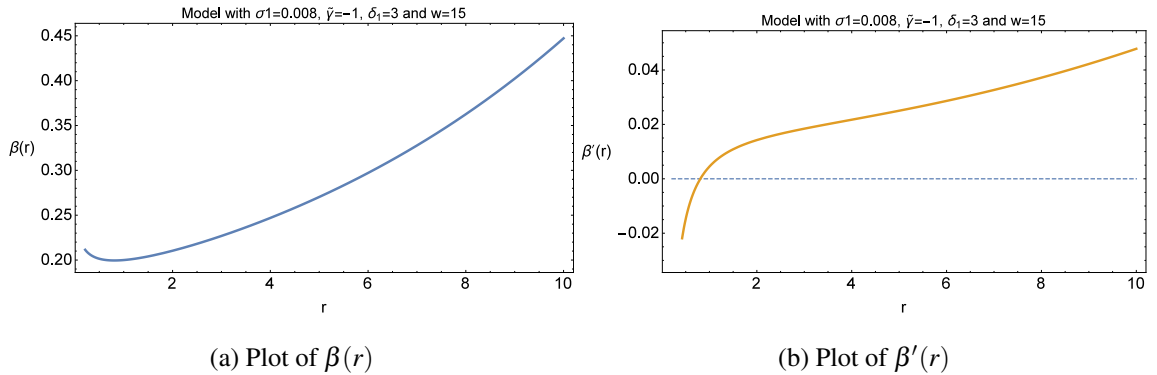


Figure 4.13: The behavior of $\beta(r)$ and $\beta'(r)$ versus r taking $\omega_0 = -2$, $\sigma_1 = 0.008$, $\tilde{\gamma} = -1$, $\delta_1 = 3$, $w = 15$, $\phi_0 = 10$, $V_0 = 0.1$.

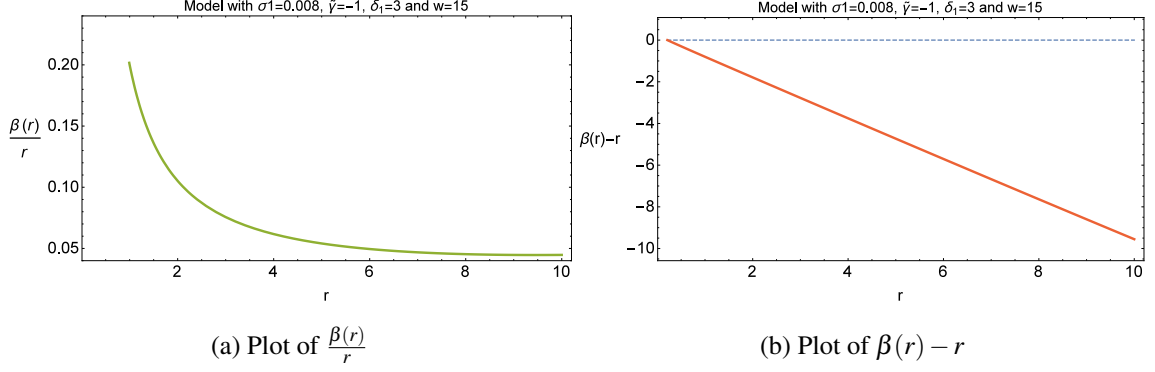


Figure 4.14: The behavior of $\frac{\beta(r)}{r}$ and $\beta(r) - r$ versus r taking $\omega_0 = -2$, $\sigma_1 = 0.008$, $\tilde{\gamma} = -1$, $\delta_1 = 3$, $w = 15$, $\phi_0 = 10$, $V_0 = 0.1$.

In Fig.4.13a behavior of the shape function has been shown. It can be analyzed that it shows the increasing behavior and meet the inequality $\beta(r) < r$. It can be seen from Fig.4.14a that $\beta(r)/r \rightarrow 0$ as $r \rightarrow \infty$ that means the spacetime is asymptotically flat. Fig.4.14b shows that $\beta(r) - r < 0$, which fulfill the condition $1 - \beta(r)/r > 0$. Using $\beta(r_0) = r_0$ we have throat at $r_0 = 0.2114$. The plot of $\beta'(r)$ is shown in Fig.4.13b and $\beta'(r_0) = -0.0709365$ which fulfill the condition $\beta'(r_0) < 1$. Evolution of NEC and WEC is shown in Fig.4.15. Here $\rho > 0$ and $\rho + p_r > 0$ are satisfied throughout the evolution but $\rho + p_t > 0$ is not satisfied.

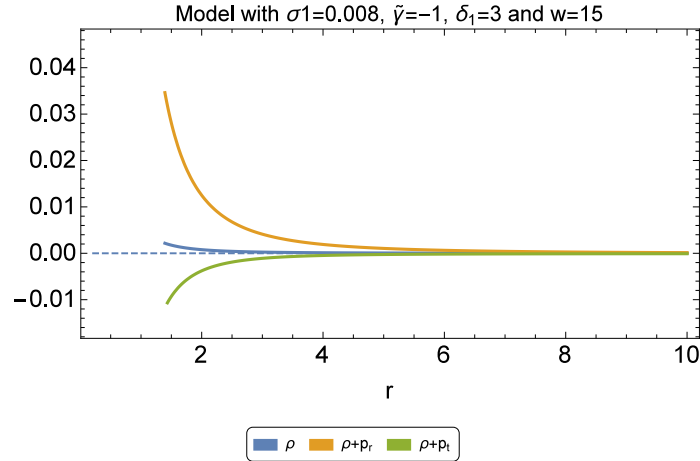


Figure 4.15: The behavior of ρ , $\rho + p_r$ and $\rho + p_t$ versus r for the parameters $\omega_0 = -2$, $\sigma_1 = 0.008$, $\tilde{\gamma} = -1$, $\delta_1 = 3$, $w = 15$, $\phi_0 = 10$, $V_0 = 0.1$.

- Induced Gravity:

For induced gravity we use $\eta = 2$, $\zeta > 0$ and by varying the parameters ω_0 , σ_1 , $\tilde{\gamma}$, δ_1 , w , ϕ_0 , V_0 , we will discuss the behavior of $\beta(r)$, $\beta'(r)$, $\frac{\beta(r)}{r}$, $\beta(r) - r$, ρ , $\rho + p_r$ and $\rho + p_t$.

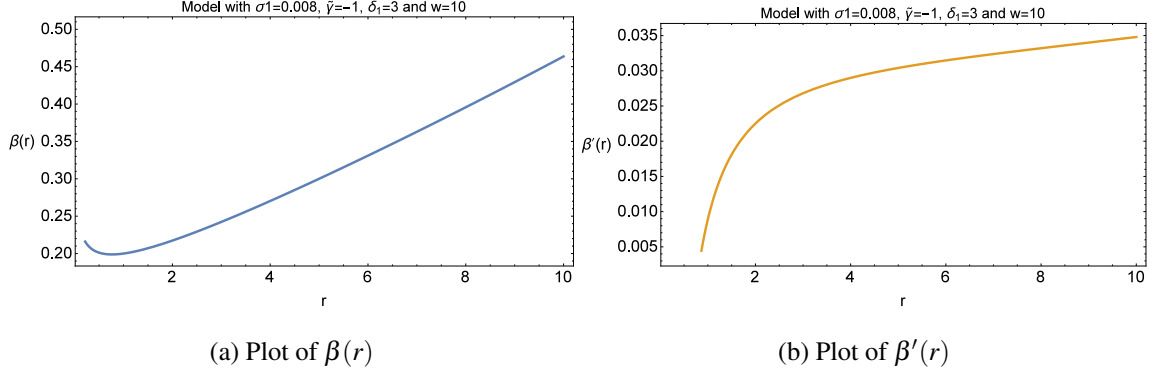


Figure 4.16: The behavior of $\beta(r)$ and $\beta'(r)$ versus r taking $\omega_0 = -2$, $\sigma_1 = 0.008$, $\tilde{\gamma} = -1$, $\delta_1 = 3$, $w = 10$, $\phi_0 = 10$, $V_0 = 0.1$.

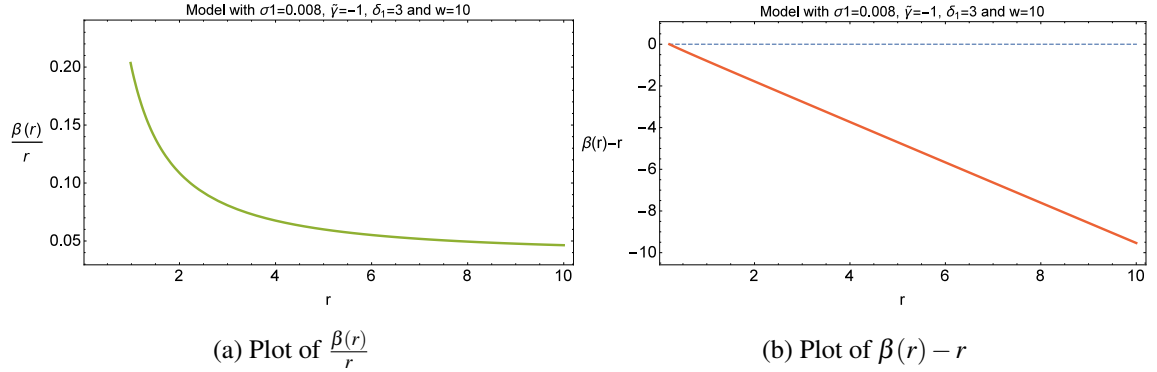


Figure 4.17: The behavior of $\frac{\beta(r)}{r}$ and $\beta(r) - r$ versus r taking $\omega_0 = -2$, $\sigma_1 = 0.008$, $\tilde{\gamma} = -1$, $\delta_1 = 3$, $w = 10$, $\phi_0 = 10$, $V_0 = 0.1$.

In Fig.4.16a behavior of the shape function has been shown. It can be analyzed that it shows the increasing behavior and meet the inequality $\beta(r) < r$. It can be seen from Fig.4.17a that $\beta(r)/r \rightarrow 0$ as $r \rightarrow \infty$ that means the spacetime is asymptotically flat. The plot in Fig.4.17b shows that $\beta(r) - r < 0$, which fulfill the condition $1 - \beta(r)/r > 0$. Using $\beta(r_0) = r_0$, we have throat at $r_0 = 0.2159$. The plot of $\beta'(r)$ is shown in Fig.4.16b and $\beta'(r_0) = -0.108932$ which fulfill the condition $\beta'(r_0) < 1$. Evolution of NEC and WEC

is shown in Fig.4.18. Here $\rho > 0$ and $\rho + p_r > 0$ are satisfied throughout the evolution but $\rho + p_t > 0$ is not satisfied in this case.

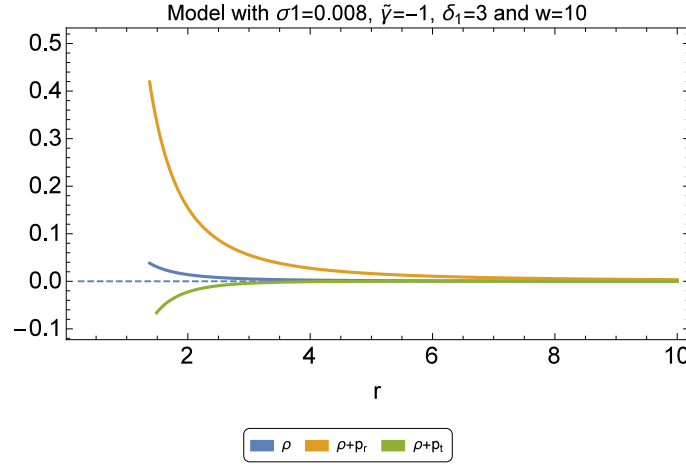


Figure 4.18: The behavior of ρ , $\rho + p_r$ and $\rho + p_t$ for the parameters $\omega_0 = -2$, $\sigma_1 = 0.008$, $\tilde{\gamma} = -1$, $\delta_1 = 3$, $w = 10$, $\phi_0 = 10$, $V_0 = 0.1$.

4.4.2 $w(r) = \tilde{B}r^l$

Now we will take $w(r) = \tilde{B}r^l$ with \tilde{B} and l as positive constants. Utilizing the above EoS with variable parameter for our field equations (4.1.14), (4.1.15) we have constraint of the following form

$$\begin{aligned} & \frac{\phi_0^{-\delta_1}}{r\kappa^2} \left(\frac{d}{r} \right)^{-\delta_1 \sigma_1} \left[-2\kappa^2 r^3 V_0 (1 + \tilde{B}r^l) + 2\eta r \tilde{\gamma} \sigma_1 (-2 + 3\tilde{B}r^l + \eta \sigma_1 \tilde{B}r^l) \phi_0^{\eta + \delta_1} \right. \\ & \times \left(\frac{d}{r} \right)^{\sigma_1 (\eta + \delta_1)} - r \omega_0 \sigma_1^2 (1 + \tilde{B}r^l) \phi_0^{\zeta + 2 + \delta_1} \left(\frac{d}{r} \right)^{\sigma_1 (\zeta + 2 + \delta_1)} + \omega_0 \sigma_1^2 (1 + \tilde{B}r^l) \phi_0^{\zeta + 2 + \delta_1} \\ & \times \left(\frac{d}{r} \right)^{\sigma_1 (\zeta + 2 + \delta_1)} \beta(r) - \tilde{\gamma} \phi_0^{\eta + \delta_1} \left(\frac{d}{r} \right)^{\sigma_1 (\eta + \delta_1)} \left\{ (2 - 4\eta \sigma_1 + 7\eta \sigma_1 \tilde{B}r^l + 2\eta^2 \sigma_1^2 \tilde{B}r^l) \right. \\ & \left. \left. \times \beta(r) + \tilde{B}r^{l+1} (2 - \eta \sigma_1) \beta'(r) \right\} \right] = 0. \end{aligned} \quad (4.4.2)$$

We are solving it numerically because analytically it cannot be solved. The results are shown below.

- Brans-Dicke Theory:

In case of BD we are using $\eta = 1$, $\zeta = -1$ and by choosing the parameters $\omega_0 = -2$, $\sigma_1 = 0.008$, $\tilde{\gamma} = -1$, $\delta_1 = 5$, $\tilde{B} = 2$, $l = 5$, $\phi_0 = 10$, $V_0 = 0.1$ we will discuss the behavior of $\beta(r)$, $\beta'(r)$, $\frac{\beta(r)}{r}$, $\beta(r) - r$, ρ , $\rho + p_r$ and $\rho + p_t$.

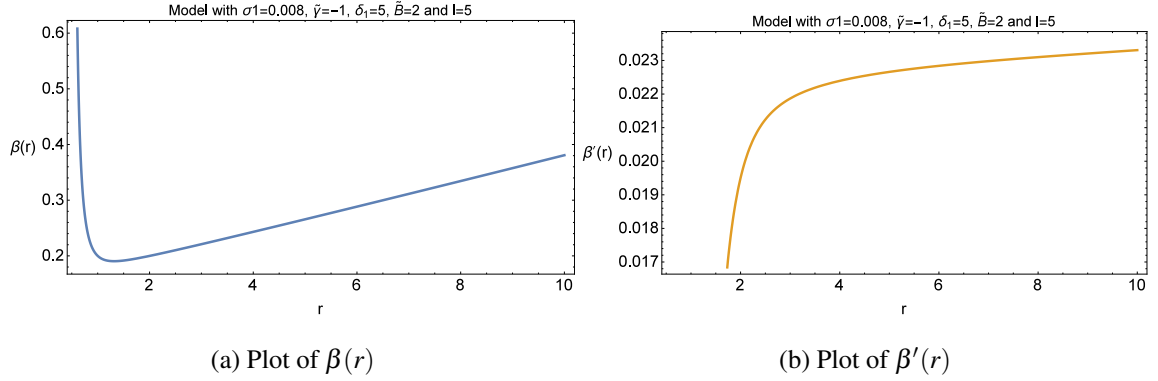


Figure 4.19: The behavior of $\beta(r)$ and $\beta'(r)$ versus r taking $\omega_0 = -2$, $\sigma_1 = 0.008$, $\tilde{\gamma} = -1$, $\delta_1 = 5$, $\tilde{B} = 2$, $l = 5$, $\phi_0 = 10$, $V_0 = 0.1$.

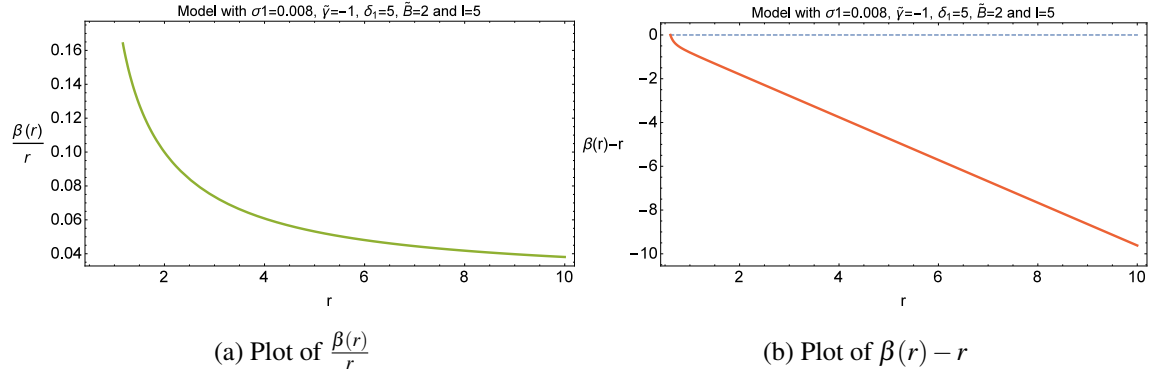


Figure 4.20: Left plot shows the behavior of $\frac{\beta(r)}{r}$ and right plot shows the behavior of $\beta(r) - r$ versus r for the parameters $\omega_0 = -2$, $\sigma_1 = 0.008$, $\tilde{\gamma} = -1$, $\delta_1 = 5$, $\tilde{B} = 2$, $l = 5$, $\phi_0 = 10$, $V_0 = 0.1$.

In Fig.4.19a behavior of the shape function has been shown. It can be analyzed that it shows the increasing behavior and meet the inequality $\beta(r) < r$. The plot in Fig.4.20a shows that $\beta(r)/r \rightarrow 0$ as $r \rightarrow \infty$ that means the spacetime is asymptotically flat. The plot in Fig.4.20b shows that $\beta(r) - r < 0$, which fulfill the condition $1 - \beta(r)/r > 0$. For

$\beta(r_0) = r_0$, the throat is located at $r_0 = 0.60765$. The plot of $\beta'(r)$ is shown in Fig.4.19b and $\beta'(r_0) = -6.06523$ which fulfill the condition $\beta'(r_0) < 1$. The Fig.4.21 shows the evolution of NEC and WEC. Here $\rho > 0$ and $\rho + p_r > 0$ are satisfied throughout the evolution but $\rho + p_t > 0$ is not satisfied.

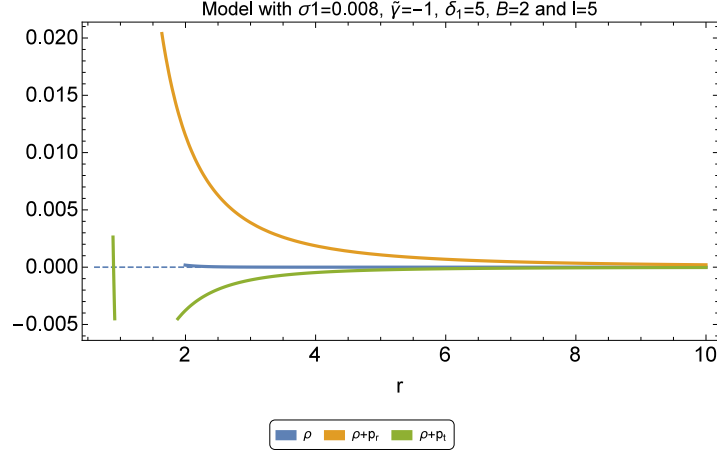


Figure 4.21: The behavior of ρ , $\rho + p_r$ and $\rho + p_t$ versus r for the parameters $\omega_0 = -2$, $\sigma_1 = 0.008$, $\tilde{\gamma} = -1$, $\delta_1 = 5$, $\tilde{B} = 2$, $l = 5$, $\phi_0 = 10$, $V_0 = 0.1$.

- Induced Gravity:

For induced gravity we use $\eta = 2$, $\zeta > 0$ and by choosing the parameters $\omega_0 = -2$, $\sigma_1 = 0.008$, $\tilde{\gamma} = -1$, $\delta_1 = 3$, $\tilde{B} = 2$, $l = 2.5$, $\phi_0 = 10$, $V_0 = 0.1$, we will discuss the behavior of $\beta(r)$, $\beta'(r)$, $\frac{\beta(r)}{r}$, $\beta(r) - r$, ρ , $\rho + p_r$ and $\rho + p_t$.

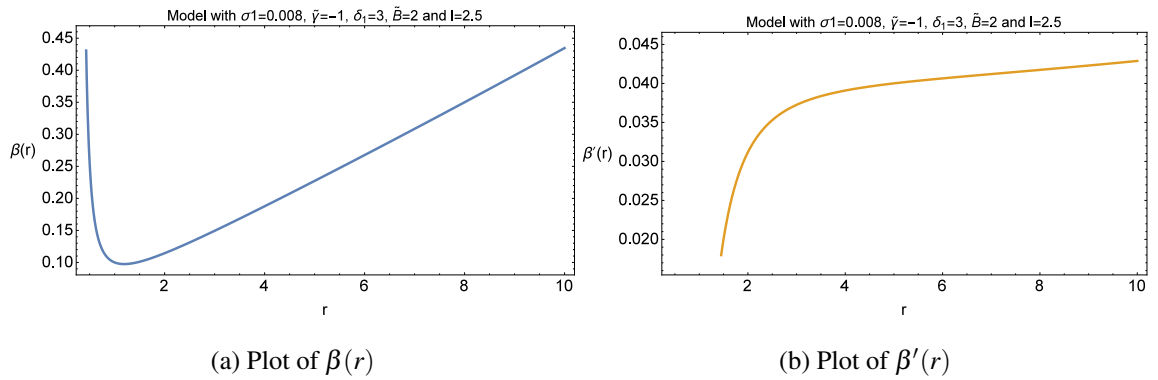


Figure 4.22: The behavior of $\beta(r)$ and $\beta'(r)$ versus r taking $\omega_0 = -2$, $\sigma_1 = 0.008$, $\tilde{\gamma} = -1$, $\delta_1 = 3$, $\tilde{B} = 2$, $l = 2.5$, $\phi_0 = 10$, $V_0 = 0.1$.

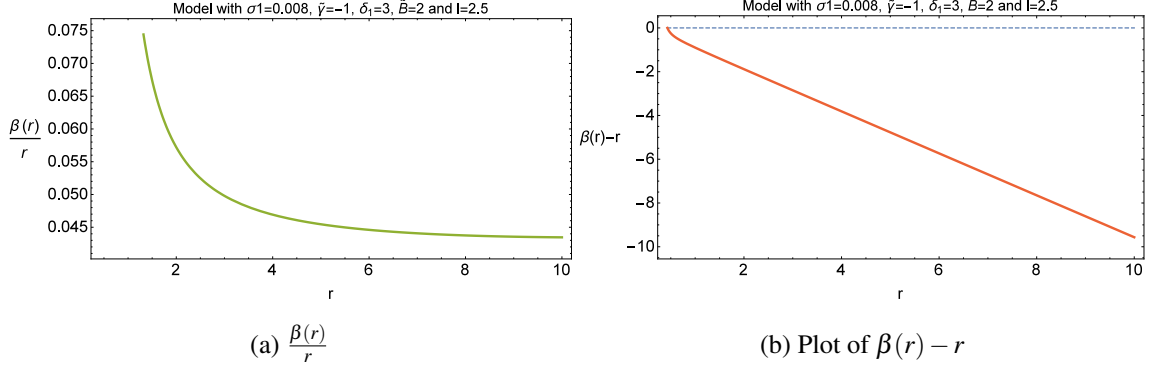


Figure 4.23: The behavior of $\frac{\beta(r)}{r}$ and $\beta(r) - r$ versus r taking $\omega_0 = -2$, $\sigma_1 = 0.008$, $\tilde{\gamma} = -1$, $\delta_1 = 3$, $\tilde{B} = 2$, $l = 2.5$, $\phi_0 = 10$, $V_0 = 0.1$.

The left plot of Fig.4.22a shows the behavior of the shape function. It can be analyzed that it shows the increasing behavior and meet the inequality $\beta(r) < r$. It can be seen from Fig.4.23a that $\beta(r)/r \rightarrow 0$ as $r \rightarrow \infty$ that means the spacetime is asymptotically flat. Fig.4.23b shows that $\beta(r) - r < 0$, which fulfill the condition $1 - \beta(r)/r > 0$. For $\beta(r_0) = r_0$, throat is located at $r_0 = 0.43055$. The plot of $\beta'(r)$ is shown in Fig.4.22b and $\beta'(r_0) = -4.15156$ which fulfill the condition $\beta'(r_0) < 1$. Evolution of NEC and WEC is shown in Fig.4.24. Here $\rho > 0$ and $\rho + p_r > 0$ are satisfied throughout the evolution but $\rho + p_t > 0$ is not satisfied in this case.

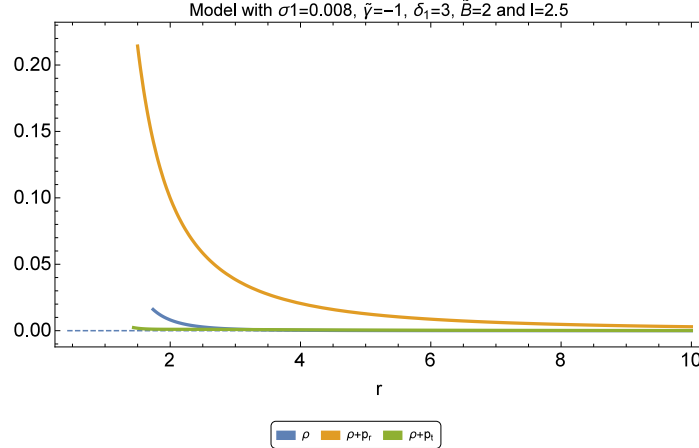


Figure 4.24: The plot shows the evolution of ρ , $\rho + p_r$ and $\rho + p_t$ for the parameters $\omega_0 = -2$, $\sigma_1 = 0.008$, $\tilde{\gamma} = -1$, $\delta_1 = 3$, $\tilde{B} = 2$, $l = 2.5$, $\phi_0 = 10$, $V_0 = 0.1$.

4.5 Barotropic fluid with EoS $p_t = w(r)\rho$

Now we will apply the EoS $p_t = w(r)\rho$ which involves lateral pressure, energy density and a positive radial function $w(r)$. In [171], Rahaman et al. has used that type of EoS with varying parameter. We are using here scalar potential of the form

$$V(\phi) = \frac{V_0}{\phi^{\delta_1}}$$

4.5.1 $w(r) = w = \text{Constant}$

First we are taking $w(r) = w = \text{constant}$. Utilizing the above EoS with constant parameter for our field equations (4.1.14), (4.1.15) we have constraint of the following form

$$\begin{aligned} & \frac{1}{r\kappa^2} \left(\frac{d}{r}\right)^{-\delta_1\sigma_1} \phi_0^{-\delta_1} \left[-2\kappa^2 r^3 V_0(w+1) + 2\eta r \tilde{\gamma} \sigma_1 (3w + \eta\sigma_1 + \eta\sigma_1 w) \phi_0^{\eta+\delta_1} \right. \\ & \times \left(\frac{d}{r}\right)^{\sigma_1(\eta+\delta_1)} - r\omega_0 \sigma_1^2 (w+1) \phi_0^{\zeta+2+\delta_1} \left(\frac{d}{r}\right)^{\sigma_1(\zeta+2+\delta_1)} + \omega_0 \sigma_1^2 (w+1) \phi_0^{\zeta+2+\delta_1} \\ & \times \left(\frac{d}{r}\right)^{\sigma_1(\zeta+2+\delta_1)} \beta(r) - \tilde{\gamma} \phi_0^{\eta+\delta_1} \left(\frac{d}{r}\right)^{\sigma_1(\eta+\delta_1)} \{ (-1 + \eta\sigma_1 + 7\eta\sigma_1 w + 2\eta^2 \sigma_1^2 \\ & \left. + 2\eta^2 \sigma_1^2 w) \beta(r) - r(-1 - 2w + \eta\sigma_1 + \eta\sigma_1 w) \beta'(r) \} \right] = 0. \end{aligned}$$

It is highly nonlinear equation, we are solving it numerically and results are shown below.

- Brans-Dicke Theory:

In case of BD we are using $\eta = 1$, $\zeta = -1$ and by choosing the parameters $\omega_0 = -2$, $\sigma_1 = 0.009$, $\tilde{\gamma} = 1$, $\delta_1 = 3$, $w = 25$, $\phi_0 = 10$, $V_0 = 0.1$ we will discuss the behavior of $\beta(r)$, $\beta'(r)$, $\frac{\beta(r)}{r}$, $\beta(r) - r$, ρ , $\rho + p_r$ and $\rho + p_t$.

In Fig.4.25a, plot shows the behavior of the shape function. It can be analyzed that it shows the increasing behavior and meet the inequality $\beta(r) < r$. It can be seen from Fig.4.26a that $\beta(r)/r \rightarrow 0$ as $r \rightarrow \infty$ that means the spacetime is asymptotically flat. Fig.4.26b shows that $\beta(r) - r < 0$, which fulfill the condition $1 - \beta(r)/r > 0$. For $\beta(r_0) = r_0$, throat is located at $r_0 = 0.18195$. The plot of $\beta'(r)$ is shown in Fig.4.25b and $\beta'(r_0) = 0.015082$ which fulfill the condition $\beta'(r_0) < 1$. Evolution of NEC and WEC is shown in right plot of

Fig.4.27. Here $\rho > 0$ and $\rho + p_t > 0$ are satisfied throughout the evolution but $\rho + p_r > 0$ is not satisfied.

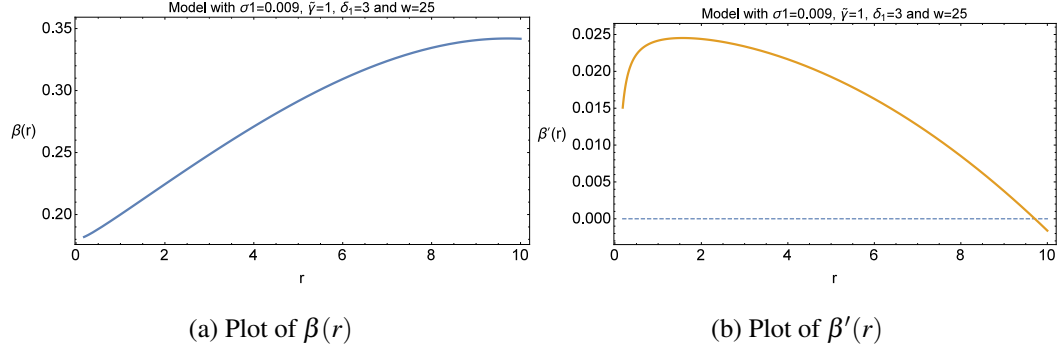


Figure 4.25: The behavior of $\beta(r)$ and $\beta'(r)$ versus r taking $\omega_0 = -2$, $\sigma_1 = 0.009$, $\tilde{\gamma} = 1$, $\delta_1 = 3$, $w = 25$, $\phi_0 = 10$, $V_0 = 0.1$.

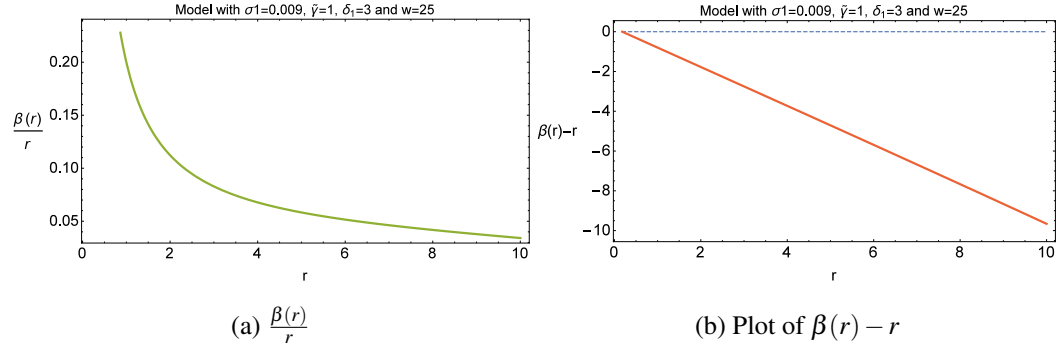


Figure 4.26: Left plot shows the behavior of $\frac{\beta(r)}{r}$ versus r and right plot shows the behavior of $\beta(r) - r$ for the parameters $\omega_0 = -2$, $\sigma_1 = 0.009$, $\tilde{\gamma} = 1$, $\delta_1 = 3$, $w = 25$, $\phi_0 = 10$, $V_0 = 0.1$.

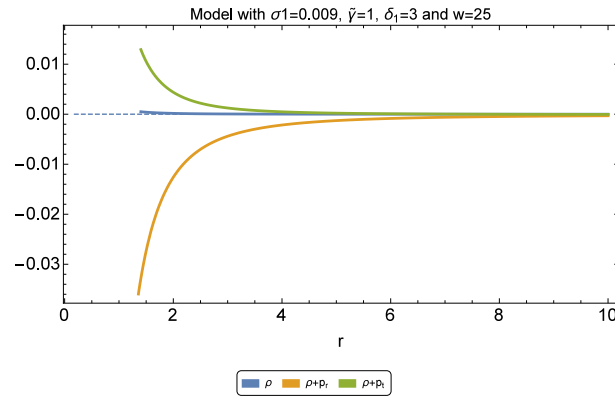


Figure 4.27: The plot shows the evolution of ρ , $\rho + p_r$ and $\rho + p_t$ for the parameters $\omega_0 = -2$, $\sigma_1 = 0.009$, $\tilde{\gamma} = 1$, $\delta_1 = 3$, $w = 25$, $\phi_0 = 10$, $V_0 = 0.1$.

- Induced Gravity:

For induced gravity we use $\eta = 2$, $\zeta > 0$ and by varying the parameters $\omega_0 = -2$, $\sigma_1 = 0.0008$, $\tilde{\gamma} = 1$, $\delta_1 = 3$, $w = 25$, $\phi_0 = 10$, $V_0 = 0.1$, we will discuss the behavior of $\beta(r)$, $\beta'(r)$, $\frac{\beta(r)}{r}$, $\beta(r) - r$, ρ , $\rho + p_r$ and $\rho + p_t$.

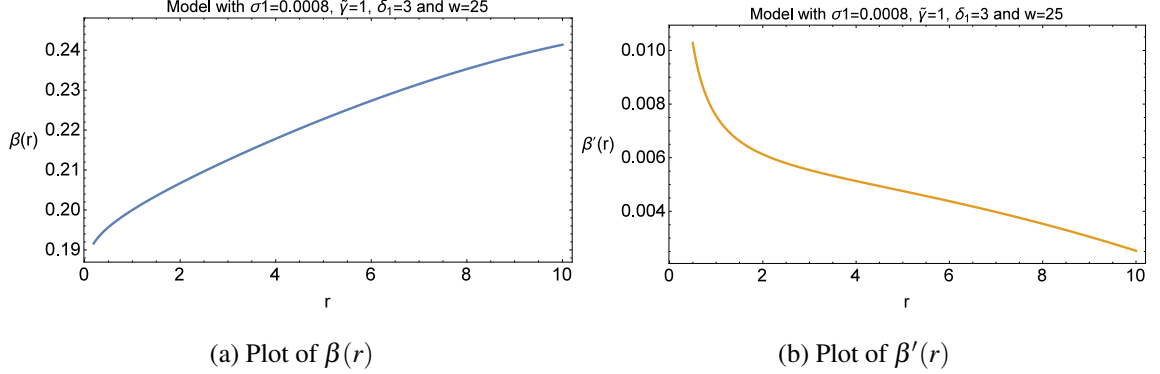


Figure 4.28: The behavior of $\beta(r)$ and $\beta'(r)$ versus r taking $\omega_0 = -2$, $\sigma_1 = 0.0008$, $\tilde{\gamma} = 1$, $\delta_1 = 3$, $w = 25$, $\phi_0 = 10$, $V_0 = 0.1$.

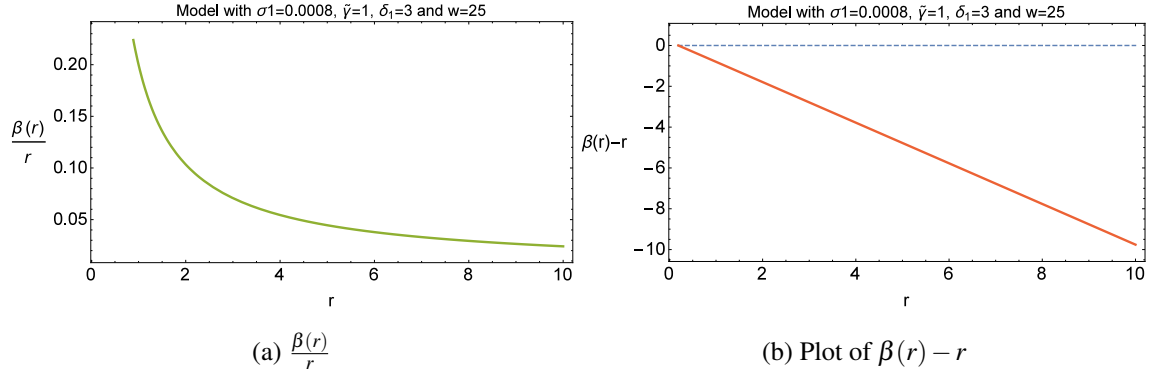


Figure 4.29: Left plot shows the behavior of $\frac{\beta(r)}{r}$ versus r and right plot shows the evolution of $\beta(r) - r$ for the parameters $\omega_0 = -2$, $\sigma_1 = 0.0008$, $\tilde{\gamma} = 1$, $\delta_1 = 3$, $w = 25$, $\phi_0 = 10$, $V_0 = 0.1$.

In Fig.4.28a behavior of the shape function has been shown. It can be analyzed that it shows the increasing behavior and meet the inequality $\beta(r) < r$. It can be seen from Fig.4.29a that $\beta(r)/r \rightarrow 0$ as $r \rightarrow \infty$ that means the spacetime is asymptotically flat. The plot of Fig.4.29b shows that $\beta(r) - r < 0$, which fulfill the condition $1 - \beta(r)/r > 0$. Using $\beta(r_0) = r_0$, we have throat at $r_0 = 0.19165$. The plot of $\beta'(r)$ is shown in Fig.4.28b and

$\beta'(r_0) = 0.0188052$ which fulfill the condition $\beta'(r_0) < 1$. Evolution of NEC and WEC is shown in Fig.4.30. Here $\rho > 0$ and $\rho + p_t > 0$ are satisfied throughout the evolution but $\rho + p_r > 0$ is not satisfied in this case.

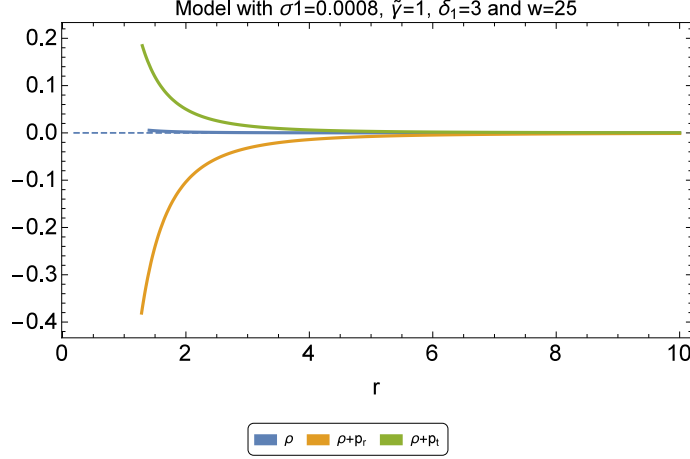


Figure 4.30: The plot shows the evolution of ρ , $\rho + p_r$ and $\rho + p_t$ for the parameters $\omega_0 = -2$, $\sigma_1 = 0.0008$, $\tilde{\gamma} = 1$, $\delta_1 = 3$, $w = 25$, $\phi_0 = 10$, $V_0 = 0.1$.

4.5.2 $w(r) = \tilde{B}r^l$

Now we will take $w(r) = \tilde{B}r^l$ with \tilde{B} and l as positive constants. Utilizing the above EoS with variable parameter for our field equations (4.1.14), (4.1.15), we have constraint of the following form

$$\begin{aligned} & \frac{1}{r\kappa^2} \left(\frac{d}{r} \right)^{-\delta_1 \sigma_1} \phi_0^{-\delta_1} \left[-2\kappa^2 r^3 V_0 (1 + \tilde{B}r^l) + 2\eta r \tilde{\gamma} \sigma_1 (3\tilde{B}r^l + \eta \sigma_1 + \eta \sigma_1 \tilde{B}r^l) \phi_0^{\eta + \delta_1} \right. \\ & \times \left(\frac{d}{r} \right)^{\sigma_1(\eta + \delta_1)} - r \omega_0 \sigma_1^2 (1 + \tilde{B}r^l) \phi_0^{\zeta + 2 + \delta_1} \left(\frac{d}{r} \right)^{\sigma_1(\zeta + 2 + \delta_1)} + \omega_0 \sigma_1^2 (1 + \tilde{B}r^l) \phi_0^{\zeta + 2 + \delta_1} \\ & \times \left(\frac{d}{r} \right)^{\sigma_1(\zeta + 2 + \delta_1)} \beta(r) - \tilde{\gamma} \phi_0^{\eta + \delta_1} \left(\frac{d}{r} \right)^{\sigma_1(\eta + \delta_1)} \left\{ (-1 + \eta \sigma_1 + 7\eta \sigma_1 \tilde{B}r^l + 2\eta^2 \sigma_1^2 \right. \\ & \left. \left. + 2\eta^2 \sigma_1^2 \tilde{B}r^l) \beta(r) - r(-1 - 2\tilde{B}r^l + \eta \sigma_1 + \eta \sigma_1 \tilde{B}r^l) \beta'(r) \right\} \right] = 0. \end{aligned}$$

We are solving it numerically because analytically it cannot be solved. The results are shown below.

- Brans-Dicke Theory:

In case of BD we are using $\eta = 1$, $\zeta = -1$ and by choosing the parameters $\omega_0 = -2$, $\sigma_1 = 0.008$, $\tilde{\gamma} = 1$, $\delta_1 = 5$, $\tilde{B} = 2$, $l = 5$, $\phi_0 = 10$, $V_0 = 1$ we will discuss the behavior of $\beta(r)$, $\beta'(r)$, $\frac{\beta(r)}{r}$, $\beta(r) - r$, ρ , $\rho + p_r$ and $\rho + p_t$.

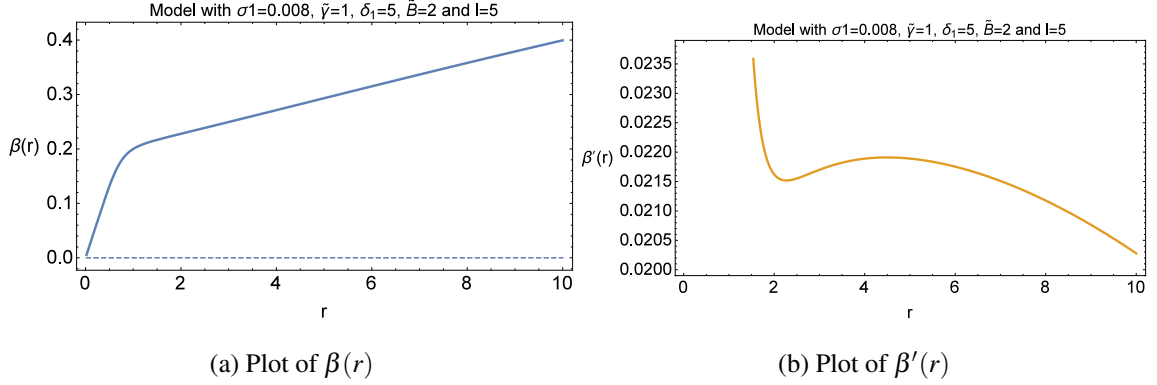


Figure 4.31: The behavior of $\beta(r)$ and $\beta'(r)$ versus r taking $\omega_0 = -2$, $\sigma_1 = 0.008$, $\tilde{\gamma} = 1$, $\delta_1 = 5$, $\tilde{B} = 2$, $l = 5$, $\phi_0 = 10$, $V_0 = 1$.

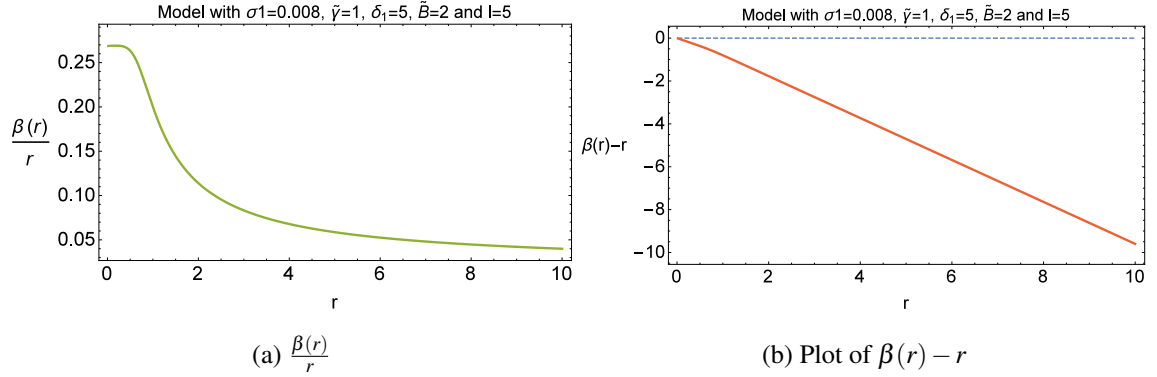


Figure 4.32: Left plot shows the behavior of $\frac{\beta(r)}{r}$ versus r and right plot shows the behavior of $\beta(r) - r$ for the parameters $\omega_0 = -2$, $\sigma_1 = 0.008$, $\tilde{\gamma} = 1$, $\delta_1 = 5$, $\tilde{B} = 2$, $l = 5$, $\phi_0 = 10$, $V_0 = 1$.

In Fig.4.31a behavior of the shape function has been shown. It can be analyzed that it shows the increasing behavior and meet the inequality $\beta(r) < r$. It can be seen from Fig.4.32a that $\beta(r)/r \rightarrow 0$ as $r \rightarrow \infty$ that means the spacetime is asymptotically flat. The plot in Fig.4.32b shows that $\beta(r) - r < 0$, which fulfil the condition $1 - \beta(r)/r > 0$ and for $\beta(r_0) = r_0$, throat is located at $r_0 = 0.0001$. The plot of $\beta'(r)$ is shown in Fig.4.31b

and $\beta'(r_0) = 0.267906$ which fulfill the condition $\beta'(r_0) < 1$. Evolution of NEC and WEC is shown in Fig.4.33. Here $\rho > 0$ and $\rho + p_t > 0$ are satisfied throughout the evolution but $\rho + p_r > 0$ is not satisfied.

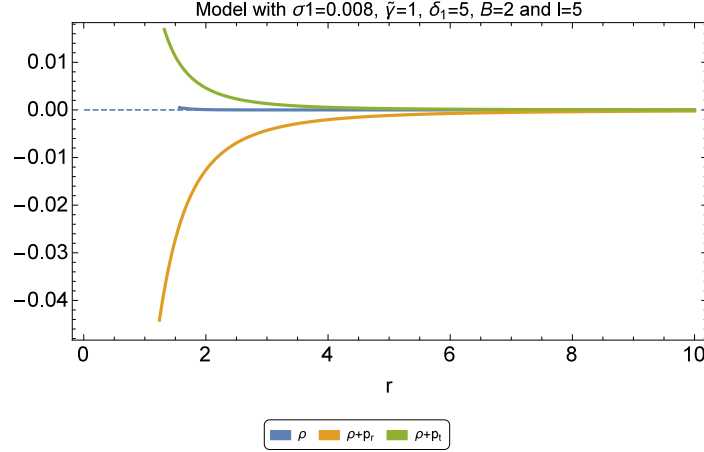


Figure 4.33: The plot shows the evolution of ρ , $\rho + p_r$ and $\rho + p_t$ for the parameters $\omega_0 = -2$, $\sigma_1 = 0.008$, $\tilde{\gamma} = 1$, $\delta_1 = 5$, $\tilde{B} = 2$, $l = 5$, $\phi_0 = 10$, $V_0 = 1$.

- Induced Gravity:

For induced gravity we use $\eta = 2$, $\zeta > 0$ and by choosing the parameters $\omega_0 = -2$, $\sigma_1 = 0.008$, $\tilde{\gamma} = 1$, $\delta_1 = 5$, $\tilde{B} = 2$, $l = 2.5$, $\phi_0 = 10$, $V_0 = 1$, we will discuss the behavior of $\beta(r)$, $\beta'(r)$, $\frac{\beta(r)}{r}$, $\beta(r) - r$, ρ , $\rho + p_r$ and $\rho + p_t$.

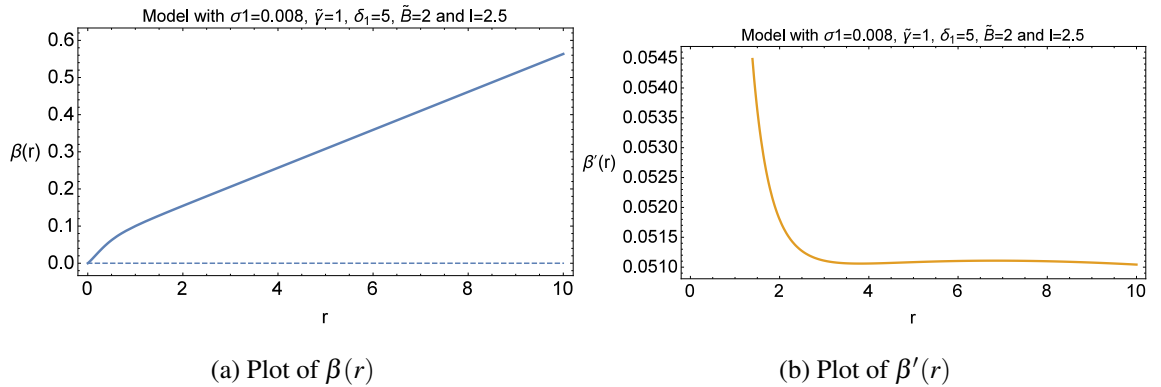


Figure 4.34: The behavior of $\beta(r)$ and $\beta'(r)$ versus r taking $\omega_0 = -2$, $\sigma_1 = 0.008$, $\tilde{\gamma} = 1$, $\delta_1 = 5$, $\tilde{B} = 2$, $l = 2.5$, $\phi_0 = 10$, $V_0 = 1$.

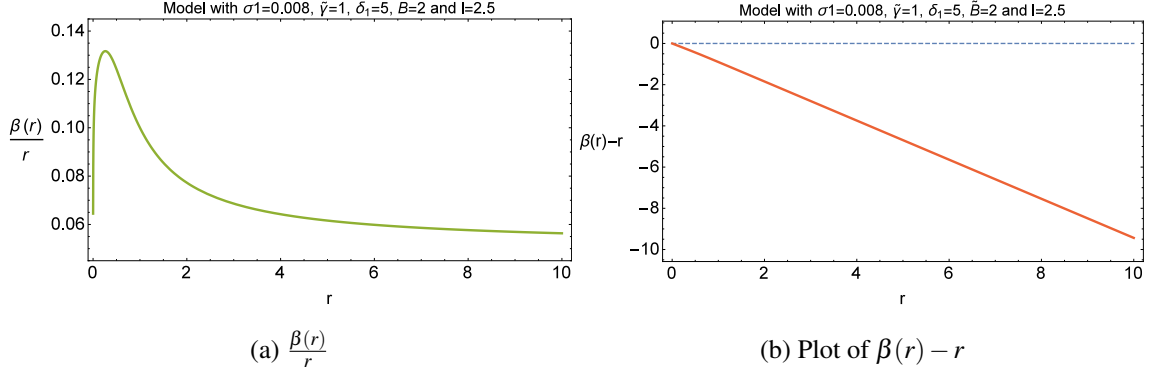


Figure 4.35: Left plot shows the behavior of $\frac{\beta(r)}{r}$ versus r and right plot shows the evolution of $\beta(r) - r$ for the parameters $\omega_0 = -2$, $\sigma_1 = 0.008$, $\tilde{\gamma} = 1$, $\delta_1 = 5$, $\tilde{B} = 2$, $l = 2.5$, $\phi_0 = 10$, $V_0 = 1$.

In Fig.4.34a behavior of the shape function has been shown. It can be analyzed that it shows the increasing behavior and meet the inequality $\beta(r) < r$. It can be seen from Fig.4.35a that $\beta(r)/r \rightarrow 0$ as $r \rightarrow \infty$ that means the spacetime is asymptotically flat. Fig.4.35b shows that $\beta(r) - r < 0$, which fulfill the condition $1 - \beta(r)/r > 0$ and for $\beta(r_0) = r_0$, throat is located at $r_0 = 0.001$. The plot of $\beta'(r)$ is shown in Fig.4.34b and $\beta'(r_0) = 0.0785625$ which fulfill the condition $\beta'(r_0) < 1$. Evolution of NEC and WEC is shown in Fig.4.36. Here $\rho > 0$ and $\rho + p_t > 0$ are satisfied throughout the evolution but $\rho + p_r > 0$ is not satisfied in this case.

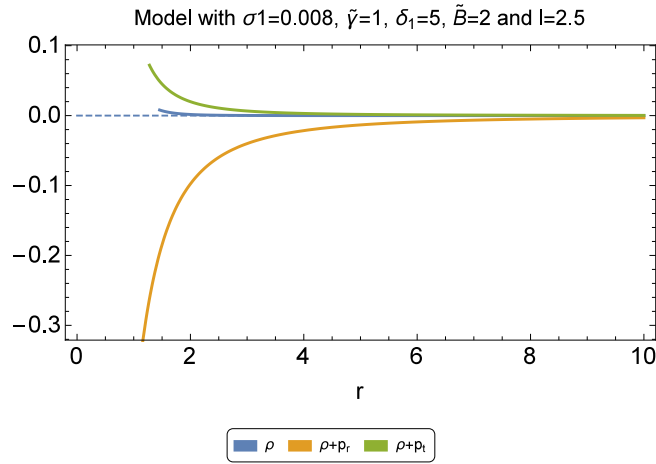


Figure 4.36: plot shows the evolution of ρ , $\rho + p_r$ and $\rho + p_t$ for the parameters $\omega_0 = -2$, $\sigma_1 = 0.008$, $\tilde{\gamma} = 1$, $\delta_1 = 5$, $\tilde{B} = 2$, $l = 2.5$, $\phi_0 = 10$, $V_0 = 1$.

Chapter 5

Inflation in $f(R, \phi)$ gravity with exponential model

5.1 Model and Background Solution

The action of $f(R, \phi)$ theory is described in (2.9.1). We are taking following $f(R, \phi)$ model

$$f(R, \phi) = \frac{1}{\kappa} [R + h(\phi) R^2 e^{\tilde{\alpha} R}], \quad (5.1.1)$$

where $h(\phi)$ is a coupling function. By expanding the exponential in terms of Ricci scalar up to the first order, we have

$$f(R, \phi) \simeq \frac{1}{\kappa} [R + h(\phi)(R^2 + \tilde{\alpha} R^3)]. \quad (5.1.2)$$

The field equations for $f(R, \phi)$ gravity are given in (2.9.2) and (2.9.3). In case of scalar field and modified gravity, the corresponding EMT are defined as, respectively

$$T_{\mu\nu}^{\phi} = \omega \left(\partial_{\mu} \phi \partial_{\nu} \phi - \frac{1}{2} g_{\mu\nu} \partial_c \phi \partial^c \phi \right) - g_{\mu\nu} V(\phi), \quad (5.1.3)$$

$$T_{\mu\nu}^{MG} = \frac{1}{2} g_{\mu\nu} (f - FR) + \nabla_{\mu} \nabla_{\nu} F - g_{\mu\nu} \square F. \quad (5.1.4)$$

Now, we will find exact solution analytically in dS case.

5.1.1 Background Inflationary Solution

Using FRW space time (3.1.1) with sign $(-, +, +, +)$, the field equations (2.9.2) and (2.9.3) can be written as

$$-\omega \dot{\phi}^2 - 6F(\dot{H} + H^2) + 6\dot{F}H + 2V - f = 0, \quad (5.1.5)$$

$$4FH^2 + 2F(\dot{H} + H^2) - \omega \dot{\phi}^2 - 2\ddot{F} - 4FH - 2V + f = 0, \quad (5.1.6)$$

$$2\omega \ddot{\phi} + 6\omega \dot{\phi} H - \frac{h_{,\phi} f}{h} + \frac{12h_{,\phi} H^2}{h\kappa} + \frac{6h_{,\phi} \dot{H}}{h\kappa} + 2V_{,\phi} = 0, \quad (5.1.7)$$

where $h = h(\phi)$ being the coupling function. Here, we are considering the following assumptions

$$a(t) = a_0 e^{H_D t} \quad \text{and} \quad \phi = \phi_0 e^{-\tilde{n} H_D t}, \quad (5.1.8)$$

where \tilde{n} , ϕ_0 and H_D are constants. Substituting (5.1.8) in Eqs. (5.1.5)-(5.1.7) and solving these equations, we get the coupling function of the form

$$h(\phi) = h_0 + h_1 \phi^2 + h_{\tilde{n}} \phi^{-1/\tilde{n}}, \quad (5.1.9)$$

where $h_1 = -\frac{\tilde{n}\omega\kappa}{48H_D^2(2\tilde{n}+1)(18\tilde{\alpha}H_D^2+1)}$ and $h_{\tilde{n}} = \tilde{n}c_1$. The scalar field potential is

$$V(\phi) = V_0 + V_1\phi^2 + V_{\tilde{n}}\phi^{-1/\tilde{n}}, \quad (5.1.10)$$

where

$$\begin{aligned} V_0 &= \frac{3H_D^2 h_0}{\kappa}, \quad V_1 = 24h_1 H_D^4 \left\{ -18\tilde{\alpha}H_D^2 + \tilde{n}^2 (36\tilde{\alpha}H_D^2 + 2) - 5\tilde{n} (18\tilde{\alpha}H_D^2 + 1) \right\}, \\ V_{\tilde{n}} &= -\frac{72h_{\tilde{n}} H_D^4 (12\tilde{\alpha}H_D^2 + 1)}{\kappa}. \end{aligned}$$

Here h_0 is the constant of integration. It can be seen that this is an exact solution obtained from the background equations. We are mentioning here some important points: First, we have obtained the solution without using conformal transformation. According to best of our knowledge, in Jordan frame no exact solution exists. Second, in case of exact dS solution, the scalar field (5.1.8) decreases with increasing time. Third, coupling function $h(\phi)$ directly depends on $V(\phi)$.

From Eqs.(5.1.9) and (5.1.10), it can be seen that V_0 depends on h_0 , similarly, $V_{\tilde{n}}$ depends on $h_{\tilde{n}}$ and h_1 is related to V_1 . If we choose $h_0 = h_{\tilde{n}} = 0$, then it is obvious that V_0 and $V_{\tilde{n}}$ also vanished.

5.2 Special Case: $h_0 = h_{\tilde{n}} = 0$

Here, we consider $h_0 = h_{\tilde{n}} = 0$. The coupling function and potential are reduced to

$$h(\phi) = h_1\phi^2, \quad V(\phi) = V_1\phi^2. \quad (5.2.1)$$

This leads to conclude the following points. It can be seen that h_1 is positive definite implies that $18\tilde{\alpha}H_D^2 + 1 < 0$ or $\tilde{\alpha} < -1/(18H_D^2)$. Since, during inflation the parameter H is large, leads to small negative value of $\tilde{\alpha}$. From the EMT (5.1.3) and (5.1.4), we can calculate $\rho + 3p$ as

$$\begin{aligned} \rho + 3p \equiv -T_0^0 + T_\mu^\mu &= 2\phi_0^2 H_D^2 e^{-2\tilde{n}H_D t} \left[\tilde{n}^2 + V_1 - h_1 \left\{ 72H_D^2 (1 + 2\tilde{n} + 2\tilde{n}^2) \right. \right. \\ &\quad \left. \left. + 648\tilde{\alpha}H_D^4 (3 + 2\tilde{n} + 4\tilde{n}^2) \right\} \right]. \end{aligned} \quad (5.2.2)$$

In (5.2.2), the first two terms correspond to the canonical scalar field while the last term corresponds to the modifications to the gravity. For $\tilde{n} < 1/2$, the third term is always

negative while positive for $\tilde{n} > 1/2$. However, $\tilde{n} \ll 1$ leads to $\rho + 3p < 0$ and for $\tilde{n} \gg 1$, we have $\rho + 3p > 0$. In the further analysis, we are taking $\tilde{n} \gg 1$. We can say from above discussion that either it corresponds to exit for large values of \tilde{n} or by varying the initial condition of $\dot{\phi}$. If $\dot{\phi}_{t=0} \neq \dot{\phi}_{t=0}^{dS}$, then we will check that what kind of inflation exists using the relation $\dot{\phi} \propto \tilde{n}$.

5.3 First Order Scalar and Tensor Perturbations for the Model

The cosmological perturbation theory is an effective and competent tool to study the universe. The universe is homogeneous, but the actual universe is not homogeneous. If universe is totally homogeneous then we cannot observe the local structures of the universe such as galaxies and clusters of galaxies. We are using the FLRW universe, which is perfectly homogeneous model and give accurate descriptions only on large scales. If we introduce inhomogeneities and anisotropies in our model then it will be very difficult to explain how stars and galaxies were formed. The correct way to explain it through perturbation theory. We are using FLRW spacetime and apply perturbation theory to deal with inhomogeneities and anisotropies. In perturbation expansion, FLRW spacetime can be seen as the zeroth order term. First we should derive the perturbation expansion, substitute it into EFEs and find the solution. In this technique, the problem is that EFEs are covariant while having metric and include perturbations is not a covariant process, it introduces the gauge dependence.

Now we will discuss the scalar and tensor power-spectra for our model (5.1.2). We have used the same notation as used in [172] then it will be easy to compare. For our model, analysis of [172] is not applicable.

5.3.1 Perturbations

For FRW space time first order perturbations are

$$ds^2 = -(1 + 2\theta)dt^2 - a(\beta_{,\alpha} + B_\alpha)dt dx^\alpha + a^2 \left[g_{\alpha\beta}^{(3)}(1 - 2\psi) + 2\gamma_{\alpha|\beta} + 2C_{\alpha|\beta} + 2C_{\alpha\beta} \right]. \quad (5.3.1)$$

In the above expression $dt \equiv ad\eta$ and $\theta(x, t)$, $\beta(x, t)$, $\psi(x, t)$, $\gamma(x, t)$ are the scalar perturbations. $B_\alpha(x, t)$ and $C_\alpha(x, t)$ denote the tracefree vector perturbation and $C_{\alpha\beta}(x, t)$ presents the tracefree and transverse tensor perturbations. The decomposed form of scalar field is $\phi(x, t) = \bar{\phi}(t) + \delta\phi(x, t)$.

In Fourier space, scalar perturbed equations of Newtonian gauge are [172, 173]:

$$-F\psi + F\theta + \delta F = 0, \quad (5.3.2)$$

$$-2F\dot{\psi} - 2FH\dot{\theta} - \dot{F}\theta + \dot{\phi}\delta\phi + \delta\dot{F} - H\delta F = 0, \quad (5.3.3)$$

$$6FH\dot{\psi} + 6FH^2\dot{\theta} + 2F\frac{k^2}{a^2}\dot{\psi} - \dot{\phi}^2\dot{\theta} + 3\dot{F}\dot{\psi} + 6\dot{F}H\dot{\theta} + \dot{\phi}\delta\dot{\phi} - \ddot{\phi}\delta\phi - 3H\dot{\phi}\delta\phi - 3H\delta\dot{F} + 3\dot{H}\delta F + 3H^2\delta F - \frac{k^2}{a^2}\delta F = 0, \quad (5.3.4)$$

$$6F\ddot{\psi} + 12F\dot{H}\dot{\theta} + 6FH\ddot{\theta} + 12FH\dot{\psi} + 12FH^2\dot{\theta} - 2F\frac{k^2}{a^2}\dot{\theta} + 3\dot{F}\dot{\psi} + 6\dot{F}H\dot{\theta} + \dot{F}\dot{\theta} + 4\dot{\phi}^2\dot{\theta} + 6\theta\ddot{F} - 4\dot{\phi}\delta\dot{\phi} - 2\ddot{\phi}\delta\phi - 6H\dot{\phi}\delta\phi - 3\delta\dot{F} - 3H\delta\dot{F} + 6H^2\delta F - \frac{k^2}{a^2}\delta F = 0, \quad (5.3.5)$$

$$\delta\ddot{\phi} + 3H\delta\dot{\phi} - \frac{1}{2}f_{\phi\phi} + V_{\phi\phi}\delta\phi + \frac{k^2}{a^2}\delta\phi - 3\dot{\phi}\dot{\psi} - 6H\dot{\phi}\dot{\theta} - \dot{\phi}\dot{\theta} - 2\ddot{\phi}\dot{\theta} + 3F_{\phi}\dot{\psi} + 6F_{\phi}\dot{H}\dot{\theta} + 3HF_{\phi}\dot{\theta} + 12F_{\phi}H\dot{\psi} + 12F_{\phi}H^2\dot{\theta} + 2F_{\phi}\frac{k^2}{a^2}\dot{\psi} - F_{\phi}\frac{k^2}{a^2}\dot{\theta} = 0, \quad (5.3.6)$$

$$\delta F - F_{\phi}\delta\phi + F_R\delta R = 0. \quad (5.3.7)$$

where $\delta R = -6\ddot{\psi} - 12\dot{H}\dot{\theta} - 6H\ddot{\theta} - 24H\dot{\psi} - 24H^2\dot{\theta} - 4\frac{k^2}{a^2}\dot{\psi} + 2\frac{k^2}{a^2}\dot{\theta}$. While the tensor perturbations are as follows [173]:

$$\ddot{C}_{\beta}^{\alpha} + \left(\frac{\dot{F}}{F} + 3H\right)\dot{C}_{\beta}^{\alpha} + \frac{k^2}{a^2}C_{\beta}^{\alpha} = 0. \quad (5.3.8)$$

5.3.2 Scalar Power Spectrum

Here we calculate the equation, which satisfy the 3-curvature perturbation \mathcal{R} and derive the related power spectrum. We are using the technique followed in [174]. The \mathcal{R} in Jordan frame is stated as

$$\mathcal{R} = \psi + \frac{H}{\dot{\phi}}\delta\phi. \quad (5.3.9)$$

The equations (5.3.2)-(5.3.7) are highly ordered and non-linear so, we use different techniques to calculate the 3-curvature perturbation equation. First, we will use $\theta + \psi = \Theta$ and find the solution of differential equation. Physically, in Einstein frame, Θ represents the Bardeen potential. Using Eqs.(5.3.3)-(5.3.5), we have differential equation in Θ as:

$$F\ddot{\Theta} + \left(3\dot{F} + FH - \frac{2F\ddot{\phi}}{\dot{\phi}}\right)\dot{\Theta} + \left(\frac{Fk^2}{a^2} + \frac{2\dot{F}\ddot{\phi}}{\dot{\phi}} - \frac{2FH\ddot{\phi}}{\dot{\phi}} - \ddot{F} + \dot{F}H + 4F\dot{H}\right)\Theta + \left(-\dot{\phi}^2 + 3\ddot{F} + 3\dot{F}H - 6F\dot{H} - \frac{6\dot{F}\ddot{\phi}}{\dot{\phi}}\right)\theta = 0. \quad (5.3.10)$$

Using background quantities for dS, assuming $\tilde{n} \ll 1$ and large values of k , we have differential equation in terms of Θ as

$$\ddot{\Theta} + (1 - 4\tilde{n})H_D\dot{\Theta} + \frac{k^2}{a^2}\Theta - 4\tilde{n}(1 - \tilde{n})H_D^2\theta = 0. \quad (5.3.11)$$

Applying the small wavelength limit $\frac{k}{a} \gg 1$, the last two terms of the left hand side can be written as

$$\left(\frac{k^2}{a^2} - 4\tilde{n}(1 - \tilde{n})H_D^2\right)\theta + \frac{k^2}{a^2}\psi \simeq \frac{k^2}{a^2}\Theta. \quad (5.3.12)$$

which can further be written as

$$\ddot{\Theta} + (1 - 4\tilde{n})H_D\dot{\Theta} + \frac{k^2}{a^2}\Theta = 0. \quad (5.3.13)$$

In terms of Θ , $\delta\phi$ is as follows

$$\delta\phi = -\frac{\phi_0 e^{-\tilde{n}H_D t}}{\tilde{n}H_D}(\dot{\Theta} + H_D\Theta). \quad (5.3.14)$$

Rewriting the perturbation equations in terms of \mathcal{R} and using Eqs. (5.3.9) and (5.3.13), we have Θ in terms of \mathcal{R} as

$$\Theta = -(3a^2\ddot{R} + 12H_D a^2\dot{R} + 2k^2 R)\frac{\tilde{n}H_D}{\phi_0}e^{\tilde{n}H_D t},$$

substituting it into the perturbation equations, we get the differential equation in terms of \mathcal{R} :

$$\ddot{\mathcal{R}} + 3H_D\dot{\mathcal{R}} + \frac{k^2}{a^2}\mathcal{R} = 0. \quad (5.3.15)$$

It is an important result which shows that higher order differential equation can be reduced to second order. For the power-spectrum, we can evaluate solution to the above differential

equation for the short wavelength limit and using the Bunch-Davies vacuum at the initial epoch of inflation as

$$R_{<} = \frac{H_D}{2a\sqrt{k}} e^{-ik\tilde{\eta}}. \quad (5.3.16)$$

In the long wavelength limit, we get $R_{>} = C$. By matching $R_{<}$ and $R_{>}$ at horizon crossing ($|k\tilde{\eta}| = 2\pi$), we get

$$C = \frac{\sqrt{2}H_D\pi}{k^{3/2}}, \quad (5.3.17)$$

leading to following scale-invariant scalar power spectrum

$$\mathcal{P}_R = H_D^2.$$

For $\tilde{n} \ll 1$, above analysis is an analytical expression. It is not possible to obtain the semi-analytical expression for other cases, which shows the tilted spectrum. Next, we derive the tensor power spectrum without using $\tilde{n} \ll 1$ limit which leads to blue tilt.

5.3.3 Tensor Power Spectrum

Following [173], we can obtain the equation of motion for the tensor perturbation of exact dS solution

$$\ddot{C}_\beta^\alpha + (3 - 2\tilde{n})H_D\dot{C}_\beta^\alpha + \frac{k^2}{a^2}C_\beta^\alpha = 0. \quad (5.3.18)$$

Defining $C_\beta^\alpha = v_g/z_g$ and $z_g = ae^{-\tilde{n}H_D t}$, we have

$$v_g'' + \left(k^2 - \frac{z_g''}{z_g}\right) = 0. \quad (5.3.19)$$

The solution to the above differential equation is again a sum of Hankel function:

$$v_g = \sqrt{-\tilde{\eta}} \left(\tilde{C}_1 H_{3/2-\tilde{n}}^{(1)}(-k\tilde{\eta}) + \tilde{C}_2 H_{3/2-\tilde{n}}^{(2)}(-k\tilde{\eta}) \right). \quad (5.3.20)$$

Fixing Bunch-Davies vacuum to the initial state, we have $\tilde{C}_2 = 0$ and $\tilde{C}_1 = \sqrt{\pi/4}$. Hence for tensor perturbation C_β^α , we have

$$v_g = \sqrt{\frac{\pi}{4}} \sqrt{-\tilde{\eta}} H_{3/2-\tilde{n}}^{(1)}(-k\tilde{\eta}). \quad (5.3.21)$$

The tensor power spectrum is given by $\mathcal{P}_g = 8 \frac{k^3}{2\pi^2} |\mathcal{C}_\beta^\alpha|^2$ and modified as

$$\mathcal{P}_g = 8 \left(\frac{k}{k_*}\right)^{2\tilde{n}} \frac{2^{-2\tilde{n}}}{4\pi^2} H_D^2 \left(\frac{\Gamma(3/2 - \tilde{n})}{\Gamma(3/2)}\right)^2 e^{2\tilde{n}H_D t_*}. \quad (5.3.22)$$

The tensor spectral index is calculated as $n_T = 2\tilde{n}$, which means that for a decaying scalar field the spectrum obtained is blue tilted i.e., blue tilted for $\tilde{n} > 1/2$ and red tilted for $\tilde{n} < 1/2$.

5.4 Stability of Inflationary Solution

Now we will discuss the stability of dS solution and will examine the variations of initial values either they show inflationary phase, super inflation or smooth exit. Hence, to show the inflationary solution many initial values exist and a mess of models have been discussed in literature which show the saddle point [175, 176]. The field Eqs (5.1.5)-(5.1.7) in terms of the variable $\Delta = \dot{\phi}/\phi$ can be written as

$$\begin{aligned}\dot{\Delta} = & 2V_1 + 2592\tilde{\alpha}h_1\dot{H}H^4 + 1296\tilde{\alpha}h_1\dot{H}^2H^2 + 1728\tilde{\alpha}h_1H^6 + 216\tilde{\alpha}h_1\dot{H}^3 - 144h_1\dot{H}H^2 \\ & - 144h_1H^4 - 36h_1\dot{H}^2 - 3H\Delta - \Delta^2,\end{aligned}\quad (5.4.1)$$

$$\begin{aligned}\ddot{H} = & \frac{1}{36h_1H - 648\tilde{\alpha}h_1H\dot{H} - 1296\tilde{\alpha}h_1H^3} \left[\frac{3H^2}{\phi_0^2} e^{2\tilde{n}H_D t} - 180h_1\dot{H}H^2 + 972\tilde{\alpha}h_1H^2\dot{H}^2 \right. \\ & - 3024\tilde{\alpha}h_1H^6 + 1296\tilde{\alpha}h_1\dot{H}H^4 + \frac{1}{2}\Delta^2 - 18h_1\dot{H}^2 + 216\tilde{\alpha}h_1\dot{H}^3 - V_1 - 72h_1H\dot{H}\Delta \\ & \left. - 144h_1H^3\Delta + 648\tilde{\alpha}h_1H\dot{H}^2\Delta + 2592\tilde{\alpha}h_1H^5\Delta + 2592\tilde{\alpha}h_1H^3\dot{H}\Delta \right].\end{aligned}\quad (5.4.2)$$

The field equations in terms of Δ shows that the evolution of Hubble parameter, No of e-folding etc. do not involve ϕ or $\dot{\phi}$, only depends on Δ .

Let us define vector v as:

$$v = \begin{pmatrix} H \\ \dot{H} \\ \Delta \end{pmatrix}.\quad (5.4.3)$$

It is important to note that the dS solution ($H = H_D$) is an equilibrium point ($\dot{v}_{eq} = 0$) and

$$\{v\}_{eq} = \begin{pmatrix} H_D \\ 0 \\ -\tilde{n}H_D \end{pmatrix},\quad (5.4.4)$$

and the equations for $\dot{v} = f(v)$ can be written as

$$\dot{v} = \begin{pmatrix} \dot{H} \\ \ddot{H} \\ \dot{\Delta} \end{pmatrix}. \quad (5.4.5)$$

As we have mentioned above, perturbing $v = v_{eq} + \delta v$ and expanding $f(v)$ for δv about the equilibrium point, we have

$$\delta v_i = \{\partial_j f_i\}_{eq} \delta v_j = J_{ij} \delta v_j. \quad (5.4.6)$$

where

$$J_{ij} = \begin{pmatrix} \partial \dot{H} / \partial H & \partial \dot{H} / \partial \dot{H} & \partial \dot{H} / \partial \Delta \\ \partial \ddot{H} / \partial H & \partial \ddot{H} / \partial \dot{H} & \partial \ddot{H} / \partial \Delta \\ \partial \dot{\Delta} / \partial H & \partial \dot{\Delta} / \partial \dot{H} & \partial \dot{\Delta} / \partial \Delta \end{pmatrix}. \quad (5.4.7)$$

Let the eigen value and eigen vector of Jacobian are λ_i and μ_i . Then the phase space trajectory is given by:

$$\delta v_i = \sum_{i=1}^{i=3} c_i \mu_i e^{(\lambda_i t)}.$$

where c_i 's are constants whose values has to be fixed from initial values of Hubble parameter (H_i) and the initial value of $\dot{\phi}$. In our case, we have one real and two complex eigen values which are too lengthy in expression due to which we did not mention them in the paper. For large values of eigen value (λ), the number of e-folding is given by

$$N \approx \frac{H_D}{\lambda} \ln \left(\frac{H_D^2}{\lambda (H_D - H_j)} \right).$$

Fig. 5.1 shows the behavior of slow-roll parameter $\varepsilon = -\frac{\dot{H}}{H^2}$ versus number of e-folds for different initial values of $\dot{\phi}$. The parameter ε can be evaluated as under

$$\varepsilon = \frac{24H^2 (18\tilde{\alpha}H^2 + 1) (2Hh_1\phi\dot{\phi} - 2h_1\dot{\phi}^2 - 2h_1\ddot{\phi}\phi)}{2H^2 \{1 - 12H^2h_1\phi^2 (36\tilde{\alpha}H^2 + 2)\}}.$$

Figure 5.1 is plotted for $\varepsilon - N$ trajectories taking some initial values. It can be observed that for $\dot{\phi} < 1.4\phi_D$, the inflationary phase sustained as $\varepsilon < 1$ and ε attains a constant value less than unity for $\dot{\phi} \geq 1.4\phi_D$, fixing the other parameters as $\omega_0 = -0.005$, $\phi_0 = -0.3$, $\tilde{n} = 200$, $H_D = 4 \times 10^4$, $H_j = 2$, $\tilde{\alpha} = -10^{-7}$. It can be seen that in the space $\dot{\phi} < \phi_D$, the

inflationary phase exist without an exit which represent ϵ is diverging to $-\infty$ while $\dot{\phi} > \phi_D$ leads to the inflationary era with an exit. The initial condition $\dot{\phi} = \phi_D$ generates $\epsilon = 0$. In this case, the results are obtained for standard No. of e-folds, i.e., $N \simeq 50, 60$, which is in good agreement with observational data. Further, it is observed that as the value of $\frac{\dot{\phi}}{\phi_D}$ is directly proportional to N , as increment in initial value produced an increase in N . Hence rate of inflation increases as $\dot{\phi}$ increases. The trajectories are attracted toward its origin with increasing initial values. This shows that deviation of initial values from de-Sitter value leads to either inflation with exit or super inflation, and that the de-Sitter solution is a saddle point.

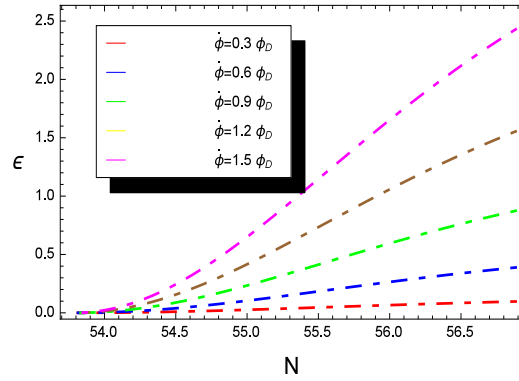


Figure 5.1: Evolution of ϵ versus N for different initial values of $\dot{\phi}$.

The scalar field ϕ is expressed as

$$\phi = \frac{6\kappa\omega H\dot{\phi}}{4\kappa v_1 - 288h_1 - 3456\tilde{\alpha}h_1H^6}.$$

Figure 5.2 is plotted for ϕ versus N (left plot) and versus time t (right plot) for standard No. of e-folds. It can be seen that scalar field is decaying with the evolution of time. The trajectories of $\phi - N$ shows the same behavior as $\epsilon - N$.

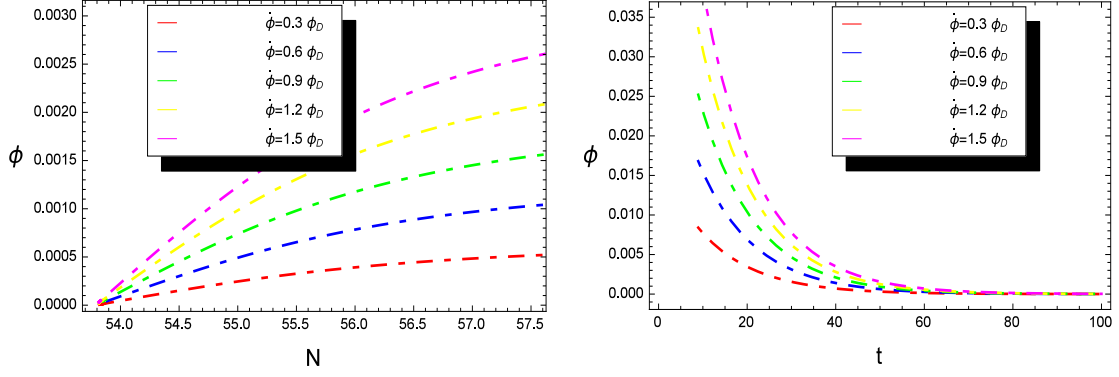


Figure 5.2: Evolution of ϕ versus N for different initial values of $\dot{\phi}$.

The scalar spectral index is defined as [177]

$$n_s = 1 - 4\varepsilon_1 - 2\varepsilon_2 + 2\varepsilon_3 - 2\varepsilon_4,$$

where

$$\varepsilon_1 = -\frac{\dot{H}}{H^2}, \quad \varepsilon_2 = \frac{\ddot{\phi}}{H\dot{\phi}}, \quad \varepsilon_3 = \frac{\dot{F}}{2HF}, \quad \varepsilon_4 = \frac{\dot{E}}{2HE}, \quad E = \omega F + \frac{3\dot{F}^2}{2\dot{\phi}^2}.$$

The tensor to scalar ratio is defined as $r = \frac{P_g}{P_r}$. For better understanding of the inflationary model's compatibility with recent data, we have plotted parametric plots (5.3) in which scalar spectral index is plotted versus tensor to scalar ratio for $\tilde{n} > 1$. It is observed that for $\tilde{n} = 1.61, 1.7$, we have the standard value of spectral index $n_s = 0.968$ and an upper bound of tensor to scalar ratio is obtained as $r < 0.11$ which is in accordance with Planck 2015 and 2018 data [5]. It can be seen that as the value of \tilde{n} increases, the range of n_s is compressed.

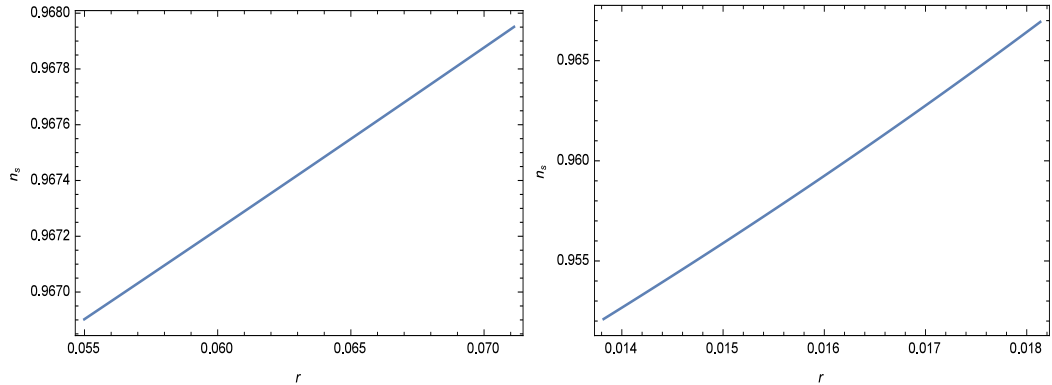


Figure 5.3: Left plot shows the behavior of r versus n_s for $\dot{\phi} = 0.0065\phi_D$ with $\tilde{n} = 1.6$ and right plot for $\dot{\phi} = 0.0065\phi_D$ with $\tilde{n} = 1.7$.

Chapter 6

Anisotropic Universe Models in $f(R, \phi)$ gravity

6.1 Field Equations for Bianchi I Model and Some General Parameters

The field equations of $f(R, \phi)$ theory are given by (2.9.2) and (2.9.3). The BI is defined in (2.11.6) for which the scalar curvature R turns out to be

$$R = -2 \left[\frac{\ddot{A}}{A} + 2 \frac{\ddot{B}}{B} + 2 \frac{\dot{A}\dot{B}}{AB} + \frac{\dot{B}^2}{B^2} \right]. \quad (6.1.1)$$

For the metric (2.11.6), mean Hubble parameter, average scale factor and volume are given by

$$H(t) = \frac{1}{3} \left(\frac{\dot{A}}{A} + 2 \frac{\dot{B}}{B} \right) \quad a(t) = (AB^2)^{1/3}, \quad V = a^3(t) = AB^2.$$

The corresponding directional Hubble parameters are defined as

$$H_x = \frac{\dot{A}}{A}, \quad H_y = \frac{\dot{B}}{B} = H_z. \quad (6.1.2)$$

The deceleration and anisotropy parameter of expansion are defined as

$$q = \frac{d}{dt} \left(\frac{1}{H} \right) - 1, \quad \Delta = \frac{1}{3} \sum_{i=1}^3 \left(\frac{H_i - H}{H} \right)^2. \quad (6.1.3)$$

For $\Delta = 0$, we can get the isotropic expansion of the universe. The shear scalar and expansion scalar are turns out to be

$$\sigma = \frac{1}{\sqrt{3}} \left(\frac{\dot{A}}{A} - \frac{\dot{B}}{B} \right), \quad \Theta = u^a_{;a} = \frac{\dot{A}}{A} + 2 \frac{\dot{B}}{B}, \quad (6.1.4)$$

It is worthwhile to mention here that when $t \rightarrow +\infty$, $V \rightarrow +\infty$, $\Delta \rightarrow 0$ and $\rho > 0$, any universe model becomes isotropic [96, 178].

Now we will define the EMT for anisotropic fluid and also formulate the field equations for LRS BI model with this matter source. To discuss the accelerated expansion of the universe, we are taking anisotropic fluid of the form [95, 96]

$$T^\mu_\nu = \text{diag}[\rho, -p_x, -p_y, -p_z], \quad (6.1.5)$$

where ρ is energy density and p_x , p_y , p_z are pressures in x , y and z directions, respectively. For anisotropic fluid, EoS is defined as $p = w\rho$, where w is a variable [179]. By defining

the directional EoS parameters along x , y and z axes, i.e., $w_x = w + \delta$, $w_y = w + \gamma$ and $w_z = w + \gamma$, we have (6.1.5) in the following form

$$T_v = \text{diag}[1, -(w + \delta), -(w + \gamma), -(w + \gamma)]\rho, \quad (6.1.6)$$

where δ represents the deviation of w on x axis and γ is the deviation on both y and z axes. Clearly, Eq.(6.1.6) with $\delta = \gamma = 0$ represents the EMT for isotropic fluid defined below

$$T_v = \text{diag}[\rho, -w\rho, -w\rho, -w\rho]. \quad (6.1.7)$$

For the anisotropic fluid, energy conservation equation can be written as

$$\dot{\rho} + (1 + w) \left(\frac{\dot{A}}{A} + 2\frac{\dot{B}}{B} \right) \rho(t) + \left(\delta \frac{\dot{A}}{A} + 2\gamma \frac{\dot{B}}{B} \right) \rho(t) = 0. \quad (6.1.8)$$

Separating the deviation free and anisotropy parts of anisotropic fluid and then by taking anisotropy part equal to zero [95, 180], we get

$$\left(\delta \frac{\dot{A}}{A} + 2\gamma \frac{\dot{B}}{B} \right) \rho(t) = 0. \quad (6.1.9)$$

Since energy density is a non-zero quantity, it means either both the deviation parameters vanish or $\frac{H_x}{H_y} = -\frac{2\gamma}{\delta}$. In order to get more general solution, if δ and γ are allowed to be function of cosmic time t and we constrained δ and γ by assuming a special dynamic which is consistent with (6.1.9). The dynamic of the deviation parameter on the x axis, $\delta(t)$, is assumed to be [95].

$$\delta(t) = \frac{2n}{3} \frac{\dot{B}}{B} \left(\frac{\dot{A}}{A} + 2\frac{\dot{B}}{B} \right) \frac{1}{\rho}, \quad (6.1.10)$$

and thus from (6.1.9) the deviation parameter on the y and z axes, $\gamma(t)$, is found as

$$\gamma(t) = -\frac{n}{3} \frac{\dot{A}}{A} \left(\frac{\dot{A}}{A} + 2\frac{\dot{B}}{B} \right) \frac{1}{\rho}, \quad (6.1.11)$$

In these assumptions $\delta(t)$ and $\gamma(t)$ are dimensionless parameters and n is a dimensionless constant that parameterizes the amplitude of the deviation from EoS parameter and can be given real values. If the deviation parameters approaches to zero or $\frac{\delta(t) - \gamma(t)}{\omega} \rightarrow 0$ then the DE is isotropic [95]. For the anisotropic fluid and LRS BI spacetime, the field equations

take the following form:

$$(m+2)\frac{\dot{B}}{B}\partial_t f_R - \left\{ m(m-1)\frac{\dot{B}^2}{B^2} + (m+2)\frac{\ddot{B}}{B} \right\} f_R + \frac{\omega(\phi)\dot{\phi}^2}{2} - \frac{f}{2} + V(\phi) = \kappa^2 \rho, \quad (6.1.12)$$

$$\partial_{tt} f_R + 2\frac{\dot{B}}{B}\partial_t f_R - \left\{ m(m+1)\frac{\dot{B}^2}{B^2} + m\frac{\ddot{B}}{B} \right\} f_R - \frac{f}{2} + V(\phi) - \frac{\omega(\phi)\dot{\phi}^2}{2} = (w+\delta)\rho \kappa^2, \quad (6.1.13)$$

$$\partial_{tt} f_R + (m+1)\frac{\dot{B}}{B}\partial_t f_R - \left\{ (m+1)\frac{\dot{B}^2}{B^2} + \frac{\ddot{B}}{B} \right\} f_R - \frac{f}{2} + V(\phi) - \frac{\omega(\phi)\dot{\phi}^2}{2} = (w+\gamma)\rho \kappa^2, \quad (6.1.14)$$

where we have used the condition $A = B^m; m \neq 0, 1$ which we have constructed by taking the term $\frac{\sigma}{\Theta}$ as a constant (assuming the relationship of proportionality between the expansion and shear scalars). This condition has been widely used in literature, e.g., [101, 102, 106]. Basically the set of field equations (6.1.12)-(6.1.14) involve only two independent equations with five unknown quantities namely B , f , w , V and ρ . Therefore in order to make a closed system of equations, we have to choose three more conditions. For this purpose, we consider the well-known power law forms of scalar field and the coupling constant [146], i.e.,

$$\phi = B^{\beta_1}, \quad \omega(\phi) = \omega_0 \phi^\zeta, \quad (6.1.15)$$

where β_1 , ω_0 and ζ all are non-zero constants. Feasible graphs can be plotted for all values of ω_0 , $-\infty < \zeta < 6.5$ and $-\infty < \beta_1 < 1.36$. Further, in the coming section, we will consider two different viable forms of the function $f(R, \phi)$.

6.2 Solution of field Equations

In this section, we will explore the solution of field equations (6.1.12)-(6.1.14) by using ansatz (6.1.15) for two different $f(R, \phi)$ models. Here we will also illustrate the physical importance of the constructed solutions graphically.

6.2.1 The Model: $f(R, \phi) = R(1 + \xi \kappa^2 \phi^2)$

First we are choosing the model (3.1.55). Subtracting Eq.(6.1.13) from Eq.(6.1.14) and then by using the ansatz (6.1.15) with the model (3.1.55), we have the following differential

equation:

$$\frac{\ddot{B}}{B} - (m+1) \frac{\dot{B}^2}{B^2} + \left(\frac{2\beta_1 \xi \kappa^2 B^{2\beta_1}}{1 + \xi \kappa^2 B^{2\beta_1}} \right) \frac{\dot{B}^2}{B^2} + \left(\frac{\eta_2}{1 + \xi \kappa^2 B^{2\beta_1}} \right) \frac{\dot{B}^2}{B^2} = 0, \quad (6.2.1)$$

where $\eta_2 = \frac{n(m+2)^2 \kappa^2}{3(m-1)}$. Its twice integration leads to the following form:

$$\frac{B^{m-\eta_2}}{m-\eta_2} + \xi \kappa^2 \left(-1 + \frac{\eta_2}{2\beta_1} \right) \frac{B^{m-\eta_2+2\beta_1}}{m-\eta_2+2\beta_1} = c_1 t + c_2, \quad (6.2.2)$$

where c_1, c_2 are constants of integration. For $x = X, y = Y, z = Z$ and $B = T$, LRS BI metric becomes

$$ds^2 = \frac{1}{c_1^2} T^{2\eta_2-2m-2} \left(1 + \xi \kappa^2 T^{2\beta_1} \right)^{2-\eta_2/\beta_1} dT^2 - T^{2m} dX^2 - T^2 (dY^2 + dZ^2). \quad (6.2.3)$$

The corresponding physical parameters become

$$\begin{aligned} V &= T^{m+2}, \quad \Delta = \frac{2(m-1)^2}{(m+2)^2}, \\ H_x &= mH_y = m c_1 T^{m-\eta_2} \left(1 + \xi \kappa^2 T^{2\beta_1} \right)^{-1+\frac{\eta_2}{2\beta_1}}, \\ H &= \left(\frac{m+2}{3} \right) c_1 T^{m-\eta_2} \left(1 + \xi \kappa^2 T^{2\beta_1} \right)^{-1+\frac{\eta_2}{2\beta_1}}, \\ \Theta &= 3H = (m+2) c_1 T^{m-\eta_2} \left(1 + \xi \kappa^2 T^{2\beta_1} \right)^{-1+\frac{\eta_2}{2\beta_1}}, \\ \sigma^2 &= \frac{1}{3} (m-1)^2 c_1^2 T^{2m-2\eta_2} \left(1 + \xi \kappa^2 T^{2\beta_1} \right)^{-2+\frac{\eta_2}{\beta_1}}, \\ q &= \frac{3}{m+2} \left\{ \frac{(\eta_2 - m) + (2\beta_1 - m) \xi \kappa^2 T^{2\beta_1}}{1 + \xi \kappa^2 T^{2\beta_1}} \right\} - 1, \end{aligned}$$

where $\beta_1 > 0$ for expanding universe and $m > 0, (m \neq 1)$. Clearly, the deceleration parameter is a dynamical quantity. Here by taking some specific values of free parameters, one can get the negative values of the deceleration parameter. In particular, for $T \rightarrow 0$, the deceleration parameter reduces to $q = \frac{3(\eta_2-m)}{m+2} - 1$ while, for later phases of universe, i.e., $T \rightarrow \infty$, it takes the value $q = \frac{3(2\beta_1-m)}{m+2} - 1$. The behavior of these specific values of deceleration parameter is shown in Fig. 6.1. The blue curve corresponds to its value when $T \rightarrow 0$ indicating a deceleration phase of the universe while red curve provides its behavior for later cosmic epochs indicating a negative behavior and hence supports to accelerated late phases of universe. For $m > 0; m \neq 1$, in earlier times, expansion and shear scalar

goes to infinity and volume is zero while in later times volume goes to infinity and expansion as well as shear scalars of the universe approaches to zero where the constraints $m < \eta_2 < 2\beta_1$ should be satisfied. Which shows the expanding universe at infinite rate of expansion from zero volume to infinitely large size. For all values of m except $m = 1$, the anisotropic parameter of expansion is constant. Hence, in later times the model does not isotropize.

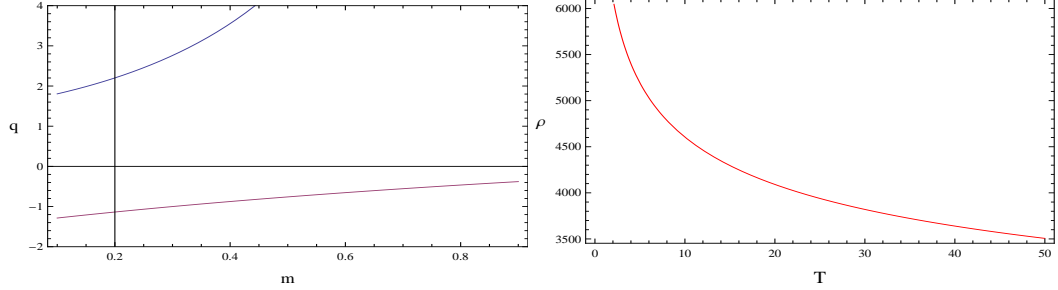


Figure 6.1: The left plot represents the behavior of deceleration parameter q versus m while right plot indicates the behavior of energy density versus T where $n = 0.02$, $\beta_1 = 0.2$, $m = 2$, $\xi = -0.5$, $\zeta = -1.5$, $\omega_0 = 0.5$, $c_1 = -0.01$ and $c_3 = 1$.

Using model (3.1.55) in (2.9.3), we can write the scalar potential V as follows

$$\begin{aligned}
V(\phi) \approx V(T) = & \omega_0 \beta_1^2 c_1^2 \{2\eta_2 - \zeta \beta_1 - 2\beta_1 - 2m\} \frac{T^{\zeta \beta_1 + 2\beta_1 + 2m - 2\eta_2}}{\zeta \beta_1 + 2\beta_1 + 2m - 2\eta_2} \\
& + \omega_0 \xi \kappa^2 c_1^2 \left\{ 2\eta_2 - 2\beta_1 - 6\eta_2 \beta_1^2 - \zeta \beta_1^2 \eta_2 - 2\beta_1^2 \eta_2 + 2\zeta \beta_1^3 + 4m\beta_1^2 - 2m\beta_1 \eta_2 \right. \\
& \left. + 8\beta_1^3 \right\} \frac{T^{\zeta \beta_1 + 4\beta_1 + 2m - 2\eta_2}}{\zeta \beta_1 + 4\beta_1 + 2m - 2\eta_2} + \frac{4\omega_0 \beta_1^2 \xi^2 \kappa^4 c_1^2 (\eta_2 - 3\beta_1)}{\zeta \beta_1 + 6\beta_1 + 2m - 2\eta_2} T^{\zeta \beta_1 + 6\beta_1 + 2m - 2\eta_2} \\
& + \frac{8\beta_1^2 \xi^2 \kappa^4 c_1^2 (m+2)}{4\beta_1 + 2m - 2\eta_2} T^{4\beta_1 + 2m - 2\eta_2} + 8\beta_1 \xi^3 \kappa^6 c_1^2 (m+2) (\eta_2 - 3\beta_1) \\
& \times \frac{T^{6\beta_1 + 2m - 2\eta_2}}{6\beta_1 + 2m - 2\eta_2} + c_3. \tag{6.2.4}
\end{aligned}$$

Substituting (6.2.4) into (6.1.12), we have

$$\begin{aligned}
\kappa^2 \rho(T) = & (2m+1)c_1^3 T^{2m-2\eta_2} + \frac{\xi \kappa^2 c_1^2}{\beta_1} \left(2m\beta_1^2 + 4\beta_1^2 + 2m\eta_2 - 2m\beta_1 + \eta_2 - \beta_1 \right) \\
& \times T^{2m-2\eta_2+2\beta_1} + \frac{\xi^2 \kappa^4 c_1^2}{\beta_1} \left\{ (\eta_2 - 2\beta_1)(2m\beta_1 + 2m + 4\beta_1 + 1) + \frac{8\beta_1^3(m+2)}{2m-2\eta_2+4\beta_1} \right\} \\
& \times T^{2m-2\eta_2+4\beta_1} + \frac{8\beta_1 \xi^3 \kappa^6 c_1^2(m+2)}{2m-2\eta_2+6\beta_1} (\eta_2 - 3\beta_1) T^{2m-2\eta_2+6\beta_1} + \omega_0 \beta_1^2 c_1^2 \{ 2\eta_2 - \zeta \beta_1 \\
& \times -2\beta_1 - 2m \} \frac{T^{\zeta \beta_1 + 2m - 2\eta_2 + 2\beta_1}}{2(\zeta \beta_1 + 2\beta_1 + 2m - 2\eta_2)} + \omega_0 \xi \kappa^2 c_1^2 \left\{ 2\eta_2^2 \beta_1 - 8\eta_2 \beta_1^2 - \zeta \beta_1^2 \eta_2 \right. \\
& \left. + 2\zeta \beta_1^3 + 8\beta_1^3 - 2m\beta_1 \eta_2 + 8m\beta_1^2 \right\} \frac{T^{\zeta \beta_1 + 2m - 2\eta_2 + 4\beta_1}}{2(\zeta \beta_1 + 4\beta_1 + 2m - 2\eta_2)} + 4\omega_0 \beta_1^2 \xi^2 \kappa^4 c_1^2 \\
& \times (\eta_2 - 3\beta_1) \frac{T^{\zeta \beta_1 + 2m - 2\eta_2 + 6\beta_1}}{\zeta \beta_1 + 2m - 2\eta_2 + 6\beta_1} + c_3, \tag{6.2.5}
\end{aligned}$$

where c_3 denotes the constant of integration. Eq's (6.1.8) and (6.1.9) leads to

$$w = -1 - \frac{\frac{d\rho}{dt}}{(m+2)\rho^{\frac{B}{B}}}. \tag{6.2.6}$$

Using (6.2.5), we can write the EoS parameter as

$$\begin{aligned}
w(T) = & -1 - \frac{1}{(m+2)\rho} \left[(2m+1)(2m-2\eta_2)c_1^3 T^{2m-2\eta_2} + \frac{\xi \kappa^2 c_1^2}{\beta_1} (2m-2\eta_2+2\beta_1) \right. \\
& \times \left(2m\beta_1^2 + 4\beta_1^2 + 2m\eta_2 - 2m\beta_1 + \eta_2 - \beta_1 \right) T^{2m-2\eta_2+2\beta_1} + \frac{\xi^2 \kappa^4 c_1^2}{\beta_1} (2m-2\eta_2 \\
& + 4\beta_1) \left\{ (2m\beta_1 + 2m + 4\beta_1 + 1)(\eta_2 - 2\beta_1) + \frac{8\beta_1^3(m+2)}{2m-2\eta_2+4\beta_1} \right\} T^{2m-2\eta_2+4\beta_1} + 8\beta_1 \xi^3 \\
& \times \kappa^6 c_1^2 (m+2)(\eta_2 - 3\beta_1) T^{2m-2\eta_2+6\beta_1} + \frac{\omega_0 \beta_1^2 c_1^2}{2} T^{\zeta \beta_1 + 2m - 2\eta_2 + 2\beta_1} \{ 2\eta_2 - \zeta \beta_1 \\
& - 2\beta_1 - 2m \} + \frac{1}{2} \omega_0 \xi \kappa^2 c_1^2 \left\{ 2\beta_1 \eta_2^2 - 2m\beta_1 \eta_2 - 8\beta_1^2 \eta_2 + 8\beta_1^3 - \zeta \beta_1^2 \eta_2 + 2\zeta \beta_1^3 \right. \\
& \left. + 8m\beta_1^2 \right\} T^{\zeta \beta_1 + 2m - 2\eta_2 + 4\beta_1} + 4\omega_0 \beta_1^2 \xi^2 \kappa^4 c_1^2 (\eta_2 - 3\beta_1) T^{\zeta \beta_1 + 2m - 2\eta_2 + 6\beta_1} \left. \right], \tag{6.2.7}
\end{aligned}$$

where ρ is given by (6.2.5) and the skewness parameters becomes

$$\delta(T) = \frac{2n(m+2)}{3\rho} c_1^2 T^{2m-2\eta_2} \left(1 + \xi \kappa^2 T^{2\beta_1} \right)^{-2 + \frac{\eta_2}{\beta_1}}, \tag{6.2.8}$$

$$\gamma(T) = -\frac{nm(m+2)}{3\rho} c_1^2 T^{2m-2\eta_2} \left(1 + \xi \kappa^2 T^{2\beta_1} \right)^{-2 + \frac{\eta_2}{\beta_1}}, \tag{6.2.9}$$

and the anisotropic expansion measure of anisotropic fluid becomes

$$\frac{\delta - \gamma}{w} = \frac{n(m+2)^2 c_1^2 T^{-2\eta_2+2m} \left(1 + \xi \kappa^2 T^{2\beta_1}\right)^{-2+\frac{\eta_2}{\beta_1}}}{3\rho(T)w(T)}, \quad (6.2.10)$$

where $\rho(T)$ is given by (6.2.5) and $w(T)$ is given in (6.2.7).

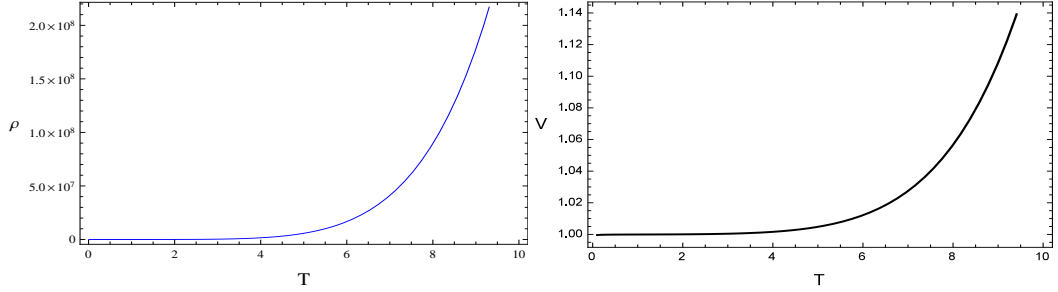


Figure 6.2: Left plot represents ρ and right plot indicates scalar potential versus T for $n = 0.02$, $\beta_1 = 1.2$, $m = 2$, $\xi = -0.5$, $\zeta = -1.5$, $\omega_0 = 0.5$, $c_1 = -0.01$ and $c_3 = 1$.

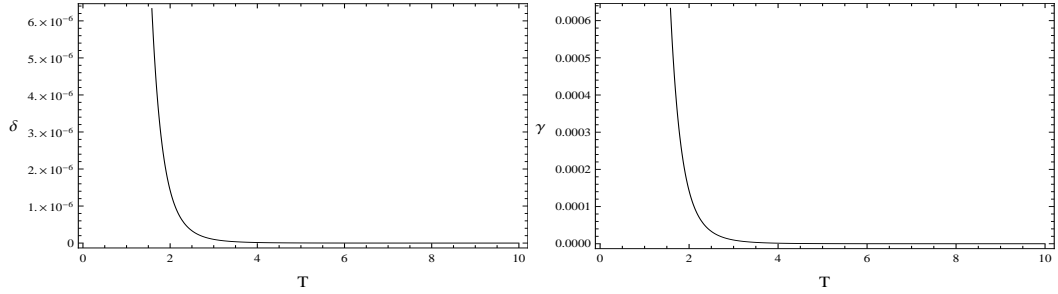


Figure 6.3: Left plot refers to skewness parameter δ while right plot provides γ versus T for $n = 0.02$, $\beta_1 = 1.2$, $m = 2$, $\xi = -0.5$, $\zeta = -1.5$, $\omega_0 = 0.5$, $c_1 = -0.01$ and $c_3 = 1$.

The Right panel of Fig. 6.1 indicates the behavior of density function versus T . Here we have taken $\beta_1 = 0.2$. Clearly ρ shows positive decreasing behavior that is consistent with phenomenon of cosmic expansion. According to which with the expanding universe $T \rightarrow \infty$, the density of cosmos will almost vanish. The left curve of Fig. 6.2 also refers to positive behavior of energy density for $\beta_1 = 1.2$ however, it shows increasing behavior that is a non-physical case. The scalar potential is also positive and shows increasing behavior. In Fig. 6.3, the behavior of skewness parameters is shown, these are finite at initial time while in later times, both tends to zero and hence supporting isotropic behavior of fluid in final stages. Now we will discuss the EoS parameter for $\beta_1 > \frac{2(\eta_2-m)}{\zeta+6}$ and $\beta_1 < \frac{2(\eta_2-m)}{\zeta+6}$. In

early times of the universe, we get EoS of the form $w = -1 + \frac{2(\eta_2 - m)}{m+2}$ which may show the quintessence or decelerated cosmic phase by an appropriate selection of free parameters. While in later times, we have $w = -1 - \frac{\beta_1(\zeta+6)-2(\eta_2-m)}{m+2}$, in case of $\beta_1 > \frac{2(\eta_2-m)}{\zeta+6}$, we have $w < -1$ which shows the phantom region and for $\beta_1 < \frac{2(\eta_2-m)}{\zeta+6}$, we can get $w > -1$ shows the quintessence region. Thus in both cases, we get accelerated phases of cosmos. In Fig. 6.4, its behavior versus cosmic time has been given. Here the EoS parameter shows negative behavior indicating the phantom cosmic phase. Also, in the same figure, the anisotropic expansion measure of anisotropic fluid indicates that in initial cosmic epochs, this parameter takes infinitely large values but later on, it decreases and converges to zero for the final stages of universe.

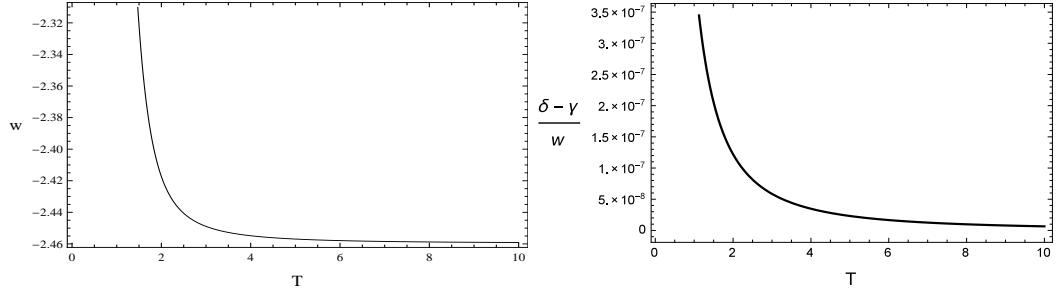


Figure 6.4: Right plot represents anisotropic expansion measure of anisotropic fluid $\frac{\delta - \gamma}{w}$ versus T and left plot corresponds to the deviation free EoS parameter w versus T for the same choice of parameters

6.2.2 The Model: $f(R, \phi) = \frac{R - 2\Lambda(1 - e^{b_1 \phi \kappa^3 R})}{\kappa^2}$

The second model we have chosen is (3.1.45). Now we will use this model to discuss the solution of field equations in the presence of anisotropic fluid.

Subtracting (6.1.13) from (6.1.14) and then by using power law ansatz (6.1.15) along with the model (3.1.45), we have the following differential equation:

$$\frac{\ddot{B}}{B} - (m+1)\frac{\dot{B}^2}{B^2} - \left(\frac{2\Lambda b_1 \kappa^3 \beta_1 B^{\beta_1}}{1 - 2\Lambda b_1 \kappa^3 B^{\beta_1}} \right) \frac{\dot{B}^2}{B^2} + \left(\frac{\eta_2}{1 - 2\Lambda b_1 \kappa^3 B^{\beta_1}} \right) \frac{\dot{B}^2}{B^2} = 0, \quad (6.2.11)$$

where $\eta_2 = \frac{n(m+2)^2 \kappa^4}{3(m-1)}$. Its twice integration yields

$$\frac{B^{\eta_2-m}}{\eta_2-m} - \frac{2\Lambda b_1 \kappa^3}{\beta_1} (2\beta_1 - 2\eta_2) \frac{B^{\eta_2-m+\beta_1}}{\eta_2-m+\beta_1} = k_1 t + k_2, \quad (6.2.12)$$

where k_1, k_2 are constants of integration. Taking $B = T, x = X, y = Y, z = Z$, the space-time reduces to

$$ds^2 = \frac{1}{k_1^2} T^{2\eta_2-2m-2} \left(1 - 2\Lambda b_1 \kappa^3 T^{\beta_1}\right)^{2-\frac{2\eta_2}{\beta_1}} dT^2 - T^{2m} dX^2 - T^2 (dY^2 + dZ^2). \quad (6.2.13)$$

The corresponding parameters become

$$\begin{aligned} \Delta &= \frac{2(m-1)^2}{(m+2)^2}, \quad V = T^{m+2}, \\ H_x &= mH_y = m k_1 T^{m-\eta_2} \left(1 - 2\Lambda b_1 \kappa^3 T^{\beta_1}\right)^{-1+\frac{\eta_2}{\beta_1}}, \\ H &= \left(\frac{m+2}{3}\right) k_1 T^{m-\eta_2} \left(1 - 2\Lambda b_1 \kappa^3 T^{\beta_1}\right)^{-1+\frac{\eta_2}{\beta_1}}, \\ \Theta &= 3H = (m+2) k_1 T^{m-\eta_2} \left(1 - 2\Lambda b_1 \kappa^3 T^{\beta_1}\right)^{-1+\frac{\eta_2}{\beta_1}}, \\ \sigma^2 &= \frac{1}{3} (m-1)^2 k_1^2 T^{2m-2\eta_2} \left(1 - 2\Lambda b_1 \kappa^3 T^{\beta_1}\right)^{-2+\frac{2\eta_2}{\beta_1}}, \\ q &= \frac{3}{m+2} \left\{ \frac{(\eta_2-m) + (m-\beta_1) 2\Lambda b_1 \kappa^3 T^{\beta_1}}{1 - 2\Lambda b_1 \kappa^3 T^{\beta_1}} \right\} - 1, \end{aligned}$$

where $\beta_1 > 0$ and $m > 0, (m \neq 1)$. Here we will illustrate the behavior of these physical parameters. For $0 < m < 1$, these parameters have increasing behavior with increasing T . Also, the appropriate selection of free constants can lead to the negative behavior of deceleration parameter. For example, for initial and later cosmic epochs, the deceleration parameter becomes $q = \frac{3(\eta_2-m)}{m+2} - 1$ and $q = \frac{3(m-\beta_1)}{m+2} - 1$, respectively. The graphical behavior of these values versus parameter m indicates a similar behavior as shown in Fig. 6.4 and hence supports to the same arguments. In earlier cosmic times, the expansion and shear scalars goes to infinity and volume turns out to be zero while in later cosmic stages, volume goes to infinity while the expansion and shear scalars of the universe model approaches to zero. That supports to expanding behavior of universe at infinite rate of expansion. For all values of m the anisotropic parameter of expansion appears constant except $m = 1$, so in final stages of cosmos it did not approach to isotropy.

Utilizing model (3.1.45) in (2.9.3), we can write the scalar potential as follows

$$\begin{aligned}
V(\phi) \approx V(T) &= \frac{\omega_0 \beta_1^2 k_1^2}{\zeta \beta_1 + 2m - 2\eta_2 + 2\beta_1} \{ \zeta \beta_1 - 2\beta_1 - 2m - 4\Lambda b_1 \kappa^3 \beta_1 + 2\eta_2 \} \\
&\times T^{\zeta \beta_1 + 2m - 2\eta_2 + 2\beta_1} + 2\omega_0 \beta_1 \Lambda b_1 \kappa^3 k_1^2 \{ (2m - \zeta \beta_1 + 2\beta_1)(2\eta_2 - 2\beta_1) + 4\beta_1 \Lambda b_1 \kappa^3 \\
&\times (2\eta_2 - 3\beta_1) - 2\eta_2(2\eta_2 - 3\beta_1) \} \frac{T^{\zeta \beta_1 + 2m - 2\eta_2 + 3\beta_1}}{\zeta \beta_1 + 2m - 2\eta_2 + 3\beta_1} + 2\Lambda b_1 \kappa \beta_1 k_1^2 \{ 2m^2 + 4m \\
&+ 3 - \eta_2(m + 2) \} \frac{T^{2m - 2\eta_2 + \beta_1}}{2m - 2\eta_2 + \beta_1} + 4\Lambda^2 b_1^2 \kappa^4 k_1^2 \{ \beta_1^2(m + 2) - (2m^2 + 4m + 3) \\
&\times (2\eta_2 - 2\beta_1) + \eta_2(m + 2)(2\eta_2 - 3\beta_1) \} \frac{T^{2m - 2\eta_2 + 2\beta_1}}{2m - 2\eta_2 + 2\beta_1} - 8\Lambda^3 b_1^3 \kappa^7 \beta_1 k_1^2(m + 2) \\
&\times (2\eta_2 - 3\beta_1) \frac{T^{2m - 2\eta_2 + 3\beta_1}}{2m - 2\eta_2 + 3\beta_1} + k_3. \tag{6.2.14}
\end{aligned}$$

Using the self-interacting potential (6.2.14) into (6.1.12), we have

$$\begin{aligned}
\kappa^2 \rho(T) &= \frac{1}{2} \omega_0 \beta_1 k_1^2 T^{\zeta \beta_1 + 2m - 2\eta_2 + \beta_1} + \omega_0 k_1^2 \left\{ \zeta \beta_1^3 - 2m\beta_1^2 - 4\Lambda b_1 \kappa^3 \beta_1^3 - 2\beta_1^3 \right. \\
&+ 2\eta_2 \beta_1^2 + \Lambda b_1 \kappa^3 (2\eta_2 - 2\beta_1)(\zeta \beta_1 + 2m - 2\eta_2 + 2\beta_1) \left. \right\} \frac{T^{\zeta \beta_1 + 2m - 2\eta_2 + 2\beta_1}}{\zeta \beta_1 + 2m - 2\eta_2 + 2\beta_1} \\
&+ \frac{2\omega_0 \beta_1 \Lambda b_1 \kappa^3 k_1^2}{\zeta \beta_1 + 2m - 2\eta_2 + 3\beta_1} \{ (2m - \zeta \beta_1 + 2\beta_1)(2\eta_2 - 2\beta_1) + 4\beta_1 \Lambda b_1 \kappa^3 (2\eta_2 - 3\beta_1) \\
&- 2\eta_2(2\eta_2 - 3\beta_1) \} T^{\zeta \beta_1 + 2m - 2\eta_2 + 3\beta_1} + \frac{(2m + 1)k_1^2}{\kappa^2} T^{2m - 2\eta_2} + \frac{2\Lambda b_1 \kappa \beta_1 k_1^2}{2m - 2\eta_2 + \beta_1} \\
&\times \left\{ (2m^2 + 4m + 3) - (m + 2)(2m + \beta_1 - 2\eta_2) - \frac{2m + 1}{\beta_1^2} (2\eta_2 - \beta_1)(2m - 2\eta_2 + \beta_1) \right. \\
&- \eta_2(m + 2) \left. \right\} T^{2m - 2\eta_2 + \beta_1} + 4\Lambda^2 b_1^2 \kappa^4 k_1^2 \{ \beta_1^2(m + 2) - (2m^2 + 4m + 3)(2\eta_2 - 2\beta_1) \\
&+ (2m + 2\beta_1 - 2\eta_2)(m + 2) + \eta_2(m + 2)(2\eta_2 - 3\beta_1) \} \frac{T^{2m - 2\eta_2 + 2\beta_1}}{2m - 2\eta_2 + 2\beta_1} - 8\Lambda^3 b_1^3 \kappa^7 \\
&\times \beta_1 k_1^2(m + 2)(2\eta_2 - 3\beta_1) \frac{T^{2m - 2\eta_2 + 3\beta_1}}{2m - 2\eta_2 + 3\beta_1} + k_3, \tag{6.2.15}
\end{aligned}$$

where k_3 is an integration constant. Equations (6.1.8) and (6.1.9) show that

$$w = -1 - \frac{\frac{d\rho}{dt}}{(m + 2)\rho^{\frac{B}{B}}}. \tag{6.2.16}$$

From (6.2.16), we can write the EoS parameter as

$$\begin{aligned}
w(T) = & -1 - \frac{1}{(m+2)\rho} \left[\frac{1}{2} \omega_0 \beta_1 k_1^2 (\zeta \beta_1 + 2m - 2\eta_2 + \beta_1) T^{\zeta \beta_1 + 2m - 2\eta_2 + \beta_1} + \omega_0 k_1^2 \right. \\
& \times \left\{ \zeta \beta_1^3 - 2\beta_1^3 - 2m\beta_1^2 - 4\Lambda b_1 \kappa^3 \beta_1^3 + \Lambda b_1 \kappa^3 (2\eta_2 - 2\beta_1) (\zeta \beta_1 + 2m - 2\eta_2 + 2\beta_1) \right. \\
& \left. + 2\eta_2 \beta_1^2 \right\} T^{\zeta \beta_1 + 2m - 2\eta_2 + 2\beta_1} + 2\omega_0 \beta_1 \Lambda b_1 \kappa^3 k_1^2 \left\{ (2m - \zeta \beta_1 + 2\beta_1) (2\eta_2 - 2\beta_1) \right. \\
& \left. + 4\beta_1 \Lambda b_1 \kappa^3 (2\eta_2 - 3\beta_1) - 2\eta_2 (2\eta_2 - 3\beta_1) \right\} T^{\zeta \beta_1 + 2m - 2\eta_2 + 3\beta_1} + \frac{1}{\kappa^2} (2m+1) k_1^2 \\
& \times (2m - 2\eta_2) T^{2m-2\eta_2} + 2\Lambda b_1 \kappa \beta_1 k_1^2 \left\{ (2m^2 + 4m + 3) - (m+2)(2m + \beta_1 - 2\eta_2) \right. \\
& \left. - \frac{2m+1}{\beta_1^2} (2\eta_2 - \beta_1) (2m - 2\eta_2 + \beta_1) - \frac{n(m+2)^3 \kappa^4}{3(m-1)} \right\} T^{2m-2\eta_2+\beta_1} + 4\Lambda^2 b_1^2 \kappa^4 k_1^2 \\
& \times T^{2m-2\eta_2+2\beta_1} \left\{ (m+2)(\beta_1^2 + 2m + 2\beta_1 - 2\eta_2) - (2\eta_2 - 2\beta_1)(2m^2 + 4m + 3) \right. \\
& \left. + \frac{n(m+2)^3 \kappa^4 (2\eta_2 - 3\beta_1)}{3(m-1)} \right\} - 8\Lambda^3 b_1^3 \kappa^7 \beta_1 k_1^2 (m+2)(2\eta_2 - 3\beta_1) T^{2m-2\eta_2+3\beta_1} + k_3 \Big],
\end{aligned} \tag{6.2.17}$$

where ρ is given by (6.2.15). Further the skewness parameters are defined below:

$$\delta(T) = \frac{2n(m+2)}{3\rho} k_1^2 T^{2m-2\eta_2} \left(1 - 2\Lambda b_1 \kappa^3 T^{\beta_1} \right)^{-2 + \frac{2\eta_2}{\beta_1}}, \tag{6.2.18}$$

$$\gamma(T) = -\frac{nm(m+2)}{3\rho} k_1^2 T^{2m-2\eta_2} \left(1 - 2\Lambda b_1 \kappa^3 T^{\beta_1} \right)^{-2 + \frac{2\eta_2}{\beta_1}}, \tag{6.2.19}$$

and the anisotropic expansion measure of anisotropic fluid is given by

$$\frac{\delta - \gamma}{w} = \frac{n(m+2)^2 k_1^2 T^{-2\eta_2+2m} \left(1 - 2\Lambda b_1 \kappa^3 T^{\beta_1} \right)^{-2 + \frac{2\eta_2}{\beta_1}}}{3\rho(T)w(T)}, \tag{6.2.20}$$

where $\rho(T)$ is given by (6.2.15) and $w(T)$ is given in (6.2.17).

The plots of energy density, potential, skewness parameters and EoS parameter denoted are shown in Figures 6.5-6.7. In Fig. 6.5, the behavior of scalar potential and energy density is given. Scalar potential shows increasing behavior and energy density shows decreasing behavior and approaches to zero in later times.

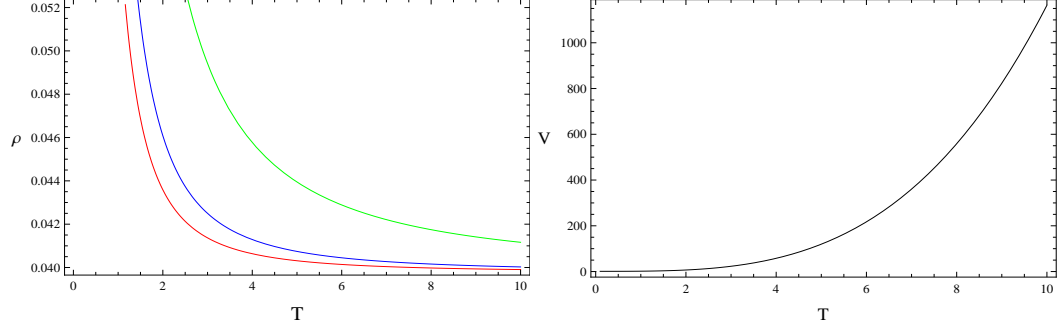


Figure 6.5: Left plot represents ρ for three values of β while right plot indicates scalar potential versus T for $n = 0.002$, $\beta_1 = 1.2$, $m = 4$, $b_1 = 1$, $\zeta = 2.5$, $\omega_0 = 0.5$, $k_1 = 1$ and $k_3 = 1$.

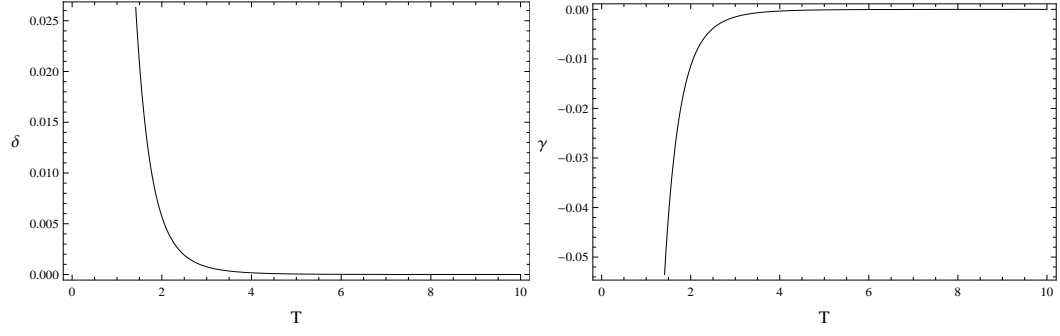


Figure 6.6: Plot represents skewness parameters δ and γ versus T for $n = 0.002$, $\beta_1 = 1.2$, $m = 4$, $b_1 = 1$, $\zeta = 2.5$, $\omega_0 = 0.5$, $k_1 = 1$ and $k_3 = 1$.

In initial cosmic epochs, the skewness parameters are finite and turns out to be zero in later cosmic times as shown in Fig. 6.6. Now we will discuss the EoS parameter for $\beta_1 > \frac{2(\eta_2-m)}{\zeta+3}$ and $\beta_1 < \frac{2(\eta_2-m)}{\zeta+3}$. The EoS parameter, in early times of the universe, turns out to be $w = -1 + \frac{2(\eta_2-m)\kappa^2}{m+2}$ which may show any of quintessence or phantom region by choosing suitable choice of free parameters. While in later times, we have $w = -1 - \frac{\{\beta_1(\zeta+3)-2(\eta_2-m)\}\kappa^2}{m+2}$ which shows the quintessence region ($w > -1$) for $\beta_1 < \frac{2(\eta_2-m)}{\zeta+3}$ and phantom region ($w < -1$) for $\beta_1 > \frac{2(\eta_2-m)}{\zeta+3}$. The EoS parameter indicates the phantom region of cosmic expansion as shown in Fig. 6.7. Also, the anisotropic expansion measure of fluid shows infinite behavior initially but goes to zero for later cosmic epochs.

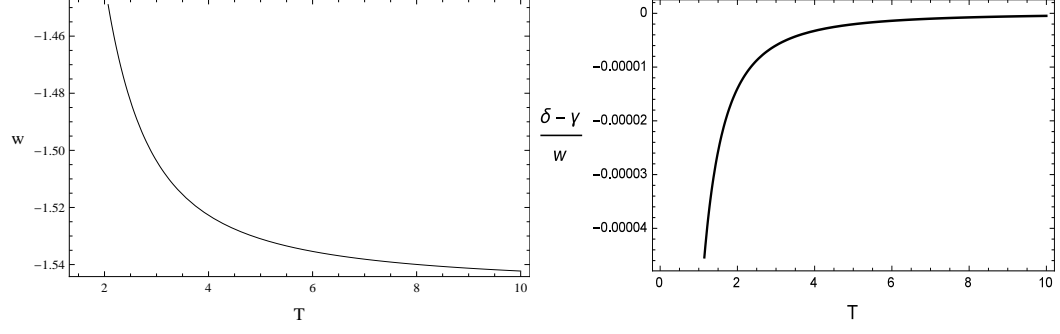


Figure 6.7: Left plot provides the behavior of EoS parameter w versus T for $n = 0.002$, $\beta_1 = 1.2$, $m = 4$, $b_1 = 1$, $\zeta = 2.5$, $\omega_0 = 0.5$, $k_1 = 1$ and $k_3 = 1$ while right plot indicates the anisotropic expansion measure of fluid versus T for the same choice of free parameters.

Chapter 7

Conclusions

Scalar tensor theories of gravity are very useful to discuss accelerated cosmic expansion and to predict the universe destiny. These theories proved to be much promising due to their vast applications in gravitation and cosmology. These theories play key role in developing models of inflation and DE. One of more general modified gravity is, $f(R, R_{\mu\nu}R^{\mu\nu}, \phi)$ which include the Ricci scalar, contraction of Ricci tensors and scalar field. In this chapter we have summarized the main results of the thesis and discuss the conclusions. Focussing on FRW, Morris-Thorne geometry and LRS BI universe models we have discussed the cosmological issues.

In first section of Chapter 3, we have applied the reconstruction programme to $f(R, R_{\mu\nu}R^{\mu\nu}, \phi)$ theory. The action (2.10.1) in the original and specific forms as regards $f(R, \phi)$, $f(Y, \phi)$ is reconstructed for some well-known solutions in FRW background. The existence of dS solutions has been investigated in modified theories [181]. Here, we have developed multiple dS solutions which may be useful in explaining the different cosmic phenomena. In a dS universe, we have constructed the more general case $f(R, Y, \phi)$ and establish $f(R, \phi)$ considering the function independent of Y and $f(Y, \phi)$ by taking function independent of R . The power law expansion history has also been reconstructed in this modified theory for both general as well as particular form of the action (2.10.1). These solutions explain the matter/radiation dominated phase that connects with the accelerating epoch. The $f(R, R_{\mu\nu}R^{\mu\nu}, \phi)$ model can also be reconstructed which will reproduce the crossing of phantom divide exhibiting the superaccelerated expansion of the universe.

The Lagrangian of $f(R, R_{\mu\nu}R^{\mu\nu}, \phi)$ gravity is more comprehensive implying that different functional forms of f can be suggested. The change in Lagrangian arouse the question how to constrain such a theory on physical grounds. In this chapter, we have formulated the constraints on $f(R, T, R_{\mu\nu}T^{\mu\nu})$ gravity and its specific forms by examining the energy conditions. The energy conditions are also developed in terms of deceleration, jerk, and snap parameters. To show how energy conditions constrain the $f(R, R_{\mu\nu}R^{\mu\nu}, \phi)$ gravity, we have examined the free parameters in reconstructed and well known models. In general dS case $f(R, Y, \phi)$ energy conditions are depending on six parameters β_1, ζ, t and α_i 's where $i = 1, 2, 3$. In this procedure we have fixed the α_i 's and observe the feasible region by varying the other parameters.

In dS $f(R, \phi)$ and $f(Y, \phi)$ models, the NEC depend on five parameters $t, \alpha_1, \alpha_2, \beta_1$ & ζ and WEC depend only on three parameters t, α_1 & α_2 . In case of NEC we have fixed α_1, α_2 and find the constraints on the other parameters. In WEC we are changing α_1 and explore the possible ranges on α_2 and t . For power law $f(R, \phi)$ and $f(Y, \phi)$ models, functions depend on six parameters $\alpha_1, \alpha_2, \beta_1, \zeta, n_1$ and t . In power law case we have $n_1 > 1$, and varying α_1, α_2 we have analyzed the viable constraints on β_1, ζ and t . Further more we have considered three particular forms of $f(R, Y, \phi)$ gravity taking function independent of Y , i.e., $f(R, \phi)$, $Rf(\phi)$, $\phi f(R)$ from which we can deeply understand the applications of energy conditions. Model-I is a function of four parameters b_1, β_1, n_1 and t , we have checked the validity of NEC and WEC by varying b_1 . Model-II is depending on β_1, ζ, n_1 and t , for $n_1 > 1$ we have explored the viability of other parameters. Next in model-III we have five parameters β_1, ξ, n_1, ζ and t , for $n_1 > 1$ we have find the feasible constraints on other parameters by fixing ζ . In model-IV the conditions are depending on five parameters $\beta_1, \alpha, n_1, \zeta$ and t . we have $n_1 > 1$ and varying β_1 we examined the possible regions for the other parameters.

Finally, we generally discuss the variations of parameters involved in power law solutions and scalar field coupling function, denoted by ζ and n_1 respectively. In dS models we have examined that the more general case $f(R, Y, \phi)$ is more effective as compared to $f(R, \phi)$ and $f(Y, \phi)$ models since in general case one can specify the parameters in more comprehensive way. In all cases of dS models, WEC is valid for all ζ and NEC is valid if ($\zeta \geq 1$ & $\zeta \leq -5$). In power law case $f(R, \phi)$, for both NEC and WEC n_1 has a fixed value $n_1 = 3$ and ζ has variations ($\zeta \geq 0$ & $\zeta \leq -5.5$). For $f(Y, \phi)$ case we have ($n_1 \geq 2.3$ with $\zeta \geq 4, \zeta \leq -1$) for WEC and for NEC we have $n_1 \geq 2$ with ($\zeta \geq 0, \zeta \leq -4$). In other known $f(R, \phi)$ models, the validity of these conditions require $n_1 > 1$ with ($\zeta \geq 0, \zeta \leq -2$).

In second section of Chapter 3, we have discussed the thermodynamical laws in the context of modified $f(R, R_{\mu\nu}R^{\mu\nu}, \phi)$ theory. This theory can be regarded as an extended form of $f(R, \phi)$ gravity. Here, we have presented the general formalism of field equations for FRW spacetime with any spatial curvature in this theory and shown that these equations can be cast to the form of FLT $T_h d\hat{S}_h + T_{in} d\hat{S}_{in} = \delta Q$, in non-equilibrium and

$T_h d\hat{S}_h = \delta Q$ in equilibrium description of thermodynamics. In this structure of FLT we find that entropy is contributed from two factors, first one corresponds to horizon entropy defined in terms of area and second represents the entropy production term $d\bar{S}$ which is produced because of the non-equilibrium description in $f(R, Y, \phi)$ gravity. It is important to mention here that no such term is present in Einstein, Gauss-Bonnet, scalar-tensor theory with non-minimally derivative coupling, Lovelock and braneworld modified theories [55]-[58]. However, in case of modified theories like $f(R)$ and scalar tensor theories people have suggested various schemes to avoid the additional entropy term in FLT [60, 61, 182]. Following such approach one can also discuss the equilibrium thermodynamics as done in [60, 65].

Moreover, the validity of GSLT at the apparent horizon of FRW universe is also tested in this modified theory. We present the general relation involving contributions from horizon entropy, auxiliary entropy terms and associated with the matter contents within the horizon is presented in comprehensive way. Here, we have assumed the proportionality relation between the temperatures related to apparent horizon and matter components inside the horizon. To discuss the validity of GSLT, we have selected the more generic models reconstructed in Sec. 3.1. The discussions are in detail as we have also considered some well known models from different backgrounds to validate the GSLT. We can retrieve the results in other modified theories depending on the choice of the Lagrangian $f(R, Y, \phi)$. When we consider function independent of Y we can reduce the results of $f(R, Y, \phi)$ into $f(R, \phi)$ gravity and choosing $f(R, Y, \phi) = R\phi$ we get the results for BD theory. Further, by considering a function independent of Y and ϕ we get the results for $f(R)$ gravity. Table 3.2 summarizes the regions where the GSLT is satisfied for all the models that we have discussed.

In a dS $f(R, Y, \phi)$ model, one can notice that the validity of the GSLT depends on five parameters $\alpha_1, \alpha_2, \alpha_3, \beta_1$ and t and hence we fixed two parameters, α_1 and α_2 to show the viable regions by varying the other parameters. Next we have considered $f(R, \phi)$ using dS model whose GSLT constraint depends on four parameters $\alpha_1, \alpha_2, \beta_1$ and t . Here we are fixing β_1 and observe the feasible regions by varying the other parameters. In power law $f(R, \phi)$ case by varying α_1, α_2 we have examined the feasible constraints on β_1, n_1 and t .

Next we have considered four known models of $f(R, Y, \phi)$ gravity independent of Y , which are of the form $f(R, \phi)$, $Rf(\phi)$, $\phi f(R)$. Model-I is depending on four parameters b_1 , n_1 , β_1 and t , we have checked the validity of $\dot{S}_{tot} \geq 0$ by varying b_1 . Model-II is a function of four parameters β_1 , ζ , n_1 and t , by fixing n_1 we have discussed the viability of the GSLT for feasible values of β_1 , ζ and t . In model-III the constraint is depending on four parameters n_1 , ξ , β_1 and t . By fixing $n_1 > 1$ we examined the possible regions for the other parameters. Next in model-IV we have four parameters n_1 , α , β_1 and t . For $n_1 > 1$ we have find the feasible constraints on other parameters.

Wormhole solutions in GR do not satisfy all the standard energy conditions. Other approach is then to modify Einstein field equations in terms of an effective EMT that satisfy the energy bounds and the exotic part of the wormholes are supported by higher order curvature terms.

In Chapter 4 we have studied whether in $f(R, \phi)$ modified theory, the ordinary matter can support wormholes. In the last decades, it has been mentioned that in highly compacted astrophysical objects, pressures are anisotropic, which means that the tangential and radial pressures are not equal for such objects. Investigating the existence of wormholes for different kind of fluids are then an interesting question to address. To investigate this we have analyzed the behavior of NEC and WEC for three different supporting fluids: a barotropic fluid, an anisotropic fluid and an isotropic fluid. Additionally, we have constructed wormholes satisfying the flaring-out condition $\beta'(r = r_0) < 1$ where r_0 is the throat which satisfies $\beta(r = r_0) = r_0$.

To analyse the physics of wormhole solutions, different methods have been discussed in the literature. One method is to find wormhole solutions giving a specific shape function. On the other hand, a second approach is considering the matter content and then calculate the shape function directly from the field equations.

We have explored $f(R, \phi)$ gravity involving coupling between the Ricci scalar and matter field. Here the resulting equations are highly non-linear and complicated involving unknowns p_t , p_r , ρ , a , b , $f(R, \phi)$. Therefore, we have focussed our study in a power-law case $f(R, \phi) = \tilde{\gamma}R\phi^\eta$, where $\tilde{\gamma}$ and η are constants. Then, by choosing $\eta = 1$ and $\zeta = -1$, BD theory is recovered and by choosing $\eta = 2$ and $\zeta > 0$, Induced gravity is recovered.

Then, for an anisotropic, isotropic and barotropic fluids, we have constructed wormhole solutions and then examine the energy conditions.

In the case of an anisotropic matter content, we assumed a specific form of the shape function (power-law type) to obtain a solution and then to check the existence of wormholes. Then, we investigated the validity of standard energy conditions. We have found that in both BD and Induced gravity, an anisotropic generic fluid verifying all the energy conditions can support a wormhole geometry. However, to satisfy all the energy conditions, we must have negative values of $\tilde{\gamma}$. For positive values of $\tilde{\gamma}$, the matter given by the anisotropic fluid will violate some of the energy conditions.

In the case of an isotropic fluid $p_r = p_t = p$, it is possible to solve the field equations to get the shape function and the potential. The shape function then can be constraint to satisfy the wormhole conditions. This is valid for a generic power-law $f(R, \phi)$ gravity. Then, we found that isotropic fluids satisfying all the energy conditions (WEC and NEC) can support wormholes in both BD and Induced gravity.

For an anisotropic matter satisfying a barotropic EoS $p_r = w(r)\rho$, the field equations are complicated to solve. Therefore, we studied some special cases numerically focussing on BD and Induced gravity. This study was carried out by choosing some special values of the parameters. We analyzed the cases where the barotropic function is a constant $w(r) = w$ and also when $w(r) = \tilde{B}r^l$, where \tilde{B} and l are constants. For both cases, we have constraint the parameters in such a way that ensures the conditions to have a traversable wormhole geometry. In both cases, we have found some models where $\rho + p_r > 0$ and also $\rho > 0$ but $\rho + p_t$ can be negative, so that WEC is not always satisfied. Then, for our potential, barotropic fluids in BD and Induced gravity do not satisfy all the energy conditions to support a wormhole geometry. Note that one can also assume a barotropic EoS $p_t = w(r)\rho$, when now the transverse pressure is related to the energy density. If ones carries out the same analysis mentioned above with the same potential, we also get a similar conclusion: wormholes can be constructed satisfying all the geometric required properties but the full WEC is not satisfied. For this case, one has that $\rho + p_t > 0$ and also $\rho > 0$ but $\rho + p_r$ can be negative.

In Chapter 5, we have derived the exact inflationary model in Jordan frame for $f(R, \phi)$

model. Even though it is common to study the $f(R)$ models in Einstein frame, we showed explicitly that in the Einstein frame, action contains non-canonical kinetic term. Thus, the advantage of the conformal transformation is negated. Thus, we performed the background and the first order perturbation analysis in the Jordan frame. The massive scalar field is non-minimally coupled to $f(R)$ action and do not have self-interacting potential. We have evaluated the expression $\rho + 3p$, which led to conclude that for the values $\tilde{n} \ll 1$, $\rho + 3p < 0$ and for $\tilde{n} \gg 1$, we have $\rho + 3p > 0$. In [115], authors also calculated the term $\rho + 3p$ and showed that for $\tilde{n} \gg 1 \Rightarrow \rho + 3p = 0$ which did not lead to inflation. While $\tilde{n} \ll 1$ leads to $\rho + 3p < 0$.

We showed explicitly that the model supports inflationary solution with an exit and the number of e-foldings depends on the deviation of initial values from dS scenario. Further, we have discussed the scalar and tensor perturbations for the chosen $f(R, \phi)$ model. We have used the new analytical method devised in [115] to reduce the higher order scalar perturbation equations to second order in 3-curvature perturbation. We analytically obtained the scalar power spectrum in $\tilde{n} \gg 1$ limit and showed that the scalar power spectrum is scale invariant. We obtained the tensor power-spectrum for $\tilde{n} > \frac{1}{2}$ and showed that the spectrum is blue tilted.

To get insight, we plotted the graphs of slow-roll parameter and scalar field for different initial values of $\dot{\phi}$ i.e., $\dot{\phi} = 0.3\phi_D$, $0.6\phi_D$, $0.9\phi_D$, $1.2\phi_D$, $1.5\phi_D$ and $\dot{\phi} = \phi_D$. The $\varepsilon - N$ trajectories showed that in the parametric space $\dot{\phi} < 1.4\phi_D$, the inflationary phase sustained as $\varepsilon < 1$ and ε attains a constant value less than unity for $\dot{\phi} \geq 1.4\phi_D$. It can be seen that in the space $\dot{\phi} < \phi_D$, the inflationary phase exist without an exit which represent ε is diverging to $-\infty$ while $\dot{\phi} > \phi_D$ leads to the inflationary era with an exit. The initial condition $\dot{\phi} = \phi_D$ generates $\varepsilon = 0$. In this case, the results are obtained for standard No. of e-folds, i.e., $N \simeq 50, 60$, which is in good agreement with observational data. Further, it is observed that as the value of $\frac{\dot{\phi}}{\phi_D}$ is directly proportional to N , as increment in initial value produced an increase in N . Hence rate of inflation increases as $\dot{\phi}$ increases. The trajectories are attracted towards its origin with increasing initial values. This shows that deviation of initial values from dS value leads to either inflation with exit or super inflation, and that the dS solution is a saddle point. The plot $\phi - N$ represents the decaying behavior with evolution of time.

The slow-roll parameter and scalar field versus N for different initial values of $\dot{\phi}$ are also plotted in [115] for $\tilde{n} = 0.01, 0.1$. These plots show inflationary era and then an exit from inflation for $\dot{\phi} < \dot{\phi}_D$ (which is opposite to our case) and No. of e-folding lies between 80 to 90. Our results are compatible with [115] for standard values of perturbed parameters.

For better understanding of the inflationary model's compatibility with recent data, we have plotted parametric plots (5.3) in which scalar spectral index is plotted versus tensor to scalar ratio for $\tilde{n} > 1$. It is observed that for $\tilde{n} = 1.61, 1.7$, we have the standard value of spectral index $n_s = 0.968$ and an upper bound of tensor to scalar ratio is obtained as $r < 0.11$ which is in accordance with Plank 2015 and 2018 data [5]. It can be seen that as the value of \tilde{n} increases, the range of n_s is compressed.

One of main point is that the inflationary models in general relativity goes to red-tilt [183, 184]. Our discussion and the references [115, 174] led to a conclusion that the modified theories of gravity and general relativity can be distinguished by the fact that in modified theories, the tensor spectrum is blue-tilted. It is worth mentioning here that our results reduced to [115, 174] by choosing $\tilde{\alpha} = 0$.

In Chapter 6, we have reconstructed different LRS BI cosmic models in $f(R, \phi)$ gravity in the presence of anisotropic matter source. For this purpose, we have chosen two $f(R, \phi)$ models and developed the exact solutions for each of these models. For the sake of simplicity in calculations, we have chosen some power law ansatz as well as a specific condition for scale factors that arises from the proportionality condition of expansion and shear scalars. We have also explored the dynamics of the constructed models by investigating the graphical behavior of scalar potential, energy density, EoS parameter and skewness parameters by taking some particular non-zero values of the involved free parameters. For this purpose, we have fixed the $m > 1$ and $n = 0.002$ through out the graphical discussions.

In [149], the authors has selected two values of the coupling constant to explore the evolution of linear density contrast and virial overdensity that are: $\xi = -0.5$ & $\xi = 0.15$. It is concluded that in such a case, the negative choices of coupling constant yield the least deviation from the Λ CDM model. We have taken that particular negative value $\xi = -0.5$ for graphing purposes everywhere. Similarly, for the second model which has been used to discuss inflation and spectral index as well as the tensor-to-scalar ratio [113]. Actually,

authors constructed this model by extending a viable class of exponential $f(R)$ models involving Λ to accommodate phenomenon of cosmic inflation. For this purpose, they introduced a substitution of the form: $\frac{1}{R_0} \rightarrow -b_1 \kappa^3 \phi$, where b_1 is a dimensionless number of order unity and κ has the usual meaning. Following this, we fixed this parameter by taking the simplest choice of $b_1 = 1$. We have also used the power law ansatz for scalar field where it can be easily seen that the scalar field as a DE candidate plays a dominant role in late time acceleration with expanding universe when $\beta_1 > 0$, whereas $\beta_1 < 0$ indicates that the scalar field vanishes with the cosmic expansion ($B \rightarrow \infty$). Thus the possible best choices of this parameter will be $\beta_1 > 0$ and particularly, we have fixed this parameter as $\beta_1 = 1.2$ in the graphical analysis of both models. A brief summary of the obtained results is given in the following.

- For both constructed models with $m > 1$, the skewness parameters approaches to zero in later cosmic epochs which supports to the isotropic expansion of models in last stages of universe. Also, the anisotropy expansion measure of anisotropic fluid $\frac{\delta-\gamma}{w}$ indicates infinite value in initial cosmic epochs while it vanishes with the passage of cosmic time and hence corresponds to the isotropic expansion of universe in final stages. This is in agreement with the results already discussed in the literature [97, 101, 185] for BVI_0 model in GR and BI model in BD scalar-tensor theory.
- In both constructed models, the energy density shows the positive decreasing behavior as indicated in Figures. This is also compatible with the discussions [5, 101, 103, 186] indicating that the universe was highly dense in initial epochs but later on, energy density decreases with the passage of time and goes to zero due to expansion.
- For both these models, the self-interacting potential is also positive and increases with the increasing time. Hence it can be concluded that the scalar field plays a dominant role in late cosmic expansion.
- The physical parameters like σ , Θ , H_x , H_y and H show decreasing behavior with the increasing cosmic time and hence approaches to zero as $T \rightarrow \infty$ under some specific conditions on the free parameters. This result is also in agreement with the literature [103].

- For the discussed models, the deceleration parameter is a dynamical quantity that can be positive or negative by choosing some appropriate values of free parameters. In particular, for the selected set of free parameters, it is observed that for final cosmic epochs, the deceleration parameter shows negative behavior and hence supports to accelerated expansion of cosmos [5, 186].
- In both cases, the graphical behavior of deviation free EoS parameter indicates strongly negative behavior and hence corresponds to quintessence or phantom phases of cosmos in late eras [5]. Thus the constructed models show the accelerated expansion of the universe. Furthermore, for all permissible values of m , we have constant value of the anisotropic parameter of expansion which leads to model anisotropy even in the later cosmic epochs.

It would be worthwhile to construct exact solutions for other Bianchi type models with anisotropic or viscous matter contents in $f(R, R_{\alpha\beta}R^{\alpha\beta}, \phi)$ theory of gravity.

Chapter 8

References

- [1] Riess, A.G. et al. (1998). Observational Evidence from Supernovae for an Accelerating Universe and a Cosmological Constant, *Astron. J.* **116**, 1009; Perlmutter, S. et al. (1999). Measurements of Ω and Λ from 42 High-Redshift Supernovae, *Astrophys. J.* **517**, 565.
- [2] Bennett, C.L. et al. (2003). First-Year Wilkinson Microwave Anisotropy Probe (WMAP) Observations: Preliminary Maps and Basic Results, *Astrophys. J. Suppl.* **148**, 1; Spergel, D.N. et al. (2007). Wilkinson Microwave Anisotropy Probe (WMAP) Three Year Results: Implications for Cosmology, *Astrophys. J. Suppl.* **170**, 377.
- [3] Allen, S.W. et. al. (2004). Constraints on dark energy from Chandra observations of the largest relaxed galaxy clusters, *Mon. Not. Roy. Astron. Soc.*, **353**, 457.
- [4] Tegmark, M. et al. (2004). Cosmological parameters from SDSS and WMAP, *Phys. Rev. D* **69**, 103501.
- [5] Ade, P., et al. (2016). Planck 2015 results-XIII. cosmological parameters, *Astronomy & Astrophysics* **594**, A13.
- [6] Sahni, V. and Starobinsky, A.A. (2000). The case for a positive cosmological Λ -Term, *Int. J. Mod. Phys. D* **9**, 373.
- [7] Carroll, S.M. (2001). The Cosmological Constant, *Living Rev. Rel.* **4**, 1.
- [8] Peebles, P.J.E. and Ratra, B. (2003). The cosmological constant and dark energy, *Rev. Mod. Phys.* **75**, 559.
- [9] Einstein, A. (1917). Cosmological Considerations in the General Theory of Relativity, *Sitzungsber. Preuss. Akad. Wiss. Phys. Math. Klasse* **VI**, 142.
- [10] Weinberg, S. (1989). The cosmological constant problem, *Rev. Mod. Phys.* **61**, 1.
- [11] Padmanabhan, T. (2008). Dark energy and gravity, *Gen. Relativ. Gravit.* **40**, 529.
- [12] Bento, M.C. et al. (2002). Generalized Chaplygin gas, accelerated expansion, and dark energy matter unification, *Phys. Rev. D* **66**, 043507; Benaoum, H.B. (2012). Modified Chaplygin Gas Cosmology, *Adv. in High Energy Phys.* **2012**, 357802.

- [13] Caldwell, R.R. et al. (1998). Cosmological Imprint of an Energy Component with General Equation of State, *Phys. Rev. Lett.* **80**, 1582; Steinhardt, P.J. et al. (1999). Cosmological tracking solutions, *Phys. Rev. Lett.* **59**, 123504.
- [14] Lobo, F.S.N. (2009). The Dark Side of Gravity: Modified Theories of Gravity *Dark Energy-Current Advances and Ideas* 173-204; Clifton, T. et. al. (2012). Modified Gravity and Cosmology, *Phys. Reports* **513**, 1.
- [15] Buchdahl, H.A. et al. (1970). Non-Linear Lagrangians and Cosmological Theory, *Astron. Soc.* **150**, 1.
- [16] Ferraro, R. and Fiorini, F. (2007). Modified teleparallel gravity: Inflation without an inflaton, *Phys. Rev. D* **75**, 084031; Bengochea, R. and Ferraro, R. (2009). Dark torsion as the cosmic speed-up, *Phys. Rev. D* **79**, 124019.
- [17] Carroll, S. et al. (2005). Cosmology of generalized modified gravity models, *Phys. Rev. D* **71**, 063513; Cognola, G. (2006). Dark energy in modified Gauss-Bonnet gravity: Late-time acceleration and the hierarchy problem, *Phys. Rev. D* **73**, 084007.
- [18] Harko, T. et al. (2011). $f(R, T)$ gravity, *Phys. Rev. D* **84**, 024020.
- [19] Fujii, Y. and Maeda, K. (2004). The Scalar Tensor Theory of Gravitation (Cambridge University); Brans, C.H. (2005). The Roots of Scalar Tensor Theory: An Approximate History, *Contributed to Conference: C04-05-31.1*
- [20] Faraoni, V. Cosmology in Scalar Tensor Gravity (Springer 2004).
- [21] Weinberg, S.: Gravitation and Cosmology (Wiley, 1972).
- [22] Bertotti, B. et al. (2003). A test of general relativity using radio links with the Cassini spacecraft, *Nature* **425**, 374; Felice, A.D. et al. (2006). Relaxing nucleosynthesis constraints on Brans-Dicke theories, *Phys. Rev. D* **74**, 103005.
- [23] Bhadra, A. et al. (2007). Brans-Dicke theory: Jordan versus Einstein frame, *Mod. Phys. Lett. A* **22**, 367.
- [24] Faraoni, V. and Gunzig, E. (1999). Einstein Frame or Jordan Frame?, *Int. J. Theor. Phys.* **38**, 217; Flanagan, E.E. (2004). The conformal frame freedom in theories of gravitation, *Class. Quantum. Grav.* **21**, 3817.

- [25] Faraoni, V. et al. (1999). Conformal transformations in classical gravitational theories and in cosmology, *Fund. Cosmic Phys.* **20**, 121.
- [26] Capozziello, S. (2002). Curvature Quintessence, *Int. J. Mod. Phys. D* **11**, 483.
- [27] Li, B. and Chu, M.C. (2006). CMB and matter power spectra of early $f(R)$ cosmology in the Palatini formulation, *Phys. Rev. D* **74**, 104010.
- [28] Nojiri, S. et al. (2010). Cosmological reconstruction of realistic modified $F(R)$ gravities, *Phys. Lett. B* **681**, 74.
- [29] Elizalde, E. et al. (2010). Λ CDM epoch reconstruction from $F(R, G)$ and modified Gauss-Bonnet gravities, *Class. Quantum Grav.* **27**, 095007.
- [30] Carloni, S. et al. (2012). A new approach to reconstruction methods in $f(R)$ gravity, *Class. Quantum Grav.* **29**, 135012.
- [31] Sharif, M and Zubair, M. (2013). Energy Conditions Constraints and Stability of Power Law Solutions in $f(R, T)$ Gravity, *J. Phys. Soc. Jpn.* **82**, 014002.
- [32] Jamil, M. et al. (2012). Reconstruction of some cosmological models in $f(R, T)$ cosmology, *Eur. Phys. J. C* **72**, 1999.
- [33] Sharif, M. and Zubair, M. (2014). Cosmological reconstruction and stability in $f(R, T)$ gravity, *Gen. Rel. Grav.* **46**, 1723.
- [34] Carroll, S.: Spacetime and Geometry: An Introduction to General Relativity (Addison Wesley, 2004).
- [35] Hawking, S.W. and Ellis, G.F.R.: The Large Scale Structure of Spacetime (Cambridge University Press, 1973).
- [36] Schon, R. and Yau, S.T. (1981). Proof of the positive mass theorem. 2, *Commun. Math. Phys.* **79**, 231.
- [37] Visser, M. (1997). General relativistic energy conditions: The Hubble expansion in the epoch of galaxy formation, *Phys. Rev. D* **56**, 7578.

- [38] Banijamali, A. et al. (2012). Energy conditions in $f(G)$ modified gravity with non-minimal coupling to matter, *Astrophys. Space Sci.* **338**, 327.
- [39] Liu, Di and Reboucas, M.J. (2012). Energy conditions bounds on $f(T)$ gravity, *Phys. Rev. D* **86**, 083515.
- [40] Atazadeh, K. et al. (2009). Energy Conditions in $f(R)$ Gravity and Brans-Dicke Theorems, *Int. J. Mod. Phys. D* **18**, 1101.
- [41] Santos, J. et al. (2010). Energy Conditions Constraints on a class of $f(R)$ -gravity, *Int. J. Mod. Phys. D* **19**, 1315; Alvarenga, A.G. et al. (2013). Testing some $f(R, T)$ gravity models from energy conditions, *J. mod. phys.* **4**, 130.
- [42] Santos, J. et al. (2007). Energy conditions in $f(R)$ gravity, *Phys. Rev. D* **76**, 083513.
- [43] Garcia, N.M. (2011). Energy conditions in modified Gauss-Bonnet gravity, *Phys. Rev. D* **83**, 104032.
- [44] Zubair, M. and Waheed, S. (2015). Energy conditions in $f(T)$ gravity with non-minimal torsion-matter coupling, *Astrophys. Space Sci.* **355**, 361-369.
- [45] Sharif, M. and Waheed, S. (2013). Energy conditions in a generalized second-order scalar-tensor gravity, *Adv. in High Energy Phys.* **2013**, 253985.
- [46] Sharif, M. and Zubair, M. (2013). Energy conditions in $f(R, T, R_{\mu\nu}T^{\mu\nu})$ gravity, *J. High. Energy Phys.* **12**, 079.
- [47] Waheed, S. and Zubair, M. (2015). Energy constraints and $F(T, T_G)$ cosmology, *Astrophys. Space Sci.* **359**, 47.
- [48] Hawking, S.W. (1975). Particle creation by black holes, *Commun. Math. Phys.* **43**, 199.
- [49] Bardeen, J.M. et al. (1973). The four laws of black hole mechanics, *Commun. Math. Phys.* **31**, 161.
- [50] Jacobson, T. (1995). Thermodynamics of Spacetime: The Einstein Equation of State, *Phys. Rev. Lett.* **75**, 1260.

- [51] Verlinde, E. (2000). On the Holographic Principle in a Radiation Dominated Universe, *hep-th/0008140*.
- [52] Padmanabhan, T. (2005). Gravity and the thermodynamics of horizons, *Phys. Rep.* **406**, 49.
- [53] Padmanabhan, T. (2002). Classical and quantum thermodynamics of horizons in spherically symmetric spacetimes, *Class. Quantum Grav.* **19**, 5387.
- [54] Paranjape, A. et al. (2006). Thermodynamic route to field equations in Lanczos-Lovelock gravity, *Phys. Rev. D* **74**, 104015; Kothawala, D. and Padmanabhan, T. (2009). Thermodynamic structure of Lanczos-Lovelock field equations from near-horizon symmetries *Phys. Rev. D* **79**, 104020.
- [55] Cai, R.G. and Kim, S.P. (2005). First law of thermodynamics and Friedmann equations of Friedmann-Robertson-Walker universe, *JHEP* **02**, 050.
- [56] Akbar, M. and Cai, R.G. (2006). Friedmann equations of FRW universe in scalar-tensor gravity, $f(R)$ gravity and first law of thermodynamics, *Phys. Lett. B* **635**, 7.
- [57] Sadjadi, H.M. (2006). Generalized second law in a phantom-dominated universe, *Phys. Rev. D* **73**, 063525.
- [58] Akbar, M. (2008). Viscous Cosmology and Thermodynamics of Apparent Horizon, *Chin. Phys. Lett.* **25**, 4199.
- [59] Cembranos, J.A.R. et al. (2015). Thermodynamic Analysis of Non-Linear Reissner-Nordström Black Holes, *Universe* **1**, 412; Cembranos, J.A.R. et al. (2015). Reissner-Nordström black holes in the inverse electrodynamics model, *JCAP* **1502**, 042; Cembranos, J.A.R. et al. (2014). KerrNewman Black Holes in $f(R)$ Theories, *Int. J. Geom. Meth. Mod. Phys.* **11**, 1450001; Cruz-Dombriz, A. de la. et al. (2009). Black holes in $f(R)$ theories, *Phys. Rev. D* **80**, 124011.
- [60] Bamba, K. and Geng, C.Q. (2010). Thermodynamics in $f(R)$ gravity in the Palatini formalism, *JCAP* **06**, 014.
- [61] Bamba, K. and Geng, C.Q. (2011). Thermodynamics of cosmological horizons in $f(T)$ gravity, *JCAP* **11**, 008.

- [62] Sharif, M. and Zubair, M. (2012). Thermodynamics in $f(R, T)$ theory of gravity, *JCAP* **03**, 028; (2013). Thermodynamic behavior of particular $f(R, T)$ -gravity models, *J. Exp. Theor. Phys.* **117**, 248; (2013). Thermodynamics in Modified Gravity with Curvature Matter Coupling, *Adv. High Energy Phys.* **2013**, 947898.
- [63] Zubair, M. and Jawad, A. (2015). Generalized second law of thermodynamics in $f(T, T_G)$ gravity, *Astrophys. Space Sci.* **360**, 11; Zubair, M. and Waheed, S. (2015). Thermodynamic study in modified $f(T)$ gravity with cosmological constant regime, *Astrophys. Space Sci.* **360**, 68.
- [64] Sharif, M. and Zubair, M. (2013). Study of thermodynamic laws in $f(R, T, R_{\mu\nu}T^{\mu\nu})$ gravity, *JCAP* **11**, 042.
- [65] Huang, Y. et al. (2015). Thermodynamics of scalar-tensor theory with non-minimally derivative coupling, *EPJC* **75**, 351.
- [66] Flamm, L. (1916). Comments on Einsteins Theory of Gravity, *Phys. Z.* **17**, 448.
- [67] Einstein, A. and Rosen, N. (1935). The particle problem in the general theory of relativity, *Phys. Rev.* **48**, 73.
- [68] Misner, C.W. and Wheeler, J.A. (1957). Classical physics as geometry, *Ann. Phys.* **2**, 525; Wheeler, J.A. (1957). On the nature of quantum geometrodynamics, *Ann. Phys. (N.Y.)* **2**, 604.
- [69] Morris, M.S. and Thorne, K.S. (1988). Wormholes in spacetime and their use for interstellar travel: A tool for teaching general relativity, *Am. J. Phys.* **56**, 395; Morris, M.S., Thorne, K.S. and Yurtsever, U. (1988). Wormholes, time machines, and the weak energy condition, *Phys. Rev. Lett.* **61**, 1446.
- [70] Teo, E. (1998). Rotating traversable wormholes, *Phys. Rev. D* **58**, 024014; Visser, M. (1989). Traversable wormholes: Some simple examples, *Phys. Rev. D* **39**, 3182-3184; Bouhmadi-López, M. et al. (2014). Wormholes minimally violating the null energy condition, *J. Cosmol. Astropart. Phys.* **11**, 007.
- [71] Visser, M. (1989). Traversable wormholes: Some simple examples, *Phys. Rev. D* **39**, 3182-3184;

- [72] Visser, M.: Lorentzian Wormholes From Einstein to Hawking, (American Institute of Physics, August 1996); Visser, M. et al. (2003). Traversable wormholes with arbitrarily small energy condition violations, *Phys. Rev. Lett.* **90**, 201102.
- [73] Lobo, F.S.N. and Oliveira, M.A. (2009). Wormhole geometries in $f(R)$ modified theories of gravity, *Phys. Rev. D* **80**, 104012; Bahamonde, S. et al. (2016). Cosmological wormholes in $f(R)$ theories of gravity, *Phys. Rev. D* **94**, 044041.
- [74] Jamil, M. et al. (2013). Wormholes in a viable $f(T)$ gravity, *EPJC* **73**, 2267; Boehmer, C.G. et al. (2012). Wormhole geometries in modified teleparallel gravity and the energy conditions, *Phys. Rev. D* **85**, 044033.
- [75] Zubair, M. et al. (2016). Static spherically symmetric wormholes in $f(R, T)$ gravity, *EPJC* **76**, 444.
- [76] Agnese, A.G. and Camera, M. La. (1995). Wormholes in the Brans-Dicke theory of gravitation, *Phys. Rev. D* **51**, 2011.
- [77] Nandi, K.K. et al. (1997). Brans wormholes, *Phys. Rev. D* **55**, 2497.
- [78] He, F. and Kim, S.W. (2002). New Brans-Dicke wormholes, *Phys. Rev. D* **65**, 084022.
- [79] Ebrahimi, E. and Riazi, N. (2010). Expanding $(n + 1)$ -dimensional wormhole solutions in Brans-Dicke cosmology, *Phys. Rev. D* **81**, 024036.
- [80] Capozziello, S. et al. (2012). Wormholes supported by hybrid metric-Palatini gravity, *Phys. Rev. D* **86**, 127504.
- [81] Bahamonde, S. et al. (2016). Scalar-tensor teleparallel wormholes by Noether symmetries, *Phys. Rev. D* **94**, 084042.
- [82] Mehdizadeh, M.R. et al. (2015). Einstein-Gauss-Bonnet traversable wormholes satisfying the weak energy condition, *Phys. Rev. D* **91**, 084004.
- [83] Accetta, F.S. et al. (1990). Wormholes and baby universes in scalar-tensor gravity, *Nuclear Physics B* **333**, 221-252.

- [84] Poisson, E. and Visser, M. (1995). Thin-shell wormholes: Linearization stability, *Phys. Rev. D* **52**, 7318.
- [85] Lobo, F.S.N. and Crawford, P. (2004). Linearized stability analysis of thin-shell wormholes with a cosmological constant, *Class. Quantum Grav* **21**, 391.
- [86] Eiroa, E.F. and Simeone, C. (2004). Cylindrical thin-shell wormholes, *Phys. Rev. D* **70**, 044008.
- [87] Eiroa, E.F. and Romero, G.E. (2004). Linearized stability of charged thin shell wormholes, *Gen. Rel. Gravit* **36**, 651.
- [88] Thibeault, M., Simeone, C. and Eiroa, E.F. (2006). Thin-shell wormholes in Einstein-Maxwell theory with a Gauss-Bonnet term, *Class. Quantum Grav* **38**, 1593; Eiroa, E.F. (2008). Stability of thin-shell wormholes with spherical symmetry, *Phys. Rev. D* **78**, 024018; Dias, G.A.S. and Lemos, J.P.S. (2010). Thin-shell wormholes in d-dimensional general relativity: Solutions, properties, and stability, *Phys. Rev. D* **82**, 084023; Garcia, N.M., Lobo, F. S.N. and Visser, M. (2012). Generic spherically symmetric dynamic thin-shell traversable wormholes in standard general relativity, *Phys. Rev. D* **86**, 044026.
- [89] M. Sharif, and M. Azam, (2013). Mechanical Stability of Cylindrical Thin-Shell Wormholes, *Eur. Phys. J. C* **73**, 2407; Sharif, M. and Yousaf, Z. (2014). Cylindrical Thin-shell Wormholes in $f(R)$ gravity, *Astrophys. Space Sci* **351**, 351; Varela, V. (2015). A note on linearized stability of Schwarzschild thin-shell wormholes with variable equations of state, *Phys. Rev. D* **92**, 044002; Richarte, M.G. et al. (2017). Relativistic Bose-Einstein condensates thin-shell wormholes, *Phys. Rev. D* **96**, 084022; Forghani, S.D., Mazharimousavi, S.H. and Halilsoy, M. (2018). Asymmetric Thin-Shell Wormholes, *Eur. Phys. J. C* **78**, 469.
- [90] Barceló, C. and Visser, M. (2000). Brane surgery: Energy conditions, traversable wormholes, and voids, *Nucl. Phys. B* **584**, 415.
- [91] Lobo, F.S.N. and Crawford, P. (2005). Stability analysis of dynamic thin shells, *Class. Quant. Grav.* **22**, 4869.

- [92] Rodrigues, D.C. (2008). Anisotropic cosmological constant and the CMB quadrupole anomaly, *Phys. Rev. D* **77**, 023534.
- [93] Koivisto, T. and Mota, D. F. (2008). Anisotropic dark energy: dynamics of the background and perturbations, *J. Cosmol. Astropart. Phys.* **806**, 18; Koivisto, T. and Mota, D. F. (2008). Accelerating cosmologies with an anisotropic equation of state, *Astrophys. J.* **679**, 1.
- [94] Yadav, A. K. and Saha, B. (2012). LRS Bianchi-I anisotropic cosmological model with dominance of dark energy, *Astrophys. Space Sci.* **337**, 759.
- [95] Akarsu, O. and Kilinc, C.B. (2010). LRS Bianchi type I models with anisotropic dark energy and constant deceleration parameter, *Gen. Relativ. Grav.* **42**, 119.
- [96] Akarsu, O. and Kilinc, C.B. (2010). Bianchi type III models with anisotropic dark energy, *Gen. Relativ. Grav.* **42**, 763.
- [97] Sharif, M. and Zubair, M. (2010). Effects of Electromagnetic Field on the Dynamics of Bianchi TYPE VI_0 Universe with Anisotropic Dark Energy, *Int. J. Mod. Phys. D* **19**, 1957.
- [98] Sharif, M. and Zubair, M. (2012). Dynamics of a magnetized Bianchi VI 0 universe with anisotropic fluid, *Astrophys Space Sci.* **339**, 45.
- [99] Sharif, M. and Zubair, M. (2012). Anisotropic Universe Models with Perfect Fluid and Scalar Field in $f(R, T)$ Gravity, *J. Phys. Soc. Japan* **81**, 114005.
- [100] Sharif, M. and Zubair, M. (2014). Study of Bianchi I anisotropic model in $f(R, T)$ gravity, *Astrophys Space Sci.* **349**, 457.
- [101] Sharif, M. and Waheed, S. (2012). Anisotropic universe models in Brans-Dicke theory, *EPJC*, **72**, 1876.
- [102] Sharif, M. and Waheed, S. (2012). Dynamics of Magnetized Bulk Viscous Strings in Brans-Dicke Gravity, *Int. J. Mod. Phys. D* **21**, 1250055.
- [103] Zubair, M. and Hassan, S. M. A. (2016). Dynamics of Bianchi type I, III and Kantowski-Sachs solutions in $f(R, T)$ gravity, *Astrophys Space Sci.* **361**, 149; Zubair, M. et al. (2016). Bianchi type I and V solutions in $f(R, T)$ gravity with time-dependent deceleration parameter, *Can. J. Phys.* **94**, 1289.

- [104] Sahoo, P. and Reddy, R. (2018). LRS Bianchi type-I bulk viscous cosmological models in $f(R, T)$ gravity, *astrophys.* **61**, 134-143.
- [105] Ramesh, G. and Umadevi, S. (2016). Cosmological models with linearly varying deceleration parameter in $f(R, T)$ gravity, *Astrophys. Space Sci.* **361**, 2.
- [106] Shamir, M.F. (2015). Locally Rotationally Symmetric Bianchi Type I Cosmology in $f(R, T)$ Gravity, *EPJC* **75**, 354.
- [107] Guth, A. (1981). Inflationary universe: A possible solution to the horizon and flatness problems, *Phys. Rev. D* **23**, 347.
- [108] Starobinsky, A.A (1980). A new type of isotropic cosmological models without singularity, *Phys. Lett. B* **91**, 99.
- [109] Liddle, A.R. and Samuel, M. (2003). How long before the end of inflation were observable perturbations produced?, *Phys. Rev. D* **68**, 103503.
- [110] Walliser, D. (1992). Successful inflation in scalar-tensor theories of gravity, *Nucl. Phys. B* **378**, 150.
- [111] Garcia Bellido, J. and Quiros, M. (1990). Extended inflation in scalar-tensor theories of gravity, *Phys. Lett. B* **243**, 1.
- [112] Lahiri, J. and Bhattacharya, G. (2006). Perturbative analysis of multiple-field cosmological inflation, *Annals Phys.* **321**, 999-1023.
- [113] Myrzakulov, R. et al. (2015). Inflation in $f(R, \phi)$ -theories and mimetic gravity scenario, *EPJC* **75**, 9444.
- [114] Sharif, M. and Saleem, R. (2014). Warm anisotropic inflationary universe model, *EPJC* **74**, 2738.
- [115] Mathew, J. et al. (2018). Inflation with $f(R, \phi)$ in Jordan frame, *Gen.Rel.Grav.* **50**, 90.
- [116] Hawking, S.: The Illustrated: A Brief Histor of Time (Bantam Books, 1996).
- [117] Hawking, S.: The Universe in A Nutshell (Bantam Books, 2001).
- [118] Wetterich, C. (1998). Cosmology and the fate of dilatation symmetry, *Nucl. Phys. B* **302**, 668.

- [119] Caldwell, R.R. et al. (1998). Cosmological imprint of an energy component with general equation of state, *Phys. Rev. Lett.* **80**, 1582.
- [120] Ratra, B. and Peebles, P.J.E. (1998). Cosmological consequences of a rolling homogeneous scalar field, *Phys. Rev. D* **37**, 3406.
- [121] Frieman, J.A. et al. (1995). Cosmology with Ultralight Pseudo Nambu-Goldstone Bosons, *Phys. Rev. Lett.* **75**, 2077.
- [122] Coble, K. et al. (1997). Dynamical Λ models of structure formation, *Phys. Rev. D* **55**, 1851.
- [123] Hawking, S.W. and Ellis, G.F.R.: *The Large Scale Structure of Spacetime* (Cambridge University Press, 1999).
- [124] Caldwell, R.R. (2002). A phantom menace? Cosmological consequences of a dark energy component with super-negative equation of state, *Phys. Lett. B* **545**, 23.
- [125] Caldwell, R.R. et al. (2003). Phantom Energy: Dark Energy with $w < -1$ Causes a Cosmic Doomsday, *Phys. Rev. Lett.* **91**, 071301.
- [126] McInnes, B. (2002). The dS/CFT correspondence and the big smash, *JHEP* **0208**, 029.
- [127] Baushev, A.N. (2010). Phantom dark energy and the steady state ‘on the average’ universe, *J. Phys. Conf. Ser.* **203**, 012055.
- [128] Feng, B. et al. (2005). Dark energy constraints from the cosmic age and supernova, *Phys. Lett. B* **607**, 35.
- [129] Guo, Z.K. et al. (2005). Cosmological evolution of a quintom model of dark energy, *Phys. Lett. B* **608**, 177.
- [130] Feng, B. et al. (2006). Oscillating quintom and the recurrent universe, *Phys. Lett. B* **634**, 101.
- [131] Narlikar, J.V.: *An Introduction to Relativity* (Cambridge University Press, 2010).

- [132] Sahni, V. et al. (2003). Statefinder-a new geometrical diagnostic of dark energy, *J. Exp. Theor. Phys. Lett.* **77**, 201.
- [133] Poisson, E.: A Relativistic Toolkit: The Mathematics of Black Hole Mechanics (Cambridge University Press, 2004).
- [134] Duggal, K.L. and Sharma, R.: Symmetries of Spacetimes and Riemannian Manifolds (Kluwer Academic Publishers, 1999).
- [135] Wald, R.M.: General Relativity (University Of Chicago Press, 1984).
- [136] Nordström, G. (1912). Relativitätsprinzip und Gravitation, *Phys. Zeitschr* **13**, 1126; Träge und schwere Masse in der Relativitätsmechanik, *Annalen der Physik* **40**, 856-878; Zur Theorie der Gravitation vom Standpunkt des Relativitätsprinzips, *Annalen der Physik* **42**, 533-554.
- [137] Dirac, P.A.M. (1937). The cosmological constants, *Nature* **139**, 323; (1937). Physical Science and Philosophy, *Nature* **139**, 1001; (1938). A New Basis for Cosmology, *Proc. R. Soc. Lon. A* **165**, 199.
- [138] Lambiase, G. et al. (2015). Astrophysical constraints on extended gravity models, *JCAP*. **07**, 003.
- [139] Bekenstein, J.D. (1974). Generalized second law of thermodynamics in black-hole physics, *Phys. Rev. D* **9**, 3292.
- [140] Hawking, S.W. (1976). Black holes and thermodynamics, *Phys. Rev. D* **13**, 191.
- [141] Sato, K. (1981). First-order phase transition of a vacuum and the expansion of the Universe, *Mon. Not. R. Astron. Soc.* **195** 467; (1981). Cosmological baryon-number domain structure and the first order phase transition of a vacuum, *Phys. Lett. B* **99**, 66.
- [142] Novello, M. and Salim, J.M. (1979). Nonlinear photons in the universe, *Phys. Rev. D* **20**, 377; Garca-Salcedo, R. and Breton, N. (2000). Born-Infeld cosmologies, *Int. J. Mod. Phys. A* **15**, 4341.

- [143] Thiemann, T. (2003). Lectures on loop quantum gravity, *Lect. Notes. Phys.* **631**, 41; Novello, M. (2005). Cosmological effects of nonlinear electrodynamics, *Int. J. Mod. Phys. A* **20**, 2421; Novello, M. et al. (2004). Nonlinear electrodynamics and the acceleration of the universe, *Phys. Rev. D* **69**, 127301; Novello, M. et al. (2007). Cosmological effects of nonlinear electrodynamics, *Class. Quantum Grav.* **24**, 3021.
- [144] De Lorenci, V.A. et al. (2002). Nonlinear electrodynamics and FRW cosmology, *Phys. Rev. D* **65**, 063501.
- [145] Wang, B. et al. (2006). Thermodynamics of an accelerated expanding universe, *Phys. Rev. D* **74**, 083520.
- [146] Banerjee, N. and Pavon, D. (2007). Holographic dark energy in Brans-Dicke theory, *Phys. Lett. B* **647**, 477; Bertolami, O. and Martins, P. J. (2000). Nonminimal coupling and quintessence, *Phys. Rev. D* **61**, 064007.
- [147] Visser, M. (2004). Jerk and the cosmological equation of state, *Class. Quantum. Grav.* **21**, 2603.
- [148] Visser, M. (2005). Cosmography: cosmology without the Einstein equations, *Gen. Rel. Grav.* **37**, 1541-1548.
- [149] Fan, Y. et al. (2015). Spherical collapse in the extended quintessence cosmological models, *Phys. Rev. D* **92**, 083529.
- [150] Bahamonde, S. et al. (2015). Generalized $f(R, \phi, X)$ Gravity and the Late-Time Cosmic Acceleration, *Universe* **1**, 186-198.
- [151] Bekenstein, J.D. (1973). Black Holes and Entropy, *Phys. Rev. D* **7**, 2333.
- [152] Wald, R. M. (1993). Black hole entropy is the Noether charge, *Phys. Rev. D* **48**, R3427.
- [153] Brustein, R. et al. (2009). Wald's entropy is equal to a quarter of the horizon area in units of the effective gravitational coupling, *Phys. Rev. D* **79**, 044025.

- [154] Misner, C. W. and Sharp, D. H. (1964). Relativistic equations for adiabatic, spherically symmetric gravitational collapse, *Phys. Rev.* **136**, B571; Bak, D. and Rey, S.J. (2000). Cosmic holography+, *Class. Quantum. Grav.* **17**, L83.
- [155] Wu, S. F., et al. (2008). The generalized second law of thermodynamics in generalized gravity theories, *Class. Quantum. Grav.* **25**, 235018.
- [156] Hayward, S. A. (1998). Unified first law of black-hole dynamics and relativistic thermodynamics, *Class. Quantum. Grav.* **15**, 3147; Hayward, S.A. et al. (1999). Dynamic black-hole entropy, *Phys. Lett. A* **256**, 347.
- [157] Bamba, K. and Geng, C.Q. (2009). Thermodynamics in $F(R)$ gravity with phantom crossing, *Phys. Lett. B* **679**, 282.
- [158] Zubair, M and Bahamonde, S. (2017). Generalized Second Law of Thermodynamic in Modified Teleparallel Theory, *EPJC* **77**, 472.
- [159] Izquierdo, G. and Pavon, D. (2006). Dark energy and the generalized second law, *Phys. Lett. B* **633**, 420.
- [160] Harko, T. et al. (2013). Modified-gravity wormholes without exotic matter, *Phys. Rev. D* **87**, 067504.
- [161] Garcia, N.M. and Lobo, F.S.N. (2010). Wormhole geometries supported by a non-minimal curvature-matter coupling, *Phys. Rev. D* **82**, 104018; (2011). Nonminimal curvature-matter coupled wormholes with matter satisfying the null energy condition, *Class. Quantum Grav.* **28**, 085018.
- [162] Lobo, F.S.N. (2007). General class of braneworld wormholes, *Phys. Rev. D* **75**, 064027.
- [163] Zubair, M. and Kousar, F. (2016). Cosmological reconstruction and energy bounds in $f(R, R_{\alpha\beta}R^{\alpha\beta}, \phi)$ gravity, *EPJC* **76**, 254.
- [164] Tian, D. W. (2016). Traversable wormholes and energy conditions in Lovelock-Brans-Dicke gravity, arXiv:1508.02291.

- [165] Pavlovic, P. and Sossich, M. (2015). Wormholes in viable $f(R)$ modified theories of gravity and weak energy condition, *EPJC* **75**, 117.
- [166] Dent, J.B. et al. (2011). $f(T)$ gravity mimicking dynamical dark energy. Background and perturbation analysis, *J. Cosmol. Astropart. Phys.* **01**, 009.
- [167] Sotiriou, T.P. (2011). Generalizations of teleparallel gravity and local Lorentz symmetry, *Phys. Rev. D* **83**, 104030.
- [168] Li, B. et al. (2011). Large-scale structure in $f(T)$ gravity, *Phys. Rev. D* **83**, 104017.
- [169] Zhang, Y., et al. (2011). Notes on $f(T)$ Theories, *J. Cosmol. Astropart. Phys.* **07**, 015.
- [170] Bhattacharya, S. and Chakraborty, S. (2017). $f(R)$ gravity solutions for evolving wormholes, *EPJC* **77**, 558.
- [171] Rahaman, F. et al. (2009). Wormholes with varying equation of state parameter, *Acta Phys. Polon. B* **40**, 25.
- [172] Hwang, J.c. and Noh, H. (1996). Cosmological perturbations in generalized gravity theories, *Phys. Rev. D* **54**, 1460.
- [173] Hwang, J.c. and Noh, H. (2000). Conserved cosmological structures in the one-loop superstring effective action, *Phys. Rev. D* **61**, 043511.
- [174] Johnson, J.P., Mathew, J. and Shankaranarayanan, S. (2017). Inflation driven by exponential non-minimal coupling of inflaton with gravity, arXiv:1706.10150.
- [175] Tambalo, G. and Rinaldi, M. (2017). Inflation and reheating in scale-invariant scalar-tensor gravity, *Gen. Rel. Gravit* **49**, 52.
- [176] Kanti, P. et al. (2015). Gauss-bonnet inflation, *Phys. Rev. D* **92**, 041302.
- [177] Hwang, J.C. and Noh, H. (2001). $f(R)$ gravity theory and CMBR constraints, *Phys. Lett. B* **506**, 13; Noh, H. and Hwang, J.C. (2001). Inflationary spectra in generalized gravity: Unified forms, *Phys. Lett. B* **515**, 231.

- [178] Collins, C.B. and Hawking, S.W. (1973). Why is the universe isotropic?, *Astrophys. J.* **180**, 317.
- [179] Carroll, S.M., Hoffman, M. and Trodden, M. (1992). Can the dark energy equation-of-state parameter w be less than -1 ?, *Phys. Rev. D* **68**, 023509.
- [180] Sharif, M., Zubair, M. (2010). Dynamics of Bianchi I universe with magnetized anisotropic Dark Energy, *Astrophys. Space Sci.* **330**, 399.
- [181] Elizalde, E. et al. (2012). De Sitter universe in nonlocal gravity, *Phys. Rev. D* **85**, 044002; Elizalde, E. and Gomez, D.S. (2009). $F(R)$ cosmology in the presence of a phantom fluid and its scalar-tensor counterpart: Towards a unified precision model of the evolution of the Universe, *Phys. Rev. D* **80**, 044030; Cognola, G. et al. (2009). Initial and final de Sitter universes from modified $f(R)$ gravity, *Phys. Rev. D* **79**, 044001; Elizalde, E. et al. (2013). Reconstruction procedure in nonlocal cosmological models, *Class. Quant. Grav.* **30**, 035002.
- [182] Gong, Y. and Wang, A. (2007). Friedmann Equations and Thermodynamics of Apparent Horizons, *Phys. Rev. Lett.* **99**, 211301; Wu, S.F. et al. (2010). Dynamical horizon entropy and equilibrium thermodynamics of generalized gravity theories, *Phys. Rev. D* **81**, 044034.
- [183] Mukhanov, V.: Physical foundations of cosmology (Cambridge University Press, 2005).
- [184] Weinberg, S.: Cosmology (Oxford University Press, Oxford New York, 2008).
- [185] Aktas, C. et al. (2012). Behaviors of dark energy and mesonic scalar field for anisotropic universe in $f(R)$ gravity, *Phys. Lett. B* **707**, 237.
- [186] Pradhan, A. et al. (2012). Dark energy models with anisotropic fluid in Bianchi Type- VI_0 space-time with time dependent deceleration parameter, *Astrophys Space Sci.* **337**, 401-413.